Investigation of BCL-2 interacting killer (BIK) as a breast cancer biomarker and its role in failed apoptosis

by

Vrajesh K Pandya

A thesis submitted in partial fulfillment of the requirements for the degree of

Doctor of Philosophy

Department of Biochemistry
University of Alberta

ABSTRACT

Breast cancer is the number one cause of cancer-associated deaths in women worldwide. It can be broadly classified into estrogen receptor (ER) positive or -negative subtypes which form the basis of treatment. Despite the therapeutic advancements, more than half a million women annually succumb to the illness suggesting critical gaps in our understanding of the disease. Chemo-, radiation- and hormonal therapies are used to reduce tumor burden work by inducing apoptosis. Hence investigation of players in the apoptotic program can uncover the mechanisms of cancer aggression. Apoptosis is regulated by the BCL-2 family of proteins, which sense and relay the death signals to the downstream machinery that executes cell death. The BH3-only proteins, a subgroup of the BCL-2 family, act as the sensors of a variety of cell-intrinsic stressors and determine therapeutic response against cancer. Thus, it is believed that if the BH3-only proteins are absent or downregulated it may create a permissive environment for the development of therapeutic resistance leading to cancer aggression.

In order to decipher how BH3 proteins affect breast cancer pathophysiology, I interrogated the gene expression levels of five BH3-only members in breast cancer tumors with respect to patient survival outcomes. Interestingly, we found that the BH3-only member BCL-2 interacting killer (BIK) was associated with worse patient survival and patients with high levels of *BIK* transcript were twice as likely to die from the disease compared to the BIK-low patients. This finding was surprising, given the pro-apoptotic nature of BIK. Hence, we validated these findings in a different cohort of patients by quantitating BIK protein levels using immunohistochemistry. Strikingly, BIK protein levels were also associated with worse survival outcomes of the patients.

Thus, high BIK expression in two independent patient cohorts (total n=327) was associated with poor patient survival. Further interrogation revealed that high *BIK* mRNA levels in association with high levels of *ATG5*, a regulator of the cytoprotective autophagic pathway, predicted worse prognostic outcomes. This provided a clue that BIK might have a tumor-promoting effect through enhanced cell survival in the face of tumor-associated stress. In order to test this, I ectopically expressed BIK in breast cancer cells and tested their autophagic response to nutrient starvation or mammalian target of rapamycin complex 1 (mTORC1) inhibition. While there was some autophagic response, BIK did not stimulate robust autophagy. Furthermore, MTT assays revealed that BIK expression did not confer a growth or survival benefit on the cells when they were nutrient starved or rapamycin-treated. Together these observations showed that BIK did not strongly regulate autophagy in the cell lines tested yet hinted that BIK may have tumor-promoting effects in patients.

More than 70% of all breast cancers are ER-positive driven by the female sex hormone estrogen. This type of cancer is treated with anti-estrogen therapy that utilizes drugs such as tamoxifen to induce cancer cell apoptosis and prevent relapse. Recent studies have identified an aberration of apoptosis called “failed apoptosis” in which apoptosis is initiated but does not go to completion, causes DNA double-strand breaks and mutations leading to tumorigenesis. Importantly, BIK is upregulated in response to anti-estrogen treatment of the ER-positive breast cancer which prompted me to interrogate BIK’s involvement in this patient subgroup. Interestingly, we discovered that high BIK levels predicted poor prognosis of anti-estrogen treated ER-positive but not alternatively treated ER-negative patients. I hypothesized that BIK facilitated tumor aggression in the ER-positive patients through failed apoptosis. Indeed, BIK expression in

breast cancer cell lines led to minimal cell death but caused caspase activation, and double-strand DNA damage dependent on caspase activated DNAse (CAD). Importantly, tamoxifen-mediated BIK expression also induced genomic damage in cells, suggesting a link between anti-estrogen stimulated DNA damage-mediated mutagenesis. Finally, I explored whether transient expression of BIK altered cell phenotypes after long-term culture. Interestingly, cells surviving this treatment produced progeny with aggressive phenotypes characterized by high clonogenic survival, elevated anchorage-independent growth, and enrichment of cancer stem cells. These results suggest that poor survivals of BIK-high ER-positive patients could be partly due to failed apoptosis which may provoke mutations and provide a means of evolution for cancer cells. Thus, in this thesis, I identified BIK as a novel biomarker of breast cancer and discovered a potential mechanism of BIK-mediated tumor evolution.

PREFACE

This thesis is an original work by Vrajesh Pandya.

A modified version chapter 3 of this thesis has been published as Pandya, V., Glubrecht, D., Vos, L., Hanson, J., Damaraju, S., Mackey, J., Hugh, J., and Goping, I.S. (2016). The pro-apoptotic paradox: the BH3-only protein Bcl-2 interacting killer (Bik) is prognostic for unfavorable outcomes in breast cancer. Oncotarget *7*, 33272-33285. I (VP) am the first author on this publication and conducted all experiments except for IHC staining. DG conducted BIK and BCL-2 IHC for Dataset-2. VP, DG, JHugh, and ISG consulted on IHC scoring and DG conducted final scoring. LV, SD, and JM provided patient samples and anonymized outcomes data. JHanson provided expert advice on statistical analysis. ISG and I designed experiments. I performed all data analysis. I wrote the first draft of the manuscript that was edited by ISG.

All experiments described in chapter 4 were designed by ISG, and VP. VP performed all the experiments and data analysis.

A modified version of chapter 5 of this thesis is in preparation for publication as Pandya V, Githaka JM, Kirschenman R, Patel N, Veldhoen R, Damaraju S, Mackey J, and Goping IS (2018). BIK is a prognostic marker for ER-positive breast cancer and induces sublethal apoptosis to promote cancer aggression (Manuscript in preparation). I (VP) will be the first author on this publication and performed the majority of the experiments except the ones specifically mentioned here. JMG performed BIK spinning disk confocal imaging, measured colony size and density, and performed mammosphere formation assays. RK performed mouse xenografts and took weekly tumor measurements. NP harvested the tumors and measured post-harvest tumor volumes. RV

made MCF-7 Tet-On cells that were characterised by VP. SD and JM provided patient samples and anonymized outcomes data. ISG and I designed experiments. I performed all data analysis. I wrote the first draft of the manuscript that was edited by ISG.

The literature review presented in chapter 1 is my original work, as is the concluding analysis presented in chapter 6.

DEDICATION

To all my teachers who taught me how to learn...

मंज़िल तो मिल ही जाएगी, चाहे भटक कर ही सही,

गुमराह तो वो है जो घर से कभी निकले ही नहीं.

[(You) will meet your destiny even if it is after an endless wondering,

the lost are those who never stepped out of their homes.]

ACKNOWLEDGMENTS

Getting a PhD has long been a dream. As I come near the end, I would like to offer my heartfelt thanks to the individuals who made it possible for me to come this far.

First and foremost, I would like to thank my supervisor Dr. Ing Swie Goping. She welcomed me in her lab and provided an excellent mentorship and happy working environment. Her approach of "leading from the back" has helped me think deeper about my project and take responsibility for it. I also thank her for the financial support she has provided for the last five years. Above everything else, I am grateful for the tremendous patience and generosity she has shown in guiding me through the academic and personal struggles. I cannot thank you enough.

I am thankful to Dr. Arun Raturi, once a boss now a friend, for introducing me to Dr. Goping and bringing me to Canada. You have been the older brother I never had. I will forever be grateful.

Sincere thanks to my supervisory committee members Dr. Thomas Simmen and Dr. Nicolas Touret for monitoring my progress through the graduate school and providing constructive criticism which has enormously helped me with my professional development.

Our collaborators whose expertise has tremendously contributed to this project. Dr. Sambasivaroa Damaraju for providing the tissue-microarrays, Dr. Judith Hugh for teaching us nuances of breast cancer pathology and giving her expert onion, and Dr. John Mackey for sharing the gene expression dataset and his in-depth knowledge about breast cancer oncology.

I would like to express my thanks to Dr. Richard Fahlman and Dr. Marek Michalak for serving on my candidacy exam and Dr. Jose Teodoro and Dr. Mary Hitt for participating in my thesis defense.

I would also like to thank the University of Alberta for the Doctoral Recruitment Scholarship and the Faculty of Medicine and Dentistry (FoMD) for the MedStar award for graduate students. Canadian Institutes of Health Research (CIHR) and Cancer Institute of Northen Alberta (CRINA) for providing travel awards. Department of Biochemistry for the valuable Biochemistry Graduate Assistantships in Teaching and Learning (BGATS).

All the past and present members of the Goping lab who are now dear friends. Diane Marganski for being a friend, philosopher and guide through thick and thin. Jasdeep Mann and Dr. John Maringa Githaka for many over-the-bench discussions, help with experiments and more. Raven Kirschenman for help with animal work. Past members Dr. Ning Yang, Dr. Namita Tripathi and Rachel Montpetit for many helpful scientific and not-so-scientific discussions. You all have made grad school bearable.

My family and friends for being always there for me. My mother Rekha Pandya for her unshakable belief, encouragement, and love. My wife Namrata for being a patient companion during the peaks and valleys of life, and also for being someone who always makes me believe that "it is gonna be okay." My son Ishan whose mere presence makes me smile and laugh for no apparent reason. Rahul and Paresh, my besties, for being my backup if I ever messed up in life.

Finally and most importantly, I would like to thank my teachers from high school to the university for instilling in me the interest in science. Mr. K.F Kachhia, Dr. Nila Bhatt, Mr. Piyush Pandya, Dr. Chetan Ambasana, Dr. Archana Gayatri, Dr. Anjana Desai, and Dr. Timishrah Bagchi. I am only here because of you.

TABLE OF CONTENTS

LIST OF TABLES

LIST OF FIGURES

LIST OF ABBREVIATIONS

°C	Degree Celsius
µ	Micron
µg	Microgram
µL	Microlitre
µM	Micromolar
3-MA	3-methyladenine
4-HT	4-hydroxytamoxifen
AE	Anti-estrogen
AI	Aromatase inhibitors
AIF	Apoptosis-inducing factor
AiP	Apoptosis induced proliferation
ALL	Acute lymphocytic leukemia
AML	Acute myeloid leukemia
ANOVA	Analysis of variance
AP-1	Activator protein 1
APAF1	Apoptotic protease activating factor 1
ATF-2	Activating transcription factor 2
ATG	Autophagy-related
ATM	Ataxia telangiectasia mutated

ATR	Ataxia telangiectasia and Rad3-related protein
BAD	BCL-2-associated death promoter
Baf A1	Bafilomycin A1
BAK	BCL2-antagonist/killer 1
BAX	BCL2 associated x
BC	Breast cancer
BCA	Bicinchoninic acid
BCL-2	B-cell lymphoma 2
BCL-XL	B-cell lymphoma-extra large
BH	BCL-2 homology
BID	BH3 interacting domain death agonist
BIK	BCL-2 interacting killer
BIM	BCL-2 interacting mediator of cell death
BRCA1	Breast cancer associated 1
BRCA2	Breast cancer associated 2
$CaCl_2$	Calcium dichloride
CAD	Caspase-activated DNase
CARD	Caspase recruitment domain
CBP/p300	CREB-binding protein
CCND1	Cyclin D1
CCNE1	Cyclin E1

CD	Cluster of differentiation
cDNA	Complementary DNA
Ced-3	Cell death protein 3
Ced-4	Cell death protein 4
ChIP	Chromatin immunoprecipitation
CI	Confidence interval
CK14	Cytokeratin 14
CK17	Cytokeratin 17
CK18	Cytokeratin 18
CK2LK	Casein kinase 2 like kinase
CK5	Cytokeratin 5
CK8	Cytokeratin 8
COX2	Cyclooxygenase 2
CQ	Chloroquine
CSC	Cancer stem cell
CXCR4	C-x-c motif chemokine receptor 4
DAB	3,3'-diaminobenzidine tetrahydrochloride
DAPI	4′,6-diamidino-2-phenylindole
DDR	DNA damage response
DED	Death-effector domain
DFS	Disease-free survival

dH_2O	Distilled water
DISC	Death-inducing signaling complex
DKO	Double knockout
DMSO	Dimethyl sulfoxide
DNA	Deoxyribonucleic acid
DNA-PKcs	DNA-dependent protein kinase, catalytic subunit,
Dox	Doxycycline
DR	Death receptor
DR3	Death receptor 3
DR6	Death receptor 6
DSB	DNA double-strand break
dsDNA	Double-stranded DNA
E2	Estradiol
EBSS	Earl's balanced salt solution
ECL	Enhanced chemiluminescence
EDTA	Ethylenediaminetetraacetic acid
EGF	Epidermal growth factor
EGF	Epidermal growth factor
EMSA	Electrophoretic mobility shift assay
EMT	Epithelial to mesenchymal transition
EndoG	Endonuclease G

ER	Estrogen receptor
ER	Endoplasmic reticulum
ERBB3	Erb-b2 receptor tyrosine kinase 3
ERBB4	Erb-b2 receptor tyrosine kinase 4
ERE	Estrogen response elements
ERK1/2	Extracellular signal-regulated kinase 1/2
ERα	Estrogen receptor alpha
ERβ	Estrogen receptor beta
ETS	E26 transformation specific
EV	Empty vector
FADD	Fas-associated protein with death domain
FATE1	Fetal and adult testis-expressed 1
FBS	Fetal bovine serum
FCS	Fetal calf serum
FDA	Food and Drug Administration
FFPE	Formalin-fixed paraffin-embedded
FGF-2	Fibroblast growth factor
FGFR	Fibroblast growth factor receptor
FISH	Fluorescence in situ hybridization
FOXA1	Forkhead box A1
FOXO3A	Forkhead box O3

GAPDH	Glyceraldehyde 3-phosphate dehydrogenase
GATA3	GATA binding protein 3
GEO	Gene expression omnibus
GFP	Green fluorescent protein
GGH	Gamma-glutamyl hydrolase
GRP78	78-kDa glucose-regulated protein
GUS	Beta-glucuronidases
h	Hour
H2AX	Histone 2 AX
H_2O_2	Hydrogen peroxide
HCL	Hydrochloric acid
HCQ	Hydroxychloroquine
HDAC1	Histone deacetylase 1
HER2	Human epidermal growth factor receptor 2
HER3	Erb-b2 receptor tyrosine kinase 3
HF	High fidelity
HML	High mutational load
HR	Homologous *recombination*
HRP	Horseradish peroxidase
IB	Immunoblot
IF	Immunofluorescence

IGFIR	Insulin-like growth factor 1 receptor
IHC	Immunohistochemistry
IMS	Intermembrane space
INDEL	Insertion or deletion
INF-γ	Interferon-gamma
IR	Ionizing radiation
JNK	C-Jun N-terminal kinases
KCL	Potassium chloride
KH_2PO_4	Monopotassium phosphate
KM	Kaplan-Meier
LAPTMB4	Lysosome-associated transmembrane protein 4-beta
LC3	Light chain 3
LML	Low mutational load
LMP	Low melting point agarose
LTC	Long-term culture
MCL-1	Myeloid leukemia cell differentiation protein
MEF	Mouse embryonic fibroblasts
MFI	Mean fluorescence intensity
mg	Milligram
MHC-I	Major histocompatibility complex I
miRISC	miRNA RISC complex

MLC	Myosin light chains
mM	Millimolar
MOMP	Mitochondrial outer membrane permeabilization
mRNA	Messenger RNA
mTORC1	Mammalian target of rapamycin complex 1
MTT	3-(4,5-Dimethylthiazol-2-yl)-2,5-Diphenyltetrazolium Bromide
$Na_2HPO_4.7H_20$	Sodium monohydrogen phosphate heptahydrate
NAC	N-acetyl cysteine
NaCl	Sodium chloride
NAF1	Nutrient-deprivation autophagy factor-1
NaH_2PO_4	Monosodium dihydrogen orthophosphate
NaOH	Sodium hydroxide
NCoR	Nuclear receptor co-repressor 1
NDS	Normal donkey serum
NF-κB	Nuclear factor kappa-light-chain-enhancer of activated B cells
ng	Nanogram
NGS	Normal goat serum
NHEJ	Non-homologous end joining
nM	Nanomolar
NP-40	Igepal ca-630
NSCLC	Non-small-cell lung carcinoma

NSEP1	Nuclease sensitive element binding protein 1
OMM	Outer mitochondrial membrane
OS	Overall survival
PABPN1	Poly(a) binding protein nuclear 1
PARP	Poly ADP ribose polymerase
PAS	Phagophore assembly site
PBS	Phosphate-buffered saline
PCD	Programmed cell death
PCD-II	Type-II Programmed cell death
PCR	Polymerase chain reaction
PD-1	Programmed cell death protein 1
PD-L1	Programmed cell death protein 1 ligand
PE	Phosphatidylethanolamines
PFA	Paraformaldehyde
PGE2	Prostaglandin E2
PI3K	Phosphatidylinositol-4,5-bisphosphate 3-kinase
PIP2	Phosphatidylinositol 4,5-bisphosphate
PIP3	Phosphatidylinositol (3,4,5)-trisphosphate
PR	Progesterone receptor
PUMA	P53 upregulated modulator of apoptosis
qRT-PCR	Quantitative reverse transcription PCR

RIPA	Radioimmunoprecipitation assay
RISC	RNA-induced silencing complex
RNA	Ribonucleic acid
ROC	Receiver operator curve
ROCK1	Rho-associated protein kinase 1
ROS	Reactive oxygen species
RPLPO	Large ribosomal protein
RPMI	Roswell Park Memorial Institute medium
RS	Recurrence score
RT	Room temperature
RTK	Receptor tyrosine kinase
SD	Standard deviation
SDS	Sodium dodecyl sulfate
SDS-PAGE	Sodium dodecyl sulfate–polyacrylamide gel electrophoresis
SEM	Standard Error of Mean
SERD	Selective estrogen receptor degrader
SERM	Selective estrogen receptor modulators
SMAC	Second mitochondria-derived activator of caspases
SMART	Silencing mediator for retinoid and thyroid hormone receptors
ssDNA	Single-stranded DNA
Star-PAP	Star-poly(A) polymerase

STAT1	Signal transducer and activator of transcription 1
STS	Staurosporine
SWI/SNF	Switch/sucrose non-fermentable
TBHP	Tert-Butyl hydroperoxide
TBS	Tris-buffered saline
TBST	Tris-buffered saline- tween 20
TE	Tris-EDTA
TFRC	Transferrin receptor protein 1
TGF- β	Transforming growth factor beta 1
TM	Transmembrane
TMA	Tissue microarray
TNF	Tumor necrosis factor
TNFR-1	Tumor necrosis factor receptor 1
TRAIL	TNF-related apoptosis-inducing ligand
TRAILR1/2	TRAIL receptor 1/2
TX-100	Triton-X 100
UV	Ultraviolet
v/v	Volume/volume
VEGF	Vascular endothelial growth factor
w/v	Weight/volume
XBP1	X-box binding protein 1

Δ	Deletion

CHAPTER 1

INTRODUCTION

1.1 Worldwide burden of breast cancer

Breast cancer is a heterogeneous spectrum of diseases of global impact. Statistics gathered for 2012 indicate that breast cancer affected more than 1.5 million women worldwide, caused more than 500,000 deaths, and accounted for the highest number of cancer-associated mortalities in women (Ferlay et al., 2015) (Tables 1.1 and 1.2). The highest incidence rate is reported in North America, Australia/New Zealand, and Northern and Western Europe, while the lowest incidence rate is in Africa and Asia (ACS, 2016; Ferlay et al., 2015). Although many low-and-middle-income countries such as sub-Saharan Africa have lower incidence rates, mortality rates are higher due to inadequate availability of early detection methods and access to treatment (ACS, 2016; Ferlay et al., 2015). Thus, morbidity and mortality associated with breast cancer remain a significant health concern throughout the world either due to high prevalence rates or lack of healthcare availability.

Increased occurrence of breast cancer in developed countries has been attributed to a variety of factors. For instance, in the two decades following 1980, an increase in breast cancer incidence was observed in Western countries. This was attributed to increased early detection, and reproductive factors such as early onset of menstrual cycles, first pregnancy at a later age, late menopause, use of hormones in the form of oral contraceptives and hormone replacement therapy (Althuis et al., 2005; Ferlay et al., 2015). After the year 2000, due to the reduction of menopausal hormone therapy and reduced participation in the mammographic screening, the incidence rate has stabilized close to 130 women per every 100,000 people (ACS, 2016; Youlden et al., 2012). Many developed countries have implemented national programs for X-ray-based mammographic screening for early detection of breast cancer. Early detection increases the likelihood of treatment

Table 1.1 Top 10 cancers diagnosed worldwide (Ferlay et al., 2015)

Site	Cases
Breast	1,671,100
Colorectum	614,300
Lung, bronchus, and trachea	583,100
Cervix uteri	527,600
Stomach	320,300
Corpus uteri	319,600
Ovary	238,700
Thyroid	229,900
Liver	228,100
Non-Hodgkin's lymphoma	168, 100
All sites	6,657,500

Table 1.2 Top 10 cancers causing high mortality worldwide (Ferlay et al., 2015)

Site	Cases
Breast	521,900
Lung, bronchus, and trachea	491,200
Colorectum	320,300
Cervix uteri	265,700
Stomach	320,300
Liver	254,100
Pancreas	156,600
Ovary	151,900
Esophagus	119,000
Leukemia	114,200
All sites	3,548,200

success resulting in improved survival outcomes for patients. Thus, while incidence has stabilized in parts of the world, substantial global challenges ranging from screening to treatment accessibility remain for a great number of countries.

Breast cancer survivals have improved over the years, and investment in cancer treatment has increased. For instance, availability of high-quality healthcare in countries such as Canada, USA, Australia, Israel and many western European countries has led to >85% 5-year survivals whereas, in less developed countries, this rate remains close to 60% (Lauby-Secretan et al., 2015; Smith et al., 2016). In 2012, 6.2 million women worldwide survived breast cancer who were diagnosed in the preceding 5-years (ACS, 2016; Ferlay et al., 2015). Successful outcomes come with substantial personal or public financial costs. For instance, a recent study estimated that in European countries the average medical cost per patient was nearly $19,000 (Capri and Russo, 2017) a value that is not possible for less-developed nations. Therefore, disease-prevention, early diagnosis, and more effective therapy are of paramount importance to reduce incidence and treatment costs.

Many risk factors including genetic, environmental and lifestyle have been found to be associated with an increased risk of developing breast cancer (Subramani and Lakshmanaswamy, 2017). Family history and presence of breast cancer associated 1 (*BRCA1*) or breast cancer associated 2 (*BRCA2*) mutations, as well as reproductive factors described earlier are a few (ACS, 2016; Bradbury and Olopade, 2007; Colditz and Bohlke, 2014). [Note, in this thesis, human gene names are italicized (e.g., *BRACA1*) whereas protein names are capitalized (e.g., BRCA1)]. Additionally, lifestyle and environmental components such as alcohol consumption, lack of physical activity, obesity, smoking and exposure to radiation are also associated with a higher

chance of developing breast cancer (ACS, 2016; Bradbury and Olopade, 2007; Carter et al., 2015; Colditz and Bohlke, 2014; Ordonez-Mena et al., 2016). Thus, although these associative relationships are ascribed, the exact causative agents are not fully characterized. In recent years, there has been an explosion of investigations into breast cancer genomics and transcriptomics with one of the aims to find causes of breast cancer (Curtis, 2015; Ellis and Perou, 2013). This has confirmed that cancer is a genetic disease and mutations of tumor suppressor genes and/or amplification of proto-oncogenes drive carcinogenesis (Anthony J.F. Griffiths et al., 2015). Continued accumulation of mutations with age overwhelms the tumor-suppressing mechanisms, facilitating cancerous growth. However, how these genomic alterations arise is not completely clear. Furthermore, cancer has a propensity to evolve and become more aggressive when intercepted with therapy. Hence, understanding the pathways that drive tumor evolution would help in designing better treatment modalities that limit disease recurrence. This would eventually improve prognosis, reduce treatment costs and improve the quality of life.

One of the standard ways to assess tumor aggressiveness and the odds of treatment success is by utilizing biomarkers, which include hormone receptors such estrogen receptor (ER), progesterone receptor (PR) and human epithelial growth factor receptor 2 (HER2). Their presence predicts a good prognosis with specific treatment. Currently, the 5-years overall survivals (OS) remain stagnant at ~85%, reflecting ongoing gaps in the understanding of the disease. Hence, the identification of novel biomarkers in the context of tumor aggressiveness can bridge this gap.

1.2 Pathological subtypes of breast cancer

Classically, breast cancer is divided into three subtypes based on the presence or absence of estrogen receptor (ER), progesterone receptor (PR), human epidermal growth factor receptor 2

(HER2), and the level of proliferation marker Ki67. This is clinically determined by analysis of protein levels or gene copy number as determined by immunohistochemistry (IHC) or fluorescent *in situ* hybridization (FISH) of the tumors. Based on this, the tumors are classified as luminal (ER and/or PR positive), HER2-enriched or triple-negative (also referred to as basal-like) (Sorlie et al., 2001; Toss and Cristofanilli, 2015). Analysis of tumor gene expression patterns identified their origins with respect to the mammary gland (Perou et al., 2000). The luminal tumors showed elevated expression of many genes commonly expressed in the breast luminal cells, defined as the polarised cells forming the inner layer of the mammary gland ducts. The elevated genes included cytokeratins (*CK8* and *CK18*) and ER-responsive genes (*LIV1*, *CCND1*, *XBP1,*) (Malhotra et al., 2010; Yersal and Barutca, 2014). Subsequent studies showed that two subbranches of the luminal group called luminal A and luminal B could be assigned wherein patients with luminal A tumors had a better prognosis than the luminal B group (Hu et al., 2006). The HER2-enriched group expressed high levels of *HER2* oncogene usually with low levels of ER (Malhotra et al., 2010; Yersal and Barutca, 2014). Tumors in the triple-negative subtype displayed many characteristics of the breast basal epithelial cells (cells forming the outer layer of the mammary gland ducts) and were positive for basal specific cytokeratins (*CK5, CK14, CK17*) (Malhotra et al., 2010; Yersal and Barutca, 2014). This led to the existing classification of luminal A, luminal B, HER2-enriched, and basal-like determined based on ER/PR/HER2 testing and proliferation marker Ki67. This clinical identification primarily dictates therapy choice.

1.2.1 Luminal

The luminal group represents 75% of all breast cancers diagnosed, and the tumors show ER and/or PR positivity. Further classification is based on the expression of HER2 and the proliferation marker Ki67.

1.2.1.1 Luminal A

Approximately 50-60% of the breast cancers are of the luminal A subtype (Toss and Cristofanilli, 2015; Yersal and Barutca, 2014). They express luminal-specific cytokeratins CK8 and CK18 in addition to the ER-associated genes such as *LIV1*, *FOXA1*, *XBP1*, *GATA3*, *BCL2*, *ERB3* and *ERB4* (Perou et al., 2000; Sotiriou et al., 2003*)*. Luminal A tumors usually have low- histological grades, nuclear pleomorphism and mitotic indices (Yersal and Barutca, 2014). Metastasis is most commonly to the bones (58.5%), lungs (21.7%), liver (15.5%) and brain (4.3%) in that order (Wu et al., 2017). Treatment usually includes hormonal therapy and have excellent survival outcomes with rates of relapse that are the lowest of all subtypes (Guarneri and Conte, 2009; Kennecke et al., 2010).

1.2.1.2 Luminal B

15-20% of the breast cancers fall into the luminal B classification (Yersal and Barutca, 2014). They are ER and/or PR-positive, with high Ki67 index (>14% cells positive) and HER2 negative; or with any Ki67 index with HER2 positivity (Malhotra et al., 2010; Yersal and Barutca, 2014). Typically the tumors show a high histological grade and increased expression of proliferation-related genes such as *v-MYB*, *GGH*, *LAPTMB4*, *NSEP1* and *CCNE1* compared to the luminal A group (Creighton, 2012). Metastatic preference in this group shifts more toward liver (26.6%) compared to 15.5 % in luminal A (Wu et al., 2017). Treatment is usually more aggressive involving endocrine, anti-HER2 and/or chemotherapeutic agents depending on the disease

presentation (Yersal and Barutca, 2014). Survival outcomes are usually poorer compared to the luminal A group (Creighton, 2012).

1.2.2 HER2-enriched

15-20% of the breast cancer tumors are classified into this category, and are typically characterized by high expression of human epidermal growth factor receptor 2 (HER2), high-histologic, nuclear and mitotic grades (Yersal and Barutca, 2014). HER2 is a member of the membrane-embedded receptor tyrosine kinases (RTK) family encoded by the proto-oncogene *ERBB2*, which maps at the 17q21 chromosomal position (Moasser, 2007). The HER2 signaling pathway promotes cell growth and division. The primary effector ligands of these RTKs are the epidermal growth factors (EGFs) that bind to the extracellular domains and promote receptor dimerization. Furthermore, HER2 can be activated in a ligand-independent manner by the homo- or heterodimerization with human epidermal growth factor receptor 3 (HER3) when present at high levels (Ménard et al., 2003; Moasser, 2007; Yersal and Barutca, 2014). HER2 dimerization causes transphosphorylation of its intracellular domains leading to the activation of downstream signaling cascades such as mitogen-activated protein kinase (MAPK) and phosphoinositide 3-kinase (PI3K/AKT) pathways (Ménard et al., 2003; Moasser, 2007). This signaling axis activates transcription factors, which regulate genes involved in proliferation, survival, invasion, angiogenesis, and metastasis (Moasser, 2007). Thus, HER2 overexpression leads to constitutive proliferative signaling and contributes to tumor progression. Furthermore, p53 mutations are found in more than 50% of the cases, compared to an average of ~26% in the luminal group suggesting possible deregulation of the cell cycle, DNA repair and apoptotic pathways (Bertheau et al., 2013). Accordingly, HER2-enriched tumors tend to grow faster than the luminal subtypes with

a worse prognosis (Loibl and Gianni, 2017). Metastasis usually occurs in bones (34.5%), liver (31.7%), lungs (25.5%) and brain (8.3%) suggesting a shift towards liver and lung colonization compared to 15.5% and 21.7% respectively in the luminal A subtype (Wu et al., 2017). HER2 directed therapies such as monoclonal antibodies (e.g., trastuzumab, pertuzumab) or tyrosine kinase inhibitors (e.g., lapatinib) that intercept different steps of the HER2 signaling pathway are usually employed (Loibl and Gianni, 2017).

1.2.3 Basal-like/Triple negative

This subtype consists of about 8-37% of all breast cancers diagnosed (Yersal and Barutca, 2014). Tumors are typically characterized by poor gland formation, high- histologic, mitotic and nuclear grades and the presence of necrotic centers or fibrotic zones (Yersal and Barutca, 2014). They are referred to as basal-like because of their high expression of basal cytokeratin markers including CK5, CK14, CK17 and laminin (Perou et al., 2000; Sorlie et al., 2001). Since these tumors do not express ER, PR, and HER2, they are also referred to as triple-negative. Nearly 88% of basal-like tumors harbor p53 mutations, show genomic instability and repression of the retinoblastoma pathway (Bertheau et al., 2013). This type of tumors are very aggressive and metastasizes to bones (36.4%), lungs (32.1%), liver (22.4%) and brain (9.12%) (Wu et al., 2017). There is no targeted therapy available for this group and treatment usually involves cytotoxic chemotherapy sometimes with poly-ADP ribose polymerase (PARP) inhibitors in BRCA1 deficient tumors (Yersal and Barutca, 2014). Survival outcomes for basal-like breast cancers are the worst compared to all other subtypes (Foulkes et al., 2010).

1.2.4 Diagnosis and survival prediction using biomarkers

Biomarkers provide useful information about disease progression and highlight critical biological pathways. In recent years, in addition to the immuno-histological subtyping of breast cancer, multigene-panel based predictors of outcomes have been developed and are in various stages of testing/acceptance for clinical use. These tests estimate expression levels of various candidate genes by using complementary deoxyribonucleic acid (cDNA) oligonucleotide arrays or multiplex polymerase chain reaction (PCR) technologies. Most of these tests classify ER-negative tumors as a high-risk group, and hence, their real utility is in predicting prognosis and therapeutic outcomes in the ER-positive group. Some of the prominent tests that are in clinical use include Oncotype Dx, PAM50, and EndoPredict (Harris et al., 2016). For brevity, only the development and utility of Oncotype Dx is described in greater detail because it is the most accepted of all the genomic tests for clinical use (Harris et al., 2016).

Oncotype Dx is a qRT-PCR based assay utilizing multi-gene expression signature to predict patient survivals. It was developed in the context of a specific early-stage breast cancer characterized by ER-positive, HER2-negative, and axillary node-negative tumors (Paik et al., 2004). Patients diagnosed with this kind of cancer usually have an excellent prognosis (85% 5-years disease-free survival) with hormonal therapy (Paik et al., 2004). However, since 15% of the cases retain the risk of disease recurrence, many (up to 85%) patients who only need hormonal therapy are also treated with chemotherapy due to the non-availability of prediction tools (Paik et al., 2004). Oncotype Dx is aimed at segregating the low-risk patients who only need endocrine therapy from the high-risk group needing chemoendocrine therapy. This decreases overtreatment of the low-risk patients and provides the benefit of chemotherapy to the high-risk group.

Oncotype Dx utilizes an associative relationship between expression levels of 16 genes to predict the likelihood of recurrence. Based on a regression analysis of the predictor genes and mathematical modeling, a recurrence score (RS) ranging from 0-100 is calculated (Paik et al., 2004). A tri-partite categorization of the RS divides patients into low- (RS<11), intermediate- (RS 11-25) and high-risk (RS>25) groups for 10-years disease-free survivals (DFS) (Sparano et al., 2018). According to the latest prospective clinical trial called TAILORx, low- and intermediate-risk groups only need to be treated with endocrine therapy whereas the high-risk group would benefit from chemoendocrine therapy. Thus, Oncotype Dx serves as a gene expression-based pre-treatment diagnostic tool in directing treatment modalities to ER-positive node negative subtypes.

Although clinically useful, Oncotype Dx is limited in its scope due to its applicability in a very restricted group of ER-positive breast cancer patients. As well, all tests are performed at a centralized laboratory of the developer (Genomic Health, Inc.), making its universal implementation challenging. Furthermore, each test costs ~$4500, compared to ~$100 for ER/PR testing using IHC. Thus, although Oncotype Dx is increasingly being used to make therapeutic decisions, there is still a need to identify biomarkers that would cover a larger group of patients at a lower cost.

1.2.5 Management of breast cancer

Breast cancer treatment involves treating the primary as well as the metastatic disease. The type of treatment is decided based on the size, stage, grade, and the intrinsic subtype of the tumor. In most cases, the primary tumor is first excised by surgery, followed by adjuvant therapy to eliminate residual cancer cells. Adjuvant therapy broadly falls into three classes named chemo-,

anti-HER2- and endocrine therapies depending on the therapeutic agents used. Chemotherapy selectively targets fast proliferating cancer cells by inflicting DNA damage or by causing cytoskeletal distress using compounds such as doxorubicin (topoisomerase II inhibitor), cyclophosphamide (DNA crosslinker), and taxanes (microtubule depolymerization inhibitor) (Ades et al., 2017). This type of therapy is most commonly used to treat basal-like cancer or other subtypes if distant metastasis is discovered (Ades et al., 2017). Anti-HER2 therapy is used to intercept proliferative signaling in HER2 enriched breast cancers. Monoclonal antibodies such as trastuzumab and pertuzumab, or drugs such as lapatinib block HER2-dependent growth signaling and are used alone or in combination with chemotherapy (Masoud and Pagès, 2017). The endocrine therapy uses drugs that target estrogen and/or progesterone receptor signaling and is used to treat luminal A and B subtypes (Ades et al., 2017; Masoud and Pagès, 2017).

1.2.5.1 Endocrine therapy of ER-positive breast cancer and its limitations

Estrogen, also referred to as 17 β-estradiol (E2) is a steroid sex hormone required for normal female sexual development. It also pathologically fuels ER- and PR-positive breast cancers. E2 binds and activates nuclear estrogen receptor α and β (ERα and ERβ) wherein ERα is the predominant effector in the context of breast cancer (Katzenellenbogen et al., 2018; Marino et al., 2006; McDonnell and Norris, 2002; Tremont, 2017). The major effects of estrogen signaling are mediated through E2: ERα interactions that stimulate cellular proliferation by transcriptional modulation (Musgrove and Sutherland, 2009). E2 binding promotes ERα dimerization followed by nuclear translocation and interaction with co-activators to stimulate transcription (Katzenellenbogen et al., 2018). E2: ERα complex can directly associate with DNA at the estrogen response elements (EREs), which are consensus palindromic sequences located in the

promoter/enhancer regions of the E2 responsive genes (Marino et al., 2006; Nicholson and Johnston, 2005; Ponglikitmongkol et al., 1988). Indirect association of E2: ERα with DNA also occurs and is mediated through DNA binding transcription factors such as SP-1, AP-1, and ATF-2/c-Jun at the non-ERE sites (Gaub et al., 1990; Marino et al., 2006; O'Lone et al., 2004). Both in the direct and indirect modes, E2: ERα does not act as the direct transcriptional controller and needs to partner with co-activator complexes such as CBP/p300 and SWI/SNF that facilitate chromatin remodeling to initiate transcription (Marino et al., 2006; Nicholson and Johnston, 2005; Smith and O'Malley, 2004). E2 responsive genes include critical cell cycle regulators and angiogenesis promoters such as cyclin D1 (activates G1 to S transition), cyclin E1 and E2 (facilitates S phase progression), and vascular endothelial growth factor (VEGF*)* (stimulates new blood vessel formation) (Marino et al., 2006; Musgrove and Sutherland, 2009). Furthermore, transcription factors such as c-MYC and c-FOS*,* which are involved in cellular growth and proliferation are also upregulated by E2 stimulation (Musgrove and Sutherland, 2009; Niu et al., 2015; Sabbah et al., 1999; Wang et al., 2011; Weisz and Rosales, 1990). Thus, constant estrogenic signaling in ER-positive cancer cells drives their growth and proliferation. This makes estrogen and ER the targets for hormonal therapy of ER-positive breast cancers.

Hormonal therapy was first conceptualized as the surgical removal of the ovaries in 1896 to deplete estrogen production (Nicholson and Johnston, 2005). Modern-day hormonal therapies mainly utilize three approaches to block E2: ERα signaling. Firstly, by decreasing estrogen availability using aromatase inhibitors (AIs) such as anastrozole, letrozole, and exemestane (Jiang, 2013). These compounds block aromatase enzymes that produce estrogen in peripheral sites such as adipose tissues to reduce the amount of circulating estrogen in post-menopausal women.

Secondly, by inhibiting the E2: ERα interactions using selective ER modulators (SERMs) such as tamoxifen. Binding of tamoxifen with ERα blocks its co-activator binding surface (Katzenellenbogen et al., 2018; Tanenbaum et al., 1998). This prevents co-activator association, effectively inhibiting the transcription of the E2-responsive growth and proliferation genes. Thirdly, by degrading the ER using selective ER downregulators (SERDs) such as fulvestrant. SERDs are steroidal mimics that engage ER with a higher affinity than E2 and promote dissociation of the E2: ER dimers (Jiang, 2013; Katzenellenbogen et al., 2018). Crucially, fulvestrant: ERα monomers do not translocate to the nucleus and are unstable, which results in accelerated ER degradation and diminished E2 signaling (Osborne et al., 2004). In general, anti-estrogens (AE) exert their anti-cancer effects by blocking cell proliferation and/or by inducing apoptosis. When cultured cells are treated with AEs, E2: ERα signaling is blocked leading to rapid decreases in the expression of proliferation factors (e.g., MYC and cyclin D1), causing cell-cycle arrest (Musgrove and Sutherland, 2009). Also, estrogen deprivation or AI treatment induces apoptosis, which occurs through the transcriptional upregulation of pro-apoptotic protein BIK that induce caspase activation (Hur et al., 2004; Viedma-Rodriguez et al., 2015). Downregulation of BIK leads to tamoxifen resistance in cultured cells highlighting its importance in the effectiveness of tamoxifen treatment (Viedma-Rodriguez et al., 2013). In addition to BIK, stress-activated kinases such as Jun N-terminal kinase (JNK) and p38 MAPK, as well as the activation of intracellular second messenger ceramide drive apoptosis (Musgrove and Sutherland, 2009). Combined effects of these two mechanisms halt tumor progression. Altogether, endocrine therapy remains the mainstay of ER-positive breast cancers and has brought 85-95% 5-year disease-free survival rates,

signifying its importance in the breast cancer treatment (Davies et al., 2013; Smith et al., 2017; Tremont, 2017).

While endocrine therapy has greatly reduced recurrence rates and mortality, it retains significant shortcomings including the risk of developing cancer at other sites, reduced sexual function and the development of treatment resistance. Tamoxifen, in addition to being an ER antagonist, also acts as an ER agonist in the uterus, liver, and bones (Marino et al., 2006; Musgrove and Sutherland, 2009; Nicholson and Johnston, 2005). This is associated with increased rates of endometrial cancer and uterine sarcoma (Bergman et al., 2000; Wickerham et al., 2002). As well, breast cancer recurrence despite tamoxifen treatment is a major clinical problem wherein one-third of the women treated with tamoxifen for five years are estimated to suffer disease relapse within 15 years (Musgrove and Sutherland, 2009).

Depending on when during the treatment resistance is encountered, it is classified as *de novo* or acquired. *De novo* resistance exists from the start of the therapy, and the underlying mechanisms are not well understood but some reports suggest that a high degree of promiscuous signaling with other growth receptors (e.g., HER2, IGFIR, FGFR, etc.) compensate for the loss of E2 signaling, rendering the E2: ERα targeted therapy ineffective (Ali et al., 2016; Musgrove and Sutherland, 2009). Acquired resistance, on the contrary, occurs upon a prolonged exposure to anti-estrogens. This could result from the loss of ER, inappropriate activation of growth factor signaling and mutations of the estrogen receptor that subvert anti-estrogen effects (Ali et al., 2016; Musgrove and Sutherland, 2009). Recent studies have elucidated a clinically relevant mechanism of acquired resistance, which involves activating mutations in the ER signaling pathway. Analysis of the circulating tumor DNA and deep sequencing of the tumors have identified activating

mutations in the ER-coding gene *ESR1* in 11-40% of relapsed patients who had previously been treated with endocrine therapy (Chu et al., 2016; Li et al., 2013). These activating mutations enable ERα to pre-fold into the agonist conformation without a ligand (Katzenellenbogen et al., 2018; Li et al., 2013). Clones harboring these mutations would no longer need estrogen for ER-dependent signaling, conferring AI and tamoxifen resistance. Whether these mutations pre-exist in certain clones or are acquired after therapy is not clear. Further investigations that focus on the effect of therapy on tumor evolution will likely answer these questions.

1.3 Apoptosis

Apoptosis is a type of programmed cell death (PCD) whereby multicellular organisms remove unwanted or aberrant cells by a genetically encoded cellular suicide sequence in response to signals originating from within or outside the cell. Naturally occurring cell death was described more than 150 years ago although a detailed characterization took place in the mid 20th century (Fuchs and Steller, 2011; Yang and Goping, 2013). Ultrastructural studies carried out in the 1970s demonstrated that cells dying under physiological conditions display distinct morphological features as opposed to the cells dying because of excessive stress causing swelling and rupture, known as necrosis (Fuchs and Steller, 2011; Kerr et al., 1972). Hallmark features of apoptosis include chromatin condensation, membrane blebbing, cytoplasmic shrinkage among others, and the cells displaying these features are rapidly cleared by other cells (Fuchs and Steller, 2011). Kerr and colleagues coined the term Apoptosis (falling of leaves from trees) for this type of cell death (Kerr et al., 1972). The next advancement in apoptotic research came from genetic studies performed in *C. elegans,* which demonstrated the effects of individual mutations on the programmed cell death pathway and elucidated that apoptosis was a genetically controlled

program with individual genes acting to execute the cascade (Fuchs and Steller, 2011). Molecular characterization of the gene products identified an evolutionarily conserved cell death machinery centered around executioner molecules termed caspases, which are a family of cysteine proteases.

Studies of apoptosis using the three model systems of the nematode *C. elegans*, the fruit fly *D. melanogaster* and mice have contributed significantly to the present day understanding of the apoptotic pathway (Fuchs and Steller, 2011). The end goal in all three systems is to activate proteases called caspases responsible for cellular dismantling. Individual players in the *C. elegans* apoptotic pathway were identified through lineage tracking experiments. The *C. elegans* embryo produces precisely 1090 cells, of which 131 undergo PCD during development (Sulston and Horvitz, 1977; Sulston et al., 1983). Loss of function mutants of *C. elegans* genes egl-1, ced-3, and ced-4 do not undergo apoptosis, and the 131 cells persist in the adult worm, whereas the loss of function mutation in ced-9 results in aberrant cell death and is developmentally lethal (Ellis and Horvitz, 1986; Ellis et al., 1991). These findings suggested that some genes promoted apoptotic induction whereas other inhibited it. This work that established *C. elegans* as a model organism, identified cell lineages during development and characterized cell death mutants was awarded a Nobel prize in Physiology or Medicine to Sydney Brenner, John Sulston and Robert Horowitz in 2002 (NobelPrize.org, 2018). In vertebrates, PCD during and after development plays critical roles in the maintenance of tissue homeostasis. Classic examples such as the creation of separated toes by interdigital tissue removal, and regression of the mammary glands after weaning illustrate the role of PCD in organ sculpting (Lindsten and Thompson, 2006; Quarrie et al., 1996). As well, apoptosis maintains the required number of cells during an animal's lifetime. Examples such as

the elimination of 80% of the oocytes in females prior to birth and the death of nearly 50% of neurons in the central nervous system during development illustrate this role (Barres and Raff, 1999; Reynaud and Driancourt, 2000). Furthermore, apoptosis acts as a stringent quality control mechanism by culling potentially dangerous cells from tissues as exemplified by the positive and negative selection of T and B cells to eliminate self-reactive clones posing a risk of autoimmunity (Opferman and Korsmeyer, 2003). Thus, apoptosis works hand in hand with cellular proliferation, differentiation and tissue remodeling but also acts as an eraser to correct mistakes made during growth and development. Due to this intricate role, defects in the apoptotic mechanisms are associated with a variety of pathological states such as neurodegenerative diseases (e.g., Alzheimer's, Parkinson and Huntington's diseases) and cancer (Okouchi et al., 2007). Thus, a properly functioning apoptotic program is crucial for the optimum fitness of animals including humans.

1.3.1 Execution of apoptosis by caspases

A defined sequence of events mediates apoptosis. The activation of caspases directly or indirectly orchestrates morphological features of apoptosis and cellular dismantling. Caspases are a family of cysteine proteases comprising of 13 members, which are synthesized as zymogens and activated in response to death stimuli by cleavage at specific aspartic acid residues (Li and Yuan, 2008; Nagata, 2018). Caspases are endo-proteases made up of three domains including, an N-terminal prodomain, which inhibits the enzyme activity, a large subunit (~20 kDa) and a small subunit (~10 kDa) (Li and Yuan, 2008; McIlwain et al., 2013). Upon activation of the apoptotic program, the first cleavage occurs between the large and small subunits and the second one occurs

between the prodomain and large subunits, in turn removing the inhibitory prodomain and separating the small and large subunits (Li and Yuan, 2008; McIlwain et al., 2013). Finally, the active caspase molecule is assembled as a heterodimer formed by a small and a large subunit. Each caspase requires the presence of a specific (yet diverse) four amino acid recognition motif (xxxD) in its substrate peptide (Earnshaw et al., 1999; Li and Yuan, 2008; McIlwain et al., 2013). Differences in the recognition motif are responsible for the preference of specific substrate proteins, which confers functional diversity to distinct caspase family members.

Caspases are divided into two groups namely initiator and executioner caspases based on their function, structure of the precursor forms and the order of activation. Initiator caspases (caspase-2, -8, and -9) have prodomains that consist of either a death effector domain (DED) or a caspase activation and recruitment domain (CARD) (Earnshaw et al., 1999; Li and Yuan, 2008; McIlwain et al., 2013). These domains allow initiator caspases to engage in protein-protein interactions with upstream adaptor molecules that trigger their activation. Subsequently, activated initiator caspases proteolytically cleave and activate executioner caspases (caspase-3, -6 and -7) (Earnshaw et al., 1999; Li and Yuan, 2008; McIlwain et al., 2013). These proteases dismantle the cellular infrastructure by large-scale proteolysis. Caspase-mediated cleavage of proteins result in the morphological features of apoptosis by one of the following means: (i) by destroying the activity of proteins (ii) by promoting activity through the removal of inhibitory domains (iii) converting a protein into its dominant negative form and (iv) by cleaving proteins with no apparent consequences (Green, 2010).

Activated caspase-3 and -7 bring about the morphological changes of apoptosis by cleaving a variety of downstream targets. As examples, caspase-dependent activation of kinases such as Rho-associated protein kinase 1 (ROCK1) promotes increased phosphorylation of myosin light chains (MLC), which causes membrane blebbing (Coleman et al., 2001; Sebbagh et al., 2001). As well, the direct destruction of cytoskeletal constituents such as actin, tubulin, and vimentin lead to loss of typical cellular morphology resulting in the rounded appearance of apoptotic cells (Ndozangue-Touriguine et al., 2008; Taylor et al., 2008). Furthermore, caspase-mediated destruction of the matrix focal adhesion sites detaches cells from the extracellular matrix (Levkau et al., 1998; Sasaki et al., 2002). Final stages of the destruction include fragmentation of the genomic DNA. This occurs through either caspase-independent DNases such as endonuclease G (EndoG) and apoptosis-inducing factor (AIF) or by caspase-dependent DNase (CAD) (Samejima and Earnshaw, 2005). This produces the characteristic agarose gel ladder appearance of the fragmented DNA (Nagata, 2000; Zhang and Xu, 2000).

CAD also called DNA fragmentation factor 40 (DFF40), was discovered through *in vitro* studies that showed that healthy nuclei underwent DNA fragmentation upon combined addition of recombinant activated caspase-3 and cytoplasmic extract of HeLa cells but not when either component were added alone (Liu et al., 1997). This meant that there was a "DNA fragmentation factor" in the cytoplasm that was activated by caspase-3. This observation led to the purification of CAD/DFF40, which was found to form a heterodimer with another subunit called the Inhibitor of caspase-activated DNAse (ICAD/DFF45) (Liu et al., 1997) (Figure 1.1). During translation of the *CAD* mRNA, ICAD serves as a chaperone that mediates cotranslational folding of the nascent CAD peptide (Figure 1.1) (Enari et al., 1998; Sakahira et al., 2000; Samejima and Earnshaw, 2005). As

well, in healthy cells, after the folding is complete, ICAD remains associated with CAD and blocks its nuclease activity (Sakahira et al., 2000; Samejima and Earnshaw, 2005). The subcellular localization of CAD: ICAD complex is controversial since some reports suggest nuclear whereas others suggest cytoplasmic localization (Enari et al., 1998; Liu et al., 1998; Samejima and Earnshaw, 1998, 2005). With the onset of apoptosis, activated caspase-3 and caspase-7 cleave ICAD, which allow CAD homodimerization through the N-terminal CIDE domains, promoting its activation (Figure 1.1) (Larsen and Sorensen, 2017). CAD explicitly targets double-stranded DNA (dsDNA) but not single-stranded DNA (ssDNA) or RNA (Widlak and Garrard, 2005; Widlak et al., 2000a). CAD homodimers form a unique scissors-like structure distinct from any other nuclease and assemble at the inter-nucleosomal positions with two active site facing the DNA strands (Samejima and Earnshaw, 2005; Woo et al., 2004). Coordinated nucleophilic attacks from both active sites induce a double-strand break (DSB), either leaving a blunt-end cut or a 1-base overhang with 5'P or 3'OH ends (Larsen and Sorensen, 2017; Widlak et al., 2000b; Woo et al., 2004). Although CAD non-selectively cleaves any inter-nucleosome sequence, it exhibits a slight preference towards purines (Rs) and pyrimidines (Ys) that show rotational symmetry (5'-R-R-R-Y-R-Y-Y-Y-3') (Widlak et al., 2000a). CAD is a crucial apoptotic nuclease, since cells derived from *CAD* knockout mice or cells with non-activable CAD are severely compromised in their ability to fragment DNA (McIlroy et al., 2000; Zhang et al., 1998). Thus, during apoptosis caspase-dependent DNA fragmentation heavily relies on CAD. Based on whether caspase activation takes place due to external stimulation or cell-intrinsic factors, two major pathways of caspase activation have been described (Figure 1.2).

1.3.1.1 Extrinsic pathway of caspase activation

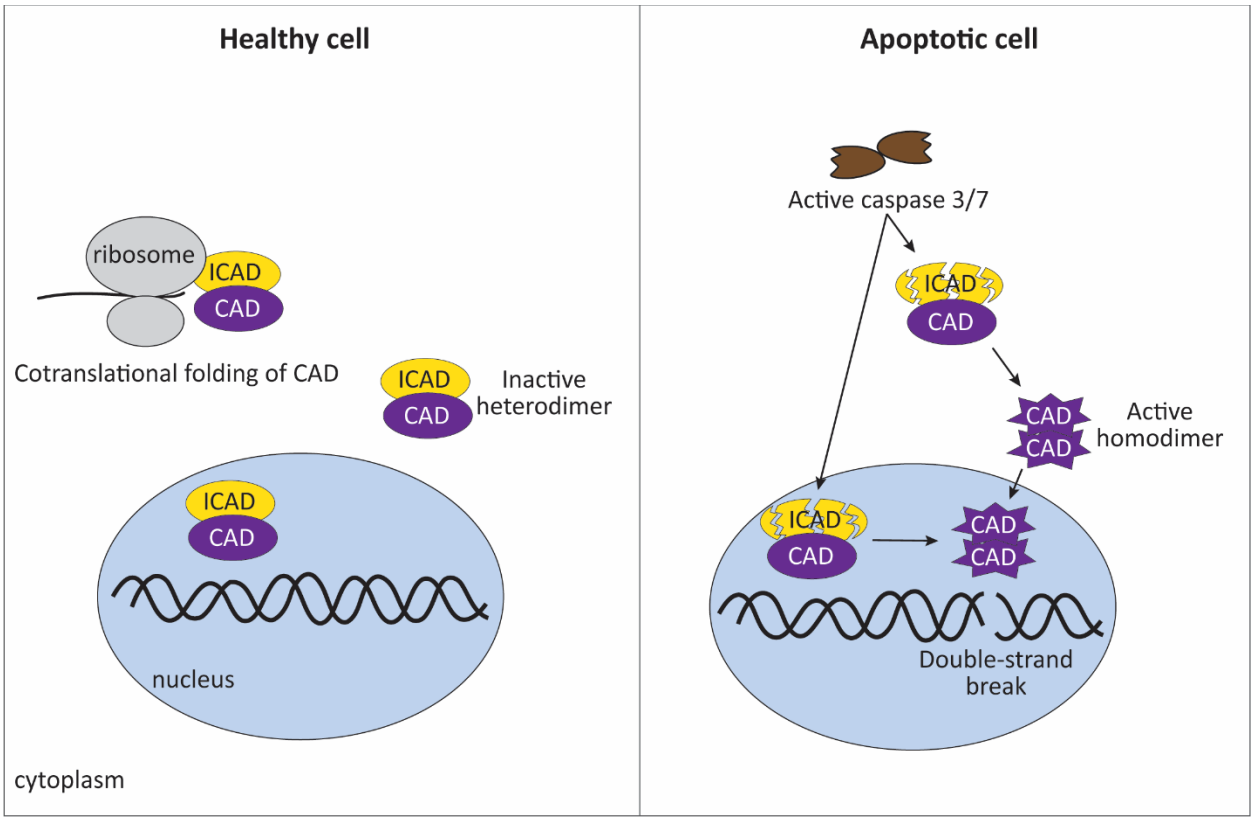

Figure 1.1 Caspase-activated DNAse (CAD) and nuclear fragmentation. Left: Inhibitor of CAD (ICAD), assists in the cotranslational folding of CAD and forms inactive heterodimers with it that localize in the cytoplasm and/or nucleus. Right: Upon apoptotic induction executioner caspases are activated, which cleave ICAD, in turn allowing CAD homodimerization and activation. CAD dimers induce DNA fragmentation by cleaving inter-nucleosomal DNA.

This pathway is initiated when specific ligands bind to receptors (referred to as death receptors) located on the surface of the cells as trimers. The death receptors belong to the tumor necrosis factor (TNF) superfamily and include FAS/CD95, TNFR-1, TRAILR1/2, DR3, and DR6 (Nagata, 2018; Taylor et al., 2008). The ligands that activate these receptors are closely related molecules and include TNF, FAS-L, and TRAIL. How ligand binding to death receptors triggers caspase activation is described here with the example of FAS-L: CD95 interaction. Death receptors contain a protein interaction domain called the death domain (DD) on their cytoplasmic tail. Binding of FAS-L to the CD95 stimulates the recruitment of the adaptor protein FAS-associated via death domain (FADD) through a DD-DD interaction (Figure 1.2) (Green, 2010; Nagata, 2018; Taylor et al., 2008). This interaction facilitates exposure of another interaction domain of the FADD called the death effector domain (DED), which allows association of death receptors with procaspase-8, in turn forming what is referred to as a death-inducing signaling complex (DISC) (Figure 1.2). In the DISC, dimerization of procaspase-8 stimulates its autocatalytic processing and activation. Activated caspase-8 can subsequently cleave executioner caspases such as caspase-3 and -7 leading to full-fledged apoptosis (Figure 1.2) (Green, 2010; Nagata, 2018). In certain cell types, caspase-8 activation alone is not sufficient and requires proteolytic processing of the pro-apoptotic B-cell lymphoma 2 (BCL-2) family member BH3 domain-interacting death agonist (BID) (Figure 1.2) (BID will be discussed in more detail in section 1.4.3), which triggers the mitochondria-mediated intrinsic pathway of apoptosis.

1.3.1.2 Intrinsic pathway of caspase activation

Cell-intrinsic stresses such as the loss of growth factor signaling, DNA damage, cytoskeletal disruption, accumulation of unfolded proteins and oxidative stress trigger this arm of apoptosis (Figure 1.2). The mitochondria play an essential role in the initiation of this pathway. It ensues with the permeabilization of the outer mitochondrial membrane (OMM), which releases the inter-membrane space (IMS) proteins such as cytochrome *c,* EndoG, apoptosis-inducing factor (AIF), and second mitochondria-derived activator of caspases (SMAC) into the cytosol (Figure 1.2) (Green, 2010; Taylor et al., 2008). This process is called mitochondrial outer membrane permeabilization (MOMP). Cytosolic cytochrome *c* interacts with an adaptor protein called the apoptotic protease activating factor 1 (APAF1) through the WD domain and promotes assembly of a wheel-shaped heptamer (Li and Yuan, 2008; McIlwain et al., 2013). This serves as a platform that promotes binding of caspase-9 through CARD, which in turn facilitates caspase-9 dimerization and activation (Li and Yuan, 2008; McIlwain et al., 2013). This complex containing APAF1, cytochrome *c,* and caspase-9 is called the apoptosome (Figure 1.2). Subsequently, activated caspase-9 proteolytically processes executioner caspases-3 and -7 leading to their activation (Li and Yuan, 2008; McIlwain et al., 2013). Thus, in the intrinsic pathway of apoptosis, death signals converge at the mitochondria, amplified in the cytoplasm and end with the activation of initiator caspases such as caspase-9. This arm of apoptosis is regulated by the BCL-2 family of proteins.

1.4 BCL-2 family proteins and regulation of apoptosis

Investigation of the BCL-2 family of proteins began with the efforts to identify cancer-causing oncogenes. The t(14;18) chromosomal translocation is a cytogenetic abnormality observed in approximately 85% of the follicular lymphomas and up to 30% of the diffuse cell lymphomas

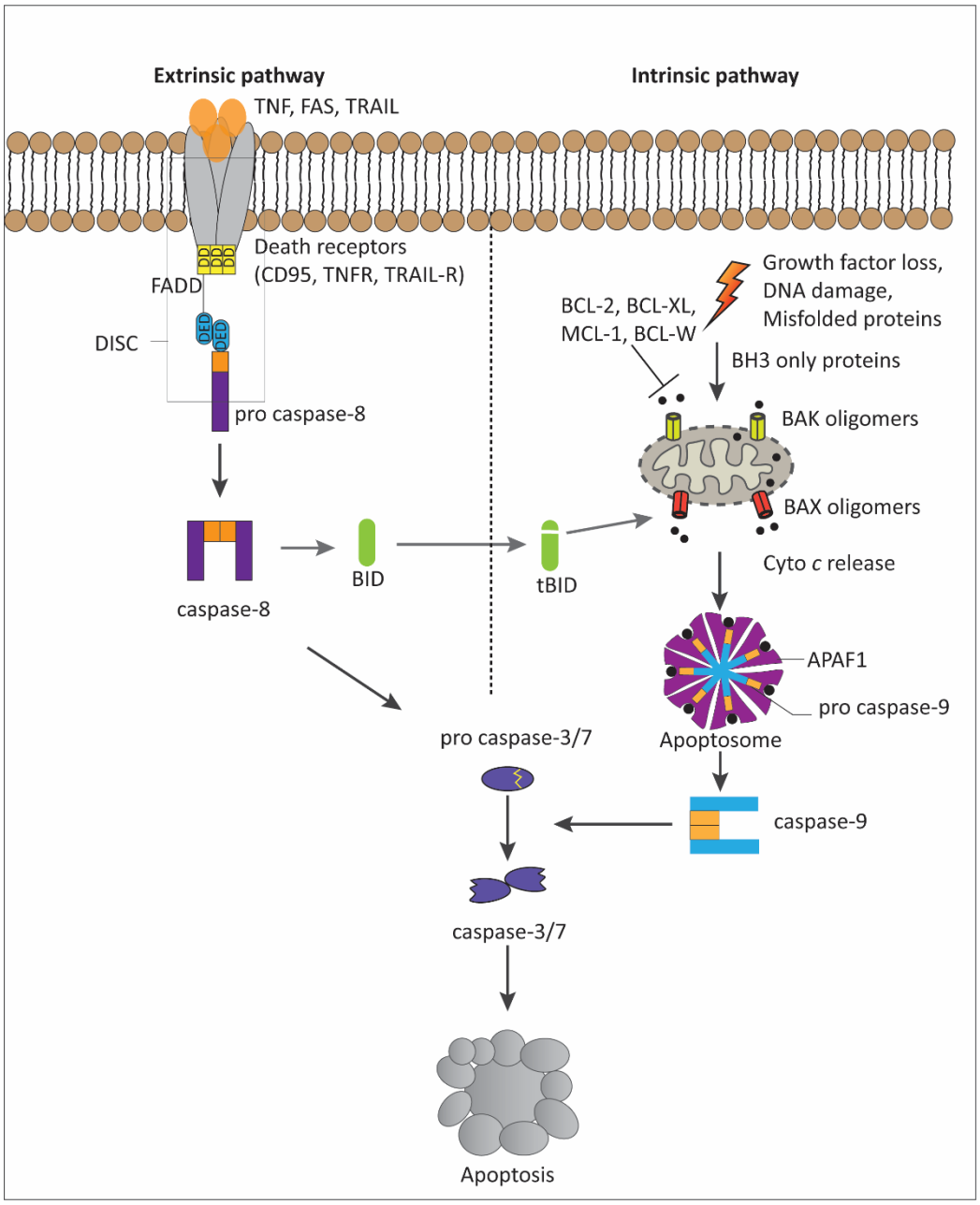

Figure 1.2 Overview of the extrinsic and intrinsic apoptotic pathways. Extrinsic apoptosis is induced upon extracellular ligand stimulation of the plasma membrane-localized death receptors, such as CD95. Activation of CD95 leads to the recruitment and activation of initiator caspase-8. Activated caspase-8, in turn, cleaves and activates caspase-3 causing apoptosis. BID cleavage by caspase-8 produces tBID, which in turn activates the intrinsic apoptotic pathway. Intrinsic apoptosis is initiated by cell-intrinsic stress, such as DNA damage or growth factor loss. These apoptotic stimuli activate BAK/BAX resulting in MOMP and the effusion of apoptotic factors such as cytochrome *c*. This pathway is tightly regulated by the BCL-2 family proteins that comprise of anti- and pro-apoptotic proteins. When the balance is in favor of pro-apoptotic proteins, cytochrome *c* is released, which stimulates the formation of apoptosome leading to caspase-9 and caspase-3 activation. Anti-apoptotic proteins on the other hand, prevent MOMP.

(Rowley, 1982; Yunis, 1983). Investigations centered around this translocation led to the identification of the *BCL-2* gene. Two groups (Bakhshi et al., 1985; Tsujimoto et al., 1985) independently cloned the t(14;18) region in human follicular B-cell lymphomas and found that the *BCL-2* gene was located next to the immunoglobulin heavy chain locus resulting in the overexpression of the BCL-2 protein. Subsequent studies revealed that *BCL-2* was different from other oncogenes in the sense that it did not promote cellular proliferation. Instead, it prolonged the survival of the existing cells (McDonnell and Korsmeyer, 1991; Vaux et al., 1988). To date, more than 20 members of the BCL-2 family have been identified by their possession of the BCL-2 homology domains (BH) (Figure 1.3). Overall the BCL-2 family is divided into pro- and anti-apoptotic groups. The pro-apoptotic group is further subdivided into multidomain effector or BH3-only groups based on the number of BH domains present (Figure 1.3). Different members of the BCL-2 family work in concert to form a relay channel for the transmission of death signals at the mitochondria.

Protein-protein interactions between pro- and anti-apoptotic proteins ultimately tip the balance on the side of survival or death. Anti-apoptotic BCL-2 proteins all have a similar globular structure with the surface-exposed hydrophobic groove. This groove allows protein-protein interactions with pro-apoptotic multidomain or BH3-only proteins via a BH3 domain (Liu et al., 2003; Sattler et al., 1997). In the absence of death signaling, the anti-apoptotic proteins sequester the pro-apoptotic effectors BCL-2-associated X protein (BAX) or BCL-2 antagonist/killer 1 (BAK), which are are the downstream effectors of MOMP. When the death signaling is triggered, the pro-apoptotic BH3-only proteins activate BAK/BAX either through a direct interaction or indirectly by displacing them from the anti-apoptotic proteins

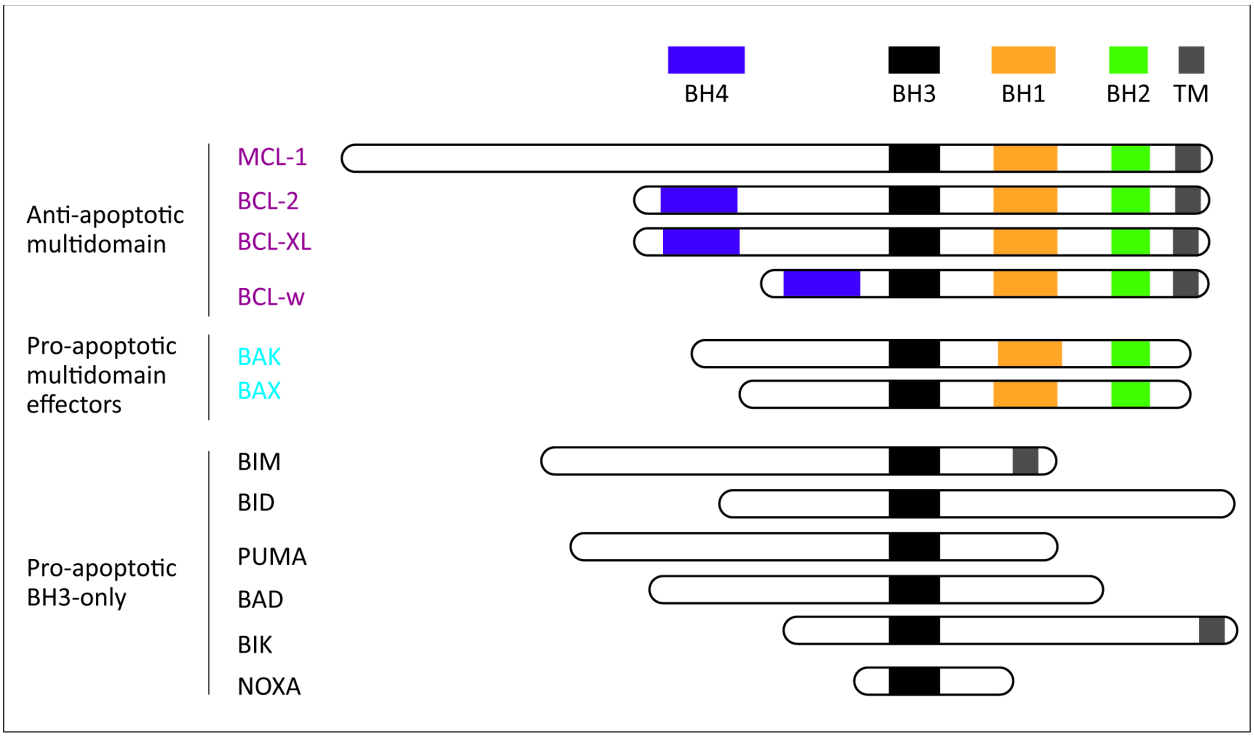

Figure 1.3 Overview of the BCL-2 family. The defining feature of all BCL-2 family proteins is the presence of at least one BH domain. The family is divided into pro- or anti-apoptotic groups that stimulate or inhibit apoptosis respectively. The pro-apoptotic proteins are subdivided into mitochondrial pore-forming effectors such as BAK/BAX, or BH3-only members (e.g., BIK, BIM, PUMA and NOXA) that directly or indirectly activate BAK/BAX. All pro-apoptotic effectors and anti-apoptotic proteins have more than one BH domains whereas the BH3-only proteins have just one BH domain. Some members of the family also contain a C-terminal transmembrane domain allowing their association with membranous structures.

(Adams and Cory, 2007a; Shamas-Din et al., 2013). The three subgroups of the BCL-2 family proteins are described here in more detail.

1.4.1 Multidomain pro-apoptotic effector proteins

BAK and BAX are the direct effectors of MOMP. Their role in apoptosis was identified through *in vitro* studies and subsequently confirmed using of BAK/BAX single and double knockout (DKO) mice. Loss of BAK had no phenotype whereas BAX deficiency produced lymphoid hyperplasia (Knudson et al., 1995). This relatively mild phenotype became more severe with the BAK/BAX DKO animals that died during the perinatal period and showed severe developmental defects such as the presence of interdigital webs, imperforate vaginal canals as well as cellular hyperplasia in the hematopoietic and central nervous systems (Lindsten et al., 2000). Furthermore, BAK/BAX DKO mouse embryonic fibroblasts (MEFs) were unable to undergo MOMP and showed a high degree of resistance to apoptotic stimuli (Zong et al., 2001). Thus, these studies highlighted a crucial yet overlapping role of BAK and BAX in the intrinsic apoptotic pathway.

Activated, BAK and BAX form homo-oligomers in the OMM in turn leading to MOMP. BAK in its monomeric form is usually tethered to the mitochondria via its C-terminal hydrophobic tail, and its activation is constitutively inhibited by anti-apoptotic BCL-2 like protein extra large (BCL-XL) and myeloid cell leukemia 1 (MCL-1) (Willis et al., 2005). Upon apoptotic stimulation, BH3-only proteins displace BAK from the anti-apoptotic proteins leading to its activation (Willis et al., 2005). In addition to the anti-apoptotic proteins, BAK activity in healthy cells has also been shown to be suppressed by binding to voltage-dependent anion-selective channel 1 (VDAC) (Kim et al., 2006). Direct binding of BH3-only proteins such as tBID, BIM or PUMA to BAK dissociates it from

VDAC and promotes its activation (Kim et al., 2006). Thus, BAK can be directly or indirectly activated by the BH3-only proteins.

The second pro-apoptotic effector BAX remains cytosolic in healthy cells and translocates to the mitochondria upon activation (Goping et al., 1998). BAX activation and mitochondrial anchoring require an exposed C-terminal tail (Gavathiotis et al., 2008). In the inactive state, this tail remains bound to a surface exposed hydrophobic groove and need to be dislodged for activation. Structural studies of BAX bound to a BH3 peptide of the BCL-2-interacting mediator of cell death (BIM) (BIM is discussed in more detail in section 1.4.3) demonstrated that BH3: BAX interaction induced a conformational change that released the C-terminal tail in turn promoting its mitochondrial insertion (Gavathiotis et al., 2008). Furthermore, similar to BAK, displacement of anti-apoptotic proteins from BAX by the BH3-only proteins also promotes its activation (Czabotar et al., 2014; Shamas-Din et al., 2011). Once activated, the BH3 domains of both BAK and BAX are exposed and interact with the adjacent BAK/BAX molecules through the surface hydrophobic groves (Dewson and Kluck, 2009). Homo-oligomers formed through this interaction create pores in the OMM, large enough to allow passage of molecules such as cytochrome *c* (Czabotar et al., 2014). Altogether, the direct or indirect activation of these multi-domain pro-apoptotic effectors results in the initiation of mitochondrial apoptosis.

1.4.2 Anti-apoptotic BCL-2 family proteins

The anti-apoptotic proteins maintain cellular health by inhibiting apoptosis. A total of 6 anti-apoptotic proteins are presently identified. Among those, BCL-2, BCL-XL, and MCL-1 are the prominent members due to their critical roles during embryonic development. These proteins act

as pro-survival factors, which was identified by gene knock out studies. BCL-2 deficient mice suffered polycystic kidney disease, hypopigmentation of hair and low numbers of circulating lymphocytes. This was attributed to the excessive cell death of the kidney and melanocyte progenitors and mature B and T lymphocytes (Veis et al., 1993). BCL-XL and MCL-1 deficient animals had a more severe phenotype. Loss of BCL-XL caused extensive apoptosis in premature hematopoietic and neuronal cells and was embryonically lethal whereas MCL-1 deficiency prevented embryo implantation (Motoyama et al., 1995; Rinkenberger et al., 2000). Furthermore, conditional knockout of MCL-1 showed excessive death in the lymphoid and hematopoietic lineages (Opferman et al., 2005; Opferman et al., 2003). Thus, these studies clearly highlighted a pro-survival role of anti-apoptotic members.

Anti-apoptotic proteins prohibit the activation of BAK/BAX and thus prevent MOMP. The solution structure of BCL-XL bound to the BH3 domain of BAK has been solved and has demonstrated a groove formed by BH1, BH2 and BH3 alpha helices (Sattler et al., 1997). This groove forms a hydrophobic pocket required for the binding of BAK/BAX (Sattler et al., 1997). Thus, in healthy cells, anti-apoptotic proteins keep BAK/BAX in an inactive state through an inhibitory interaction, which can be relieved by the BH3-only proteins discussed next.

1.4.3 BH3-only pro-apoptotic proteins

BH3-only proteins serve as the molecular sensors of distinct stress stimuli and act alone or in combination depending on the nature of the stress. Accordingly, deletions of any of the BH3-only members in mice were not embryonically lethal but showed apoptotic resistance when challenged with specific death triggers. As examples, BID deficient hepatocytes were impaired in

FAS stimulated apoptosis, but many of the *Bid*$^{-/-}$ cell lines underwent normal apoptosis in response to DNA damage or cell cycle arrest suggesting a prominent role of the BID in the extrinsic arm of apoptosis (Kaufmann et al., 2007; Yin et al., 1999). On the other hand, cell lines derived from p53 upregulated modulator of apoptosis (PUMA) and Noxa deficient mice were incompetent in undergoing DNA damage-induced apoptosis, highlighting their particular role in response to genotoxic insults (Jeffers et al., 2003; Villunger et al., 2003). Of all the BH-3 only knockouts, *Bim*$^{-/-}$ mice had the most severe phenotype of excessive accumulation of lymphoid and myeloid cells, which eventually led to a fatal autoimmune state resembling systemic lupus erythematosus (Bouillet et al., 1999). BIM deficient lymphocytes were resistant to cytokine deprivation, Ca^{2+} influx and microtubule distress but not to FAS ligand stimulated apoptosis (Bouillet et al., 1999). These observations highlighted that individual BH3-only members respond to specific death signals.

BH3-only members are positioned at the top of the intrinsic apoptotic program, and their job is to activate BAK/BAX. Individual BH3-only proteins differ in their capacity to bind other BCL-2 family members, which allows for another level of regulation. BH3-only proteins such as tBID and BIM can physically associate with BAK and BAX respectively and induce a conformational change promoting BAK/BAX oligomerization (Sarosiek et al., 2013a). Other BH3-only proteins (e.g., BIK, BAD, BMF, HRK) act as sensitizers (Adams and Cory, 2007b). In healthy cells, BAK/BAX remain sequestered by anti-apoptotic BCL-2 proteins. Sensitizer BH3-only proteins compete with BAK/BAX for binding to anti-apoptotic proteins, in turn displacing BAK/BAX for activation (Chipuk et al., 2010; Wu et al., 2018). Thus, in this case, sensitizer BH3-only proteins act as the

inhibitors of inhibitors. In the end, BAK/BAX activated by direct activation or sensitization induce MOMP.

Due to their death-promoting activity, BH3-only proteins are either not synthesized or are kept inactive in healthy cells until a death signal is encountered. This is achieved through a tight transcriptional and post-transcriptional control. Stress-activated transcription factors such as p53, FOXO3A, E2F-1, and NF-κB induce transcription of the BH3-only genes under specific stress signals (Lomonosova and Chinnadurai, 2008). As a specific example, the presence of growth factor signaling promotes Akt dependent phosphorylation of the transcription factor FOXO3A, facilitating its binding to 14-3-3 proteins and sequestration in the cytosol (Dijkers et al., 2000). When the growth factor signaling diminishes, FOXO3A is dephosphorylated, moves to the nucleus and stimulates *BIM* transcription (Dijkers et al., 2000; Lomonosova and Chinnadurai, 2008). A different stressor such as DNA damage promotes stabilization of p53 by halting its proteasomal degradation, which in turn stimulates *PUMA* and *NOXA* transcription (Lomonosova and Chinnadurai, 2008; Nakano and Vousden, 2001; Oda et al., 2000). Post-translational modifications serve as another mechanism to regulate the activity of BH3-only proteins. As examples, BID activation requires an N-terminal cleavage by proteases such as caspase-8, granzyme B, and calpain to presumably expose its BH3 domain and initiate the mitochondrial apoptotic program (Chen et al., 2001; Li et al., 1998; Sutton, 2000). Further, the pro-apoptotic activity of BCL-2-associated death promoter (BAD) is kept in check by its phosphorylation by Akt and RAF-1 kinases when growth factors are abundant (Datta et al., 1997; Ye et al., 2011). Phosphorylated BAD binds to 14-3-3 proteins and remains sequestered in the cytosol. Upon growth factor withdrawal, calcineurin mediated dephosphorylation promotes its mitochondrial translocation where it

sequesters BCL-XL to trigger apoptosis (Wang et al., 1999). Altogether, BH3-only proteins act as the key initiators of MOMP that propagate specific death signals through their interaction with other BCL-2 family members and are tightly regulated to ensure cellular fitness in the absence of death signaling.

1.5 BCL-2 interacting killer (BIK)– the founding member of BH3-only proteins

BCl-2 interacting killer (BIK) also known as Natural born killer (NBK), is a 160 amino acid long protein with a unique localization at the endoplasmic reticulum (*ER*)(Chinnadurai et al., 2008; Mathai et al., 2002). It was identified in a yeast two-hybrid screen as a candidate that interacted with cellular anti-apoptotic proteins BCL-2 and BCL-XL as well as viral survival proteins EBV-BHRF1 and E1B-19K (Boyd et al., 1995). Ectopic expression of BIK triggered cell death, which could be blocked by coexpression of BCL-2 and BCL-XL, which suggested its pro-apoptotic function (Boyd et al., 1995). The human *BIK* gene is located at the chromosome 22q13.3 locus spanning over a 19 kb region (Verma et al., 2000). Subsequent gene knockout studies performed in mice uncovered BIK's role in normal animal development. $Bik^{-/-}$ animals developed normally and did not show cellular hyperplasia in most of the tissues, unlike the $Bim^{-/-}$ mice that had lympho-myeloid hyperplasia (Coultas et al., 2004). As well, hematopoietic cells derived from $Bik^{-/-}$ mice were not protected from cytokine deprivation-induced apoptosis (Coultas et al., 2004). This lack of a notable phenotype suggested that BIK may either have overlapping roles with other BH3-only proteins or only respond to context-specific signals that preferentially funnel through BIK. A follow-up study investigated this possibility in *Bik/Bim* double knockout (DKO) mice (Coultas et al., 2005). While testes development is normal in individual $Bik^{-/-}$ and $Bim^{-/-}$ animals,

Bik/*Bim* DKO males were sterile due to impaired spermatogenesis. These animals had an excess of spermatocytes, but mature sperm was never produced. All the other characteristics of *Bik*/*Bim* DKO mice were identical to the $Bim^{-/-}$ mice, suggesting a tissue-specific overlapping role of BIK (Coultas et al., 2005). This phenotype could potentially result because both BIM and BIK activate the same MOMP effector, BAX (Gillissen et al., 2003; Gillissen et al., 2007; Sarosiek et al., 2013b). Hence, in this scenario, BAK dependent MOMP presumably remains functional, and apoptosis is not severely compromised. However, investigation of BIK deficiency combined with a deficiency of other BH3-only proteins that activate BAK (e.g., NOXA, tBID) may uncover novel phenotypes not observed with *Bik*/*Bim* DKO mice. Altogether, the BH3-only protein BIK localizes to the *ER*, interacts with pro-survival factors and plays a role with BIM in the mouse testicular development.

Functional dissection of BIK provided an insight into how it may exert its pro-apoptotic activity (Figure 1.4). Regions of BIK important for BCL-2 interaction and apoptotic induction were identified using a yeast two-hybrid system and co-immunoprecipitation (Co-IP) assays (Elangovan and Chinnadurai, 1997). It was discovered that a 52-amino acid (aa 43-94) region of BIK was sufficient for heterodimerization with BCL-2, which was further narrowed down to an 18-amino acid region (aa 57-74) encompassing the BH3 domain as evidenced by Co-IP experiments (Figure 1.4) (Elangovan and Chinnadurai, 1997). Deletion of as few as 5 amino acids in this region left the protein completely inactive (Elangovan and Chinnadurai, 1997). Thus the BH3 domain is critical for BIK pro-apoptotic activity. BIK also contains a C-terminal motif (aa 121-135) that is required for maximal apoptotic activity (Elangovan and Chinnadurai, 1997). As well, a transmembrane domain (TM) domain of BIK (aa 136-156) anchors it into the ER membrane, making it the only BH3-only protein localized at this organelle.

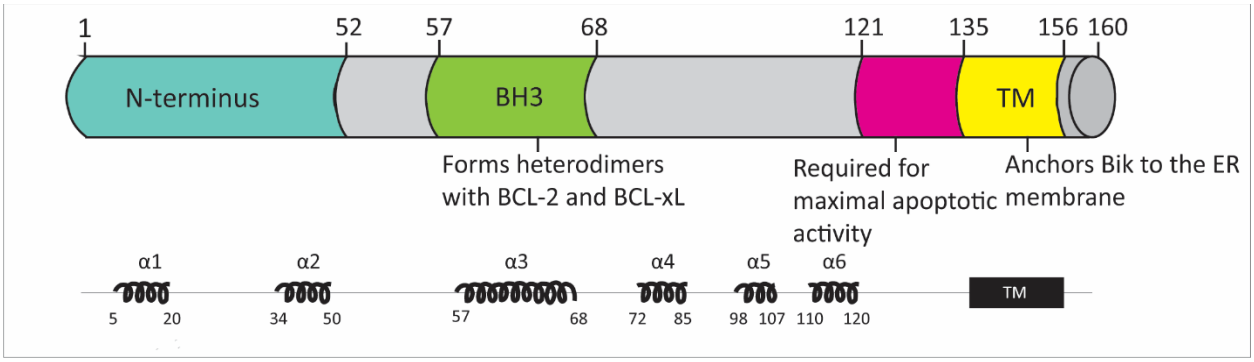

Figure 1.4 BIK domain structure. Top: Three functional domains of BIK have been identified. The BH3-domain is critical for the association with anti-apoptotic proteins and for apoptosis induction. The C-terminal motif is formed by amino acids 121 to 135, and although the exact function is not known, it is important for maximal BIK pro-apoptotic activity. The TM domain anchors BIK into the *ER* membrane and although not required for pro-apoptotic activity, is important for protein stability. Bottom: Based on computation modeling, BIK contains six alpha helices, making it the only structured protein in the BH3-only group.

Endoplasmic reticulum (*ER*) is a membrane-bound organelle in eukaryotic cells. Commonly known functions of the *ER* include protein folding and glycosylation, lipid metabolism, and Ca^{+2} homeostasis (Bravo-Sagua et al., 2013). Additionally, *ER* is the largest intracellular store of Ca^{+2} ions required for a multitude of functions such as regulation of muscle contraction, metabolism, protein folding, and apoptosis (Bravo-Sagua et al., 2013). Cancer cells often encounter excessive protein folding load causing accumulation of misfolded proteins (Bravo-Sagua et al., 2013; Clarke et al., 2014). This leads to ER-stress, which if unresolved, triggers apoptosis. As well, deregulated Ca^{+2} signaling can cause mitochondrial Ca^{+2} overload and trigger apoptosis (Bravo-Sagua et al., 2013; Clarke et al., 2014). Thus, although the intrinsic apoptotic pathway typically involves mitochondrial disruption, sensing of death stimuli originating from the *ER* is critical for an effective response. In healthy cells, most BH3-only proteins including BIM, BID and BAD exist away from the *ER*, and upon encountering a death stimulus, migrate to the mitochondria to activate BAK/BAX (Shamas-Din et al., 2011). BIK, on the other hand, resides at the *ER*, making it a strategically positioned BH3-only sensor for this organelle (Germain et al., 2005; Germain et al., 2002; Mathai, 2005; Mathai et al., 2002). Further, in addition to the mitochondrial outer membrane, anti-apoptotic BCL-2 proteins also localize at the ER where BIK can engage them (Heath-Engel et al., 2008). Thus, in scenarios where *ER*-specific homeostatic processes are perturbed, BIK may be critical in communicating these perturbations to the mitochondria.

1.5.1 Mechanisms of BIK induced cell death

BIK mediated cell death occurs by three distinct mechanisms in different cell types in a context-dependent manner (Figure 1.5).

1.5.1.1 By inhibition of anti-apoptotic proteins

BIK induces cell death through the canonical apoptotic pathway. Early studies demonstrated that ectopic BIK expression caused cytochrome *c* release and caspase activation leading to cell death, which was dependent on the BH3 domain of BIK (Germain et al., 2002; Tong et al., 2001). This suggested that BIK induced apoptotic cell death, however, the mechanism of mitochondrial perforation necessary for this process was unknown. BH3-only proteins can activate pro-apoptotic effectors BAK/BAX by direct physical interaction or indirectly by inhibiting the anti-apoptotic members such as BCL-2, BCL-XL, and MCL-1. BIK interacts with BCL-2 and BCL-XL but not with BAK or BAX, indicating an indirect activation mode (Boyd et al., 1995; Elangovan and Chinnadurai, 1997; Gillissen et al., 2003). Gillissen et al. elucidated that BAX was the sole effector of BIK induced cytochrome *c* release (Gillissen et al., 2003). These authors found that BIK expression triggered apoptosis in BAX proficient but BAK deficient cells whereas BAK proficient BAX deficient cells were protected. Further, BAX re-expression conferred sensitivity to BIK induced apoptosis indicating that BAK was dispensable for BIK mediated apoptosis.
BIK competes with BAX for BCL-2 and BCL-XL binding presumably leading to BAX dissociation and activation (Figure 1.5). The obvious question as to why BIK does not activate BAK was addressed in a subsequent study (Gillissen et al., 2007). While BAK is known to be sequestered by BCL-XL and MCL-1, Gillissen et al. found that BIK failed to break the MCL-1: BAK complex (Gillissen et al., 2007). This suggested that MCL-1 prohibited BAK activation, which was confirmed by MCL-1 silencing, which in fact led to BAK activation and apoptosis in BAX deficient cells (Gillissen et al., 2007). Why BIK could not activate BAK bound to BCL-XL was explained by the observation that BIK expression somehow upregulated MCL-1 levels in cells (Gillissen et al., 2007).

This excess MCL-1 may potentially sequester BAK released from BCL-XL and prevent its oligomerization. In conclusion, the inability of BIK to dissociate BAK: MCL-1 complex results in the selective activation of BAX bound to BCL-2 and BCL-XL. This is an excellent demonstration of the selective nature of the BH3-only proteins for specific anti-apoptotic members.

1.5.1.2 By mitochondrial Ca^{+2} overload

While protein-protein interactions between BCL-2 family members have been shown to regulate the mitochondrial pathway of apoptosis, Shore and colleagues demonstrated that the endoplasmic reticulum (*ER*) and mitochondrial fission machinery could also trigger cytochrome *c* release in BIK expressing cells (Germain et al., 2005; Mathai et al., 2005). These authors found that BIK expression in the presence of caspase inhibition promoted BAX localization and oligomerization at the *ER* that was associated with *ER* Ca^{+2} release (Mathai et al., 2005). Ectopic BIK expression in BAK/BAX DKO baby mouse kidney cells failed to trigger *ER* Ca^{+2} release, which confirmed that in this system BAK and BAX both played a role in calcium mobilization (Figure 1.5). Cytosolic Ca^{+2} can be taken up by the mitochondria, and the overload of Ca^{+2} in mitochondria can lead to apoptosis. Interestingly, ectopic or p53 stimulated BIK expression led to mitochondrial fragmentation and cytochrome *c* release, which could be prevented by pharmacological inhibition of the mitochondrial calcium uptake (Figure 1.5). This uncovered a novel mechanism of cytochrome *c* release different from the one involving BAX oligomerization at the mitochondria (Germain et al., 2005). Additionally, the authors identified that in BIK expressing cells Dynamin-related protein 1 (DRP1), a GTPase enzyme essential for normal mitochondrial fission, was recruited to the mitochondria and facilitated their fragmentation to augment cytochrome *c* release

(Figure 1.5) (Germain et al., 2005). All in all, this model suggested that BIK can induce MOMP through *ER* Ca^{+2} release, mitochondrial calcium overload and subsequent fragmentation.

1.5.1.3 By autophagic cell death

While the above mechanisms focussed on the induction of the mitochondrial pathway of apoptosis, BIK mediated cell death was also reported to occur by an alternative pathway. Autophagy can act as a cell survival or cell death mechanism depending on the context (Marino et al., 2014). Investigations of BIK induced cell death in melanoma and glioma cell lines showed that cytochrome *c* release and caspase activation was not seen in these experimental systems, which hinted that a novel cell death pathway might be at play (Naumann et al., 2003; Oppermann et al., 2005). Subsequently, Rashmi et al. provided insight into the underlying mechanism by ectopically expressing BIK in *Bcl-2* $^{+/+}$ or *Bcl-2* $^{-/-}$ MEFs (Rashmi et al., 2008). The cell death occurred in a cytochrome *c* and caspase-independent manner in *Bcl-2* $^{+/+}$ and *Bcl-2* $^{-/-}$ MEFs (Rashmi et al., 2008). This suggested that this mode of cell death did not require BAK/BAX activation and MOMP. Interestingly, upon ectopic BIK expression, *Bcl-2* $^{-/-}$ but not *Bcl-2* $^{+/+}$ cells displayed hallmarks of autophagy such as cytoplasmic vacuoles and punctate distribution of microtubule-associated proteins 1A/1B light chain 3B (LC3B), suggesting that BIK induced autophagy in the absence of BCL-2 (Figure 1.5) (Rashmi et al., 2008). Further, pharmacological inhibition of autophagy or silencing of critical autophagic components *Atg5* and *Beclin1* conferred a protective effect on cellular health, which confirmed that autophagy was the cause of cell death (Rashmi et al., 2008).

In conclusion, in the BCL-2 proficient cells, BIK acts as a sensitizer to induce cytochrome *c* release by either activating BAX oligomerization at the mitochondria or by promoting BAK/BAX mediated Ca^{+2} release from the *ER* and mitochondrial Ca^{+2} overload. This eventually leads to

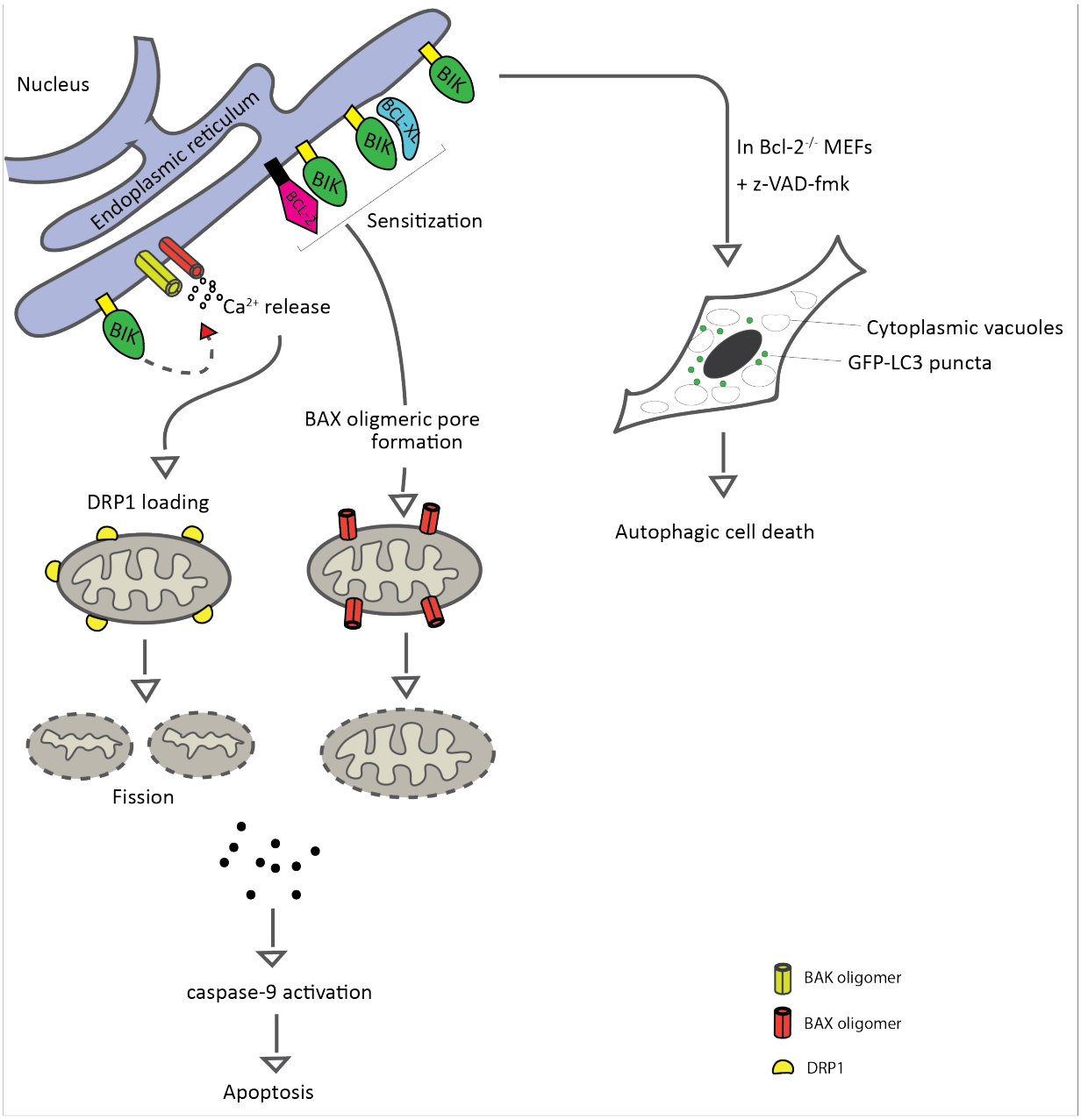

Figure 1.5 Mechanisms of BIK induced cell death. *ER*-localized BIK induces cell death through apoptotic and autophagic pathways. The cytochrome c release necessary for the apoptotic pathway is triggered in one of the two ways. First, BIK can sequester BCL-2 and BCL-XL, in turn activating BAX, which leads to MOMP and cytochrome *c* effusion. Second, BIK can stimulate *ER* Ca^{+2} release through *ER*-localised BAK/BAX. Subsequent mitochondrial Ca^{+2} uptake promotes loading of the fission enzyme DRP1, which in turn promotes mitochondrial fragmentation causing cytochrome *c* release. Downstream caspase cascade then dismantles the cell. BIK mediated autophagic cell death occurs in *Bcl-2*$^{-/-}$ mouse embryonic fibroblasts. This mode of cell death is defined by cellular vacuolization, the formation of GFP-LC3 puncta and protective effect of autophagic downregulation.

caspase activation and cell death. In the absence of BCL-2 however, BIK induces autophagic cell death possibly by assisting the core autophagic machinery.

1.5.2 Regulation of BIK expression

While most BH3-only proteins are unstructured, a computationally predicted structure of BIK is available (McDonnell et al., 1999). According to this study, BIK consists of 6 alpha helices and an exposed BH3 domain suggesting that it might be a constitutively active molecule (Figure 1.3) (McDonnell et al., 1999). Furthermore, BIK induces apoptosis in most models tested and therefore investigators have resorted to using BCL-2 coexpression or pharmacological inhibition of caspases to study upstream events (Germain et al., 2005; Mathai et al., 2002; Mathai et al., 2005). Hence, it is essential that BIK be under tight transcriptional and post-transcriptional regulation in healthy cells to prevent the onset of apoptosis.

1.5.2.1 Levels of *BIK* mRNA in normal tissues and transformed cell lines

BIK gene is expressed in a tissue-restricted manner that may be deregulated in cancer. Daniel et al. investigated levels of BIK transcript in a variety of human tissues using northern blot analysis and found a restricted pattern (Daniel et al., 1999). *BIK* mRNA expression was highest in the kidney and pancreas followed by placenta, lungs, and liver. No detectable expression was observed in the heart, brain, skeletal muscle, small intestine, colon, spleen, thymus, ovary or in the blood leukocytes (Daniel et al., 1999). However, cancerous cell lines that belong to some of these compartments showed *BIK* elevation. For instance, Ravji (Burkitt's lymphoma) and SW480 (colon adenocarcinoma), as well as 9 of the 24 human myeloma cell lines that were screened, had a moderate to high *BIK* expression (Bodet et al., 2010; Daniel et al., 1999). Furthermore, RNAseq data available in the Cancer Cell Line Encyclopedia show that cell lines derived from Burkitt's

lymphoma, pancreatic and colorectal cancers have the highest *BIK* expression; lung, ovarian and breast cancer cell lines have a moderate expression whereas glioma, Hodgkin's lymphoma, and osteosarcoma cell lines show the lowest expression (Broadinstitute.org, 2018). Collectively, this suggests that *BIK* mRNA expression might be upregulated upon neoplastic transformation in tissues that otherwise do not express *BIK*.

1.5.2.2 Regulation of *BIK* mRNA expression and its stability

Various transcription factors have been found to regulate the transcriptional activity of the *BIK* gene depending on the death signal. *BIK* transcriptional upregulation upon genotoxic stress has been demonstrated both in a p53-dependent and -independent manner (Hur et al., 2006; Mathai et al., 2002; Paquet et al., 2004; Real et al., 2006). Treatment of oral epithelial (KB) or MCF-7 cells with γ-radiation or doxorubicin upregulated *BIK* mRNA in a p53-dependent manner, and the *BIK* promoter was shown to be a direct transcriptional target of p53 in MCF-7 cells (Hur et al., 2006; Mathai et al., 2005). Conversely, human lymphoma and colon cancer cell lines deficient in p53 also showed *BIK* upregulation in response to genotoxic challenge demonstrating that in different cell lines, even in response to the same challenge, *BIK* upregulation can occur through alternative mechanisms (Paquet et al., 2004; Real et al., 2006).

BIK upregulation upon cytokine stimulation occurs through alternative transcription factors. For instance, interferon-γ (INF-γ) led to an increase in *BIK* mRNA and protein, which was dependent on the transcription factor signal transducer and activator of transcription 1 (STAT1) (Mebratu et al., 2008). Another cytokine, tumor growth factor β (TGF- β) upregulated *BIK* expression through transcription factor SMAD3/4, which associated with the *BIK* promoter at -1055 location determined through chromatin immunoprecipitation (ChIP) and electrophoretic

mobility shift assays (EMSA) (Spender et al., 2009). *BIK* transcription in other cell line models has also been shown. As examples, in neuroblastoma and human embryonic carcinoma cell lines, *BIK* transcription occurred in response to the chemotherapeutic agent adriamycin. This response was regulated by E2F transcription factors that bound at -104 position of the *BIK* promoter (Real et al., 2006). BIK expression in human myeloma cell lines was seen in the absence of any stress stimuli, and this upregulation was dependent on TEF transcription factor (Bodet et al., 2010). Lastly, PAR-bZIP transcription factors stimulate *BIK* transcription in mouse fibroblasts and HEK293 cells (Ritchie et al., 2009). Loss of PAR-bZIP protects cells from oxidative stress-induced apoptosis (Ritchie et al., 2009). Thus, *BIK* upregulation by distinct transcription factors acts as a stress sensing mechanism in response to a diverse set of stress stimuli.

One of the stimuli specifically relevant to breast cancer that trigger *BIK* transcriptional activity is estrogen deprivation or anti-estrogen (e.g., tamoxifen, fulvestrant) treatment of ER-positive breast cancer cell lines (Hur et al., 2006; Hur et al., 2004; Viedma-Rodriguez et al., 2013; Viedma-Rodriguez et al., 2015). This transcriptional stimulation occurs in a p53 dependent manner, and p53 knockdown or expression of a dominant negative form abolishes *BIK* transcriptional activity (Bowman et al., 1996; Hur et al., 2006). How p53 upregulates *BIK* transcription upon ER inhibition is not completely clear. However, it is known that the interplay between estrogen and p53 signaling pathways determines the growth or apoptosis in the ER-positive cancers. Estrogen binds with the estrogen receptor α (ERα) and stimulates the expression of many growth and proliferation genes that fuel the progression of ER-positive breast cancers (Figure 1.6 A) (Musgrove and Sutherland, 2009; Nicholson and Johnston, 2005). On the other hand, the p53 tumor suppressor stimulates growth inhibitory and/or apoptotic genes (Bieging et

al., 2014). Interestingly, estrogen bound ERα blocks p53 mediated transcription by directly associating with it at the p53 target gene promoters (Figure 1.6 A) (Liu et al., 2006). ERα:p53 recruits transcriptional repressors such as nuclear receptor corepressors (NCoR and SMRT) and histone deacetylase 1 (HDAC1) which prevent p53 mediated transcription initiation (Konduri et al., 2010). Contrary to estrogen, anti-estrogens prevent the ERα:p53 interaction, which allows p53 to initiate transcription at its target genes (Figure 1.6 B). Accordingly, it can be postulated that anti-estrogen mediated *BIK* transcription is mediated by ERα:p53 dissociation or ERα loss through p53. BIK synthesized in this manner determines the apoptotic response of ER-positive cells when they encounter endocrine therapy (Viedma-Rodriguez et al., 2013; Viedma-Rodriguez et al., 2015).

In addition to transcriptional stimulation, the post-transcriptional regulation also determines steady-state levels of *BIK* transcripts. Two distinct mechanisms have been demonstrated. First, mRNA stability is modulated by polyadenylation. The poly(A) polymerase Star-PAP was shown to associate with nascent *BIK* mRNA and polyadenylate it on the 3' end in HEK293 and breast cancer cells (Li et al., 2012; Yu et al., 2017). The poly(A) tail stabilizes the mRNA by its binding to polyadenylate-binding nuclear protein 1 (PABPN1) and facilitates nuclear export (Hollerer et al., 2014). Accordingly, ectopic expression of Star-PAP increased *BIK* mRNA levels, and Star-PAP silencing in breast cancer cells prevented *BIK* mediated apoptosis (Yu et al., 2017). Thus, the Star-PAP-mediated stability of BIK mRNA functionally regulates BIK killing potential. Second, specific miRNAs up- or downregulate *BIK* expression. In human monocytes, *BIK* is silenced by miR-125B presumably through the RNA induced silencing complex (RISC) mediated cytoplasmic degradation of the mRNA (Duroux-Richard et al., 2016). On the contrary, miR-28-5p, -510-5p and -608 in human lung carcinoma cells upregulate *BIK* levels (Choi et al., 2015). The

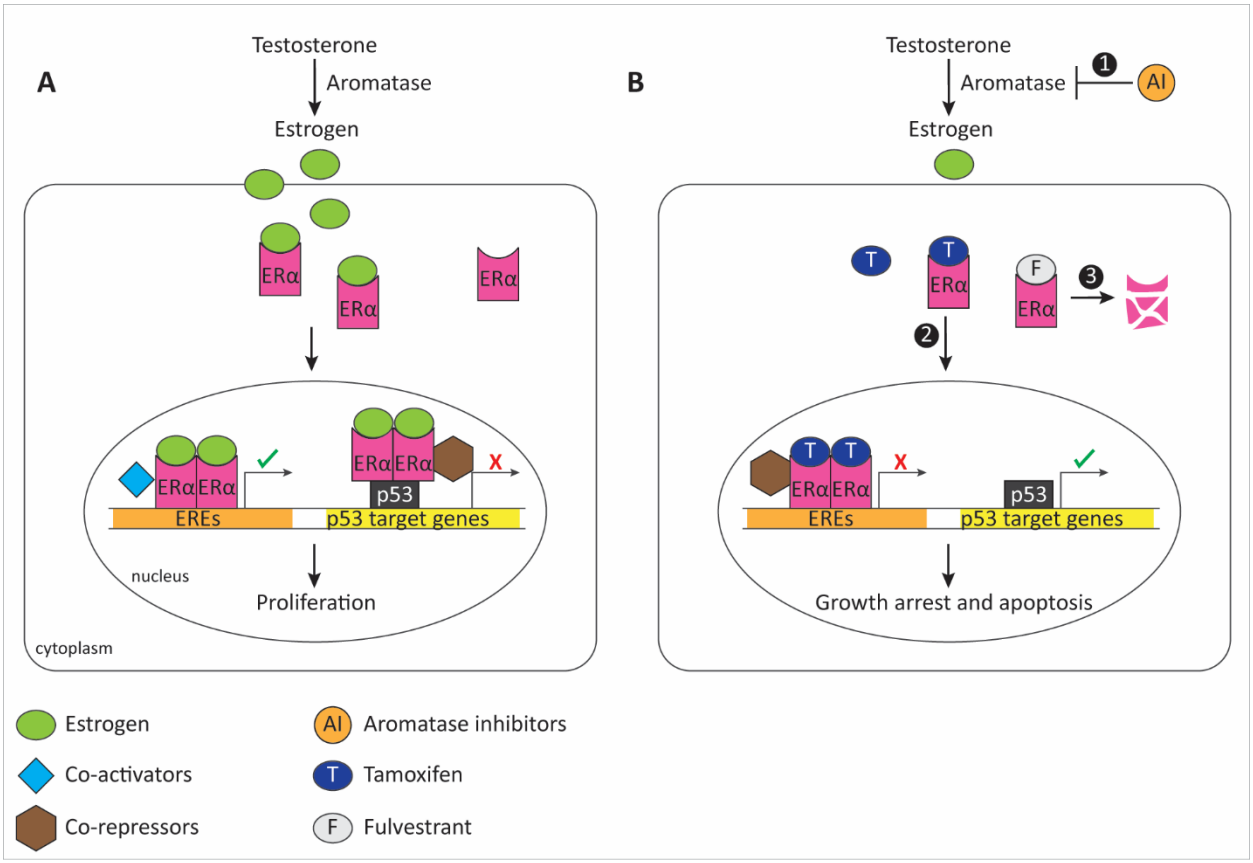

Figure 1.6 Model of mechanisms of gene regulation by estrogen. A. Estrogen (E2) is produced by aromatization of the hormone testosterone by aromatase enzymes. E2 binding to ERα promotes cell proliferation in two ways. E2: ERα dimers assemble at the estrogen-response elements (ERE) where they recruit co-activators that stimulate the transcription of growth-promoting genes. Additionally, E2: ERα physically interacts with p53 and recruits co-repressors such as NcoR, SMART and HDAC1 at the p53 binding sites which inhibit the transcription of p53 target genes. **B.** Anti-estrogens inhibit E2: ERα signaling as well as disrupt the ERα: p53 interaction, which in turn, allows p53 mediated transcriptional upregulation. ❶ Aromatase inhibitors block the production of circulating estrogen causing a direct estrogen deprivation and inhibition of the ERα mediated signaling. Also, in the absence of E2, ERα does not have an inhibitory effect on p53. ❷ Tamoxifen binding to ERα promotes recruitment of co-repressors at the EREs, causing cessation of the proliferation-associated gene transcription. As well, tamoxifen bound ERα cannot associate with p53, which reactivates p53-dependent transcription of growth inhibitory and pro-apoptotic genes. ❸ Fulvestrant has a higher binding affinity for ERα than E2. Fulvestrant bound ERα cannot dimerize, or nuclear translocate, causing a loss of E2 signaling. Also, fulvestrant bound ERα is unstable and is degraded, which would allow p53-mediated transcription. Cell cycle inhibitor p21, and pro-apoptotic genes *BIK, PUMA,* and Noxa are well-known targets of p53.

underlying mechanism of this miRNA mediated transcriptional upregulation is not completely clear. However, recent reports have suggested that in addition to the cytoplasm, miRNA: RISC (miRISC) complex also exists in the nucleus (Catalanotto et al., 2016). It is proposed, that in this case, the miRNA would recognize a specific sequence in the gene promoter and the miRISC complex would recruit activating chromatin modifiers, which may in turn, shift the chromatin architecture towards a more permissive one, thereby increasing transcription (Catalanotto et al., 2016). All in all, transcriptional upregulators, mRNA modifying enzymes, and miRNAs regulate *BIK* mRNA expression in a highly context-dependent manner.

1.5.2.3 Regulation of BIK protein

BIK mRNA levels do not predict BIK protein levels. This is attributed to the constant turnover of the protein. BIK has been shown to undergo degradation in leukemia, lymphoma, prostate, breast, and colon cancer cell lines, and proteasomal inhibitors such as MG132 or bortezomib upregulate BIK levels (Marshansky et al., 2001; Nikrad et al., 2005; Zhu et al., 2005). Furthermore, in ER-positive breast cancer cell lines, anti-estrogen stimulated BIK protein levels are augmented by proteasomal inhibition suggesting that deregulated or overwhelmed proteasomal machinery in cancer cells can promote high levels of BIK protein (Hur et al., 2006).

The underlying mechanism of BIK targeting to the proteasome and the residues necessary for this process were identified by Lopez et al. (Lopez et al., 2012). These authors demonstrated that high survival signaling leads to the phosphorylation of extracellular signal-regulated kinase ½ (ERK1/2) (Lopez et al., 2012). Phosho-ERK1/2 directly interacted with BIK and phosphorylated it on the serine 124 residue. This phosphorylation was critical for BIK polyubiquitination at lysine 34 and proteasomal degradation (Lopez et al., 2012). Thus, in the presence of survival signaling, S124

phosphorylation followed by K34 polyubiquitination promotes BIK degradation and keeps apoptotic induction in check. Additionally, loss of the survival signaling induced by pharmacological inhibition of the upstream players (e.g., c-SRC) stabilized BIK protein, suggesting that BIK protein levels may increase in the absence of survival inputs (Lopez et al., 2012). The follow-up question was, what is the nature of the machinery that ubiquitinates BIK? Maxfield et al. demonstrated that BIK was part of a protein complex formed by adaptor protein fetal and adult testis-expressed 1 (FATE1) and an E3 ubiquitin ligase RNF 183, which promoted its ubiquitination and degradation (Maxfield et al., 2015). Loss of FATE1 by siRNA mediated knockdown or diminished expression in tumor tissues upregulated BIK protein levels (Maxfield et al., 2015). Thus, these studies elucidated the details of BIK proteasomal degradation pathways and provided insight into how BIK protein levels might be elevated in cancer. The second mechanism of BIK degradation was demonstrated in myeloma cell lines. Here the authors showed that BIK underwent autophagic degradation (Chen et al., 2014). BIK protein levels were upregulated by pharmacological inhibition of the lysosomal acidification, which blocks autophagic cargo degradation suggesting that BIK is an autophagy target (Chen et al., 2014). As well, siRNA mediated depletion of the p62 protein, which is required for cargo loading, also increased BIK levels and stimulated apoptosis (Chen et al., 2014). This uncovered how inefficient autophagy could be converted into apoptosis by BIK stabilization. Altogether in healthy cells, BIK protein is produced, and normal protein turn-over mechanisms induce its rapid degradation.

1.5.3 *BIK* mutations and expression in cancer

Tumor suppressor genes are frequently mutated in cancer (e.g., p53). According to cBioPortal, the observed frequency of *BIK* mutations across all cancers is ~0.1%, suggesting that

loss of *BIK* may not confer a considerable advantage to the tumors (cBioPortal.org, 2018). Nevertheless, in some cancer cell lines deletions or mutations of BIK have been observed that reduce their sensitivity to apoptotic stimuli (Chinnadurai et al., 2008). In contrast to the loss of BIK, some investigations have also reported its overexpression in cancers. For instance, *BIK* mRNA upregulation in non-small cell lung cancer (NSCLC) has been observed along with a concomitant increase in the *BCL-2* levels, and it was found that *BIK*-high patients had worse survival outcomes (Lu et al., 2006). This poor prognosis of patients was speculated to be due to a BCL-2 blockade of BIK mediated apoptosis (Chinnadurai et al., 2008). Specifically, in the context of breast cancer, both *BIK* mRNA and protein were demonstrated to be upregulated in patient tumors, but its association with patient outcomes was not known (Garcia et al., 2005; Lopez-Munoz et al., 2012). Thus while these observations suggested that cancer cells could tolerate BIK overexpression, no clear explanation was available concerning benefit or disadvantage to the cancer cells.

1.5.3.1 Use of BIK overexpression to eradicate tumor cells

Since BIK is a robust pro-apoptotic protein, various groups have explored applications directed at using BIK as a therapeutic. By exogenously expressing BIK, melanoma and glioblastoma cells can be killed *in vitro* (Naumann et al., 2003; Oppermann et al., 2005). Furthermore, BIK overexpression overcame chemoresistance in breast, prostate, and colon cancer cells as well in acute lymphoblastic/lymphocytic leukemia cell lines (Chinnadurai et al., 2008). Human BIK protein has two closely located (Thr33 and Ser35) phosphorylation sites that undergo phosphorylation by casein kinase 2 like kinase (CK2LK) (Verma et al., 2001). Phosphonull mutants of these sites reduce BIK pro-apoptotic activity whereas phosphomimetic mutation (referred to as BIKDD) enhances the activity (Verma et al., 2001). Liposome encapsulation of plasmids encoding

wt BIK or BIKDD, and their systemic administration to specific cancers such as breast, pancreas, melanoma, and colon in xenograft or orthotopic mouse models led to tumor clearance (Jiao et al., 2014; Xie et al., 2007; Zou et al., 2002). Thus, BIK with enhanced apoptotic activity when used as a gene therapy molecule, can efficiently kill cancer cells.

1.6 Evasion of apoptosis

Avoiding cell death is a hallmark of cancer (Hanahan and Weinberg, 2011). Cancer cells routinely encounter stress due to physiological malfunctioning (e.g., overt oncogenic signaling, DNA damage due to excess cell proliferation) or anti-cancer therapy, which induce apoptotic signaling (Hanahan and Weinberg, 2011). Therefore, cells that somehow attenuate the apoptotic signaling gain a significant survival advantage. In cancer cells, this is achieved by impairment of the regulators or effectors of the apoptotic machinery.

Aberrations of the extrinsic pathway have been reported. As examples, reduced expression or mutations of CD95 (FAS death receptor) in a variety of cancers confer insensitivity to FAS ligand as well chemoresistance (Friesen et al., 1997; Fulda et al., 1998; Lee et al., 1999; Yang and Goping, 2013). Additionally, abnormal transport of TNF-related apoptosis-inducing ligand receptor (TRAIL-R) from the *ER* to the cell surface results in resistance to TRAIL-induced apoptosis in colon cancer cells (Fulda, 2009; Jin et al., 2004). A defective intrinsic apoptotic program has wider-ranging implications in cancer. Overall, two main groups of abnormalities have been observed. The first is the deregulation of the BCL-2 family proteins. As mentioned earlier, the anti-apoptotic BCL-2 was identified as a t(14;18) translocation in B-cell lymphomas. Although this aberration was oncogenic in the transgenic mice (*Eμ-bcl-2*) mimicking the translocation, the tumor incidence was low, and tumors developed after an extended latency

period, which suggested that mere anti-apoptotic upregulation was insufficient for fulminant tumorigenesis (McDonnell et al., 1989; Strasser et al., 1993). Intriguingly, a subsequent study showed that bi-transgenic mice (E*μ-bcl-2*/E*μ-myc*) harboring *Myc* and *Bcl-2* oncogenes developed tumors rapidly compared to their single transgenic counterparts (Strasser et al., 1990). This critical observation showed that excessive oncogenic signaling by Myc increased the susceptibility to apoptosis, which was counteracted by BCL-2 expression casusing faster tumor progression. In addition to BCL-2, other anti-apoptotic proteins are also implicated in apoptosis evasion. For instance, MCL-1 overexpression predicted worse prognosis in chronic lymphocytic leukemia while BCL-XL elevation in NCI-60 cell lines was associated with resistance to 122 chemotherapeutic agents (Amundson et al., 2000; Pepper et al., 2008). Thus, increased anti-apoptotic factors can promote tumorigenesis, chemotherapeutic resistance, and associate with poor survival outcomes. Defective pro-apoptotic signaling is similarly pro-oncogenic. Monoallelic deletion of *Bim* or homozygous deletion of *Puma* in E*μ-myc* mice increased the rate of hematological malignancies (Adams and Cory, 2007b; Egle et al., 2004). Furthermore, *BAX* mutations are found in ~50% of the colorectal cancers (Miquel et al., 2005). Thus, genetic or functional downregulation of the pro-apoptotic group, or upregulation of anti-apoptotic proteins favor tumorigenesis.

The second major abnormality is the deregulation of the tumor suppressor p53. In the absence of stress, p53 protein levels remain low due to its proteasomal degradation mediated through E3 ligase mouse double minute 2 homolog (MDM2) (Aubrey et al., 2018). In response to activated oncogenes, DNA damage or metabolic stress, p53 is stabilized and modulates the transcription of ~500 genes including cell cycle regulators, DNA repair factors as well BH3 only members *BIK*, *NOXA*, and *PUMA* (Aubrey et al., 2018). When untransformed cells face

unresolved stress, these BH3-only proteins induce apoptosis and protect cells from oncogenic transformation. Thus, p53-mediated apoptosis protects against cancer. Accordingly, loss of p53 in mice leads to spontaneous tumor formation at 4.5 months of age and nearly 50% of all human cancers have mutations in the p53 gene (Adams and Cory, 2007a; Donehower, 1996). Altogether, the attenuation of mitochondrial apoptosis can initiate tumorigenesis, facilitate tumor progression and impart chemoresistance.

1.7 Research objective

Breast cancer is the number one cause of cancer associated female mortalities in the world. Cancer is a heterogeneous disease. Hence, treatments guided by conventional diagnostic tools experience significant shortcomings. Therefore there is a growing need to identify new biomarkers and their association with patient outcomes to understand disease biology. Biomarker-based identification of cancer subgroups would streamline the existing therapy and open new venues for the personalized approach to treating cancer. To this end, we decided to explore breast cancer biomarkers from the regulators of the apoptotic program, specifically the BH3-only proteins. BCL-2 interacting killer (BIK) emerged as a potential candidate. Using gene and protein expression analysis of 327 patient tumors, we established BIK's role as a biomarker associated with unfavorable patient prognosis. Additionally, from the patient data analyses, we got a hint that BIK might have a pro-survival role through its interaction with the autophagy pathway (Chapter 3). Hence, I sought to interrogate whether BIK promoted cell survival using *in vitro* assays. While there was some indication that BIK promoted autophagy, there was no survival benefit at the cellular level, suggesting that BIK mediated tumor promotion may not occur through autophagy (Chapter 4). This led me to explore an alternative mechanism wherein elevation of BIK expression

in breast cancer cells engaged failed apoptosis, induced genomic damage and aggressive phenotype through the same machinery as the tumor-suppressing apoptosis (Chapter 5). Thus, the discoveries from this thesis identified a biomarker of aggressive breast cancer and elucidated the underlying mechanism of tumor evolution.

References

ACS (2016). The Global Burden of Cancer in Women. World Cancer Congress.

Adams, J.M., and Cory, S. (2007a). Bcl-2-regulated apoptosis: mechanism and therapeutic potential. Current opinion in immunology *19*, 488-496.

Adams, J.M., and Cory, S. (2007b). The Bcl-2 apoptotic switch in cancer development and therapy. Oncogene *26*, 1324-1337.

Ades, F., Tryfonidis, K., and Zardavas, D. (2017). The past and future of breast cancer treatment—from the papyrus to individualised treatment approaches. ecancermedicalscience *11*, 746.

Ali, S., Rasool, M., Chaoudhry, H., P, N.P., Jha, P., Hafiz, A., Mahfooz, M., Abdus Sami, G., Azhar Kamal, M., Bashir, S.*, et al.* (2016). Molecular mechanisms and mode of tamoxifen resistance in breast cancer. Bioinformation *12*, 135-139.

Althuis, M.D., Dozier, J.M., Anderson, W.F., Devesa, S.S., and Brinton, L.A. (2005). Global trends in breast cancer incidence and mortality 1973-1997. Int J Epidemiol *34*, 405-412.

Amundson, S.A., Myers, T.G., Scudiero, D., Kitada, S., Reed, J.C., and Fornace, A.J., Jr. (2000). An informatics approach identifying markers of chemosensitivity in human cancer cell lines. Cancer Res *60*, 6101-6110.

Anthony J.F. Griffiths, U.o.B.C., Susan R. Wessler, U.o.C.R., Sean B. Carroll, H.H.M.I.U.o.W.-M., and John Doebley, U.o.W.-M. (2015). Introduction to genetic analysis (Eleventh edition. New York, NY : W.H. Freeman & Company, [2015] ©2015).

Aubrey, B.J., Kelly, G.L., Janic, A., Herold, M.J., and Strasser, A. (2018). How does p53 induce apoptosis and how does this relate to p53-mediated tumour suppression? Cell Death Differ *25*, 104-113.

Bakhshi, A., Jensen, J.P., Goldman, P., Wright, J.J., McBride, O.W., Epstein, A.L., and Korsmeyer, S.J. (1985). Cloning the chromosomal breakpoint of t(14;18) human lymphomas: clustering around JH on chromosome 14 and near a transcriptional unit on 18. Cell *41*, 899-906.

Barres, B.A., and Raff, M.C. (1999). Axonal control of oligodendrocyte development. The Journal of cell biology *147*, 1123-1128.

Bergman, L., Beelen, M.L.R., Gallee, M.P.W., Hollema, H., Benraadt, J., and van Leeuwen, F.E. (2000). Risk and prognosis of endometrial cancer after tamoxifen for breast cancer. The Lancet *356*, 881-887.

Bertheau, P., Lehmann-Che, J., Varna, M., Dumay, A., Poirot, B., Porcher, R., Turpin, E., Plassa, L.F., de Roquancourt, A., Bourstyn, E.*, et al.* (2013). p53 in breast cancer subtypes and new insights into response to chemotherapy. Breast *22 Suppl 2*, S27-29.

Bieging, K.T., Mello, S.S., and Attardi, L.D. (2014). Unravelling mechanisms of p53-mediated tumour suppression. Nature Reviews Cancer *14*, 359.

Bodet, L., Menoret, E., Descamps, G., Pellat-Deceunynck, C., Bataille, R., Le Gouill, S., Moreau, P., Amiot, M., and Gomez-Bougie, P. (2010). BH3-only protein Bik is involved in both apoptosis induction and sensitivity to oxidative stress in multiple myeloma. British Journal of Cancer *103*, 1808-1814.

Bouillet, P., Metcalf, D., Huang, D.C., Tarlinton, D.M., Kay, T.W., Kontgen, F., Adams, J.M., and Strasser, A. (1999). Proapoptotic Bcl-2 relative Bim required for certain apoptotic responses, leukocyte homeostasis, and to preclude autoimmunity. Science (New York, NY) *286*, 1735-1738.

Bowman, T., Symonds, H., Gu, L., Yin, C., Oren, M., and Van Dyke, T. (1996). Tissue-specific inactivation of p53 tumor suppression in the mouse. Genes & development *10*, 826-835.

Boyd, J.M., Gallo, G.J., Elangovan, B., Houghton, A.B., Malstrom, S., Avery, B.J., Ebb, R.G., Subramanian, T., Chittenden, T., Lutz, R.J.*, et al.* (1995). Bik, a novel death-inducing protein shares a distinct sequence motif with Bcl-2 family proteins and interacts with viral and cellular survival-promoting proteins. Oncogene *11*, 1921-1928.

Bradbury, A.R., and Olopade, O.I. (2007). Genetic susceptibility to breast cancer. Rev Endocr Metab Disord *8*, 255-267.

Bravo-Sagua, R., Rodriguez, A.E., Kuzmicic, J., Gutierrez, T., Lopez-Crisosto, C., Quiroga, C., Díaz-Elizondo, J., Chiong, M., Gillette, T.G., Rothermel, B.A.*, et al.* (2013). Cell Death and Survival Through the Endoplasmic Reticulum-Mitochondrial Axis. Current molecular medicine *13*, 317-329.

Broadinstitute.org (2018). BIK expression in cancer cell lines.

Capri, S., and Russo, A. (2017). Cost of breast cancer based on real-world data: a cancer registry study in Italy. BMC Health Serv Res *17*, 84.

Carter, B.D., Freedman, N.D., and Jacobs, E.J. (2015). Smoking and mortality--beyond established causes. N Engl J Med *372*, 2170.

Catalanotto, C., Cogoni, C., and Zardo, G. (2016). MicroRNA in Control of Gene Expression: An Overview of Nuclear Functions. Int J Mol Sci *17*.

cBioPortal.org (2018). BIK alterations in cancer.

Chen, M., He, H., Zhan, S., Krajewski, S., Reed, J.C., and Gottlieb, R.A. (2001). Bid is cleaved by calpain to an active fragment in vitro and during myocardial ischemia/reperfusion. The Journal of biological chemistry *276*, 30724-30728.

Chen, S., Zhou, L., Zhang, Y., Leng, Y., Pei, X.Y., Lin, H., Jones, R., Orlowski, R.Z., Dai, Y., and Grant, S. (2014). Targeting SQSTM1/p62 induces cargo loading failure and converts autophagy to apoptosis via NBK/Bik. Mol Cell Biol *34*, 3435-3449.

Chinnadurai, G., Vijayalingam, S., and Rashmi, R. (2008). BIK, the founding member of the BH3-only family proteins: mechanisms of cell death and role in cancer and pathogenic processes. Oncogene *27 Suppl 1*, S20-29.

Chipuk, J.E., Moldoveanu, T., Llambi, F., Parsons, M.J., and Green, D.R. (2010). The BCL-2 Family Reunion. Molecular cell *37*, 299-310.

Choi, Y.C., Yoon, S., Byun, Y., Lee, G., Kee, H., Jeong, Y., Yoon, J., and Baek, K. (2015). MicroRNA library screening identifies growth-suppressive microRNAs that regulate genes involved in cell cycle progression and apoptosis. Experimental cell research *339*, 320-332.

Chu, D., Paoletti, C., Gersch, C., VanDenBerg, D.A., Zabransky, D.J., Cochran, R.L., Wong, H.Y., Toro, P.V., Cidado, J., Croessmann, S.*, et al.* (2016). ESR1 Mutations in Circulating Plasma Tumor DNA from Metastatic Breast Cancer Patients. Clinical cancer research : an official journal of the American Association for Cancer Research *22*, 993-999.

Clarke, H.J., Chambers, J.E., Liniker, E., and Marciniak, S.J. (2014). Endoplasmic reticulum stress in malignancy. Cancer cell *25*, 563-573.

Colditz, G.A., and Bohlke, K. (2014). Priorities for the primary prevention of breast cancer. CA Cancer J Clin *64*, 186-194.

Coleman, M.L., Sahai, E.A., Yeo, M., Bosch, M., Dewar, A., and Olson, M.F. (2001). Membrane blebbing during apoptosis results from caspase-mediated activation of ROCK I. Nature cell biology *3*, 339-345.

Coultas, L., Bouillet, P., Loveland, K.L., Meachem, S., Perlman, H., Adams, J.M., and Strasser, A. (2005). Concomitant loss of proapoptotic BH3-only Bcl-2 antagonists Bik and Bim arrests spermatogenesis. The EMBO Journal *24*, 3963-3973.

Coultas, L., Bouillet, P., Stanley, E.G., Brodnicki, T.C., Adams, J.M., and Strasser, A. (2004). Proapoptotic BH3-only Bcl-2 family member Bik/Blk/Nbk is expressed in hemopoietic and endothelial cells but is redundant for their programmed death. Mol Cell Biol *24*, 1570-1581.

Creighton, C.J. (2012). The molecular profile of luminal B breast cancer. Biologics *6*, 289-297.

Curtis, C. (2015). Genomic profiling of breast cancers. Current opinion in obstetrics & gynecology *27*, 34-39.

Czabotar, P.E., Lessene, G., Strasser, A., and Adams, J.M. (2014). Control of apoptosis by the BCL-2 protein family: implications for physiology and therapy. Nature reviews Molecular cell biology *15*, 49-63.

Daniel, P.T., Pun, K.T., Ritschel, S., Sturm, I., Holler, J., Dorken, B., and Brown, R. (1999). Expression of the death gene Bik/Nbk promotes sensitivity to drug-induced apoptosis in corticosteroid-resistant T-cell lymphoma and prevents tumor growth in severe combined immunodeficient mice. Blood *94*, 1100-1107.

Datta, S.R., Dudek, H., Tao, X., Masters, S., Fu, H., Gotoh, Y., and Greenberg, M.E. (1997). Akt phosphorylation of BAD couples survival signals to the cell-intrinsic death machinery. Cell *91*, 231-241.

Davies, C., Pan, H., Godwin, J., Gray, R., Arriagada, R., Raina, V., Abraham, M., Alencar, V.H.M., Badran, A., Bonfill, X.*, et al.* (2013). Long-term effects of continuing adjuvant tamoxifen to 10 years versus stopping at 5 years after diagnosis of oestrogen receptor-positive breast cancer: ATLAS, a randomised trial. Lancet (London, England) *381*, 805-816.

Dewson, G., and Kluck, R.M. (2009). Mechanisms by which Bak and Bax permeabilise mitochondria during apoptosis. Journal of Cell Science *122*, 2801-2808.

Dijkers, P.F., Medema, R.H., Lammers, J.W., Koenderman, L., and Coffer, P.J. (2000). Expression of the pro-apoptotic Bcl-2 family member Bim is regulated by the forkhead transcription factor FKHR-L1. Current biology : CB *10*, 1201-1204.

Donehower, L.A. (1996). The p53-deficient mouse: a model for basic and applied cancer studies. Semin Cancer Biol *7*, 269-278.

Duroux-Richard, I., Roubert, C., Ammari, M., Presumey, J., Grun, J.R., Haupl, T., Grutzkau, A., Lecellier, C.H., Boitez, V., Codogno, P.*, et al.* (2016). miR-125b controls monocyte adaptation to inflammation through mitochondrial metabolism and dynamics. Blood *128*, 3125-3136.

Earnshaw, W.C., Martins, L.M., and Kaufmann, S.H. (1999). Mammalian caspases: structure, activation, substrates, and functions during apoptosis. Annu Rev Biochem *68*, 383-424.

Egle, A., Harris, A.W., Bouillet, P., and Cory, S. (2004). Bim is a suppressor of Myc-induced mouse B cell leukemia. Proceedings of the National Academy of Sciences of the United States of America *101*, 6164-6169.

Elangovan, B., and Chinnadurai, G. (1997). Functional dissection of the pro-apoptotic protein Bik. Heterodimerization with anti-apoptosis proteins is insufficient for induction of cell death. The Journal of biological chemistry *272*, 24494-24498.

Ellis, H.M., and Horvitz, H.R. (1986). Genetic control of programmed cell death in the nematode C. elegans. Cell *44*, 817-829.

Ellis, M.J., and Perou, C.M. (2013). The Genomic Landscape of Breast Cancer as a Therapeutic Roadmap. Cancer discovery *3*, 27-34.

Ellis, R.E., Yuan, J.Y., and Horvitz, H.R. (1991). Mechanisms and functions of cell death. Annual review of cell biology *7*, 663-698.

Enari, M., Sakahira, H., Yokoyama, H., Okawa, K., Iwamatsu, A., and Nagata, S. (1998). A caspase-activated DNase that degrades DNA during apoptosis, and its inhibitor ICAD. Nature *391*, 43-50.

Ferlay, J., Soerjomataram, I., Dikshit, R., Eser, S., Mathers, C., Rebelo, M., Parkin, D.M., Forman, D., and Bray, F. (2015). Cancer incidence and mortality worldwide: sources, methods and major patterns in GLOBOCAN 2012. Int J Cancer *136*, E359-386.

Foulkes, W.D., Smith, I.E., and Reis-Filho, J.S. (2010). Triple-negative breast cancer. N Engl J Med *363*, 1938-1948.

Friesen, C., Fulda, S., and Debatin, K.M. (1997). Deficient activation of the CD95 (APO-1/Fas) system in drug-resistant cells. Leukemia *11*, 1833.

Fuchs, Y., and Steller, H. (2011). Programmed cell death in animal development and disease. Cell *147*, 742-758.

Fulda, S. (2009). Tumor resistance to apoptosis. Int J Cancer *124*, 511-515.

Fulda, S., Los, M., Friesen, C., and Debatin, K.M. (1998). Chemosensitivity of solid tumor cells in vitro is related to activation of the CD95 system. Int J Cancer *76*, 105-114.

Garcia, N., Salamanca, F., Astudillo-de la Vega, H., Curiel-Quesada, E., Alvarado, I., Penaloza, R., and Arenas, D. (2005). A molecular analysis by gene expression profiling reveals Bik/NBK overexpression in sporadic breast tumor samples of Mexican females. BMC Cancer *5*, 93.

Gaub, M.-P., Bellard, M., Scheuer, I., Chambon, P., and Sassone-Corsi, P. (1990). Activation of the ovalbumin gene by the estrogen receptor involves the Fos-Jun complex. Cell *63*, 1267-1276.

Gavathiotis, E., Suzuki, M., Davis, M.L., Pitter, K., Bird, G.H., Katz, S.G., Tu, H.C., Kim, H., Cheng, E.H., Tjandra, N.*, et al.* (2008). BAX activation is initiated at a novel interaction site. Nature *455*, 1076-1081.

Germain, M., Mathai, J.P., McBride, H.M., and Shore, G.C. (2005). Endoplasmic reticulum BIK initiates DRP1-regulated remodelling of mitochondrial cristae during apoptosis. The EMBO Journal *24*, 1546-1556.

Germain, M., Mathai, J.P., and Shore, G.C. (2002). BH-3-only BIK functions at the endoplasmic reticulum to stimulate cytochrome c release from mitochondria. The Journal of biological chemistry *277*, 18053-18060.

Gillissen, B., Essmann, F., Graupner, V., Starck, L., Radetzki, S., Dorken, B., Schulze-Osthoff, K., and Daniel, P.T. (2003). Induction of cell death by the BH3-only Bcl-2 homolog Nbk/Bik is mediated by an entirely Bax-dependent mitochondrial pathway. The EMBO Journal *22*, 3580-3590.

Gillissen, B., Essmann, F., Hemmati, P.G., Richter, A., Richter, A., Oztop, I., Chinnadurai, G., Dorken, B., and Daniel, P.T. (2007). Mcl-1 determines the Bax dependency of Nbk/Bik-induced apoptosis. The Journal of cell biology *179*, 701-715.

Goping, I.S., Gross, A., Lavoie, J.N., Nguyen, M., Jemmerson, R., Roth, K., Korsmeyer, S.J., and Shore, G.C. (1998). Regulated Targeting of BAX to Mitochondria. The Journal of cell biology *143*, 207-215.

Green, D.R. (2010). Means to an End: Apoptosis and Other Cell Death Mechanisms (Cold Spring Harbor Laboratory Press).

Guarneri, V., and Conte, P. (2009). Metastatic breast cancer: therapeutic options according to molecular subtypes and prior adjuvant therapy. Oncologist *14*, 645-656.

Hanahan, D., and Weinberg, R.A. (2011). Hallmarks of cancer: the next generation. Cell *144*, 646-674.

Harris, L.N., Ismaila, N., McShane, L.M., Andre, F., Collyar, D.E., Gonzalez-Angulo, A.M., Hammond, E.H., Kuderer, N.M., Liu, M.C., Mennel, R.G.*, et al.* (2016). Use of Biomarkers to Guide Decisions on Adjuvant Systemic Therapy for Women With Early-Stage Invasive Breast Cancer: American Society of Clinical Oncology Clinical Practice Guideline. J Clin Oncol *34*, 1134-1150.

Heath-Engel, H.M., Chang, N.C., and Shore, G.C. (2008). The endoplasmic reticulum in apoptosis and autophagy: role of the BCL-2 protein family. Oncogene *27*, 6419.

Hollerer, I., Grund, K., Hentze, M.W., and Kulozik, A.E. (2014). mRNA 3′end processing: A tale of the tail reaches the clinic. EMBO Molecular Medicine *6*, 16-26.

Hu, Z., Fan, C., Oh, D.S., Marron, J.S., He, X., Qaqish, B.F., Livasy, C., Carey, L.A., Reynolds, E., Dressler, L.*, et al.* (2006). The molecular portraits of breast tumors are conserved across microarray platforms. BMC genomics *7*, 96.

Hur, J., Bell, D.W., Dean, K.L., Coser, K.R., Hilario, P.C., Okimoto, R.A., Tobey, E.M., Smith, S.L., Isselbacher, K.J., and Shioda, T. (2006). Regulation of expression of BIK proapoptotic protein in human breast cancer cells: p53-dependent induction of BIK mRNA by fulvestrant and proteasomal degradation of BIK protein. Cancer Res *66*, 10153-10161.

Hur, J., Chesnes, J., Coser, K.R., Lee, R.S., Geck, P., Isselbacher, K.J., and Shioda, T. (2004). The Bik BH3-only protein is induced in estrogen-starved and antiestrogen-exposed breast cancer cells and provokes apoptosis. Proceedings of the National Academy of Sciences of the United States of America *101*, 2351-2356.

Jeffers, J.R., Parganas, E., Lee, Y., Yang, C., Wang, J., Brennan, J., MacLean, K.H., Han, J., Chittenden, T., Ihle, J.N.*, et al.* (2003). Puma is an essential mediator of p53-dependent and -independent apoptotic pathways. Cancer cell *4*, 321-328.

Jiang, Q. (2013). Development of new estrogen receptor-targeting therapeutic agents for tamoxifen-resistant breast cancer. *5*.

Jiao, S., Wu, M., Ye, F., Tang, H., Xie, X., and Xie, X. (2014). BikDDA, a Mutant of Bik with Longer Half-Life Expression Protein, Can Be a Novel Therapeutic Gene for Triple-Negative Breast Cancer. PloS one *9*, e92172.

Jin, Z., McDonald, E.R., 3rd, Dicker, D.T., and El-Deiry, W.S. (2004). Deficient tumor necrosis factor-related apoptosis-inducing ligand (TRAIL) death receptor transport to the cell surface in human colon cancer cells selected for resistance to TRAIL-induced apoptosis. The Journal of biological chemistry *279*, 35829-35839.

Katzenellenbogen, J.A., Mayne, C.G., Katzenellenbogen, B.S., Greene, G.L., and Chandarlapaty, S. (2018). Structural underpinnings of oestrogen receptor mutations in endocrine therapy resistance. Nature Reviews Cancer *18*, 377-388.

Kaufmann, T., Tai, L., Ekert, P.G., Huang, D.C., Norris, F., Lindemann, R.K., Johnstone, R.W., Dixit, V.M., and Strasser, A. (2007). The BH3-only protein bid is dispensable for DNA damage- and replicative stress-induced apoptosis or cell-cycle arrest. Cell *129*, 423-433.

Kennecke, H., Yerushalmi, R., Woods, R., Cheang, M.C., Voduc, D., Speers, C.H., Nielsen, T.O., and Gelmon, K. (2010). Metastatic behavior of breast cancer subtypes. J Clin Oncol *28*, 3271-3277.

Kerr, J.F.R., Wyllie, A.H., and Currie, A.R. (1972). Apoptosis: A Basic Biological Phenomenon with Wide-ranging Implications in Tissue Kinetics. British Journal of Cancer *26*, 239-257.

Kim, H., Rafiuddin-Shah, M., Tu, H.C., Jeffers, J.R., Zambetti, G.P., Hsieh, J.J., and Cheng, E.H. (2006). Hierarchical regulation of mitochondrion-dependent apoptosis by BCL-2 subfamilies. Nature cell biology *8*, 1348-1358.

Knudson, C.M., Tung, K.S., Tourtellotte, W.G., Brown, G.A., and Korsmeyer, S.J. (1995). Bax-deficient mice with lymphoid hyperplasia and male germ cell death. Science (New York, NY) *270*, 96-99.

Konduri, S.D., Medisetty, R., Liu, W., Kaipparettu, B.A., Srivastava, P., Brauch, H., Fritz, P., Swetzig, W.M., Gardner, A.E., Khan, S.A.*, et al.* (2010). Mechanisms of estrogen receptor antagonism toward p53 and its implications in breast cancer therapeutic response and stem cell regulation. Proceedings of the National Academy of Sciences *107*, 15081-15086.

Larsen, B.D., and Sorensen, C.S. (2017). The caspase-activated DNase: apoptosis and beyond. FEBS J *284*, 1160-1170.

Lauby-Secretan, B., Scoccianti, C., Loomis, D., Benbrahim-Tallaa, L., Bouvard, V., Bianchini, F., Straif, K., and International Agency for Research on Cancer Handbook Working, G. (2015). Breast-cancer screening--viewpoint of the IARC Working Group. N Engl J Med *372*, 2353-2358.

Lee, S.H., Shin, M.S., Park, W.S., Kim, S.Y., Kim, H.S., Han, J.Y., Park, G.S., Dong, S.M., Pi, J.H., Kim, C.S.*, et al.* (1999). Alterations of Fas (Apo-1/CD95) gene in non-small cell lung cancer. Oncogene *18*, 3754-3760.

Levkau, B., Herren, B., Koyama, H., Ross, R., and Raines, E.W. (1998). Caspase-mediated Cleavage of Focal Adhesion Kinase pp125(FAK) and Disassembly of Focal Adhesions in Human Endothelial Cell Apoptosis. The Journal of Experimental Medicine *187*, 579-586.

Li, H., Zhu, H., Xu, C.J., and Yuan, J. (1998). Cleavage of BID by caspase 8 mediates the mitochondrial damage in the Fas pathway of apoptosis. Cell *94*, 491-501.

Li, J., and Yuan, J. (2008). Caspases in apoptosis and beyond. Oncogene *27*, 6194.

Li, S., Shen, D., Shao, J., Crowder, R., Liu, W., Prat, A., He, X., Liu, S., Hoog, J., Lu, C.*, et al.* (2013). Endocrine-therapy-resistant ESR1 variants revealed by genomic characterization of breast-cancer-derived xenografts. Cell reports *4*, 1116-1130.

Li, W., Laishram, R.S., Ji, Z., Barlow, C.A., Tian, B., and Anderson, R.A. (2012). Star-PAP control of BIK expression and apoptosis is regulated by nuclear PIPKIalpha and PKCdelta signaling. Molecular cell *45*, 25-37.

Lindsten, T., Ross, A.J., King, A., Zong, W.X., Rathmell, J.C., Shiels, H.A., Ulrich, E., Waymire, K.G., Mahar, P., Frauwirth, K.*, et al.* (2000). The combined functions of proapoptotic Bcl-2 family members bak and bax are essential for normal development of multiple tissues. Molecular cell *6*, 1389-1399.

Lindsten, T., and Thompson, C.B. (2006). Cell death in the absence of Bax and Bak. Cell Death And Differentiation *13*, 1272.

Liu, W., Konduri, S.D., Bansal, S., Nayak, B.K., Rajasekaran, S.A., Karuppayil, S.M., Rajasekaran, A.K., and Das, G.M. (2006). Estrogen Receptor-α Binds p53 Tumor Suppressor Protein Directly and Represses Its Function. Journal of Biological Chemistry *281*, 9837-9840.

Liu, X., Dai, S., Zhu, Y., Marrack, P., and Kappler, J.W. (2003). The structure of a Bcl-xL/Bim fragment complex: implications for Bim function. Immunity *19*, 341-352.

Liu, X., Li, P., Widlak, P., Zou, H., Luo, X., Garrard, W.T., and Wang, X. (1998). The 40-kDa subunit of DNA fragmentation factor induces DNA fragmentation and chromatin condensation during apoptosis. Proceedings of the National Academy of Sciences of the United States of America *95*, 8461-8466.

Liu, X., Zou, H., Slaughter, C., and Wang, X. (1997). DFF, a heterodimeric protein that functions downstream of caspase-3 to trigger DNA fragmentation during apoptosis. Cell *89*, 175-184.

Loibl, S., and Gianni, L. (2017). HER2-positive breast cancer. Lancet (London, England) *389*, 2415-2429.

Lomonosova, E., and Chinnadurai, G. (2008). BH3-only proteins in apoptosis and beyond: an overview. Oncogene *27*, S2-19.

Lopez-Munoz, E., Hernandez-Zarco, A., Garcia-Hernandez, N., Alvarado-Cabrero, I., Zarco-Espinosa, G., Salamanca-Gomez, F., and Arenas-Aranda, D. (2012). BIK/NBK gene as potential marker of prognostic and therapeutic target in breast cancer patients. Clin Transl Oncol *14*, 586-591.

Lopez, J., Hesling, C., Prudent, J., Popgeorgiev, N., Gadet, R., Mikaelian, I., Rimokh, R., Gillet, G., and Gonzalo, P. (2012). Src tyrosine kinase inhibits apoptosis through the Erk1/2- dependent degradation of the death accelerator Bik. Cell Death Differ *19*, 1459-1469.

Lu, Y., Lemon, W., Liu, P.Y., Yi, Y., Morrison, C., Yang, P., Sun, Z., Szoke, J., Gerald, W.L., Watson, M.*, et al.* (2006). A gene expression signature predicts survival of patients with stage I non-small cell lung cancer. PLoS Med *3*, e467.

Malhotra, G.K., Zhao, X., Band, H., and Band, V. (2010). Histological, molecular and functional subtypes of breast cancers. Cancer Biol Ther *10*, 955-960.

Marino, G., Niso-Santano, M., Baehrecke, E.H., and Kroemer, G. (2014). Self-consumption: the interplay of autophagy and apoptosis. Nature reviews Molecular cell biology *15*, 81-94.

Marino, M., Galluzzo, P., and Ascenzi, P. (2006). Estrogen signaling multiple pathways to impact gene transcription. Curr Genomics *7*, 497-508.

Marshansky, V., Wang, X., Bertrand, R., Luo, H., Duguid, W., Chinnadurai, G., Kanaan, N., Vu, M.D., and Wu, J. (2001). Proteasomes Modulate Balance Among Proapoptotic and Antiapoptotic Bcl-2 Family Members and Compromise Functioning of the Electron Transport Chain in Leukemic Cells. The Journal of Immunology *166*, 3130-3142.

Masoud, V., and Pagès, G. (2017). Targeted therapies in breast cancer: New challenges to fight against resistance. World Journal of Clinical Oncology *8*, 120-134.

Mathai, J.P. (2005). The role of endoplasmic reticulum BIK in p53-mediated apoptosis In Biochemistry (Montreal: McGill University).

Mathai, J.P., Germain, M., Marcellus, R.C., and Shore, G.C. (2002). Induction and endoplasmic reticulum location of BIK/NBK in response to apoptotic signaling by E1A and p53. Oncogene *21*, 2534-2544.

Mathai, J.P., Germain, M., and Shore, G.C. (2005). BH3-only BIK regulates BAX,BAK-dependent release of Ca2+ from endoplasmic reticulum stores and mitochondrial apoptosis during stress-induced cell death. The Journal of biological chemistry *280*, 23829-23836.

Maxfield, K.E., Taus, P.J., Corcoran, K., Wooten, J., Macion, J., Zhou, Y., Borromeo, M., Kollipara, R.K., Yan, J., Xie, Y.*, et al.* (2015). Comprehensive functional characterization of cancer-testis antigens defines obligate participation in multiple hallmarks of cancer. Nat Commun *6*, 8840.

McDonnell, D.P., and Norris, J.D. (2002). Connections and regulation of the human estrogen receptor. Science (New York, NY) *296*, 1642-1644.

McDonnell, J.M., Fushman, D., Milliman, C.L., Korsmeyer, S.J., and Cowburn, D. (1999). Solution Structure of the Proapoptotic Molecule BID: A Structural Basis for Apoptotic Agonists and Antagonists. Cell *96*, 625-634.

McDonnell, T.J., Deane, N., Platt, F.M., Nunez, G., Jaeger, U., McKearn, J.P., and Korsmeyer, S.J. (1989). bcl-2-immunoglobulin transgenic mice demonstrate extended B cell survival and follicular lymphoproliferation. Cell *57*, 79-88.

McDonnell, T.J., and Korsmeyer, S.J. (1991). Progression from lymphoid hyperplasia to high-grade malignant lymphoma in mice transgenic for the t(14; 18). Nature *349*, 254-256.

McIlroy, D., Tanaka, M., Sakahira, H., Fukuyama, H., Suzuki, M., Yamamura, K., Ohsawa, Y., Uchiyama, Y., and Nagata, S. (2000). An auxiliary mode of apoptotic DNA fragmentation provided by phagocytes. Genes & development *14*, 549-558.

McIlwain, D.R., Berger, T., and Mak, T.W. (2013). Caspase functions in cell death and disease. Cold Spring Harbor perspectives in biology *5*, a008656.

Mebratu, Y.A., Dickey, B.F., Evans, C., and Tesfaigzi, Y. (2008). The BH3-only protein Bik/Blk/Nbk inhibits nuclear translocation of activated ERK1/2 to mediate IFNgamma-induced cell death. The Journal of cell biology *183*, 429-439.

Ménard, S., Pupa, S.M., Campiglio, M., and Tagliabue, E. (2003). Biologic and therapeutic role of HER2 in cancer. Oncogene *22*, 6570.

Miquel, C., Borrini, F., Grandjouan, S., Auperin, A., Viguier, J., Velasco, V., Duvillard, P., Praz, F., and Sabourin, J.C. (2005). Role of bax mutations in apoptosis in colorectal cancers with microsatellite instability. American journal of clinical pathology *123*, 562-570.

Moasser, M.M. (2007). The oncogene HER2: its signaling and transforming functions and its role in human cancer pathogenesis. Oncogene *26*, 6469-6487.

Motoyama, N., Wang, F., Roth, K.A., Sawa, H., Nakayama, K., Nakayama, K., Negishi, I., Senju, S., Zhang, Q., Fujii, S.*, et al.* (1995). Massive cell death of immature hematopoietic cells and neurons in Bcl-x-deficient mice. Science (New York, NY) *267*, 1506-1510.

Musgrove, E.A., and Sutherland, R.L. (2009). Biological determinants of endocrine resistance in breast cancer. Nature Reviews Cancer *9*, 631.

Nagata, S. (2000). Apoptotic DNA fragmentation. Experimental cell research *256*, 12-18.

Nagata, S. (2018). Apoptosis and Clearance of Apoptotic Cells. Annu Rev Immunol *36*, 489-517.

Nakano, K., and Vousden, K.H. (2001). PUMA, a novel proapoptotic gene, is induced by p53. Molecular cell *7*, 683-694.

Naumann, U., Schmidt, F., Wick, W., Frank, B., Weit, S., Gillissen, B., Daniel, P., and Weller, M. (2003). Adenoviral natural born killer gene therapy for malignant glioma. Hum Gene Ther *14*, 1235-1246.

Ndozangue-Touriguine, O., Hamelin, J., and Breard, J. (2008). Cytoskeleton and apoptosis. Biochemical pharmacology *76*, 11-18.

Nicholson, R.I., and Johnston, S.R. (2005). Endocrine therapy--current benefits and limitations. Breast cancer research and treatment *93 Suppl 1*, S3-10.

Nikrad, M., Johnson, T., Puthalalath, H., Coultas, L., Adams, J., and Kraft, A.S. (2005). The proteasome inhibitor bortezomib sensitizes cells to killing by death receptor ligand TRAIL via BH3-only proteins Bik and Bim. Mol Cancer Ther *4*, 443-449.

Niu, D., Wang, G., and Wang, X. (2015). Up-regulation of cyclin E in breast cancer via estrogen receptor pathway. International Journal of Clinical and Experimental Medicine *8*, 910-915.

NobelPrize.org (2018).

O'Lone, R., Frith, M.C., Karlsson, E.K., and Hansen, U. (2004). Genomic targets of nuclear estrogen receptors. Molecular endocrinology (Baltimore, Md) *18*, 1859-1875.

Oda, E., Ohki, R., Murasawa, H., Nemoto, J., Shibue, T., Yamashita, T., Tokino, T., Taniguchi, T., and Tanaka, N. (2000). Noxa, a BH3-only member of the Bcl-2 family and candidate mediator of p53-induced apoptosis. Science (New York, NY) *288*, 1053-1058.

Okouchi, M., Ekshyyan, O., Maracine, M., and Aw, T.Y. (2007). Neuronal apoptosis in neurodegeneration. Antioxidants & redox signaling *9*, 1059-1096.

Opferman, J.T., Iwasaki, H., Ong, C.C., Suh, H., Mizuno, S., Akashi, K., and Korsmeyer, S.J. (2005). Obligate role of anti-apoptotic MCL-1 in the survival of hematopoietic stem cells. Science (New York, NY) *307*, 1101-1104.

Opferman, J.T., and Korsmeyer, S.J. (2003). Apoptosis in the development and maintenance of the immune system. Nature immunology *4*, 410-415.

Opferman, J.T., Letai, A., Beard, C., Sorcinelli, M.D., Ong, C.C., and Korsmeyer, S.J. (2003). Development and maintenance of B and T lymphocytes requires antiapoptotic MCL-1. Nature *426*, 671-676.

Oppermann, M., Geilen, C.C., Fecker, L.F., Gillissen, B., Daniel, P.T., and Eberle, J. (2005). Caspase-independent induction of apoptosis in human melanoma cells by the proapoptotic Bcl-2-related protein Nbk / Bik. Oncogene *24*, 7369-7380.

Ordonez-Mena, J.M., Schottker, B., Mons, U., Jenab, M., Freisling, H., Bueno-de-Mesquita, B., O'Doherty, M.G., Scott, A., Kee, F., Stricker, B.H.*, et al.* (2016). Quantification of the smoking-associated cancer risk with rate advancement periods: meta-analysis of individual participant data from cohorts of the CHANCES consortium. BMC Med *14*, 62.

Osborne, C.K., Wakeling, A., and Nicholson, R.I. (2004). Fulvestrant: an oestrogen receptor antagonist with a novel mechanism of action. British Journal of Cancer *90*, S2-6.

Paik, S., Shak, S., Tang, G., Kim, C., Baker, J., Cronin, M., Baehner, F.L., Walker, M.G., Watson, D., Park, T.*, et al.* (2004). A Multigene Assay to Predict Recurrence of Tamoxifen-Treated, Node-Negative Breast Cancer. New England Journal of Medicine *351*, 2817-2826.

Paquet, C., Schmitt, E., Beauchemin, M., and Bertrand, R. (2004). Activation of multidomain and BH3-only pro-apoptotic Bcl-2 family members in p53-defective cells. Apoptosis *9*, 815-831.

Pepper, C., Lin, T.T., Pratt, G., Hewamana, S., Brennan, P., Hiller, L., Hills, R., Ward, R., Starczynski, J., Austen, B.*, et al.* (2008). Mcl-1 expression has in vitro and in vivo significance in chronic lymphocytic leukemia and is associated with other poor prognostic markers. Blood *112*, 3807-3817.

Perou, C.M., Sørlie, T., Eisen, M.B., van de Rijn, M., Jeffrey, S.S., Rees, C.A., Pollack, J.R., Ross, D.T., Johnsen, H., Akslen, L.A.*, et al.* (2000). Molecular portraits of human breast tumours. Nature *406*, 747.

Ponglikitmongkol, M., Green, S., and Chambon, P. (1988). Genomic organization of the human oestrogen receptor gene. The EMBO Journal *7*, 3385-3388.

Quarrie, L.H., Addey, C.V., and Wilde, C.J. (1996). Programmed cell death during mammary tissue involution induced by weaning, litter removal, and milk stasis. Journal of cellular physiology *168*, 559-569.

Rashmi, R., Pillai, S.G., Vijayalingam, S., Ryerse, J., and Chinnadurai, G. (2008). BH3-only protein BIK induces caspase-independent cell death with autophagic features in Bcl-2 null cells. Oncogene *27*, 1366-1375.

Real, P.J., Sanz, C., Gutierrez, O., Pipaon, C., Zubiaga, A.M., and Fernandez-Luna, J.L. (2006). Transcriptional activation of the proapoptotic bik gene by E2F proteins in cancer cells. FEBS Lett *580*, 5905-5909.

Reynaud, K., and Driancourt, M.A. (2000). Oocyte attrition. Molecular and cellular endocrinology *163*, 101-108.

Rinkenberger, J.L., Horning, S., Klocke, B., Roth, K., and Korsmeyer, S.J. (2000). Mcl-1 deficiency results in peri-implantation embryonic lethality. Genes & development *14*, 23-27.

Ritchie, A., Gutierrez, O., and Fernandez-Luna, J.L. (2009). PAR bZIP-bik is a novel transcriptional pathway that mediates oxidative stress-induced apoptosis in fibroblasts. Cell Death Differ *16*, 838-846.

Rowley, J.D. (1982). Identification of the constant chromosome regions involved in human hematologic malignant disease. Science (New York, NY) *216*, 749-751.

Sabbah, M., Courilleau, D., Mester, J., and Redeuilh, G. (1999). Estrogen induction of the cyclin D1 promoter: Involvement of a cAMP response-like element. Proceedings of the National Academy of Sciences of the United States of America *96*, 11217-11222.

Sakahira, H., Iwamatsu, A., and Nagata, S. (2000). Specific Chaperone-like Activity of Inhibitor of Caspase-activated DNase for Caspase-activated DNase. Journal of Biological Chemistry *275*, 8091-8096.

Samejima, K., and Earnshaw, W.C. (1998). ICAD/DFF regulator of apoptotic nuclease is nuclear. Experimental cell research *243*, 453-459.

Samejima, K., and Earnshaw, W.C. (2005). Trashing the genome: the role of nucleases during apoptosis. Nature reviews Molecular cell biology *6*, 677-688.

Sarosiek, K.A., Chi, X., Bachman, J.A., Sims, J.J., Montero, J., Patel, L., Flanagan, A., Andrews, D.W., Sorger, P., and Letai, A. (2013a). BID preferentially activates BAK while BIM preferentially activates BAX, affecting chemotherapy response. Molecular cell *51*, 751-765.

Sarosiek, K.A., Chi, X., Bachman, J.A., Sims, J.J., Montero, J., Patel, L., Flanagan, A., Andrews, D.W., Sorger, P., and Letai, A. (2013b). BID preferentially activates BAK while BIM preferentially activates BAX, affecting chemotherapy response. Mol Cell *51*, 751-765.

Sasaki, H., Kotsuji, F., and Tsang, B.K. (2002). Caspase 3-mediated focal adhesion kinase processing in human ovarian cancer cells: possible regulation by X-linked inhibitor of apoptosis protein. Gynecologic oncology *85*, 339-350.

Sattler, M., Liang, H., Nettesheim, D., Meadows, R.P., Harlan, J.E., Eberstadt, M., Yoon, H.S., Shuker, S.B., Chang, B.S., Minn, A.J.*, et al.* (1997). Structure of Bcl-xL-Bak peptide complex: recognition between regulators of apoptosis. Science (New York, NY) *275*, 983-986.

Sebbagh, M., Renvoize, C., Hamelin, J., Riche, N., Bertoglio, J., and Breard, J. (2001). Caspase-3-mediated cleavage of ROCK I induces MLC phosphorylation and apoptotic membrane blebbing. Nature cell biology *3*, 346-352.

Shamas-Din, A., Brahmbhatt, H., Leber, B., and Andrews, D.W. (2011). BH3-only proteins: Orchestrators of apoptosis. Biochim Biophys Acta *1813*, 508-520.

Shamas-Din, A., Kale, J., Leber, B., and Andrews, D.W. (2013). Mechanisms of Action of Bcl-2 Family Proteins. Cold Spring Harbor perspectives in biology *5*.

Smith, C.L., and O'Malley, B.W. (2004). Coregulator function: a key to understanding tissue specificity of selective receptor modulators. Endocrine reviews *25*, 45-71.

Smith, I., Yardley, D., Burris, H., De Boer, R., Amadori, D., McIntyre, K., Ejlertsen, B., Gnant, M., Jonat, W., Pritchard, K.I.*, et al.* (2017). Comparative Efficacy and Safety of Adjuvant Letrozole Versus Anastrozole in Postmenopausal Patients With Hormone Receptor-Positive, Node-Positive Early Breast Cancer: Final Results of the Randomized Phase III Femara Versus Anastrozole Clinical Evaluation (FACE) Trial. J Clin Oncol *35*, 1041-1048.

Smith, R.A., Andrews, K., Brooks, D., DeSantis, C.E., Fedewa, S.A., Lortet-Tieulent, J., Manassaram-Baptiste, D., Brawley, O.W., and Wender, R.C. (2016). Cancer screening in the United States, 2016: A review of current American Cancer Society guidelines and current issues in cancer screening. CA Cancer J Clin *66*, 96-114.

Sorlie, T., Perou, C.M., Tibshirani, R., Aas, T., Geisler, S., Johnsen, H., Hastie, T., Eisen, M.B., van de Rijn, M., Jeffrey, S.S., *et al.* (2001). Gene expression patterns of breast carcinomas distinguish tumor subclasses with clinical implications. Proceedings of the National Academy of Sciences of the United States of America *98*, 10869-10874.

Sotiriou, C., Neo, S.Y., McShane, L.M., Korn, E.L., Long, P.M., Jazaeri, A., Martiat, P., Fox, S.B., Harris, A.L., and Liu, E.T. (2003). Breast cancer classification and prognosis based on gene expression profiles from a population-based study. Proceedings of the National Academy of Sciences of the United States of America *100*, 10393-10398.

Sparano, J.A., Gray, R.J., Makower, D.F., Pritchard, K.I., Albain, K.S., Hayes, D.F., Geyer, C.E., Dees, E.C., Goetz, M.P., Olson, J.A., *et al.* (2018). Adjuvant Chemotherapy Guided by a 21-Gene Expression Assay in Breast Cancer. New England Journal of Medicine *379*, 111-121.

Spender, L.C., O'Brien, D.I., Simpson, D., Dutt, D., Gregory, C.D., Allday, M.J., Clark, L.J., and Inman, G.J. (2009). TGF-beta induces apoptosis in human B cells by transcriptional regulation of BIK and BCL-XL. Cell Death Differ *16*, 593-602.

Strasser, A., Harris, A.W., Bath, M.L., and Cory, S. (1990). Novel primitive lymphoid tumours induced in transgenic mice by cooperation between myc and bcl-2. Nature *348*, 331-333.

Strasser, A., Harris, A.W., and Cory, S. (1993). E mu-bcl-2 transgene facilitates spontaneous transformation of early pre-B and immunoglobulin-secreting cells but not T cells. Oncogene *8*, 1-9.

Subramani, R., and Lakshmanaswamy, R. (2017). Pregnancy and Breast Cancer. Prog Mol Biol Transl Sci *151*, 81-111.

Sulston, J.E., and Horvitz, H.R. (1977). Post-embryonic cell lineages of the nematode, Caenorhabditis elegans. Developmental Biology *56*, 110-156.

Sulston, J.E., Schierenberg, E., White, J.G., and Thomson, J.N. (1983). The embryonic cell lineage of the nematode Caenorhabditis elegans. Dev Biol *100*, 64-119.

Sutton, V.R. (2000). Initiation of Apoptosis by Granzyme B Requires Direct Cleavage of Bid, but Not Direct Granzyme B–Mediated Caspase Activation. *192*, 1403-1414.

Tanenbaum, D.M., Wang, Y., Williams, S.P., and Sigler, P.B. (1998). Crystallographic comparison of the estrogen and progesterone receptor's ligand binding domains. Proceedings of the National Academy of Sciences *95*, 5998-6003.

Taylor, R.C., Cullen, S.P., and Martin, S.J. (2008). Apoptosis: controlled demolition at the cellular level. Nature reviews Molecular cell biology *9*, 231-241.

Tong, Y., Yang, Q., Vater, C., Venkatesh, L.K., Custeau, D., Chittenden, T., Chinnadurai, G., and Gourdeau, H. (2001). The Pro-apoptotic Protein, Bik, Exhibits Potent Antitumor Activity That Is Dependent on Its BH3 Domain¹. Molecular Cancer Therapeutics *1*, 95-102.

Toss, A., and Cristofanilli, M. (2015). Molecular characterization and targeted therapeutic approaches in breast cancer. Breast Cancer Res *17*, 60.

Tremont, A. (2017). Endocrine Therapy for Early Breast Cancer: Updated Review. *17*, 405-411.

Tsujimoto, Y., Cossman, J., Jaffe, E., and Croce, C.M. (1985). Involvement of the bcl-2 gene in human follicular lymphoma. Science (New York, NY) *228*, 1440-1443.

Vaux, D.L., Cory, S., and Adams, J.M. (1988). Bcl-2 gene promotes haemopoietic cell survival and cooperates with c-myc to immortalize pre-B cells. Nature *335*, 440-442.

Veis, D.J., Sorenson, C.M., Shutter, J.R., and Korsmeyer, S.J. (1993). Bcl-2-deficient mice demonstrate fulminant lymphoid apoptosis, polycystic kidneys, and hypopigmented hair. Cell *75*, 229-240.

Verma, S., Budarf, M.L., Emanuel, B.S., and Chinnadurai, G. (2000). Structural analysis of the human pro-apoptotic gene Bik: chromosomal localization, genomic organization and localization of promoter sequences. Gene *254*, 157-162.

Verma, S., Zhao, L.J., and Chinnadurai, G. (2001). Phosphorylation of the pro-apoptotic protein BIK: mapping of phosphorylation sites and effect on apoptosis. The Journal of biological chemistry *276*, 4671-4676.

Viedma-Rodriguez, R., Baiza-Gutman, L.A., Garcia-Carranca, A., Moreno-Fierros, L., Salamanca-Gomez, F., and Arenas-Aranda, D. (2013). Suppression of the death gene BIK is a critical factor for resistance to tamoxifen in MCF-7 breast cancer cells. Int J Oncol *43*, 1777-1786.

Viedma-Rodriguez, R., Ruiz Esparza-Garrido, R., Baiza-Gutman, L.A., Velazquez-Flores, M.A., Garcia-Carranca, A., Salamanca-Gomez, F., and Arenas-Aranda, D. (2015). Involvement of multiple cellular pathways in regulating resistance to tamoxifen in BIK-suppressed MCF-7 cells. Tumour Biol *36*, 6991-7005.

Villunger, A., Michalak, E.M., Coultas, L., Mullauer, F., Bock, G., Ausserlechner, M.J., Adams, J.M., and Strasser, A. (2003). p53- and drug-induced apoptotic responses mediated by BH3-only proteins puma and noxa. Science (New York, NY) *302*, 1036-1038.

Wang, C., Mayer, J.A., Mazumdar, A., Fertuck, K., Kim, H., Brown, M., and Brown, P.H. (2011). Estrogen Induces c-myc Gene Expression via an Upstream Enhancer Activated by the Estrogen Receptor and the AP-1 Transcription Factor. Molecular endocrinology (Baltimore, Md) *25*, 1527-1538.

Wang, H.G., Pathan, N., Ethell, I.M., Krajewski, S., Yamaguchi, Y., Shibasaki, F., McKeon, F., Bobo, T., Franke, T.F., and Reed, J.C. (1999). Ca2+-induced apoptosis through calcineurin dephosphorylation of BAD. Science (New York, NY) *284*, 339-343.

Weisz, A., and Rosales, R. (1990). Identification of an estrogen response element upstream of the human c-fos gene that binds the estrogen receptor and the AP-1 transcription factor. Nucleic Acids Research *18*, 5097-5106.

Wickerham, D.L., Fisher, B., Wolmark, N., Bryant, J., Costantino, J., Bernstein, L., and Runowicz, C.D. (2002). Association of tamoxifen and uterine sarcoma. J Clin Oncol *20*, 2758-2760.

Widlak, P., and Garrard, W.T. (2005). Discovery, regulation, and action of the major apoptotic nucleases DFF40/CAD and endonuclease G. Journal of cellular biochemistry *94*, 1078-1087.

Widlak, P., Li, P., Wang, X., and Garrard, W.T. (2000a). Cleavage Preferences of the Apoptotic Endonuclease DFF40 (Caspase-activated DNase or Nuclease) on Naked DNA and Chromatin Substrates. Journal of Biological Chemistry *275*, 8226-8232.

Widlak, P., Li, P., Wang, X., and Garrard, W.T. (2000b). Cleavage preferences of the apoptotic endonuclease DFF40 (caspase-activated DNase or nuclease) on naked DNA and chromatin substrates. J Biol Chem *275*, 8226-8232.

Willis, S.N., Chen, L., Dewson, G., Wei, A., Naik, E., Fletcher, J.I., Adams, J.M., and Huang, D.C. (2005). Proapoptotic Bak is sequestered by Mcl-1 and Bcl-xL, but not Bcl-2, until displaced by BH3-only proteins. Genes & development *19*, 1294-1305.

Woo, E.J., Kim, Y.G., Kim, M.S., Han, W.D., Shin, S., Robinson, H., Park, S.Y., and Oh, B.H. (2004). Structural mechanism for inactivation and activation of CAD/DFF40 in the apoptotic pathway. Molecular cell *14*, 531-539.

Wu, H., Medeiros, L.J., and Young, K.H. (2018). Apoptosis signaling and BCL-2 pathways provide opportunities for novel targeted therapeutic strategies in hematologic malignances. Blood reviews *32*, 8-28.

Wu, Q., Li, J., Zhu, S., Wu, J., Chen, C., Liu, Q., Wei, W., Zhang, Y., and Sun, S. (2017). Breast cancer subtypes predict the preferential site of distant metastases: a SEER based study. Oncotarget *8*, 27990-27996.

Xie, X., Xia, W., Li, Z., Kuo, H.P., Liu, Y., Li, Z., Ding, Q., Zhang, S., Spohn, B., Yang, Y., *et al.* (2007). Targeted expression of BikDD eradicates pancreatic tumors in noninvasive imaging models. Cancer cell *12*, 52-65.

Yang, N., and Goping, I.S. (2013). Apoptosis. Colloquium Series on Building Blocks of the Cell: Cell Structure and Function *1*, 1-101.

Ye, D.Z., Jin, S., Zhuo, Y., and Field, J. (2011). p21-Activated kinase 1 (Pak1) phosphorylates BAD directly at serine 111 in vitro and indirectly through Raf-1 at serine 112. PloS one *6*, e27637.

Yersal, O., and Barutca, S. (2014). Biological subtypes of breast cancer: Prognostic and therapeutic implications. World J Clin Oncol *5*, 412-424.

Yin, X.M., Wang, K., Gross, A., Zhao, Y., Zinkel, S., Klocke, B., Roth, K.A., and Korsmeyer, S.J. (1999). Bid-deficient mice are resistant to Fas-induced hepatocellular apoptosis. Nature *400*, 886-891.

Youlden, D.R., Cramb, S.M., Dunn, N.A., Muller, J.M., Pyke, C.M., and Baade, P.D. (2012). The descriptive epidemiology of female breast cancer: an international comparison of screening, incidence, survival and mortality. Cancer Epidemiol *36*, 237-248.

Yu, C., Gong, Y., Zhou, H., Wang, M., Kong, L., Liu, J., An, T., Zhu, H., and Li, Y. (2017). Star-PAP, a poly(A) polymerase, functions as a tumor suppressor in an orthotopic human breast cancer model. Cell Death Dis *8*, e2582.

Yunis, J.J. (1983). The chromosomal basis of human neoplasia. Science (New York, NY) *221*, 227-236.

Zhang, J., Liu, X., Scherer, D.C., van Kaer, L., Wang, X., and Xu, M. (1998). Resistance to DNA fragmentation and chromatin condensation in mice lacking the DNA fragmentation factor 45. Proceedings of the National Academy of Sciences of the United States of America *95*, 12480-12485.

Zhang, J.H., and Xu, M. (2000). DNA fragmentation in apoptosis. Cell Research *10*, 205.

Zhu, H., Zhang, L., Dong, F., Guo, W., Wu, S., Teraishi, F., Davis, J.J., Chiao, P.J., and Fang, B. (2005). Bik/NBK accumulation correlates with apoptosis-induction by bortezomib (PS-341, Velcade) and other proteasome inhibitors. Oncogene *24*, 4993-4999.

Zong, W.X., Lindsten, T., Ross, A.J., MacGregor, G.R., and Thompson, C.B. (2001). BH3-only proteins that bind pro-survival Bcl-2 family members fail to induce apoptosis in the absence of Bax and Bak. Genes & development *15*, 1481-1486.

Zou, Y., Peng, H., Zhou, B., Wen, Y., Wang, S.-C., Tsai, E.-M., and Hung, M.-C. (2002). Systemic Tumor Suppression by the Proapoptotic Gene bik. Cancer Research *62*, 8-12.

CHAPTER 2

MATERIALS AND METHODS

2.1 Gene expression and tissue microarray data collection and analysis

2.1.1 Origins of Dataset-1 and Dataset-2

Dataset-1 consisted of gene expression analysis collected from 175 primary breast cancer patients as described by (Germain et al., 2011). Briefly; gene expression was obtained by hybridization of cy3-labeled mRNA to Agilent Whole Genome Arrays (Agilent #5188-5339 and 5188-5282). Hybridized arrays were scanned using an Agilent scanner; data were extracted and evaluated for quality using Feature Extraction Software 9.5 (Agilent, USA). The data was normalized against internal controls using GeneSpring GX 7.3.1 (Agilent, USA) program. The mRNA expression values were deposited in the Gene Expression Omnibus (*GEO*) database repository (https://www.ncbi.nlm.nih.gov/geo/) with GEO accession ID GSE22820. This cohort is referred to as Dataset-1 in this study and is originally labeled as the BREAD study (Germain et al., 2011).

Dataset-2 consisted of a tissue microarray (TMA) that was generated from formalin-fixed tumor samples obtained for 152 primary breast cancer patients as described by Craik et al. (Craik et al., 2010). Briefly, the TMA was prepared by punching at least two 0.6 mm tumor cores from formalin fixed paraffin embedded (FFPE) blocks and embedding them in recipient paraffin blocks. 6 μm sections were cut, and glass slides were generated for subsequent immunohistochemistry analysis. This TMA is referred to as Dataset-2 and is originally labeled as the TUBULIN study (Craik et al., 2010). There was 8% overlap with 13 patients represented in both datasets (% overlap=2 x 13 patients in both/[175+152]).

2.1.2 Tissue microarray immunohistochemistry

TMAs were deparaffinized by dipping in xylene (Fisher scientific, #X3p-1GA) 3 times for 10 min each. Serial rehydration of the slides was performed by incubating in 95%, 80%, 50 % and to 0% ethanol (Commercial alcohols, #P016EA95) solutions for 20 min each. Epitope retrieval was performed by microwaving in epitope retrieval buffer (10 mM citrate, 0.05% Tween-20; pH 6.0) in a pressure cooker for 5 min at high power (750 W). After the pressure cooker was cool, slides were placed into TBST (50 mM Tris-Cl, 150 mM NaCl, 0.05% Tween 20, pH 7.6) for a few minutes. Excess liquid was removed by wiping the slides at the edges, and a hydrophobic barrier was created using a wax pencil to retain the immunostaining reagents on the tissues. TMAs were blocked using 0.5% w/v fish gelatin (Sigma, #G7041) made in TBST. Subsequently, the slides were incubated with anti-BIK (1:300; Santa Cruz Biotechnology, #SC-1710) or anti-BCL-2 antibodies (1:300; Dako, #M0887) diluted in Dako antibody diluent (Dako, #S080983) at 4°C overnight. Next day, the slides were rinsed with TBS (50 mM Tris-Cl, 150 mM NaCl, pH 7.6) for 1 min followed by a wash in TBST once for 10 min. Tissue-intrinsic peroxidase was inactivated by treating the slides with 3% H_2O_2 (Fisher scientific, #H325) in TBS for 15 min followed by washing 2 times with TBST for 2 min each. Next, signal amplification was achieved by incubation of slides in Dako EnVision+System-HRP (Dako, #K4006) system secondary antibody for 1 h at room temperature. Immunostaining signal was detected by treating slides using Dako Liquid Dab + Substrate chromogen System (Dako, #K3467) and monitoring under a microscope for proper signal strength development. Excess substrate was washed off using tap water. The immunohistochemical signal was further darkened by treating with 1% Copper sulfate (Sigma,

#C7631) prepared in distilled water for 5 min. Subsequently, nuclear counterstaining was performed using 0.5% hematoxylin (Fisher Scientific, #3530-32) for 1-5 min until a sufficient staining intensity was obtained. Slides were dehydrated by subsequent incubations in 0%, 50%, 80% and 95% ethanol solutions for 20 min each followed by mounting under glass coverslips with Permount mounting medium (Fisher scientific, #SP15-100). Scoring of the TMA was performed in an outcome blinded fashion in consultation with pathologist Dr. Judith Hugh (University of Alberta). Score values were assigned on a scale of 0 to 3 with 0 being the weakest and 3 being the darkest staining intensities.

2.1.3 Statistical correlation analysis of *BIK* mRNA and protein levels

13 patients in Datasets 1 and 2 had the same patient IDs, and therefore both *BIK* transcript and protein expression data were available for that group. Linear correlation between continuous *BIK* transcript and protein levels was graphed as a scatter plot (MedCalc Software bvba, Ostend, Belgium; http://www.medcalc.org; 2017), followed by calculation of Pearson's (parametric) and Spearman's (non-parametric) coefficients with a p value (MedCalc Software bvba, Ostend, Belgium; http://www.medcalc.org; 2017) (Altman, 1991; Armitage, 2002). Next, *BIK* transcript and protein levels were converted into categorical variables (0=low, 1=high) using ROC curve analysis discussed in section 2.2.2. Correlations between the *BIK* transcript and proteins levels (in the categorical form) were analyzed using Chi-squared analysis and Fisher's exact tests (MedCalc Software bvba, Ostend, Belgium; http://www.medcalc.org; 2017).

2.2 Patient survival analyses with respect to gene and protein expression

2.2.1 Calculation of 5-years prognostic outcomes of patients

Disease recurrence or death was calculated for 5 years (1825 days) from the date of diagnosis using 'If, AND/OR' functions in Microsoft Excel (Microsoft Corp. USA).

2.2.2 Receiver operator curve (ROC) analysis

Raw data for gene and protein expression were represented in a continuous form. In order to identify a cutpoint to dichotomize these values into "low" and "high" groups with the best combination of sensitivity and specificity to predict outcome, ROC analysis was performed with 5-year disease recurrence as the classification variable using MedCalc Version 17.9.6 program (MedCalc Software bvba, Ostend, Belgium; http://www.medcalc.org; 2017). Marker expression values in their continuous form were entered in the "variables" category, and presence or absence of recurrence in the 5-years was entered in the "classification variable" category. The program calculated the best cutpoint based on the methodology of DeLong et al. (DeLong et al., 1988).

2.2.3 Kaplan-Meier survival curves and log-rank test

5 years disease-free or overall survivals of the patients was calculated using the MedCalc Version 17.9.6 program (MedCalc Software bvba, Ostend, Belgium; http://www.medcalc.org; 2017). Kaplan-Meier curves were plotted by entering 5-years disease-free or overall survival (calculated in Microsoft Excel) in the "survival time" category. Recurrence/death was entered as categorical variables (calculated for 5 years in Microsoft Excel) in the "endpoint" category and marker expression values were entered as categorical variables (calculated using ROC curve analysis) in the "variables" category. The MedCalc program automatically calculated hazard ratio

and p values based on the log-rank test. Patients lost to follow-up before 5-years were censored and indicated with a small vertical line on the Kaplan-Meier survival curves.

2.2.4 Cox regression (univariate and multivariate) analyses

Cox regression analysis was performed using the MedCalc Version 17.9.6 program (MedCalc Software bvba, Ostend, Belgium; http://www.medcalc.org; 2017). For univariate analysis, the 5-years disease-free survival time calculated using Microsoft Excel (Microsoft Corp. USA) was entered in the "survival time" category. Recurrence was entered as a categorical variable (calculated for 5 years in Microsoft Excel) in the "endpoint" category. Marker expression values were entered as categorical variables in the "predictor variables" category. The MedCalc program calculated the cumulative hazard and p-value.

For multivariate analysis, the 5-years disease-free survival time calculated using Microsoft Excel (Microsoft Corp. USA) was entered in the "survival time" category. Recurrence was entered as a categorical variable (calculated for 5 years in Microsoft Excel) in the "endpoint" category. More than one marker was selected and their expression values were entered as categorical variables in the "predictor variables" category. In the options menu, the method was selected as "stepwise". The p-value threshold was set at 0.05. The MedCalc program calculated the cumulative hazard and p-value for multiple variables entered simultaneously.

2.3 Reagents, cell culture, molecular cloning, and treatments

2.3.1 Reagents

All commonly used chemicals for reagent and buffer preparation were purchased from either (Fisher Scientific, USA) or (Sigma, USA) unless otherwise stated. Pan-caspase inhibitor z-VAD-fmk was obtained from either (BD Pharmingen, #550377) or (Promega, #G7232). Ampicillin, doxycycline, and puromycin were purchased from (Sigma, #A9518, D9891, P8833 respectively), and G418 was purchased from (Invitrogen, #11811031).

2.3.2 Antibodies used in the study

Protein	**Assay method**	**Cat. No**	**Dilution medium**	**Dilution**
Phospho Ser139-H2AX	IF	Cell Signalling Technologies-8718S	4%NDS	1:500
	IB		5% BSA	1:3000
BIK	IHC	Santa Cruz Biotechnology-SC-1710	3% BSA	1:300
	IF		4% NDS	1:500
	IB		5% Milk	1:500
Calnexin	IF	(Lynes et al., 2012)	4% NGS	1:250
Caspase-7 (full length)	IB	Cell Signalling Technologies -9492	5% Milk	1:1000
Caspase-7 (cleaved)	IB	Cell Signalling Technologies -9491	5% Milk	1:1000
CAD	IB	ProScie-2107	5% Milk	1:200
GRP78	IB	Abcam-Ab21685	5% Milk	1:2000
BCL-2	IB	Cell Signalling Technologies -2872S	5% Milk	1:2000
BCL-XL	IB	Cell Signalling Technologies -2762S	5% Milk	1:1000
MCL-1	IB	Sigma-M8434	5% Milk	1:1000
LC3B	IB	Cell Signalling Technologies -2775s	5% Milk	1:1000
α-Tubulin	IB	Sigma-5168	5% milk	1:100,000

2.3.3 Common solutions/buffers used in the study

Buffer	**Formulation**
Epitope retrieval buffer	10 mM citrate, 0.05% Tween-20; pH 6.0
1X TBST	50 mM Tris-Cl, 150 mM NaCl, 0.05% Tween 20, pH 7.6
2X sample solubilization buffer	250 mM Tris-HCL pH 6.8, 4% SDS, 30% glycerol, 0.003% bromophenol blue and 10% 2-mercaptoethanol
10X PBS	27 mM KCl, 15 mM KH_2PO_4, 1380 mM NaCl, 81 mM $Na_2HPO_4.7H_2O$ pH 7.4
RIPA cell lysis buffer	50 mM Tris-cl, 150 mM NaCl, 0.1% SDS, 1% NP-40, 0.5% deoxycholate, and 1 mM EDTA, pH 7.5 supplemented with protease inhibitor cocktail- (Roche, #11873580001) and phosphatase inhibitor cocktail (Roche, #04906837001,)
Comet assay *in situ* lysis buffer	2.5 M NaCl, 100 mM EDTA, 10 mM Trizma base, 1% TX-100, pH 8
Comet assay alkaline unwinding solution	200 mM NaOH, 1 mM EDTA, pH 10
Comet assay alkaline electrophoresis solution	200 mM NaOH, 1 mM EDTA, pH>13
SDS-PAGE running buffer	3.5 mM SDS, 25 mM Tris, 192 mM Glycine
Western blot transfer buffer	192 mM glycine, 25 mM Tris, 20% methanol
1X TE buffer	10 mM Tris pH 7.5, 1 mM EDTA pH 8.0
10X PBS	27 mM KCl, 15 mM KH_2PO_4, 1380 mM NaCl, 81 mM $Na_2HPO_4.7H_2O$ pH 7.4
Crystal violet colony staining solution	0.4% (w/v) Crystal Violet, 1% Formaldehyde (v/v), 1% Methanol (v/v) made in 1XPBS
Crystal violet soft-agar colony staining solution	0.005% Crystal Violet (w/v), 1% Formaldehyde (v/v), 1% Methanol (v/v) made in 1XPBS

2.3.4 Cell culture

All cell lines were cultured in RPMI-1640 medium (Invitrogen, #11835-030) with 10% fetal bovine serum (FBS) (Sigma, #F1051) unless otherwise described. Cell lines were periodically tested for mycoplasma contamination by MycoSensor PCR assay kit (Agilent Technologies, #302107) and were found to be mycoplasma-free.

2.3.5 Molecular cloning

2.3.5.1 Generation of pCDNA3.2 -DEST- BIKΔBH3

Human *BIK* cDNA in the pCDNA3.2-DEST mammalian vector was a kind gift from Dr. Michele Barry (University of Alberta). BIKΔBH3 cDNA was generated by using inverse PCR utilizing the following two oppositely oriented 5'-phospho primers:

ΔBH3 FW	5'P- ATGGACGTGAGCCTCAGGGCCCCG
ΔBH3 RV	5'P-CCGCAGGGCCAATGCGTC

The following PCR mixture and cycling conditions were used to perform inverse PCR reaction:

PCR mixture:

Ingredient	Volume (µL)
dH_2O	32.5
5X HF buffer (NEB, #B0518S)	10
10 mM dNTPs	1.0
10 µM BIK FW BamH I	2.5
10 µM BIK RV EcoR I	2.5
50 ng Template DNA	1.0
Phusion DNA polymerase (NEB, #M0530s)	0.5
Total volume	50

Cycling conditions:

Step	Condition	Temp °C	Time
1	Initial denaturation	98	30 sec
2	Denaturation	98	10 sec
3	Annealing	60	20 sec
4	Extension	72	20 sec
5	Go to step 2 x 29 times		
6	Final extension	72	5 min
7	Hold	12	∞

This caused exclusion of the region encoding the core 7 amino acids (LACIGDE) of the BH3 domain of BIK. The PCR product (plasmid minus the BH3 domain) was blunt-end ligated using T4 DNA ligase (New England Biolabs, #M0202S) to produce pCDNA3.2-DEST BIKΔBH3 (Figure 2.1). Deletion of the BH3 domain was confirmed by sequencing the plasmid and also by running a western blot that confirmed a faster running product immunoreactive with the anti-BIK antibody.

2.3.5.2 Generation of pRetroX-Tight-pur-BIK and pRetroX-Tight-pur-BIKΔBH3

Sub-cloning of Wt BIK and BIKΔBH3 into a rTet responsive pRetroX-Tight-pur vector (Clontech, #631128) was performed to produce pRetroX-Tight-pur-BIK (Figure 2.2A) and pRetroX-Tight-pur-BIKΔBH3 (Figure 2.2B), as described below. Wt BIK or BIKΔBH3 cDNA were amplified from the pCDNA3.2-DEST vector using the following primers containing restriction sites for directional cloning:

BIK FW BamH I	5'GTCAGAGGATCCATGTCTGAAGTAAGACCCCTCTCC3'
BIK RV EcoR I	5'ATGCACGAATTCTCACTTGAGCAGCAGGTGCAG3'

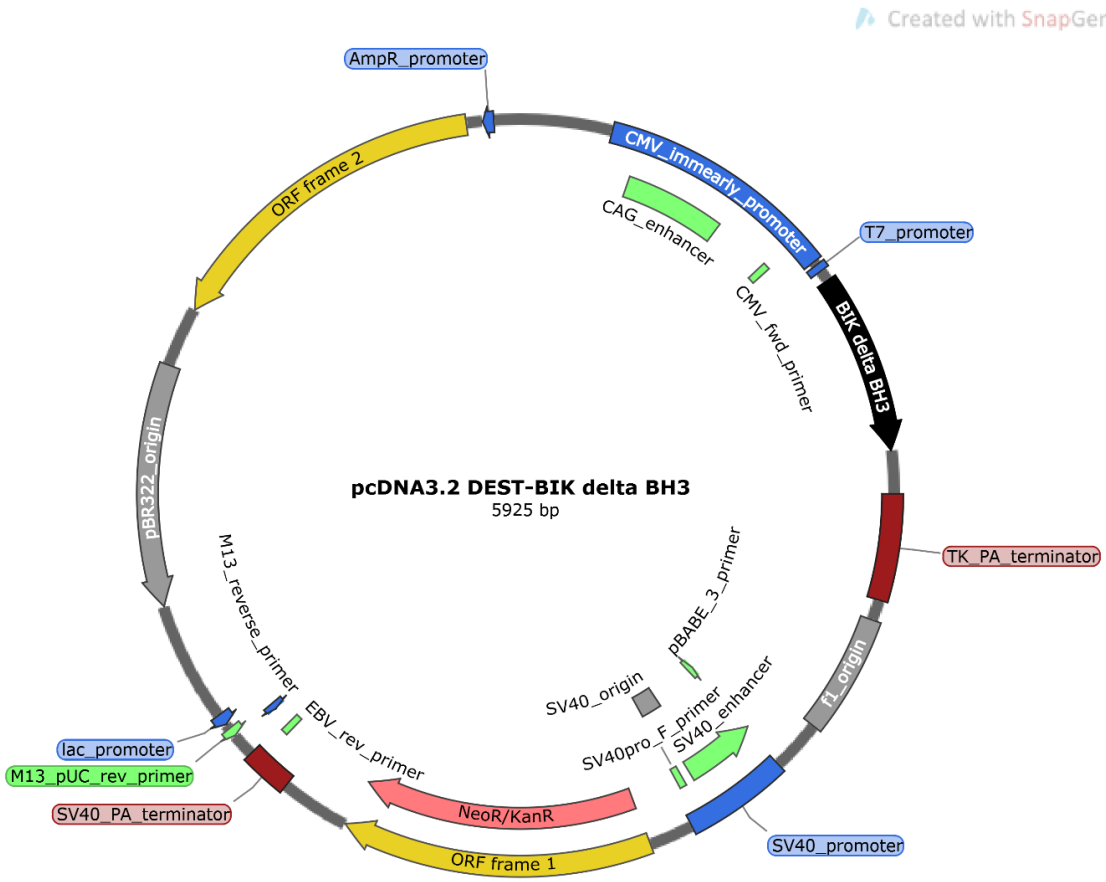

Figure 2.1 Plasmid map of pCDNA3.2-DEST-BIKΔBH3

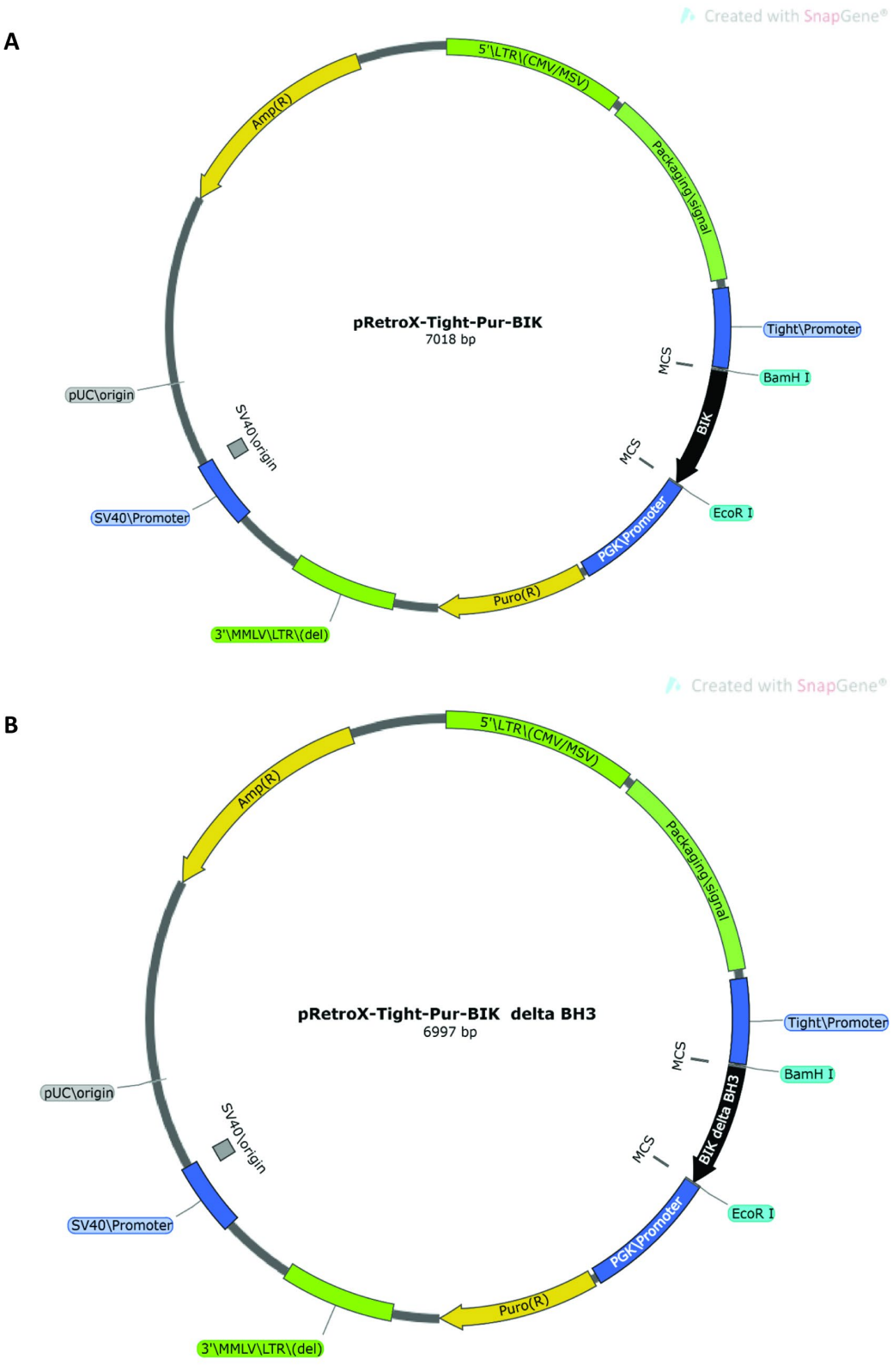

Figure 2.2 Plasmid maps of A. pRetroX-Tight-Pur-BIK and B. pRetroX-Tight-Pur-BIK delta BH3

The following PCR mixture and cycling conditions were used:

PCR mixture:

Ingredient	Volume (µL)
dH_2O	32.5
5X HF buffer (NEB, #B0518S)	10
10 mM dNTPs	1.0
10 µM BIK FW BamH I	2.5
10 µM BIK RV EcoR I	2.5
50 ng Template DNA	1.0
Phusion DNA polymerase (NEB, #M0530s)	0.5
Total volume	50

Cycling conditions:

Step	Condition	Temp °C	Time
1	Initial denaturation	98	30 sec
2	Denaturation	98	10 sec
3	Annealing	60	20 sec
4	Extension	72	20 sec
5	Go to step 2 x 29 times		
6	Final extension	72	5 min
7	Hold	12	∞

The PCR product was gel purified using GeneJET gel extraction kit (Fermentas, #K0691), followed by restriction digestion of the PCR product and pRetroX- Tight- pur vector using BamHI and EcoRI high fidelity restriction enzymes (New England Biolabs, #R3136S and R3101S respectively). pRetroX-Tight-pur vector was dephosphorylated by calf intestinal alkaline phosphatase (New England Biolabs, #M0290S) to prevent any vector self-ligation. Insert and vector were phenol:

chloroform extracted, ethanol precipitated, and relative amounts assessed by agarose gel electrophoresis followed by nucleic acid staining with SYBR Safe (Invitrogen, #S33102) and visualization by a dual UV transilluminator (VWR, #89131-468). The ligation reaction was assembled at a molar ratio of (3:1=insert: vector) with T4 DNA ligase (New England Biolabs, #M0202S) at 12°C overnight on a thermal cycler (Bio-Rad, #184-1100). Ligated plasmids were transformed into E. coli DH5α chemically competent cells (Invitrogen, #18265017) and ampicillin resistant colonies were isolated. The presence of an insert from purified plasmid DNA was screened using restriction digestion and gel electrophoresis. Thee positive clones were sequenced and were 100% identical to human BIK cDNA sequence (GeneBank Accession #CR541863) when compared using SnapGene software (from GSL Biotech; available at snapgene.com).

2.3.6 Anti-estrogen treatments of ER-positive breast cancer cells

Tamoxifen (Sigma, #T5648) and (Z)-4-hydroxytamoxifen (4-HT) (Abcam, #ab141943) were dissolved in DMSO (Sigma, #276855) at a stock concentration of 1 mM. The experiment was performed under low light conditions to minimize changes in chirality of Tamoxifen and 4-HT. MCF-7 cells were grown in phenol red-free RPMI (ThermoFisher Scientific, #11835-030) +10% FCS growth medium and treated with Tamoxifen or 4-HT at the indicated concentrations for 72 h. Cell lysates were prepared in RIPA buffer (50 mM Tris-HCl, 150 mM NaCl, 0.1% SDS, 1% NP-40, 0.5% deoxycholate, and 1 mM EDTA, pH 7.5) supplemented with protease inhibitor cocktail- (Roche, #11873580001) and phosphatase inhibitor cocktail (Roche, #04906837001), according the manufacturers' instructions.

2.4 Western blotting

Cells were harvested with 0.05% trypsin-EDTA solution (Life Technologies, #25300-062). Trypsin was neutralized with 5 times volume of the growth medium, and the cell suspension was centrifuged at 230 x g for 5 min at 4°C in an Eppendorf 5810 centrifuge equipped with a swinging bucket rotor. Cell pellets were washed once with 1mL PBS and resuspended in RIPA lysis buffer (50 mM Tris-cl, 150 mM NaCl, 0.1% SDS, 1% NP-40, 0.5% deoxycholate, and 1 mM EDTA, pH 7.5) supplemented with protease (Roche, #11873580001) and phosphatase inhibitors (Roche, #04906837001) on ice for 10 min. Cell homogenates were sonicated using a Branson SONIFIER 450 model sonicator (BRANSON Ultrasonics corporation, #S-450) for 5 sec at the lowest amplitude followed by centrifugation at 12,000 x g for 10 min at 4°C. The supernatant was collected, and protein concentration was measured using a Pierce BCA protein assay kit (ThermoFisher Scientific, #23225). 20µg of cell lysates were then mixed with equal volume of 2X sample solubilization buffer (250 mM Tris-HCl pH 6.8, 4% SDS, 30% glycerol, 0.003% bromophenol blue and 10% 2-mercaptoethanol) and boiled for 10 min. Boiled lysates were loaded onto 12% SDS polyacrylamide gels (SDS-PAGE), along with 5 µL of PageRuler Prestained Protein Ladder (ThermoFisher Scientific, #26616). Proteins were resolved at 120 V for 100 min and transferred to nitrocellulose membranes (Amersham, #45004004) using a Bio-Rad wet-transfer apparatus (Bio-Rad, #1703930) for 75 min at 400 mA. Membranes were blocked in Tris-buffered saline (50 mM Tris-HCl, 150 mM NaCl, pH 7.5) containing 0.1% Tween-20 (TBST) and 5% skim milk as mentioned on section 2.3.2 1 for 1 h at room temperature. Membranes were incubated with specific primary antibodies (refer to section 2.3.2) diluted in 5% Milk or 5% BSA as mentioned in Table 2.1 overnight at 4°C. After washing 4 times in TBST for 5 min each on a rotary shaker (56 revolutions/min), membranes were incubated with the appropriate HRP-conjugated

secondary antibodies (1:5000) (Santa Cruz Biotechnology, BioRad and Cell signalling technologies, USA) followed by signal detection using ECL reagent (Amersham, #45000875) and X-ray film (FUJIFILM, #4741019291). Blots were scanned using an Epson scanner (Epson, #J192A) at 600 dpi resolution with Epson Scan program. Densitometric analysis of the images of the scanned blots was performed using ImageJ (1.51j8) program.

2.5 Generation of BIK expressing breast cancer cell lines

A total of 3 categories of cell lines are mentioned in this thesis. A summary of their names, plasmids integrated and section explaining how they were generated are mentioned in Table 2.1.

2.5.1 Doxycycline inducible cell lines

A Doxycycline (Dox)-inducible MCF-7 Tet-On cell line was generated by transfecting MCF-7 cells with pTet-On vector (Clontech, #631018) followed by selection with 100 μg/mL G418 (Invitrogen, #11811031). A single clone was picked, and Tet repressor expression was confirmed using western blot with the anti-TetR antibody (Clontech, #631131). MDA-MB-231 Tet-On cell line was a gift from Dr. Judith Hugh (University of Alberta). Dox-inducible BIK expressing cell lines were produced by retroviral transduction with replication-deficient retroviral particles containing BIK or BIKΔBH3/pRetroX-Tight-pur vector following the manufacturer's instructions (Clontech, #632104). Briefly, GP2-293 cells plated in 10 cm tissue culture dishes were transiently transfected with 1:1 ratio of pRetroX-Tight-pur-BIK and pAmpho (Clontech, #632104) plasmids using 60 μL Lipofectamine 2000 (Invitrogen, #11668-027) and a total of 24 μg DNA in a total volume of 1.5 mL OptiMEM (Life Technologies, #31985-070) to produce retroviral particles. Growth medium

Table 2.1 Summary of the cell lines used in the study

Reference to section	Category	Cell line name	Name in the freezer if different	Plasmid(s) integrated
2.5.1	Dox-inducible cell lines	MCF-7 Tet-On EV	N/A	pTet-On, pRetroX-Tight-pur
		MCF-7 Tet-On BIK	N/A	pTet-On, pRetroX-Tight-pur BIK
		MCF-7 Tet-On BIKΔBH3	N/A	pTet-On, pRetroX-Tight-pur BIKΔBH3
		MDA MB 231 Tet-On EV	N/A	pLVX-Tet-On Advanced, pRetroX-Tight-pur
		MDA MB 231 Tet-On BIK	N/A	pLVX-Tet-On Advanced, pRetroX-Tight-pur BIK
2.5.2	BIK expressing stable cell lines	MCF-7 V6	N/A	pCDNA3.2-DEST
		MCF-7 B1	N/A	pCDNA3.2-DEST-BIK
		MCF-7 B5	N/A	pCDNA3.2-DEST-BIK
		MDA-MB-231 V13	N/A	pCDNA3.2-DEST
		MDA-MB-231 V16	N/A	pCDNA3.2-DEST
		MDA-MB-231 B28	N/A	pCDNA3.2-DEST-BIK
		MDA-MB-231 B33	N/A	pCDNA3.2-DEST-BIK
2.5.3	Long term cultured cell lines	EV-LTC-0	MCF-7 Tet-On EV_ 0 Dox_p10	pTet-On, pRetroX-Tight-pur
		EV-LTC-10	MCF-7 Tet-On EV_ 10 Dox_p10	pTet-On, pRetroX-Tight-pur
		EV-LTC-25	MCF-7 Tet-On EV_ 25 Dox_p10	pTet-On, pRetroX-Tight-pur
		EV-LTC-50	MCF-7 Tet-On EV_ 50 Dox_p10	pTet-On, pRetroX-Tight-pur
		EV-LTC-250	MCF-7 Tet-On EV_ 250 Dox_p10	pTet-On, pRetroX-Tight-pur
		BIK-LTC-0	MCF-7 Tet-On BIK_ 0 Dox_p10	pTet-On, pRetroX-Tight-pur BIK
		BIK-LTC-10	MCF-7 Tet-On_BIK_10 Dox_p10	pTet-On, pRetroX-Tight-pur BIK
		BIK-LTC-25	MCF-7 Tet-On BIK_25 Dox_p10	pTet-On, pRetroX-Tight-pur BIK
		BIK-LTC-50	MCF-7 Tet-	pTet-On, pRetroX-Tight-

			On_BIK_50 Dox_p10	pur BIK
		BIK-LTC-250	MCF-7 Tet-On_BIK_250 Dox_p10	pTet-On, pRetroX-Tight-pur BIK

containing viral particles was harvested at 24, 48 and 72 h intervals, filtered through a low protein binding filter (Millipore, #SLHP033RS) and supplemented with 4 μg/mL polybrene (Sigma, #H9268). MCF-7-Tet-On or MDA-MB-231 Tet-On cells were grown parallel to the GP2-293 cells producing viral particles and transduced with freshly harvested particles at 24, 48 and 72 h intervals by adding 1.5 mL viral supernatant to 12-well plates seeded with 2 x 10^5 cells. Immediately after the addition of viral particles, the tissue culture plates were placed in a plate-holder adapter within a swinging bucket equipped with a screw cap for containment and centrifuged at 300 x g for 1 h at RT. Plates were then placed in the tissue culture incubator. Twenty-four hours after transduction, medium was changed to selection medium containing 1 μg/mL puromycin (Sigma, #P8833) and 100 μg/mL G418 (Invitrogen, #11811031) for 7 days to eliminate untransduced cells. G418 selection is for maintaining selective pressure on cells containing pTet-On vector and Puromycin selection is for selecting cells positive for pRetroX-Tight-pur integrations. Stable colonies formed by selected cells were pooled and expanded. Dox-titration to test dose-dependent increase in BIK protein levels were assessed by western blot and immunofluorescence. All cell manipulations up to this point were performed in Tet-free serum (Clontech, #631101) and then switched to regular serum (Sigma, #F1051) after confirmation of lack of leaky BIK expression by western blots. For subsequent experiments, MCF-7 Tet-On BIK and MDA-MB-231 Tet-On BIK cell lines were grown in RPMI-1640 + 10% FBS medium after confirming the absence of any leaky expression.

2.5.2 BIK expressing stable cell lines

1.5 x 10^5 MCF-7 or MDA-MB-231 cells were plated in 24-well plates. The following day, cells were transfected with 0.8 μg of pCDNA3.2-DEST-BIK or pCDNA3.2-DEST plasmids for 24 h

using Lipofectamine 2000 (Invitrogen, #11668-027) with the following procedure. 0.8 µg plasmid DNA was diluted in 50 µL OptiMEM reduced serum medium (Life Technologies, #31985-070) and incubated for 5 min at room temperature. 2 µL Lipofectamine 2000 (Invitrogen, #11668-027) was mixed with 50 µL OptiMEM reduced serum medium (Life Technologies, #31985-070) and incubated for 5 min at room temperature. Subsequently, plasmid DNA and Lipofectamine 2000 were mixed by vigorous pipetting and incubated for 20 min at room temperature. These transfection complexes were added to the cells along with 400 µL regular growth medium. 6 h later, transfection complexes were removed, fresh growth medium was added, and cells were allowed to grow for 48 h. Subsequently, cells were harvested with trypsinization and transferred to 15 cm diameter cell culture plates. The following day, growth medium containing 1 mg/mL G418 was added (selection agent concentration was previously optimized by a kill curve assay) to select for stable clones. Selection medium was replaced every 3 days, colonies were allowed to form for 10 days, and visible colonies were circle-marked on the bottom of the cell culture plate using a marker pen. Single clones were picked by washing the plates with 1XPBS followed by spot trypsinization, transferred to 24-well plates and expanded. Clones were tested for BIK expression by western blot analysis using the anti-BIK antibody as described in section 2.4. All stable cell lines were subsequently cultured in growth medium containing 0.5 mg/mL G418 (Invitrogen, #11811031) to maintain selective pressure.

2.5.3 Long-term culture (LTC) cell lines

2.5×10^5 MCF-7 Tet-On BIK or Empty vector (EV) cells were seeded in 6-well dishes in RPMI-1640 + 10% FBS growth medium supplemented with 100 µg/mL G418 (Invitrogen, #11811031) and 1 µg/mL puromycin (Sigma, #P8833). 24 h later, cells were induced with 10, 25,

50 or 250 ng/mL doxycycline (Sigma, #D9891) containing growth medium. Cells were split every 3 days for 10 passages and continually maintained under doxycycline stimulation. At the end of 10 passages, an aliquot of cells was obtained by trypsinization and tested using western blotting for expression of BIK and persistence of γH2AX signal. These cells that underwent long-term culture were designated by the plasmid they contained (EV or BIK) followed by the acronym LTC for 'Long-Term Culture' followed by the corresponding doxycycline concentration. For example, BIK-LTC-250 refers to MCF-7 Tet-On BIK cells cultured for 10 passages with continual doxycycline stimulation at 250 ng/mL.

2.6 Cell viability assays

2.6.1 Apoptotic DNA fragmentation assay

Extensive DNA fragmentation is a hallmark of apoptotic cell death, which can be measured by immunostaining with DNA double-strand break marker γH2AX and fluorescent microscopy (Solier and Pommier, 2014). 1.5 x 10^5 MCF-7 Tet-On-BIK or Empty vector cells were grown on glass coverslips (Electron Microscopy Sciences, #72222-01) in 24-well plates and either induced with doxycycline (Sigma, #D9891) for 24 h. Cells were fixed in 4% PFA (Thermo Scientific, #PI28906) for 15 min at room temperature, permeabilized with 0.1% Triton X-100 (Sigma, #T8787) prepared in 1XPBS, and blocked for 1 h with 4% normal goat serum (Life technologies, #PCN5000) at room temperature. Cells were then incubated with 1:500 dilution of anti-γH2AX antibody (Cell Signalling Technologies, #8718s) in the blocking buffer overnight at 4°C. The next day, coverslips were washed 4 times with 1XPBS for 5min each and incubated with 1:250 dilution of Alexa Fluor 488 conjugated secondary antibodies (Life technologies, #A11008) along with DAPI

(0.25 µg/mL) (Invitrogen, #D1306). After washing with 1XPBS for 3 times for 5 min each, coverslips were mounted on glass slides using ProLong Gold antifade reagent (Invitrogen, #P36934). Fluorescent images were acquired using AxioObserver.Z1 microscope (Carl Zeiss, Germany) at 40X (NA: 1.4) objective using ZEN2 image acquisition program (Carl Zeiss, Germany). Cells with diffuse or punctate γH2AX nuclear staining morphology were counted using MatLab program. At least 6 random frames were analyzed, and at least 200 cells were counted.

2.6.2 Clonogenic survival assay

1 x 10^3 MCF-7 Tet-On-BIK cells were plated in 6-well dishes in triplicate and induced with the indicated concentrations of doxycycline (Sigma, #D9891). Fresh growth medium with added doxycycline was supplied every 3 days for a total of 12 days. Resulting colonies were stained with 500 µL of crystal violet staining solution and counted as described in the next paragraph.

1 x 10^3 cells were plated and grown for 12 days in RPMI-1640 + 10% FBS growth medium with fresh medium supplied every 3 days. Resulting colonies were stained with 500 µL of crystal violet colony staining solution (0.4% w/v crystal violet (Sigma, #C3886), 1% PFA v/v (ThermoFisher Scientific, #PI28906), 1% Methanol #67-56-1 in 1XPBS) for 15 min. Subsequently, the plates were washed with 3 mL of 1XPBS/well 4 times for 2 min each followed by one wash with dH_2O. Plates were dried overnight, and colonies were manually counted. Representative images of the colonies were acquired using an Epson scanner.

2.6.2.1 Analysis of colony size and cellular density

6-well colony plates were converted into digital images using an Epson Perfection scanner with a resolution of 1200 dpi, resulting in 20 μm pixel size images. Image analyses was performed in MATLAB (MathWorks). To extract colony size, colonies were segmented from the background using K-means clustering functions, followed by manual inspection of each image to ensure correct colony boundary detection. To compute colony densities, colony pixels were normalized, and colony density taken as the mean pixel intensity per colony. Individual colony area and colony density were calculated for at least 300 colonies from 3 independent experiments.

2.6.2.2 MTT growth assay

1 x 10^4 MCF-7 or MDA-MB-231 vector or stable BIK expressing cells were seeded in 24-well plates in duplicates. The following day, growth medium was removed, and fresh growth medium was added, or in case of EBSS treatments, cells were washed twice with 1 mL EBSS (Invitrogen, #24010043) followed by a 4 h incubation in EBSS. Subsequently, EBSS was replaced with growth medium and cells were allowed to grow for 48 h. Growth medium was removed, cells were gently washed once with 1mL 1XPBS and 250 μL of MTT solution (0.5 mg/mL MTT (Invitrogen, #M-6494) diluted in phenol-red free RPMI-1640 (Invitrogen, #11835-030) + 10% FBS was added for 4 h at 37°C in cell culture incubator. MTT solution was carefully aspirated with a 200 μL pipette. 150 μL DMSO (Sigma, #276855) was added to lyse the cells and solubilize formazan precipitates. This solution was transferred to a flat-bottom 96-well plate, and absorbance was measured at 570 nm using a MultiSkan Ascent plate reader (MTX lab systems, #P97266). 3 independent experiments were performed.

2.7 Immunofluorescence imaging of BIK expressing cells and determination of BIK subcellular localization

1.5 x 10^5 MCF-7 Tet-On BIK or MDA-MB-231 Tet-On BIK cells were grown on glass coverslips (Electron Microscopy Sciences, #72222-01) in 24-well plates and induced with the indicated doxycycline (Sigma, #D9891) concentrations for 24 h. Cells were fixed in 4% PFA (Thermo Scientific, #PI28906) at room temperature, permeabilized with 0.1% Triton X-100 (Sigma, #T8787) prepared in 1XPBS and blocked for 1 h with 4% normal donkey serum (Millipore, #S30). Cells were then incubated with 1:250 dilution of anti-BIK antibody (SC-1710, Santa Cruz Biotechnology, USA), washed 4 times with 1XPBS for 5 min each and incubated with 1:250 Alexa Fluor 488 conjugated secondary antibodies (Life technologies, #A11055) along with DAPI (0.25 µg/mL) (Invitrogen, #D1306). After washing with 1XPBS for 3 times, coverslips were mounted on glass slides using ProLong Gold antifade reagent (Invitrogen, #P36934). Fluorescent images were captured using AxioObserver.Z1 microscope (Carl Zeiss, Germany) at 40X (NA: 1.4) objective using ZEN2 imaging program. Confocal images were acquired using WaveFx spinning-disk microscope (Quorum Technologies, ON, Canada) using 20X (NA: 0.85) or 100X (NA: 1.4) oil immersion objectives using EM-CDD camera (Hamamatsu, Japan) and Volocity software (PerkinElmer, USA) set up on Olympus IX-81 inverted stand (Olympus, Japan).

In order to determine the subcellular localization of BIK, 1 x 10^5 MCF-7 Tet-On BIK cells were induced with 250 ng/mL of doxycycline (Sigma, #D9891) for 24 h. Mitochondria in the cells were stained by incubating cells for 30 min in 250 nM MitoTracker Red CMXRos (Molecular Probes, #M7512) in the growth medium. Subsequently, cells were fixed in 4% PFA (Thermo

Scientific, #PI28906) at room temperature, permeabilized with 0.1% Triton X-100 (Sigma, #T8787) prepared in 1XPBS and blocked for 1 h with 4% normal donkey and goat serum (Millipore #S30 and Life Technologies #I-M07, respectively). Cells were then incubated with 1:250 dilution of goat anti-BIK antibody (Santa Cruz Biotechnology, #SC-1710) and 1:250 dilution of rabbit anti-Calnexin antibody (kindly provided by Dr. Thomas Simmen) at 4°C overnight. The next day, coverslips were washed 4 times with 1XPBS for 5 min each and incubated with 1:250 dilution of Alexa Fluor-conjugated secondary antibodies (Life Technologies, USA) along with DAPI (0.25 µg/mL) (Invitrogen, #D1306). Anti-goat Alexa Fluor 488, and anti-rabbit Alexa Fluor 647 (Life Technologies, #A11055, and #A21246 respectively) antibodies were used to detect BIK and Calnexin signals respectively. After washing with 1XPBS for 3 times for 5 min each, coverslips were mounted on glass slides using ProLong Gold antifade reagent (Invitrogen, #P36934). Confocal images were acquired using WaveFx spinning-disk microscope (Quorum Technologies, ON, Canada) using a 100X (NA: 1.4) oil immersion objectives using EM-CDD camera (Hamamatsu, Japan) and Volocity software (PerkinElmer, USA) set up on Olympus IX-81 inverted stand (Olympus, Japan). Colocalization between immunofluorescence signals between BIK and Calnexin, or between BIK and MitoTracker Red CMXRos was performed using Coloc 2 image analysis plugin (https://imagej.net/Coloc_2) on ImageJ (1.51j8) platform. Coloc 2 was set to automatically determine Coste's threshold, followed by determination of Mander's coefficients for above threshold pixel intensities.

2.8 Assessment of DNA double-strand damage

2.8.1 Detection of γH2AX puncta as a surrogate marker for DNA double-strand breaks

Histone 2 AX (H2AX) undergoes Ser139 phosphorylation at the site of DNA double-strand breaks, which can be detected by immunofluorescence analysis. 1.5 x 10^5 MCF-7 Tet-On BIK cells were grown on glass coverslips (Electron Microscopy Sciences, #72222-01) in 24-well plates and were induced with doxycycline (Sigma, #D9891) at the indicated concentrations. Immunofluorescence analysis was performed as described in section 2.6.1 using rabbit anti-γH2AX antibody (Cell Signalling Technology, #8718s). Fluorescent images were acquired using AxioObserver.Z1 microscope (Carl Zeiss, Germany) at 40X (NA: 1.4) objective using ZEN2 image acquisition program (Carl Zeiss, Germany). Cells with punctate γH2AX nuclear staining morphology were considered to contain damaged DNA. 8 random fields of view were analyzed. At least 50 cells were used to count γH2AX puncta in 3 independent experiments.

2.8.2 Alkaline comet assay

Alkaline comet assay was performed as described by (Liu et al., 2015; Singh et al., 1988). The assay was performed under low light conditions to minimize light-induced DNA damage. Briefly, 2.5 x 10^5 MCF-7 Tet-On BIK or Empty vector cells were plated in 6-well dishes and induced with 250 ng/mL of doxycycline (Sigma, #D9891) for 24 h. Cells were harvested by trypsinization followed by centrifugation (230 x g at 4°C), resuspended in 1XPBS and counted using a hemocytometer (Fisher scientific, #S17040). Subsequently, cells were resuspended in 1% low melting point agarose (LMP) (Invitrogen, #16520050) prepared in 1XPBS (LMP) at a density of 50 cells/µL. 50 µL of this agarose was put on glass slides (pre-coated with 1% LMP agarose) and was allowed to bond with the coated agarose for 30 min at 4°C. Next, agarose-embedded cells were covered with *in situ* lysis in lysis buffer (2.5 M NaCl, 100 mM EDTA, 10 mM Trizma base, 1% TX-

100, pH 8) at 4°C for 60 min. Subsequently, nuclear DNA was unwound using freshly prepared alkaline unwinding solution (200 mM NaOH, 1 mM EDTA, pH 10) for 1 h at 4°C. Slides were aligned equidistance from the electrodes and electrophoresis was performed at 300mA for 30min in alkaline electrophoresis solution (200 mM NaOH, 1 mM EDTA, pH>13) using a Bio-Rad sub-cell electrophoresis apparatus (Bio-Rad, #1704502). The slides were washed with dH_2O twice followed by 70% ethanol fixation for 10 min and left to air dry overnight. Electrophoresed DNA was stained with RedSafe DNA stain (iNtRON Biotechnology, #21141) for 15 min. Resulting comets were imaged using AxioObserver.Z1 microscope (Carl Zeiss, Germany) at 10x magnification. The %DNA in the tail was calculated using CasPLab comet analysis program (http://casplab.com/download) (Konca et al., 2003), wherein 50 random nuclei were analyzed for 3 independent experiments.

2.8.3 Measurement of γH2AX levels using western blotting

Double-strand DNA damage was also quantified using western blotting (refer to section 2.4) and probing with the anti-γH2AX antibody (Cell Signalling Technology, #8718s). X-ray films used to detect chemiluminescence signal were scanned using an Epson scanner, and 8-bit greyscale images were obtained. Densitometric analysis of γH2AX signal was performed using tubulin as a loading control using ImageJ (1.51j8) program. At least 3 independent western blots were analyzed for this analysis.

2.9 Assays to detect ROS and DNA damage mediated by ROS

2.9.1 Flow cytometry analysis to quantitate ROS levels

Cellular ROS levels were quantitated using a cell-permeable oxidative stress sensor dye, CellRox Green (ThermoFisher Scientific, #C10444). MCF-7 Tet-On BIK or Empty vector cells were induced with indicated concentrations of doxycycline (Sigma, #D9891) for 24 h. 2.5 µM CellRox Green reagent was added to the growth medium and cells were incubated for 30 min in a cell culture incubator at 37°C. Cells were harvested by trypsinization, centrifuged and washed twice with 1XPBS followed by flow cytometry in the FL-1 channel using a BD Accuri flow cytometer (BD Biosciences, #7820018) equipped with C6 acquisition software. At least 10,000 individual cells were analyzed in 3 independent experiments. Mean fluorescence intensity (MFI) in individual cells were analyzed using FlowJo version 10 (FlowJo, LLC, USA) program. 100 μM *tert*-butyl hydroperoxide (TBHP) (Sigma, #458149) was used as positive control. Freshly prepared 2.5 µM N-acetyl cysteine NAC (Sigma #A9165) was used as a ROS scavenger for 30 min prior to treatment.

2.9.2 Detection of ROS mediated DNA damage by western blotting

2.5 x 10^5 MCF-7 Tet-On BIK cells were induced with 50 ng/mL doxycycline (Sigma, #D9891) for 24 h in the presence or absence of the pan-caspase inhibitor z-VAD-fmk (10 µM) (Promega, #G7232) or ROS scavenger NAC (2.5 mM) (Sigma, #A9165). 50µM H_2O_2 (Fisher scientific, #H325) added for 30 min in the presence or absence of caspase inhibitor z-VAD-fmk (Promega, #G7232) or ROS scavenger NAC (Sigma, #A9165) was used as a positive control. Cells were harvested by trypsinization, cell lysates were prepared, and western blotting was performed to confirm DNA damage using anti-γH2AX and anti-BIK antibodies along with tubulin as a loading control. Resulting western blots were quantitated using ImageJ (1.51j8) program.

2.10 siRNA transfections

2 x 10^5 MCF-7 Tet-On BIK cells were seeded in 12-well plates. The following day, siRNA oligos were diluted to 100 nM in 100 µL OptiMEM reduced serum medium (Life Technologies, #31985-070) and incubated for 5 min at room temperature. 2 µL Lipofectamine 2000 (Invitrogen, #11668-027) was mixed with 100 µL OptiMEM reduced serum medium (Life Technologies, #31985-070) and incubated for 5 min at room temperature. Subsequently, siRNA oligos and Lipofectamine 2000 were mixed by vigorous pipetting and incubated for 20 min at room temperature. These transfection complexes were added to the cells along with 800 µL regular growth medium. 6 h later, transfection complexes were removed, and fresh growth medium was added. Specifically for BIK, knock-down of Dox-induced BIK was performed by transfecting with 2 previously reported anti-*BIK* siRNA sequences (Mathai et al., 2005) 24 h in advance, and fresh growth medium containing Dox was added for 24 h. *CAD* silencing was performed in a similar manner. Anti-estrogen mediated *BIK* expression was silenced by *BIK* siRNA transfection for 7 hours, transfection complexes were removed, followed by anti-estrogen treatment for 48 h. Details of siRNA oligos used in the study are as follows.

Target gene	**Oligo name**	**Target Sequence**	**Manufacturer**
BIK	*BIK* siRNA-1	AUGCAUGGAGGGCAGUGAC	IDT and Dharmacon
	BIK siRNA-2	GUCACUGCCCUCCAU GCAU	IDT and Dharmacon
CAD	*CAD* siRNA-1	GAACCUGGAUCACAUAAUA	Dharmacon
	CAD siRNA-2	GGACAGCUGCUUAUCAAGA	Dharmacon

2.11 Analysis of autophagic flux

2.11.1 Autophagic flux in the presence of transient transfection of *BIK*

2.5 x 10^5 MCF-7 cells were seeded in 12-well plates. The following day, cells were either mock transfected or transiently transfected with 1.6 µg of pCDNA3.2-DEST-BIK plasmid for 24 h using Lipofectamine 2000 (Invitrogen, #11668-027). The following procedure was used for transfections. 1.6 µg plasmid DNA was diluted in 100 µL OptiMEM reduced serum medium (Life Technologies, #31985-070) and incubated for 5 min at room temperature. 4 µL Lipofectamine 2000 (Invitrogen, #11668-027) was mixed with 100 µL OptiMEM reduced serum medium (Life Technologies, #31985-070) and incubated for 5 min at room temperature. Subsequently, plasmid DNA and Lipofectamine 2000 were mixed by rigorous pipetting and incubated for 20 min at room temperature. These transfection complexes were added to the cells along with 800 µL regular growth medium. 6 h later, transfection complexes were removed, and fresh growth medium was added. 24 h later cells were incubated in Earl's balanced salt solution (Invitrogen, #24010043) or kept in regular growth media with or without 200 nM Bafilomycin A1 (LC laboratories, #B-1080) for 4 h. Cells were harvested by trypsinization, cell lysates were prepared in RIPA buffer supplemented with protease and phosphates inhibitors as described in section 2.4 and western blotting was performed with anti-LC3 antibody (Cell Signalling Technology, #2775s). Conversion of LC3 I to LC3 II was measured by densitometric analysis of lower (LC3 II) to upper (LC3 I) band on western blots where tubulin was used as a loading control. Three independent western blots were quantitated using ImageJ (1.51j8) program.

2.11.2 Autophagic flux in stable BIK expressing cell lines

2.5 x 10^5 MCF-7 or MDA-MB-231 vector or BIK expressing cells were seeded in 12-well plates. 24 h later cells were incubated in Earl's balanced salt solution (Invitrogen, #24010043) or

kept in regular growth media with or without 200 nM Bafilomycin A1 (LC laboratories, #B-1080) for 4 h. For rapamycin treatment, cells were treated with 0.5 μM rapamycin (Assay Designs, #89156-362) or DMSO (Sigma, #276855) for a total of 12 h with 200 nM Bafilomycin A1 (LC laboratories, #B-1080) treatment during the last 4 h. Cells were harvested by trypsinization, cell lysates were prepared in RIPA buffer supplemented with protease and phosphates inhibitors as described in section 2.4 and western blotting was performed with anti-LC3 antibody (Cell Signalling Technology, #2775s). Conversion of LC3 I to LC3 II was measured by densitometric analysis of lower (LC3 II) to upper (LC3 I) band on western blots where tubulin was used as a loading control using ImageJ (1.51j8) program.

2.12 *In vitro* assays of cell aggressiveness

2.12.1 Soft-agar colony formation assay

Soft-agar colony formation was done as described (Borowicz et al., 2014; Liu et al., 2015). Briefly, 2500 cells were resuspended in 0.35% agarose (Invitrogen, #16500-500) mixed with complete growth medium (RPMI-1640+ 10% FBS) and layered on top of a pre-solidified 1% agarose: growth medium mix. Colonies were allowed to form for 7 weeks, and the agarose layer was kept hydrated by addition of 200 μL of growth medium (RPMI-1640 + 10% FBS) every 5 days. To visualise colonies, growth medium on the surface of the agar was gently absorbed by a filter paper and colonies were stained with crystal violet colony staining solution (0.005% w/v crystal violet (Sigma, #C3886), 1% PFA v/v (ThermoFisher Scientific, #PI28906), 1% Methanol #67-56-1 in 1XPBS), solution overnight at 4°C. Cell culture plates were scanned using an Epson scanner (Epson, #J192A) and colonies were counted manually.

2.12.2 Mammosphere formation assay

Low cell attachment plates were prepared by incubating 24-well plates with 0.5 mL of 20 mg/mL poly-HEMA (Sigma, #P3932) in 95% EtOH followed by overnight evaporation in the cell culture hood. EV-LTC-250, BIK-LTC-0 and BIK-LTC-250 single cells were plated in replicates in poly-HEMA (Sigma, #P3932) coated 24-well plates at 5 cells/mm^3 suspension (500 µL suspension volume per well) in DMEM/F12 (1:1) (Invitrogen, #11320033) supplemented with 20 ng/mL FGF-2 (Sigma, #FO291), 20 ng/mL EGF (PeproTech, #AF100-15), 2% B27 without vitamin A (GIBCO, #12587010) and 1X ITS (insulin-transferrin-selenium, Fisher Scientific, #51500056). 0.5% Methylcellulose (Sigma, #MO387) was included to prevent cell aggregation, allowing growth of mammospheres in different z-planes of the medium. Every 3 days, 500 µL of fresh medium was added to each well without removing the old medium. Mammospheres were imaged in brightfield (Zeiss AxioObserver.Z1 microscope) at 10x magnification on day 4, 8 and 12 using ZEN2 image acquisition program. Mammosphere formation efficiency was determined on day 12 and was calculated from the number of spheres per well, divided by the number of cells plated, multiplied by 100 (to convert it to percentage).

2.12.2.1 Analysis of mammosphere size and shape

Image analyses was performed in MatLab (MathWorks). To segment mammospheres in brightfield images and determine their areas, a binary gradient image mask of the mammosphere(s) was calculated from a threshold value determined by edge and Sobel operator. Linear gaps in the gradient images were dilated using linear structuring elements, interior holes filled and resultant mammosphere boundary smoothened by eroding the image twice with a

diamond structuring element. The isoperimetric quotient of mammospheres was analyzed using MatLab (MathWorks) program. Manual inspection of each image was done to ensure correct boundary detection.

2.13 Orthotopic mouse xenografts of LTC cells

2.13.1 Implantation of 17 β-estradiol pellets

Animal procedures were performed in compliance with the Canadian Council on Animal Care and approved by the University of Alberta Animal Care and Use Committee (AUP00000386). CrTac: NCR-Fox$^{nu/nu}$ Balb/C nude female mice were obtained from Taconic Biosciences and acclimatized to the facility for 1 week. Mice were anesthetized by isoflurane inhalation, and a 60-day slow-release 17 β-estradiol pellet (Innovative Research of America, #SE-121) was subcutaneously implanted in the neck using a sterile trochar (Innovative Research of America, #MP-182) to facilitate the growth of estrogen-dependent MCF-7 cells. The incision was sealed using a tissue adhesive (3M Vetbond, #1496C). Appropriate animal ethics were followed by the use of approved SOP (ISG 011).

2.13.2 Orthotopic injection of LTC cells and measurement of tumor growth

Prior to injection, all LTC cell lines were tested using MycoSensor mycoplasma detection PCR kit (Agilent Technologies, #302109) following the manufacturer's protocol to ensure the cell lines were free of mycoplasma contamination. Seven days after the 17 β-estradiol pellet implantation, 5 x 10^6 EV-LTC-250, BIK-LTC-0 and BIK-LTC-250 cells were resuspended in 100 µL of 50/50 mix of RPMI-1640 (Invitrogen, #22400-105) and the basement membrane matrix

Matrigel (Corning, #354234) and injected in the 4L or 4R mammary gland fat pads of the mice. Tumors were allowed to grow for 7 weeks. Non-tumor takers and mice dead due to the unknown causes were removed from the analysis (final n=5 for each group). Tumor volume was monitored weekly using Vernier calipers using (Length x Width x Height)/2 formula. After 7 weeks, mice were euthanized by CO_2 inhalation and tumors were harvested. Post-harvest tumor volume was calculated using (Length x Width x Height)/2.

2.14 Statistical analyses

All bar and line graphs were prepared using GraphPad Prism version 7.03 (GraphPad Software, USA, www.graphpad.com) and represent mean ± standard deviation (SD) unless otherwise stated. Statistical significance between two groups was determined using a two-tailed unpaired t-test where the alpha was set at 0.05. To determine statistical significance among more than two groups of data, one-way analysis of variance (ANOVA) was used. Where ANOVA was significant, differences between the two selected groups were analyzed by Sidak's post-hoc test, and p values were obtained. Following ANOVA where every mean was compared with every other mean, p values were calculated using Tukey's post-hoc test, whereas where every mean was compared to a control mean, p values were calculated using Dunnett's post-hoc test. Slopes of lines for weekly monitored tumor volumes were calculated by linear regression analysis, and statistical significance was determined using GraphPad Prism version 7.03 (GraphPad Software, USA, www.graphpad.com).

References

Altman, D.G. (1991). Practical statistics for medical research (London ;: Chapman and Hall).

Armitage, P. (2002). Statistical methods in medical research, G. Berry, and J.N.S. Matthews, eds. (Oxford ;: Blackwell Scientific Publications).

Borowicz, S., Van Scoyk, M., Avasarala, S., Karuppusamy Rathinam, M.K., Tauler, J., Bikkavilli, R.K., and Winn, R.A. (2014). The soft agar colony formation assay. J Vis Exp, e51998.

Craik, A.C., Veldhoen, R.A., Czernick, M., Buckland, T.W., Kyselytzia, K., Ghosh, S., Lai, R., Damaraju, S., Underhill, D.A., Mackey, J.R., *et al.* (2010). The BH3-only protein Bad confers breast cancer taxane sensitivity through a nonapoptotic mechanism. Oncogene *29*, 5381-5391.

DeLong, E.R., DeLong, D.M., and Clarke-Pearson, D.L. (1988). Comparing the areas under two or more correlated receiver operating characteristic curves: a nonparametric approach. Biometrics *44*, 837-845.

Germain, D.R., Graham, K., Glubrecht, D.D., Hugh, J.C., Mackey, J.R., and Godbout, R. (2011). DEAD box 1: a novel and independent prognostic marker for early recurrence in breast cancer. Breast Cancer Res Treat *127*, 53-63.

Konca, K., Lankoff, A., Banasik, A., Lisowska, H., Kuszewski, T., Gozdz, S., Koza, Z., and Wojcik, A. (2003). A cross-platform public domain PC image-analysis program for the comet assay. Mutat Res *534*, 15-20.

Liu, X., He, Y., Li, F., Huang, Q., Kato, T.A., Hall, R.P., and Li, C.Y. (2015). Caspase-3 promotes genetic instability and carcinogenesis. Mol Cell *58*, 284-296.

Lynes, E.M., Bui, M., Yap, M.C., Benson, M.D., Schneider, B., Ellgaard, L., Berthiaume, L.G., and Simmen, T. (2012). Palmitoylated TMX and calnexin target to the mitochondria-associated membrane. EMBO J *31*, 457-470.

Mathai, J.P., Germain, M., and Shore, G.C. (2005). BH3-only BIK regulates BAX,BAK-dependent release of Ca2+ from endoplasmic reticulum stores and mitochondrial apoptosis during stress-induced cell death. J Biol Chem *280*, 23829-23836.

Singh, N.P., McCoy, M.T., Tice, R.R., and Schneider, E.L. (1988). A simple technique for quantitation of low levels of DNA damage in individual cells. Exp Cell Res *175*, 184-191.

Solier, S., and Pommier, Y. (2014). The nuclear gamma-H2AX apoptotic ring: implications for cancers and autoimmune diseases. Cell Mol Life Sci *71*, 2289-2297.

CHAPTER 3

BH3-ONLY PROTEIN BIK IS PROGNOSTIC FOR POOR DISEASE-FREE AND OVERALL SURVIVAL OUTCOMES IN BREAST CANCER

A modified version chapter 3 of this thesis has been published as Pandya, V., Glubrecht, D., Vos, L., Hanson, J., Damaraju, S., Mackey, J., Hugh, J., and Goping, I.S. (2016). The pro-apoptotic paradox: the BH3-only protein Bcl-2 interacting killer (Bik) is prognostic for unfavorable outcomes in breast cancer. Oncotarget *7*, 33272-33285.

3.1 Introduction

Breast cancer is the most prevalent cancer in women worldwide accounting for the highest number of cancer-associated deaths (Ferlay J, 2013; Ferlay et al., 2015; Jemal et al., 2011). Cancer is a heterogeneous disease with many factors affecting the accurate estimation of prognosis, treatment decisions and quality of life. Identification of clinical biomarkers and elucidation of their roles has paved the way for a better understanding of the disease and improved patient survival (Henry and Hayes, 2012; Van Poznak et al., 2015). Since many unknown factors still determine variable clinical outcomes, we decided to search for additional prognostic markers. We reasoned that due to inherent genomic instability, compensatory mutations would uncouple upstream molecular drivers from the clinical outcome. We thus decided to analyze apoptotic markers and in particular focussed on the BCL-2 family of proteins that are downstream effectors of cell-death or cell-survival decisions (Czabotar et al., 2014; Puthalakath and Strasser, 2002). The BH3-only proteins are a subgroup of the BCL-2 family of proteins (Czabotar et al., 2013; Doerflinger et al., 2015). BH3-only proteins have both distinct and overlapping developmental and tissue-specific expression patterns, highlighting both unique and redundant roles in cellular processes (Lomonosova and Chinnadurai, 2008; Puthalakath and Strasser, 2002). In addition to regulating apoptosis, members of this family also interact with such diverse cellular pathways as autophagy, checkpoint regulation and metabolism. Therefore, we examined whether specific BH3-only proteins were prognostic for the breast cancer patient outcome and correlated expression with specific biological pathways.

Analysis of gene expression datasets linked to clinical outcomes can identify biomarkers that are significantly regulated at the transcriptional level. Indeed, many of the BH3-only proteins

are transcriptionally regulated with subsequent effects on apoptotic, survival, metabolic and autophagic pathways (Lomonosova and Chinnadurai, 2008; Maiuri et al., 2007). Genomic stress-mediated upregulation of *BIK, PUMA,* and *NOXA* genes is dependent on the p53 tumor suppressor (Mathai, 2005; Nakano and Vousden, 2001; Oda et al., 2000; Puthalakath and Strasser, 2002). As well, ectopically expressed E2F-1 transcription factor stimulates *BIK, PUMA, NOXA, BIM* and *HRK* transcription (Hershko and Ginsberg, 2004; Real et al., 2006). Loss of endogenous E2F-1 mediated transcriptional response protects cells from PUMA and BIK mediated apoptosis in response to genotoxic stress (Hershko and Ginsberg, 2004; Real et al., 2006). Furthermore, FOXO3a transcription factor upregulates *BIM* transcription in response to taxol-induced cytoskeletal stress whereas *PUMA* transcription upon growth factor withdrawal (Sunters et al., 2003; You et al., 2006). In response to hypoxia, HIF1-α induces *NOXA* and *BNIP3* transcription (Kim et al., 2004; Sowter et al., 2001). Thus, when cells are challenged with stressors such as DNA damage, growth factor loss or hypoxia, distinct BH3-only genes are upregulated by specific transcription factors that ultimately determine cell fate.

Importantly, BH3-only protein levels are also regulated at the post-transcriptional level (Chinnadurai et al., 2008; Lomonosova and Chinnadurai, 2008). For instance, BIK is degraded by both proteasomal- and autophagic pathways (Chen et al., 2014; Lopez et al., 2012), indicating that mRNA levels will not necessarily predict protein levels. In addition, post-translational modifications of BH3-proteins alter protein function and can act as a signaling switch from apoptosis to cell survival. It is thus important to compare gene expression studies with protein analysis to generate mechanistic models for clinical outcome.

Thus, we investigated the prognostic potential of BH3-only gene expression followed by validation at the protein level. Of the five BH3-only genes analyzed, *BIK* was the only independent prognostic indicator for breast cancer patient outcomes. Surprisingly, *BIK* was associated with unfavorable clinical outcomes suggesting that *BIK* pro-apoptotic function did not cause tumor regression. Further *BIK* prognostic value was not dependent on anti-apoptotic gene expression, indicating that *BIK*-high tumors were not addicted to anti-apoptotic proteins and that *BIK* was not merely a marker of increased tumor survival pathways. To explore a causal link between *BIK* expression and outcomes we interrogated other non-apoptotic BIK-dependent molecular pathways and identified an association between the autophagy marker *ATG-5* and *BIK*. Our work suggests that *BIK* may be an indicator of enhanced autophagy and cell survival, contributing to disease recurrence.

3.2 Results

3.2.1 High *BIK* and *BID* gene expression is significantly associated with poor breast cancer patient outcomes

To investigate how BH3-only expression correlates with patient survival, I analyzed a gene expression microarray to identify, which if any, BH3-only genes were associated with clinical outcome. This patient cohort (Dataset-1) consisted of 175 patients treated with standardized therapy and tumors were excised before treatment. Of these 111 (64%) were of the luminal, 9 (5%) of the HER2 amplified and 55 (32%) of the triple negative pathological subtypes where mRNA was extracted, and gene expression determined by array analysis (Figure 3.1). Dr. John Mackey's group

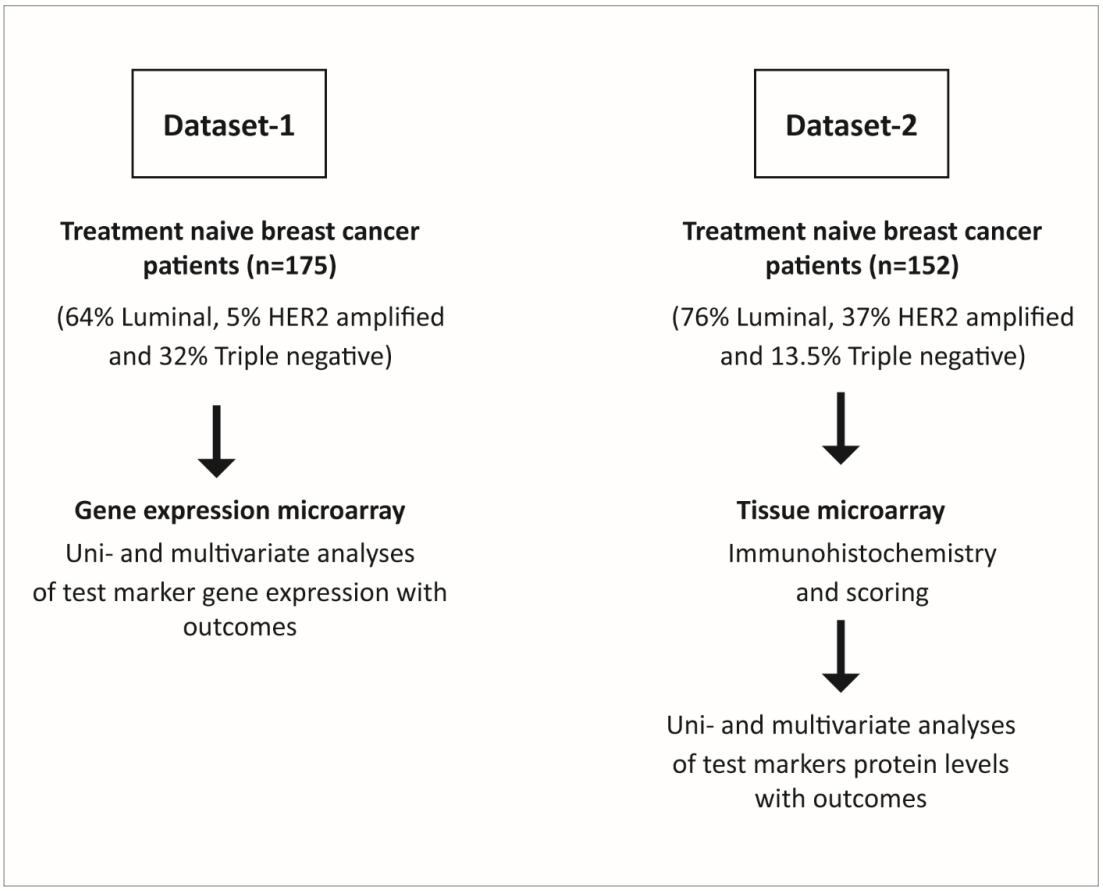

Figure 3.1 Flow chart depicting selection of patients and experimental scheme. Two different patient cohorts were chosen for the study. Treatment-naïve tumor tissue was collected for gene expression studies (Dataset-1) and protein expression studies (Dataset-2). All patients subsequently received standard guideline-based therapy and outcomes associated with marker gene expression/protein was determined as indicated.

generated this array, which we utilized to probe for BH3-only gene expression analyses (Germain et al., 2011; Liu et al., 2011).

To identify markers of early recurrence, I assessed five-year disease-free survival in relation to clinicopathophysiological markers of breast cancer such as age, tumor size, mitotic grade, vascular invasion, ER, PR and HER2 status, overall grade and menopausal status that are known to be associated with outcomes (Table 3.1). This was done by determining the hazard ratio (HR), which indicates the likelihood of relapse of the marker-high group versus the marker-low group. Patients with high mitotic and overall grades had a high hazard ratio of 2.05 and 1.95 respectively, suggesting that these patients had a poor prognosis. PR-positive patients, on the contrary, had a lower HR value (0.66) indicating that these patients had favorable outcomes likely due to a successful endocrine therapy. Therefore, this cohort appeared to be a reasonable collection that reflects the typical biology of breast cancer.

Next we wanted to investigate the correlation of BH3-only gene expression with patient survivals. Gene expression data was available for the BH3-members *BAD*, *BID*, *BIK*, *NOXA* and *PUMA*. Univariate Cox regression analysis identified that mRNA levels were significantly different with respect to disease-free survival of only *BID* (HR 1.75, p=0.011) and *BIK* (HR 1.79, p=0.021) (Table 3.1). Further, elevation of mRNA levels for both *BIK* and *BID* were significantly associated with poor survival outcomes.

3.2.2 *BIK* gene expression is an independent predictor of breast cancer survival

Disease related factors can be dependent on each other, meaning that they likely function in the same biological pathway. If the factors are independent, it suggests that they potentially work in different pathways. In order to assess whether *BIK* or *BID* were independently prognostic, I performed multivariate Cox analysis (Table 3.1). I carried out stepwise multivariate analysis on all variables associated with recurrence (*BID*, *BIK*, PR, overall grade and mitotic grade). Only *BIK* and mitotic grade were retained as independent variables (Table 3.1). I then performed pairwise multivariate analysis to assess the relationships between variables (Table 3.2). *BID* was independent of *BIK* (HR 1.78, p=0.009) but was dependent on mitotic-grade and overall grade. On the other hand, *BIK* was independent of mitotic grade, overall grade, PR status and *BID*. This finding that BIK is an independent marker of disease relapse suggested that BIK may function in a pathway unrelated to the ones that classical markers of disease aggression represent.

To quantify the risk of recurrence and death for patients with tumors that showed high levels of *BIK* mRNA expression, I conducted Kaplan-Meier (KM) analysis. Receiver Operating Curve (ROC) analysis using MedCalc program was first performed to dichotomize patients into two groups. Recurrence was set as the classification variable and a cut-point of (≤1.71) was identified that dichotomized patients into *BIK*-high and *BIK*-low groups. Kaplan-Meier analysis of those groups for disease-free survival revealed worse prognosis for *BIK*-high patients with a HR of 1.78 (p=0.019, log-rank test) (Figure 3.2 A). Similar analysis was performed for overall survival. Kaplan-Meier analysis revealed a higher risk of death for *BIK*-high patients with a hazard ratio of 2.05 (p=0.021, log-rank test) (Figure 3.2 B). Thus, elevated *BIK* mRNA level was an independent prognostic indicator of recurrence and death.

Table 3.1 Uni- and multivariate analyses of pathophysiological parameters and BH-3 only gene expression in association with disease-free survival from Dataset-1

Variable	**Univariate (Cox)**			**Multivariate (Cox) - Stepwise**		
n=175	**HR**	**95% CI**	***p***	**HR**	**95% CI**	***P***
Age>50	1.10	0.81 to 1.67	0.670		ns	
Tumor size >2 cm	1.16	0.76 to 1.78	0.486		ns	
Mitotic grade	2.05	1.32 to 3.17	0.002	2.11	1.36 to 3.27	0.001
Vascular invasion	1.50	0.97 to 2.33	0.068		ns	
ER status	0.72	0.47 to 1.11	0.140		ns	
PR status	0.66	0.43 to 1.0	0.050		ns	
HER2 status	1.14	0.67 to 1.97	0.628		ns	
Overall grade	1.95	1.18 to 3.21	0.009		ns	
Menopausal status	0.87	0.57 to 1.33	0.527		ns	
BAD	0.73	0.48 to 1.11	0.145		ns	
BID	1.75	1.14 to 2.68	0.011		ns	
BIK	1.79	1.09 to 2.92	0.021	1.89	1.16 to 3.09	0.011
NOXA	0.73	0.47 to 1.11	0.143		ns	
PUMA	1.35	0.89 to 2.10	0.166		ns	

ns= non-significant

Table-3.2 Pairwise multivariate analysis of *BIK* and *BID* gene expression against significant pathophysiological variables in association with disease-free survival from Dataset-1

Variable	**Multivariate (Cox) - Stepwise**		
n=175	**HR**	**95% CI**	***p***
Mitotic grade	2.11	1.36 to 3.27	0.001
BIK	1.89	1.16 to 3.09	0.011
BID	1.78	1.65 to 2.74	0.009
BIK	1.84	1.12 to 3.00	0.016
BIK	1.93	1.20 to 3.20	0.009
PR status	0.61	0.40 to 0.94	0.024
BIK	1.86	1.14 to 3.05	0.001
Overall grade	2.00	1.21 to 3.30	0.007
Mitotic grade	2.04	1.32 to 3.17	0.002
BID			ns
Overall grade	1.95	1.18 to 3.21	0.009
BID			ns
PR status			ns
BID	1.74	1.14 to 2.70	0.01

ns= non- significant

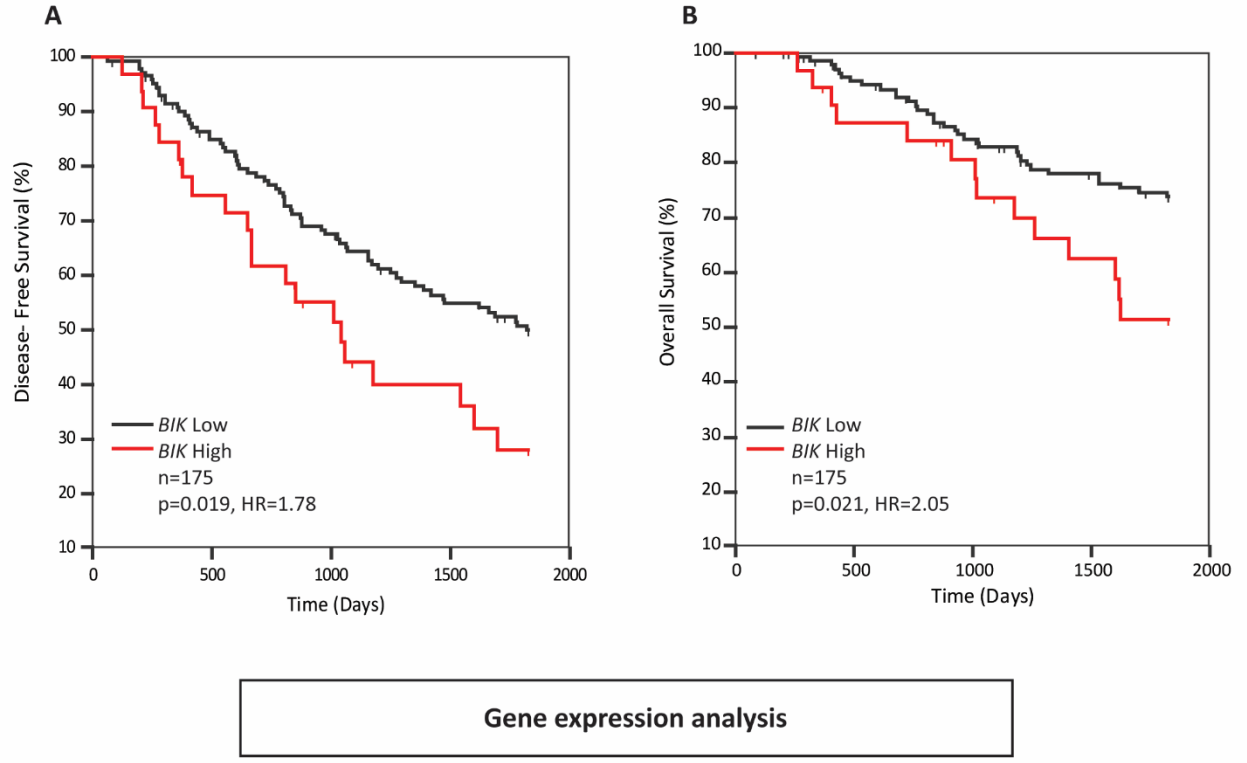

Figure 3.2 *BIK* transcript levels are elevated in breast cancer patients with poor survival outcomes. Kaplan-Meier survival curves depicting **A.** five-year disease-free (HR=1.78, 95% CI: 0.99 to 3.20) and **B.** overall survival (HR= 2.05, 95% CI: 0.96 to 4.37) outcomes of 175 patients based on *BIK* transcript levels. Patients with low levels of *BIK* transcript (n=143) were compared to patients with high levels of *BIK* transcript (n=32). The HR value of greater than 1.0 estimates the predicted risk of poor prognosis.

3.2.3 Elevated BIK protein levels are associated with poor prognosis of breast cancer patients

We were curious as to whether BIK protein was also prognostic of outcome. To rigorously test the prognostic value of BIK, we queried a different cohort of patients. We examined a tissue microarray (TMA) from 152 treatment naïve patients (Dataset-2) composed of luminal (76%), HER2 amplified (37%) and triple negative (13.5%) pathological subtypes of variable grade and stage with 11 % recurrence and 16.5 % death (Figure 3.1, page#116). The statistical significance of clinicopathological factors of age, tumor size, mitotic grade, overall grade, vascular invasion, estrogen receptor (ER)/PR and HER2 protein levels are shown in Table 3.3. Mitotic grade (HR 3.91, p=0.006), overall grade (HR 3.29, p=0.037) and ER status (HR 0.37, p=0.05) were significantly associated with disease-free survival.

The TMA was immunostained with an anti-BIK antibody and tumor cells within each tissue core were analyzed for BIK staining. Immunohistochemistry (IHC) offers a unique advantage over a whole tissue RNA/Protein extraction in that one could visualize localized staining within different cells of the whole tissue. BIK was identified by brown staining resulting from the conversion of 3,3′-Diaminobenzidine (DAB) substrate to a brown precipitate in the presence of antibody-bound horseradish peroxidase (HRP), and the nuclei were stained blue by hematoxylin. BIK was localized to the cytoplasm and staining intensity for each core was scored on a relative scale between 0-3 by personnel blinded to outcomes (Figure 3.3 A). The tumor core values were only taken from areas of invasive disease with cytoplasmic staining.

A BIK score generated from the average value of each associated core was assigned for each patient. ROC analysis identified a cut-point of ≥1.5. Multivariate analysis showed that mitotic

Table 3.3 Uni- and multivariate analyses of pathophysiological parameters and BIK protein level in association with disease-free survival from Dataset-2

Variable	Univariate (Cox)			Multivariate (Cox) - Stepwise		
n=152	**HR**	**95% CI**	***p***	**HR**	**95% CI**	***p***
Age>50	0.36	0.12 to 1.10	0.074		ns	
Tumor size >2 cm	1.18	0.44 to 3.09	0.743		ns	
Mitotic grade	3.91	1.49 to 10.27	0.006	3.97	1.51 to 10.44	0.005
Vascular invasion	0.81	0.31 to 2.14	0.673		ns	
ER status	0.37	0.14 to 0.99	0.050		ns	
PR status	0.40	0.16 to 1.05	0.062		ns	
HER2 status	0.53	0.14 to 1.95	0.336		ns	
Overall grade	3.29	1.07 to 10.09	0.037		ns	
Menopausal status	0.58	0.21 to 1.56	0.277		ns	
BIK	3.60	1.33 to 9.73	0.012	3.66	1.35 to 9.89	0.011

ns= non-significant

grade and BIK protein expression were the only two variables that retained significance (Table 3.3). I then carried out pairwise multivariate analysis to identify dependence of BIK prognostic signature on pathophysiological factors (Table 3.4). Similar to the gene expression analysis, BIK prognostic signature was independent of mitotic grade, overall grade and ER status. These results provided additional evidence that BIK may function in a novel pathway of cancer aggression. Moreover, Kaplan-Meier analysis confirmed that high levels of BIK protein were also associated with worse disease-free survival (Figure 3.3 B). Patients with high BIK protein levels had poor disease-free survival with a hazard ratio of 3.59 (p=0.007) compared to BIK-low patients. Similarly, BIK-high patients had a worse overall survival with a hazard ratio of 3.40 (p=0.04) compared with BIK-low patients (Figure 3.3 C). Altogether, mRNA and protein analysis identify BIK as a novel independent marker for breast cancer clinical outcomes.

3.2.4 BIK association with poor outcomes is not explained by compensatory increase in anti-apoptotic gene or protein expression

BIK has a well-documented role as a pro-apoptotic protein, so we were initially surprised that higher levels of *BIK* mRNA and protein were associated with poor clinical outcomes. A possible explanation was that anti-apoptotic protein levels were upregulated and compensated for BIK activity. For example, BCL-2 and BIK levels are significantly correlated in multiple myeloma cell lines where BCL-2 inhibits BIK-induced apoptosis (Bodet et al., 2010). Therefore, we investigated whether a similar *BIK: BCL-2* association was recapitulated in the clinical samples in our study. I found no correlation with *BIK* and *BCL-2* gene expression levels (r=-0.02, P=0.79, Pearson's correlation), which did not support a BCL-2-mediated tumor adaptation model for *BIK*-

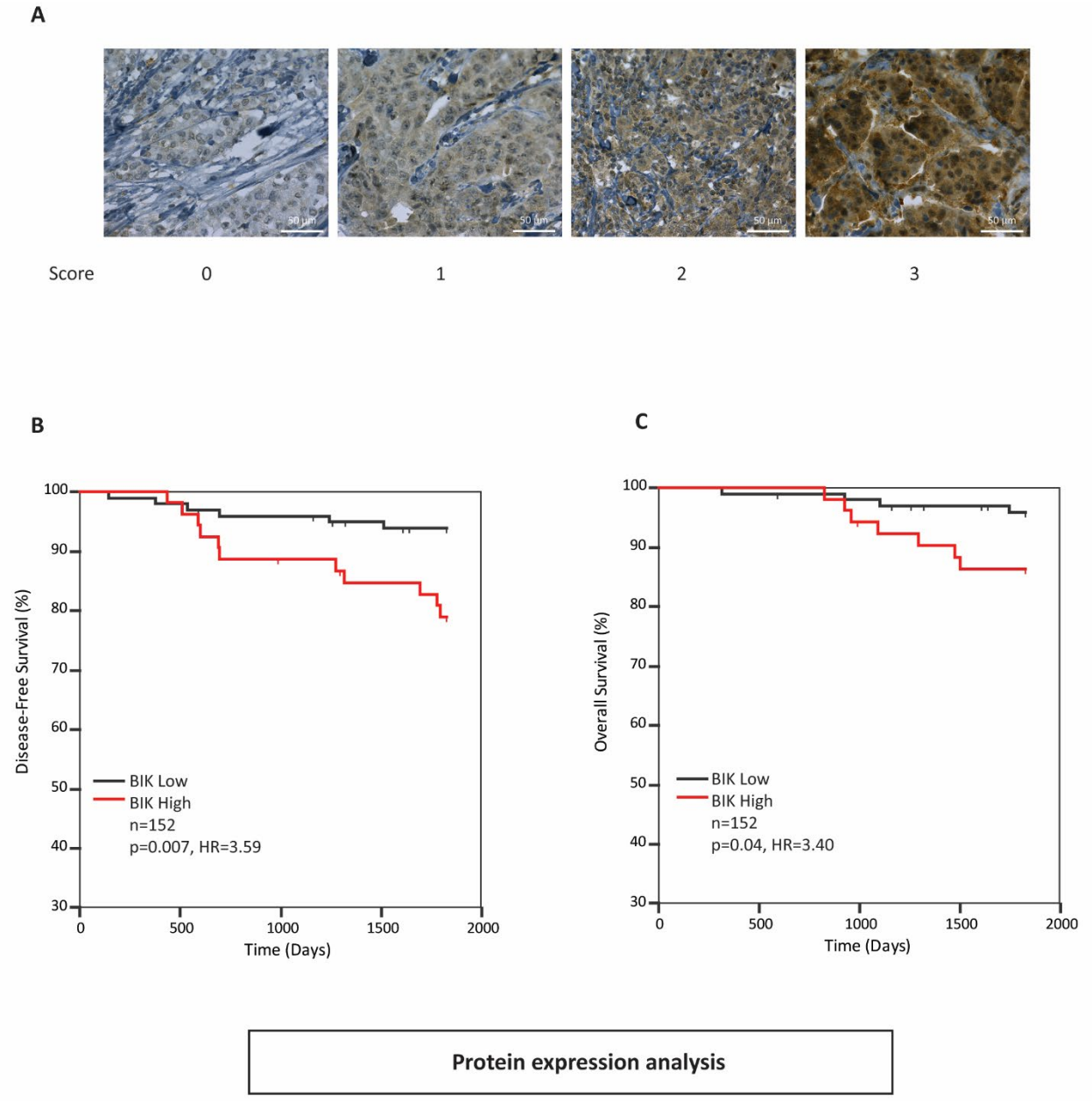
A
Score
0
1
2
3
B
Disease-Free Survival (%)
BIK Low
BIK High
n=152
p=0.007, HR=3.59
Time (Days)
C
Overall Survival (%)
BIK Low
BIK High
n=152
p=0.04, HR=3.40
Time (Days)
Protein expression analysis

Figure 3.3 BIK protein levels are elevated in breast cancer patients with poor survival outcomes. A. Immunohistochemistry analysis of patient tumors stained with anti-BIK antibody. Score values are based on antibody staining intensity (brown) on a scale of 0 to 3. Images are representative of tumor cores with typical score values. Scale bars, 50µm. *Contributed by Darryl Glubrecht* **B.** and **C.** Kaplan-Meier survival analysis depicting five-year disease-free (HR=3.59, 95% CI: 1.32 to 9.82) (B) and overall survival (HR=3.40, 95% CI: 1.10 to 11.69) (C) outcomes of 152 patients based on BIK protein levels in tumor cores. Patients with low levels of BIK protein (n=99) were compared to patients with high levels of BIK protein (n=53). The associated HR value of greater than 1.0 estimates the predicted risk of poor prognosis.

Table 3.4 Pairwise multivariate analysis of BIK against significant pathophysiological variables from Dataset-2

Variable	Multivariate (Cox) - Stepwise		
n=152	**HR**	**95% CI**	***p***
BIK	3.66	1.35 to 9.89	0.011
Mitotic grade	3.97	1.51 to 10.4	0.005
BIK	3.54	1.31 to 9.57	0.013
Overall grade	3.22	1.05 to 9.90	0.040
BIK	3.6	1.33 to 9.73	0.010
ER status			ns

ns= non-significant

high tumors. I next examined levels of anti-apoptotic genes in relation to disease-free survival. Data was available for four anti-apoptotic genes (*BCL-2*, *BCL-XL*, *MCL-1* and *BCL-w*). Univariate Cox analysis identified that elevated levels of *BCL-2*, *BCL-XL* and *MCL-1* transcripts were associated with favourable disease-free survival (Table 3.5). Stepwise multivariate Cox analysis demonstrated that all variables remained significant and were independent of each other. In KM survival analyses (Figure 3.4 A-C) elevated levels of BCL-2, BCL-XL and MCL-1 were associated with significantly improved disease-free survival with HRs of 0.41, 0.65 and 0.55, respectively. This is opposite to what would be expected if elevated *BCL-2*, *BCL-XL* and *MCL-1* were indeed inhibiting apoptosis as this would be associated with higher likelihood of recurrence with a HR greater than 1. Finally, using the *BIK: BCL-2* relationship as a model, I stratified patients with respect to their individual *BIK* and *BCL-2* gene expression levels and looked for correlations between subgroup expression levels and recurrence (Figure 3.5). If the tumor adaption model were dominant, we would expect a lower recurrence rate in the *BIK*-high patient subgroup with low *BCL-2* and presumably unencumbered apoptotic signaling, whereas the *BIK*-high patients with high *BCL-2* would show significantly higher recurrence rates. However, I see no significant difference between these two subgroups, and in fact the majority of patients show the opposite effect. Thus, elevated *BIK* levels and diminished *BCL-2* levels are both prognostic for poor outcomes, but potentially function in separate pathways.

We next examined BCL-2 protein levels in the previously described TMA from Dataset-2. Tumor cells within each core were assessed for BCL-2 protein levels (Figure 3.6 A). ROC analysis identified a cutpoint of >0. Kaplan-Meier analysis confirmed that high levels of BCL-2 protein were associated with improved disease-free survival (Figure 3.6 B). Patients with high BCL-2

Table 3.5 Uni- and multivariate analyses of *BIK* and anti-apoptotic BCL-2 family members gene expression in association with disease-free survival from Dataset-1

Variable	Univariate (Cox)			Multivariate (Cox) - Stepwise		
n=175	**HR**	**95% CI**	***p***	**HR**	**95% CI**	***p***
Mitotic grade	2.05	1.32 to 3.17	0.002	1.83	1.16 to 2.89	0.010
BIK	1.79	1.09 to 2.92	0.021	1.66	1.01 to 2.74	0.047
BCL-2	0.40	0.26 to 0.62	<0.0001	0.47	0.30 to 0.73	0.031
BCL-XL	0.65	0.43 to 0.99	0.045	0.63	0.41 to 0.96	0.031
MCL-1	0.55	0.34 to 0.87	0.010	0.48	0.30 to 0.77	0.003
BCL-w	1.24	0.75 to 2.04	0.399		ns	

ns=non-significant

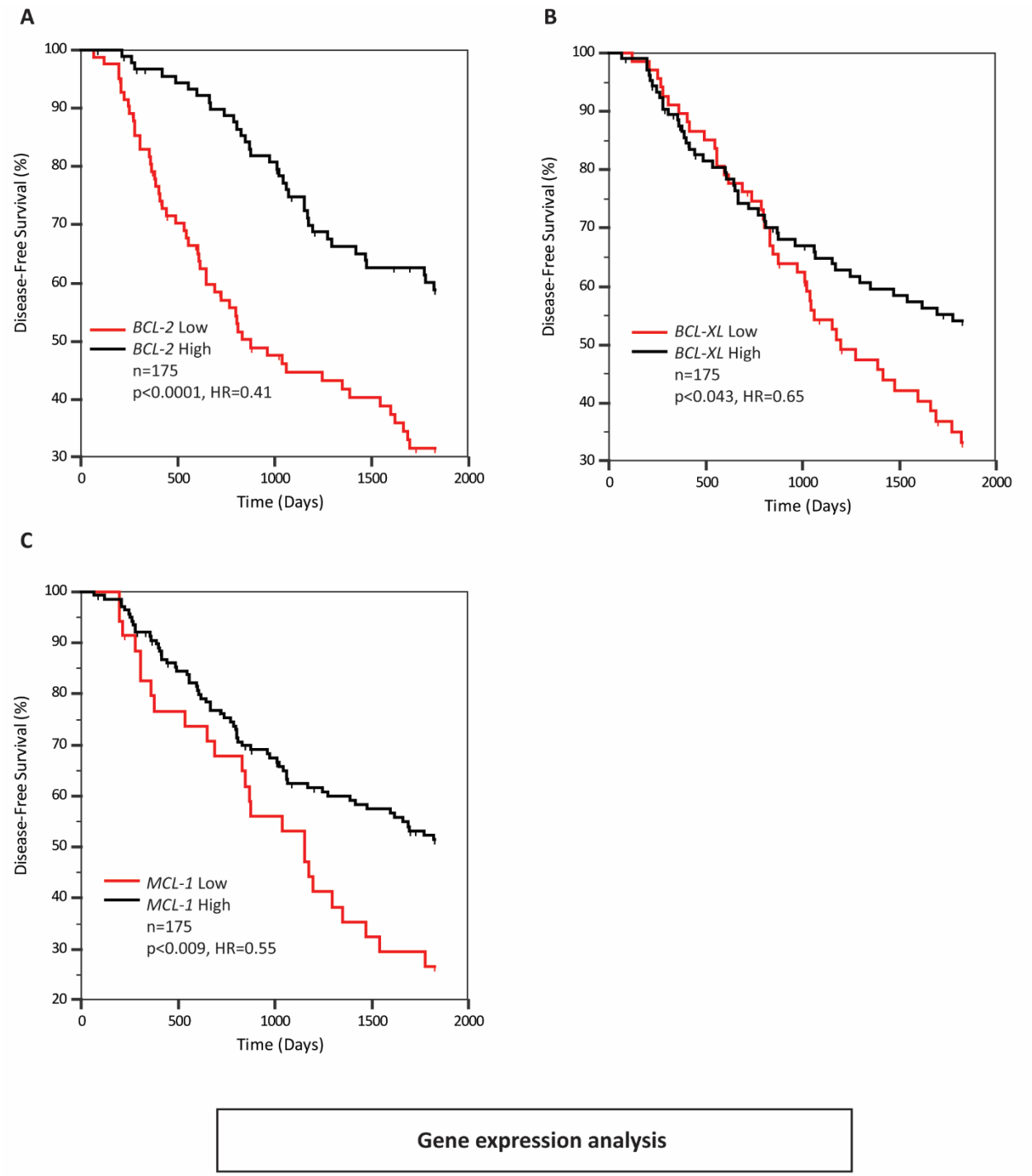

Figure 3.4 Elevated expression of anti-apoptotic BCL-2 family members is not associated with poor patient prognosis. A, B and C. Kaplan-Meier survival curves representing disease-free survival outcomes of 175 patients based on *BCL-2*, *BCL-XL* and *MCL-1* gene expression levels respectively.

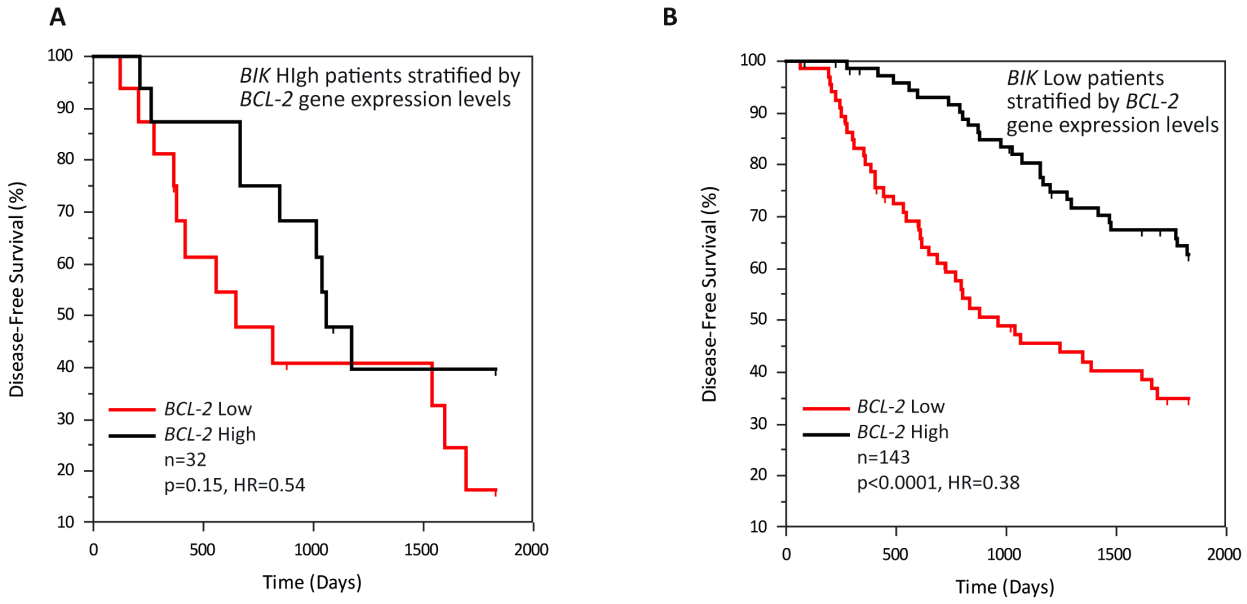

Figure 3.5 Kaplan-Meier survival curves depicting five-year disease-free survival outcomes of A. *BIK*-high (n=32) patients stratified into *BCL-2*-high and -low groups **B.** *BIK*-low (n=143) patients stratified into *BCL-2*-high or -low groups. Outcomes of patients are based on *BIK* and *BCL-2* transcript levels.

protein levels had a higher recurrence-free survival with a hazard ratio of 0.13 ($p<0.002$) compared to BCL-2-low patients. Similarly, BCL-2-high patients had a higher overall survival with a hazard ratio of 0.18 ($p=0.01$) compared with BCL-2-low patients (Figure 3.6 C). Additionally, I performed a multivariate Cox analysis of BIK and BCL-2 protein levels; BIK and BCL-2 were found to be independent variables (Table 3.6). Furthermore, I performed Kaplan-Meir survival analysis of BIK-high or BIK-low patients with respect to BCL-2 protein levels (Figure 3.7) to dissect BIK: BCL-2 relationship at the protein level. Similar to our results with *BIK: BCL-2* gene expression model, BCL-2 levels in BIK-high patients did not predict survival outcomes ($p=0.08$), confirming the absence of BCL-2 dependent tumor adaptation in BIK-high tumors. Altogether, our analyses indicate that BIK prognostic value is independent of anti-apoptotic protein levels, suggesting that a non-apoptotic activity of BIK contributes to poor clinical outcomes.

3.2.5 High *BIK* and *ATG-5* levels are associated with worse patient outcome

We sought to identify a tumor-promoting pathway that accounts for the poor prognosis in BIK-high patients. Autophagy is a stress-response pathway that recycles nutrients and removes damaged organelles to maintain cellular health (Dikic and Elazar, 2018; Kaur and Debnath, 2015). Interestingly, in addition to stimulating apoptotic pathways, BIK facilitates autophagy (Chang et al., 2010; Rashmi et al., 2008; Ruiz Esparza-Garrido et al., 2015) and enhanced autophagy is associated with poor clinical outcomes (Guo et al., 2013; Wei et al., 2011; Yang et al., 2011). Therefore, using the gene expression microarray as a screening tool, I looked for a correlation between high *BIK* expression levels and markers of autophagy. Four autophagy gene sets (*ATG-5*, *ATG-7*, Beclin1 and p62) were captured in the gene expression microarray (Table 3.7). *ATG-5*,

A

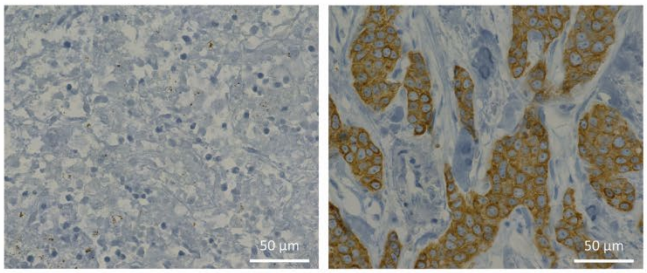

Score 0 1

B

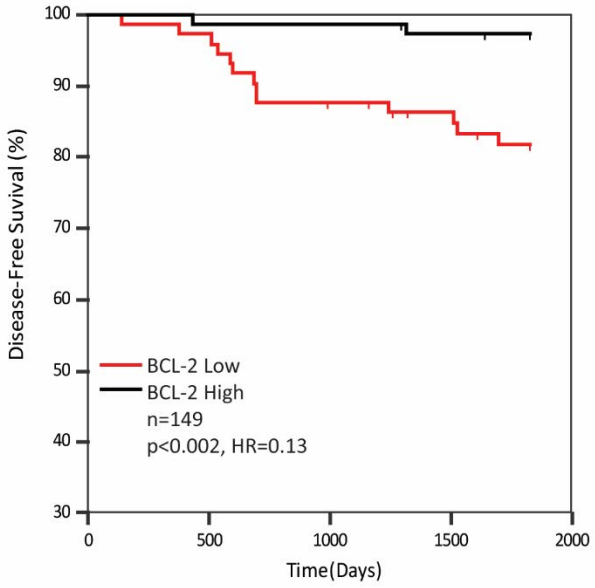

C

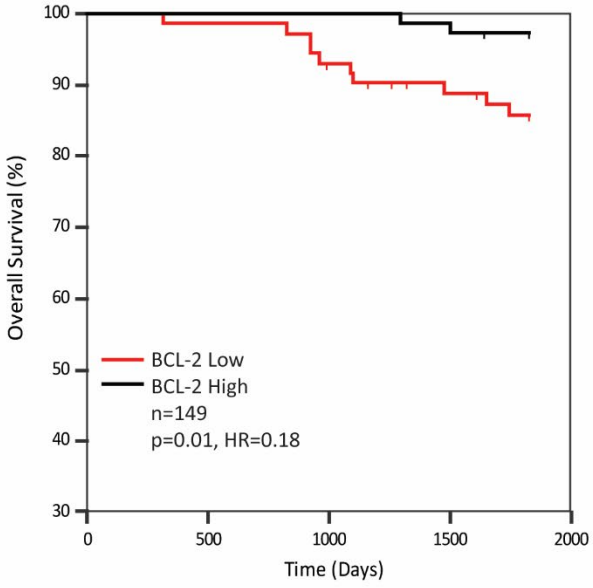

Protein expression analysis

Figure 3.6 BCL-2 protein levels are elevated in breast cancer patients with favorable survival outcomes. A. Immunohistochemistry analysis of patient tumors stained with anti-BCL-2 antibody. Score values are based on antibody staining intensity (brown) on a scale of 0 and 1. Images are representative of tumor cores with typical score values. Scale bars, 50μm. *Contributed by Darryl Glubrecht* **B.** and **C.** Kaplan-Meier survival analysis depicting 5-year disease-free (HR=0.13, 95% CI: 0.15 to 0.37) and overall survival outcomes (HR= 0.33, 95% CI: 0.15 to 0.55) of 149 breast cancer patients based on BCL-2 protein levels in tumor cores. Patients with low levels of BCL-2 protein (n=73) were compared to patients with high levels of BCL-2 protein (n=76). The associated HR value of less than 1.0 estimates the predicted risk of poor prognosis.

Table 3.6 Uni- and multivariate analyses of BIK and BCL-2 protein levels in association with disease-free survival from Dataset-2

Variable	Univariate (Cox)			Multivariate (Cox) - Stepwise		
n=139	**HR**	**95% CI**	***p***	**HR**	**95% CI**	***p***
BIK	2.99	1.07 to 8.35	0.038	3.52	1.25 to 9.88	0.017
BCL-2	0.21	0.06 to 0.74	0.016	0.18	0.05 to 0.65	0.009

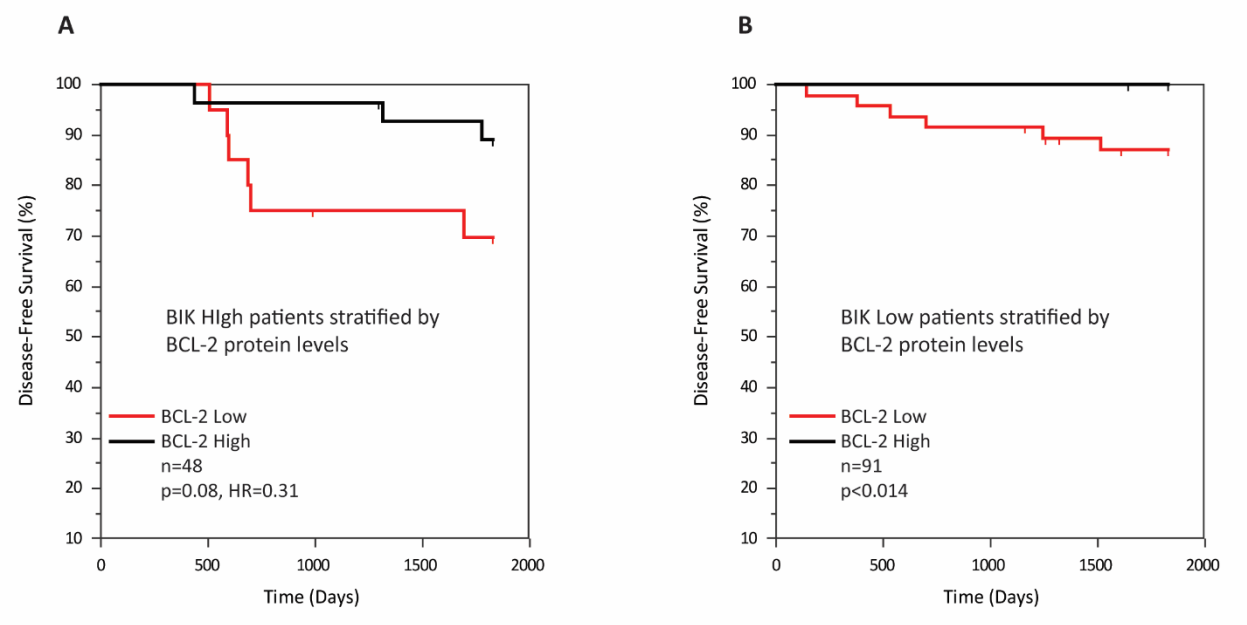

Figure 3.7 Kaplan-Meier survival curves depicting five-year disease-free survival outcomes of A. BIK-high (n=48) patients stratified into BCL-2-high and -low groups and **B.** BIK-low (n=91) patients stratified into BCL-2-high or -low groups. Outcomes of patients are based on BIK and BCL-2 protein levels.

Table 3.7 Univariate analysis of autophagy marker gene expression in association with disease-free survival from Dataset-1

Variable	Multivariate (Cox) - Stepwise		
n=175	**HR**	**95% CI**	***p***
ATG-5	1.69	1.1114 to 2.5795	0.018
ATG-7	2.38	0.8223 to 6.8692	0.016
Beclin1	0.56	0.3488 to 0.9042	0.008
p62	0.17	0.038 to 0.7882	<0.001

ATG-7 and *p62* showed clear association of high autophagy flux with poor patient outcomes. ROC curve was plotted for each of these autophagy markers to determine a cutpoint. *ATG-5* had the highest area under the curve suggesting the best combination of sensitivity and specificity parameters. Therefore, I analyzed an association of *ATG-5* with *BIK* as well as their combined effect on patient survivals.

The *ATG-5* gene product is an E3 ubiquitin ligase involved in elongation of autophagosomal membranes that facilitates tumor survival in nutrient deprivation (Kim et al., 2011; Tang et al., 2013). Overexpression of *ATG-5* is associated with aggressive tumors in squamous cell carcinoma, colorectal and prostate cancers and chemoresistant tumors in gastric cancer (Cho et al., 2012; Ge et al., 2014; Kim et al., 2011; Tang et al., 2013). To examine the dependence of *BIK* and *ATG-5*, I performed ROC curve analysis and identified a cut-point (>0.939) that dichotomized patients into *ATG-5*-high and -low groups. Kaplan-Meier survival analysis of patients with respect to *ATG-5* gene expression levels demonstrated that patients with high levels of *ATG-5* mRNA had a disease-free survival HR of 1.69 (p=0.018, log-rank test) compared to *ATG-5*-low patients (Figure 3.8 A). As well, *ATG-5*-high patients had a lower overall survival with an HR of 1.90 (p=0.04) compared to *ATG-5*-low patients (Figure 3.8 B). In order to dissect the relationship between *BIK* and *ATG-5*, I performed multivariate Cox analysis and found that *BIK* and *ATG-5* were independent variables (p=0.02 and p=0.02 respectively). I performed a bivariable KM analysis in order to further examine potential relationships between *BIK* and *ATG-5* (Figure 3.8 C). I found that while *ATG-5*-high was a stand-alone significant prognostic indicator (Figure 3.8 A), *BIK*-high was significant only when *ATG-5* was also high (Figure 3.8 C), suggesting

that the mechanism whereby high *BIK* contributes to poor outcomes may be through an *ATG-5*-dependent autophagy pathway. To interrogate this further, I generated a scatter plot to correlate patients with respect to their individual *BIK* and *ATG-5* gene levels and examined recurrence rates for each subgroup (Figure 3.8 D). I observed that *BIK*-high patients with high levels of *ATG-5* mRNA had 88% recurrence (p=0.009, log-rank test) compared to a 44% recurrence rate in the *BIK*-high/*ATG-5*-low patient subgroup. Of the *BIK*-low patient subgroups, there was no significant difference in recurrence rates relative to *ATG-5* levels. Collectively, this data supports a mutual association of BIK and ATG-5 in determining patient outcome.

3.3 Discussion

We identified that the BH3-only protein BIK was a novel prognostic marker for breast cancer. BIK levels were prognostic for disease-free and overall survival in two independent cohorts of primary breast cancer patients. Importantly, elevated BIK levels were associated with poor outcomes (average HR= 2.75). This result suggested that BIK may have tumor-promoting activity. However, there is substantial evidence that BIK is a tumor-suppressor. For example, the *BIK* gene was mutated in peripheral B-cell lymphomas, deleted in gliomas, head and neck and colorectal cancers or silenced in renal cell carcinomas (Arena et al., 2003; Bredel et al., 2005; Castells et al., 1999; Chinnadurai et al., 2008; Sturm et al., 2006). Additionally, a genetically-engineered mutant of BIK (BIKDD) induced apoptosis in pancreatic, breast and colon cancer models resulting in tumor clearance (Day et al., 2006; Jiao et al., 2014; Lan et al., 2007; Li et al., 2008). On the other hand, BIK expression was elevated in breast, pancreas, multiple myeloma and colon cancers, suggestive of a tumor-promoting role for BIK

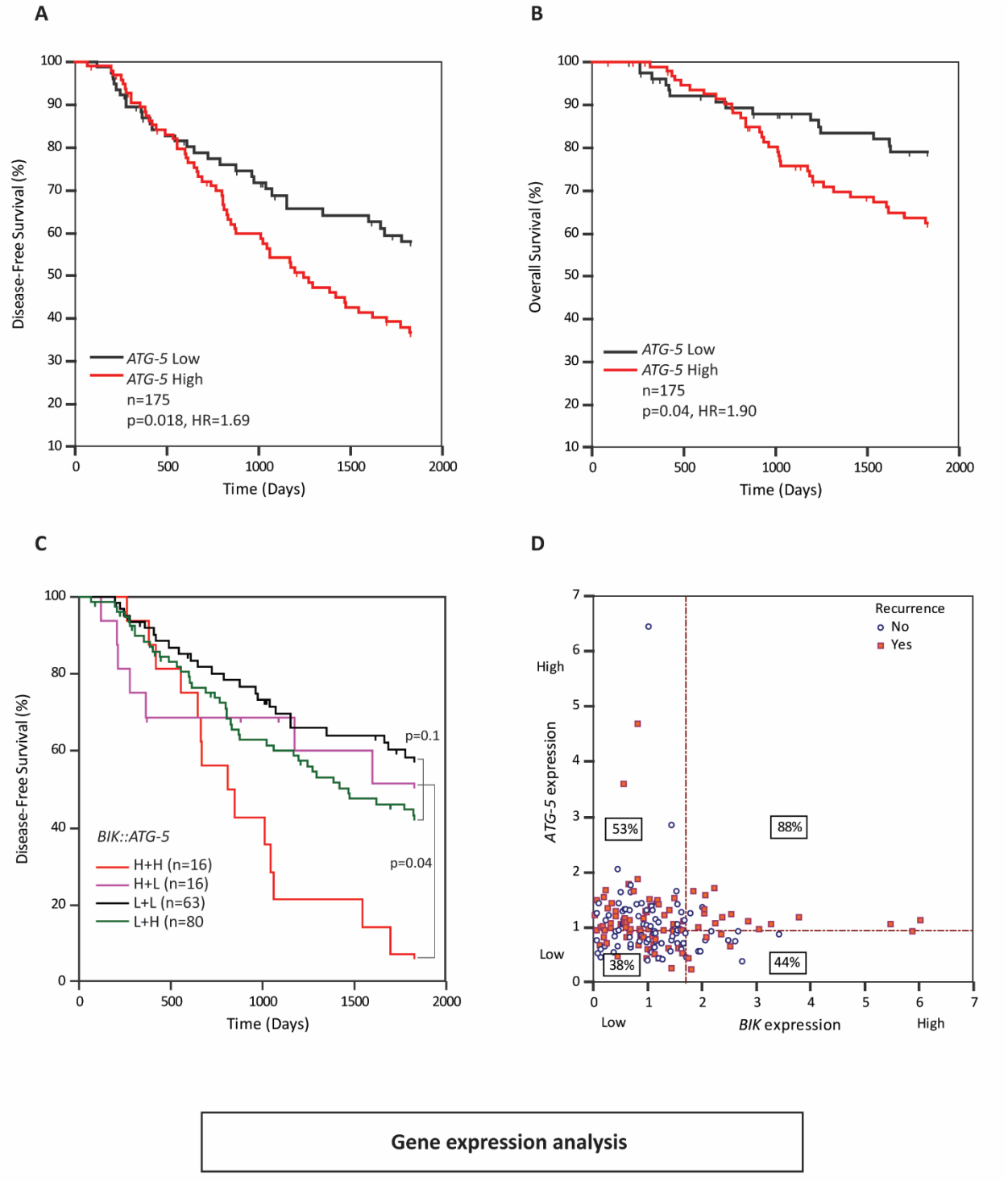

Gene expression analysis

Figure 3.8 *ATG-5* transcript levels are elevated in breast cancer patients with poor survival outcomes. A. and **B.** Kaplan Meier survival curves representing disease-free (HR=1.69, 95% CI: 1.11 to 2.65) survival and overall survival (HR=1.90, 95% CI: 1.11 to 3.41) outcomes of 175 BC patients based on *ATG-5* mRNA levels. **C.** Paired KM curves demonstrating individual or combined effects of high *ATG-5* and *BIK* expression levels on recurrence-free survival of patients. **D.** Scatter-plot comparing gene expression levels of *ATG-5* and *BIK* per patient with respect to disease recurrence. Horizontal and vertical dotted lines indicate dichotomizing score cut-points as determined by ROC analysis. Percentage values in rectangles indicate percent of patients that recurred within each quadrant.

(Garcia et al., 2005; Lopez-Munoz et al., 2012; Maxfield et al., 2015; Zhan et al., 2006). These studies, however, correlated BIK levels to disease, but did not correlate BIK levels to the outcome. As far as we know, our study is the first to report that high *BIK* transcript and protein levels correlated with poor outcomes and thus provide potential insights into the biological role of BIK in breast cancer.

While both high *BIK* mRNA and protein levels predicted unfavorable patient outcomes in Dataset-1 and -2 respectively, inherent differences between the two datasets exist. The first being in the proportion of the breast cancer subtypes. Dataset-1 consisted of 64% luminal, 5% HER2-enriched and 32% basal-like subtypes whereas in Dataset-2 this proportion was 76%, 37%, and 13.5% respectively, implying that Dataset-1 represented the highly aggressive basal-like disease. Accordingly, the 5-years DFS rate in Dataset-1 was 38.3%, and the 5-years OS rate was 57.8% compared to 83.5% and 88.2% respectively in Dataset-2. According to a 2017 estimate by Canadian Cancer Society, the 5-years overall net survival in various provinces of Canada ranged between 84 to 88% suggesting that Dataset-2 more closely represented typical breast cancer cohorts than Dataset-1 (CCS, 2018). *BIK* gene expression values were obtained from Dataset-1 while BIK protein expression values were obtained from Dataset-2. Interestingly the HR associated with high BIK protein expression was 2-times more compared to high *BIK* gene expression (3.60 vs. 1.79). This deviation could possibly suggest that BIK protein levels available in the tumors may more accurately represent the disease biology than *BIK* mRNA. However, other simpler explanations such as the differential composition of the two datasets and its effect on the hazard ratios of BIK cannot be ruled out.

How BIK association with poor clinical outcome is manifested at the molecular level is unclear. BIK could either be a marker of aggressive tumors that have evolved anti-apoptotic strategies, or BIK could have a direct tumor-promoting role. To address the first point, it is possible that tumors upregulate BCL-2 expression. This compensatory mechanism to ablate apoptotic pathways is well-documented in multiple myeloma and non-small cell lung cancer (NSCLC) tumor models (Bodet et al., 2010; Lu et al., 2006). Of particular interest, Lu et al reported that poorly surviving non-small cell lung cancer (NSCLC) patients had high *BIK* expression and hypothesized that compensatory increase in anti-apoptotic protein BCL-2 led to tumor adaptation (Chinnadurai et al., 2008; Lu et al., 2006). Contrary to their findings, in breast cancer we found that BIK and BCL-2 were independent variables and the increase in *BIK* expression was not correlated with expression levels of 4 anti-apoptotic members of the BCL-2 family. Furthermore, the anti-apoptotic genes *BCL-2*, *BCL-XL* and *MCL-1* were all independently prognostic of favourable outcome, which argues against a simple anti-apoptotic/tumor-promoting role for these genes. In addition, loss of apoptosis in the face of BIK elevation may involve dysregulation of downstream apoptotic effectors and their regulators. Additionally, recent studies report BH3-only proteins can lead to tumorigenesis by compromising mitochondrial integrity, facilitating low caspase activation and chronic genomic damage (Ichim et al., 2015). It is possible that BIK-expressing tumors have greater genomic instability driving tumor adaptation and the development of more aggressive subtypes of cancer. Taken together, our data suggest that a complex network may be at play.

In the past, conflicting results have been obtained with respect to high expression levels of anti-apoptotic proteins and their association with patient survivals. Negative outcome associations

are seen in Hodgkin's lymphoma, myeloid leukemia and follicular lymphoma, and positive outcome associations are seen in NSCLC, breast and liver cancers (Abdel-Fatah et al., 2013; Anagnostou et al., 2010; Karakas et al., 1998; Sup et al., 2005). In our case, BCL-2 levels were associated with good outcome, and this is in agreement with other studies (Abdel-Fatah et al., 2013; Gasparini et al., 1995; Lipponen et al., 1995). While BCL-2 can also inhibit cell proliferation and autophagy (Chang et al., 2010; Mazel et al., 1996; Pattingre et al., 2005; Vairo et al., 1996; Wei et al., 2008), the mechanism behind the positive prognostic signature of the anti-apoptotic genes in our study, is not clear.

It is possible that BIK stimulates tumor-promoting autophagy. BIK stimulates autophagy through BCL-2-dependent and -independent mechanisms. In the first case, BIK indirectly stimulates autophagy by ablating BCL-2: Beclin 1 interactions (Chang et al., 2010). Specifically, Chang et al. reported that BCL-2 interaction with the *ER*-resident protein, nutrient-deprivation autophagy factor-1 (NAF-1) was crucial for inhibition of Beclin1-mediated autophagy and BIK suppressed this BCL-2: NAF-1 interaction (Chang et al., 2010). In the case of the BCL-2-independent autophagy pathway, ectopic expression of BIK induced autophagy in *BCL-2* $^{-/-}$ MEFs (Rashmi et al., 2008). BIK was a target of autophagy and also actively contributed to autophagy induction (Chen et al., 2014). Finally, silencing of endogenous BIK expression in the breast cancer cell line MDA-MB-231 downregulated crucial components of autophagic machinery (Ruiz Esparza-Garrido et al., 2015). Thus, overall BIK can stimulate a BCL-2 dependent or independent autophagy both of which can be blocked by BCL-2 expression. I found that high BIK expression in breast cancer patients was significantly correlated with increased levels of the autophagy marker, *ATG-5*. ATG-5 is a prognostic indicator of squamous cell carcinoma, prostate, and colorectal

cancers relapse (An et al., 2011; Cho et al., 2012; Tang et al., 2013). This is consistent with a model whereby BIK induced-autophagy promotes breast cancer relapse (Figure 3.9). According to this model, BIK stimulates autophagy, which is presumably favored in the tumors containing high amounts of ATG-5. This high autophagic flux likely alleviates the stress arising due to nutrient scarcity and provides survival benefit to the tumors resulting in poor patient outcomes. Additionally, I speculate that anti-apoptotic BCL-2-like proteins act downstream of BIK and/or directly antagonize BIK to inhibit autophagic processes. This may explain in part, why elevated BCL-2 is associated with favorable outcomes. This multiple interaction network of BIK, BCL-2 and the marker of autophagy ATG-5 may then have subset interactions, and thus retain statistical independence. As well, I expect that other signals stimulate ATG-5 and autophagy independently of BIK, again resulting in the retention of the independent prognostic value of *BIK* and *ATG-5*. Although I propose that BIK promotes tumor survival by facilitating autophagy, other possible mechanisms could lead to BIK prognostic association with poor outcomes.

Altogether, multiple models of BIK-induced tumor survival signaling could be at play and lead to the observation of poor clinical outcome. Our study provides a rationale to investigate non-canonical roles of BIK related to tumor growth. In addition, exploration of interactions of BIK with autophagy and clinical response in breast cancer patients could set the stage for novel therapeutic regimens in the future.

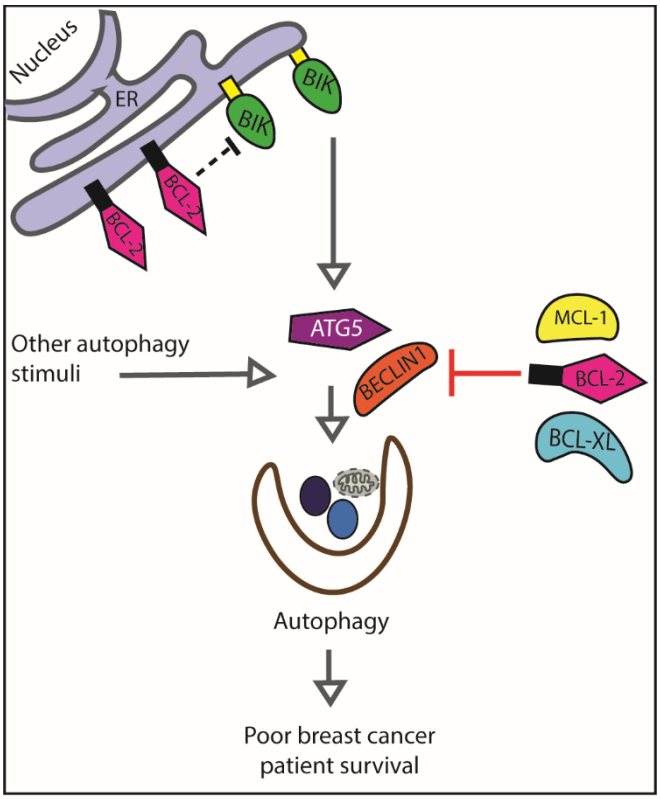

Figure 3.9 Model describing relationships between BIK, BCL-2 and ATG-5 with respect to patient survival. I propose that BIK stimulates autophagy and BCL-2 inhibits autophagy. Thus, BIK and BCL-2 function in two separates yet converging pathways associated with poor patient prognosis.

References

Abdel-Fatah, T.M., Perry, C., Dickinson, P., Ball, G., Moseley, P., Madhusudan, S., Ellis, I.O., and Chan, S.Y. (2013). Bcl2 is an independent prognostic marker of triple negative breast cancer (TNBC) and predicts response to anthracycline combination (ATC) chemotherapy (CT) in adjuvant and neoadjuvant settings. Ann Oncol *24*, 2801-2807.

An, C.H., Kim, M.S., Yoo, N.J., Park, S.W., and Lee, S.H. (2011). Mutational and expressional analyses of ATG5, an autophagy-related gene, in gastrointestinal cancers. Pathology, research and practice *207*, 433-437.

Anagnostou, V.K., Lowery, F.J., Zolota, V., Tzelepi, V., Gopinath, A., Liceaga, C., Panagopoulos, N., Frangia, K., Tanoue, L., Boffa, D.*, et al.* (2010). High expression of BCL-2 predicts favorable outcome in non-small cell lung cancer patients with non squamous histology. BMC Cancer *10*, 186.

Arena, V., Martini, M., Luongo, M., Capelli, A., and Larocca, L.M. (2003). Mutations of the BIK gene in human peripheral B-cell lymphomas. Genes Chromosomes Cancer *38*, 91-96.

Bodet, L., Menoret, E., Descamps, G., Pellat-Deceunynck, C., Bataille, R., Le Gouill, S., Moreau, P., Amiot, M., and Gomez-Bougie, P. (2010). BH3-only protein Bik is involved in both apoptosis induction and sensitivity to oxidative stress in multiple myeloma. Br J Cancer *103*, 1808-1814.

Bredel, M., Bredel, C., Juric, D., Harsh, G.R., Vogel, H., Recht, L.D., and Sikic, B.I. (2005). High-resolution genome-wide mapping of genetic alterations in human glial brain tumors. Cancer Res *65*, 4088-4096.

Castells, A., Ino, Y., Louis, D.N., Ramesh, V., Gusella, J.F., and Rustgi, A.K. (1999). Mapping of a target region of allelic loss to a 0.5-cM interval on chromosome 22q13 in human colorectal cancer. Gastroenterology *117*, 831-837.

CCS (2018). Canadian Cancer Statistics 2018 (Canadian Cancer Society).

Chang, N.C., Nguyen, M., Germain, M., and Shore, G.C. (2010). Antagonism of Beclin 1-dependent autophagy by BCL-2 at the endoplasmic reticulum requires NAF-1. EMBO J *29*, 606-618.

Chen, S., Zhou, L., Zhang, Y., Leng, Y., Pei, X.Y., Lin, H., Jones, R., Orlowski, R.Z., Dai, Y., and Grant, S. (2014). Targeting SQSTM1/p62 Induces Cargo-Loading Failure and Converts Autophagy to Apoptosis via NBK/Bik. Mol Cell Biol.

Chinnadurai, G., Vijayalingam, S., and Rashmi, R. (2008). BIK, the founding member of the BH3-only family proteins: mechanisms of cell death and role in cancer and pathogenic processes. Oncogene *27 Suppl 1*, S20-29.

Cho, D.H., Jo, Y.K., Kim, S.C., Park, I.J., and Kim, J.C. (2012). Down-regulated expression of ATG5 in colorectal cancer. Anticancer Res *32*, 4091-4096.

Czabotar, P.E., Lessene, G., Strasser, A., and Adams, J.M. (2013). Control of apoptosis by the BCL-2 protein family: implications for physiology and therapy. Nature Reviews Molecular Cell Biology *15*, 49.

Czabotar, P.E., Lessene, G., Strasser, A., and Adams, J.M. (2014). Control of apoptosis by the BCL-2 protein family: implications for physiology and therapy. Nat Rev Mol Cell Biol *15*, 49-63.

Day, C.P., Rau, K.M., Qiu, L., Liu, C.W., Kuo, H.P., Xie, X., Lopez-Berestein, G., Hortobagyi, G.N., and Hung, M.C. (2006). Mutant Bik expression mediated by the enhanced minimal topoisomerase IIalpha promoter selectively suppressed breast tumors in an animal model. Cancer gene therapy *13*, 706-719.

Dikic, I., and Elazar, Z. (2018). Mechanism and medical implications of mammalian autophagy. Nature Reviews Molecular Cell Biology *19*, 349-364.

Doerflinger, M., Glab, J.A., and Puthalakath, H. (2015). BH3-only proteins: a 20-year stock-take. Febs j *282*, 1006-1016.

Ferlay J, S.I., Ervik M, Dikshit R, Eser S, Mathers C, Rebelo M, Parkin DM, Forman D, Bray, F. (2013). Cancer Incidence and Mortality Worldwide: IARC CancerBase No. 11 [Internet]. In GLOBOCAN 2012 v10, .

Ferlay, J., Soerjomataram, I., Dikshit, R., Eser, S., Mathers, C., Rebelo, M., Parkin, D.M., Forman, D., and Bray, F. (2015). Cancer incidence and mortality worldwide: sources, methods and major patterns in GLOBOCAN 2012. International journal of cancer Journal international du cancer *136*, E359-386.

Garcia, N., Salamanca, F., Astudillo-de la Vega, H., Curiel-Quesada, E., Alvarado, I., Penaloza, R., and Arenas, D. (2005). A molecular analysis by gene expression profiling reveals Bik/NBK overexpression in sporadic breast tumor samples of Mexican females. BMC cancer *5*, 93.

Gasparini, G., Barbareschi, M., Doglioni, C., Palma, P.D., Mauri, F.A., Boracchi, P., Bevilacqua, P., Caffo, O., Morelli, L., Verderio, P.*, et al.* (1995). Expression of bcl-2 protein predicts efficacy of adjuvant treatments in operable node-positive breast cancer. Clin Cancer Res *1*, 189-198.

Ge, J., Chen, Z., Huang, J., Chen, J., Yuan, W., Deng, Z., and Chen, Z. (2014). Upregulation of autophagy-related gene-5 (ATG-5) is associated with chemoresistance in human gastric cancer. PLoS One *9*, e110293.

Germain, D.R., Graham, K., Glubrecht, D.D., Hugh, J.C., Mackey, J.R., and Godbout, R. (2011). DEAD box 1: a novel and independent prognostic marker for early recurrence in breast cancer. Breast Cancer Res Treat *127*, 53-63.

Guo, J.Y., Xia, B., and White, E. (2013). Autophagy-mediated tumor promotion. Cell *155*, 1216-1219.

Henry, N.L., and Hayes, D.F. (2012). Cancer biomarkers. Mol Oncol *6*, 140-146.

Hershko, T., and Ginsberg, D. (2004). Up-regulation of Bcl-2 homology 3 (BH3)-only proteins by E2F1 mediates apoptosis. J Biol Chem *279*, 8627-8634.

Ichim, G., Lopez, J., Ahmed, S.U., Muthalagu, N., Giampazolias, E., Delgado, M.E., Haller, M., Riley, J.S., Mason, S.M., Athineos, D.*, et al.* (2015). Limited mitochondrial permeabilization causes DNA damage and genomic instability in the absence of cell death. Molecular cell *57*, 860-872.

Jemal, A., Bray, F., Center, M.M., Ferlay, J., Ward, E., and Forman, D. (2011). Global cancer statistics. CA Cancer J Clin *61*, 69-90.

Jiao, S., Wu, M., Ye, F., Tang, H., Xie, X., and Xie, X. (2014). BikDDA, a mutant of Bik with longer half-life expression protein, can be a novel therapeutic gene for triple-negative breast cancer. PloS one *9*, e92172.

Karakas, T., Maurer, U., Weidmann, E., Miething, C.C., Hoelzer, D., and Bergmann, L. (1998). High expression of bcl-2 mRNA as a determinant of poor prognosis in acute myeloid leukemia. Ann Oncol *9*, 159-165.

Kaur, J., and Debnath, J. (2015). Autophagy at the crossroads of catabolism and anabolism. Nat Rev Mol Cell Biol *16*, 461-472.

Kim, J.-Y., Ahn, H.-J., Ryu, J.-H., Suk, K., and Park, J.-H. (2004). BH3-only Protein Noxa Is a Mediator of Hypoxic Cell Death Induced by Hypoxia-inducible Factor 1α. The Journal of Experimental Medicine *199*, 113-124.

Kim, M.S., Song, S.Y., Lee, J.Y., Yoo, N.J., and Lee, S.H. (2011). Expressional and mutational analyses of ATG5 gene in prostate cancers. APMIS : acta pathologica, microbiologica, et immunologica Scandinavica *119*, 802-807.

Lan, K.L., Yen, S.H., Liu, R.S., Shih, H.L., Tseng, F.W., and Lan, K.H. (2007). Mutant Bik gene transferred by cationic liposome inhibits peritoneal disseminated murine colon cancer. Clinical & experimental metastasis *24*, 461-470.

Li, C., Li, R., Grandis, J.R., and Johnson, D.E. (2008). Bortezomib induces apoptosis via Bim and Bik up-regulation and synergizes with cisplatin in the killing of head and neck squamous cell carcinoma cells. Mol Cancer Ther *7*, 1647-1655.

Lipponen, P., Pietilainen, T., Kosma, V.M., Aaltomaa, S., Eskelinen, M., and Syrjanen, K. (1995). Apoptosis suppressing protein bcl-2 is expressed in well-differentiated breast carcinomas with favourable prognosis. J Pathol *177*, 49-55.

Liu, R.Z., Graham, K., Glubrecht, D.D., Germain, D.R., Mackey, J.R., and Godbout, R. (2011). Association of FABP5 expression with poor survival in triple-negative breast cancer: implication for retinoic acid therapy. Am J Pathol *178*, 997-1008.

Lomonosova, E., and Chinnadurai, G. (2008). BH3-only proteins in apoptosis and beyond: an overview. Oncogene *27 Suppl 1*, S2-19.

Lopez-Munoz, E., Hernandez-Zarco, A., Garcia-Hernandez, N., Alvarado-Cabrero, I., Zarco-Espinosa, G., Salamanca-Gomez, F., and Arenas-Aranda, D. (2012). BIK/NBK gene as potential marker of prognostic and therapeutic target in breast cancer patients. Clinical & translational oncology : official publication of the Federation of Spanish Oncology Societies and of the National Cancer Institute of Mexico *14*, 586-591.

Lopez, J., Hesling, C., Prudent, J., Popgeorgiev, N., Gadet, R., Mikaelian, I., Rimokh, R., Gillet, G., and Gonzalo, P. (2012). Src tyrosine kinase inhibits apoptosis through the Erk1/2- dependent degradation of the death accelerator Bik. Cell death and differentiation *19*, 1459-1469.

Lu, Y., Lemon, W., Liu, P.Y., Yi, Y., Morrison, C., Yang, P., Sun, Z., Szoke, J., Gerald, W.L., Watson, M.*, et al.* (2006). A gene expression signature predicts survival of patients with stage I non-small cell lung cancer. PLoS medicine *3*, e467.

Maiuri, M.C., Criollo, A., Tasdemir, E., Vicencio, J.M., Tajeddine, N., Hickman, J.A., Geneste, O., and Kroemer, G. (2007). BH3-only proteins and BH3 mimetics induce autophagy by competitively disrupting the interaction between Beclin 1 and Bcl-2/Bcl-X(L). Autophagy *3*, 374-376.

Mathai, J.P. (2005). The role of endoplasmic reticulum BIK in p53-mediated apoptosis In Biochemistry (Montreal: McGill University).

Maxfield, K.E., Taus, P.J., Corcoran, K., Wooten, J., Macion, J., Zhou, Y., Borromeo, M., Kollipara, R.K., Yan, J., Xie, Y.*, et al.* (2015). Comprehensive functional characterization of cancer-testis antigens defines obligate participation in multiple hallmarks of cancer. Nat Commun *6*, 8840.

Mazel, S., Burtrum, D., and Petrie, H.T. (1996). Regulation of cell division cycle progression by bcl-2 expression: a potential mechanism for inhibition of programmed cell death. J Exp Med *183*, 2219-2226.

Nakano, K., and Vousden, K.H. (2001). PUMA, a novel proapoptotic gene, is induced by p53. Mol Cell *7*, 683-694.

Oda, E., Ohki, R., Murasawa, H., Nemoto, J., Shibue, T., Yamashita, T., Tokino, T., Taniguchi, T., and Tanaka, N. (2000). Noxa, a BH3-only member of the Bcl-2 family and candidate mediator of p53-induced apoptosis. Science *288*, 1053-1058.

Pattingre, S., Tassa, A., Qu, X., Garuti, R., Liang, X.H., Mizushima, N., Packer, M., Schneider, M.D., and Levine, B. (2005). Bcl-2 antiapoptotic proteins inhibit Beclin 1-dependent autophagy. Cell *122*, 927-939.

Puthalakath, H., and Strasser, A. (2002). Keeping killers on a tight leash: transcriptional and post-translational control of the pro-apoptotic activity of BH3-only proteins. Cell Death Differ *9*, 505-512.

Rashmi, R., Pillai, S.G., Vijayalingam, S., Ryerse, J., and Chinnadurai, G. (2008). BH3-only protein BIK induces caspase-independent cell death with autophagic features in Bcl-2 null cells. Oncogene *27*, 1366-1375.

Real, P.J., Sanz, C., Gutierrez, O., Pipaon, C., Zubiaga, A.M., and Fernandez-Luna, J.L. (2006). Transcriptional activation of the proapoptotic bik gene by E2F proteins in cancer cells. FEBS Lett *580*, 5905-5909.

Ruiz Esparza-Garrido, R., Torres-Marquez, M.E., Viedma-Rodriguez, R., Velazquez-Wong, A.C., Salamanca-Gomez, F., Rosas-Vargas, H., and Velazquez-Flores, M.A. (2015). Breast cancer cell line MDA-MB-231 miRNA profile expression after BIK interference: BIK involvement in autophagy. Tumour Biol.

Sowter, H.M., Ratcliffe, P.J., Watson, P., Greenberg, A.H., and Harris, A.L. (2001). HIF-1-dependent regulation of hypoxic induction of the cell death factors BNIP3 and NIX in human tumors. Cancer Res *61*, 6669-6673.

Sturm, I., Stephan, C., Gillissen, B., Siebert, R., Janz, M., Radetzki, S., Jung, K., Loening, S., Dorken, B., and Daniel, P.T. (2006). Loss of the tissue-specific proapoptotic BH3-only protein Nbk/Bik is a unifying feature of renal cell carcinoma. Cell Death Differ *13*, 619-627.

Sunters, A., Fernandez de Mattos, S., Stahl, M., Brosens, J.J., Zoumpoulidou, G., Saunders, C.A., Coffer, P.J., Medema, R.H., Coombes, R.C., and Lam, E.W. (2003). FoxO3a transcriptional regulation of Bim controls apoptosis in paclitaxel-treated breast cancer cell lines. J Biol Chem *278*, 49795-49805.

Sup, S.J., Alemany, C.A., Pohlman, B., Elson, P., Malhi, S., Thakkar, S., Steinle, R., and Hsi, E.D. (2005). Expression of bcl-2 in classical Hodgkin's lymphoma: an independent predictor of poor outcome. J Clin Oncol *23*, 3773-3779.

Tang, J.Y., Fang, Y.Y., Hsi, E., Huang, Y.C., Hsu, N.C., Yang, W.C., Chang, H.W., Chai, C.Y., and Chu, P.Y. (2013). Immunopositivity of Beclin-1 and ATG5 as indicators of survival and disease recurrence in oral squamous cell carcinoma. Anticancer Res *33*, 5611-5616.

Vairo, G., Innes, K.M., and Adams, J.M. (1996). Bcl-2 has a cell cycle inhibitory function separable from its enhancement of cell survival. Oncogene *13*, 1511-1519.

Van Poznak, C., Somerfield, M.R., Bast, R.C., Cristofanilli, M., Goetz, M.P., Gonzalez-Angulo, A.M., Hicks, D.G., Hill, E.G., Liu, M.C., Lucas, W.*, et al.* (2015). Use of Biomarkers to Guide Decisions on Systemic Therapy for Women With Metastatic Breast Cancer: American Society of Clinical Oncology Clinical Practice Guideline. J Clin Oncol *33*, 2695-2704.

Wei, H., Wei, S., Gan, B., Peng, X., Zou, W., and Guan, J.L. (2011). Suppression of autophagy by FIP200 deletion inhibits mammary tumorigenesis. Genes Dev *25*, 1510-1527.

Wei, Y., Pattingre, S., Sinha, S., Bassik, M., and Levine, B. (2008). JNK1-mediated phosphorylation of Bcl-2 regulates starvation-induced autophagy. Mol Cell *30*, 678-688.

Yang, S., Wang, X., Contino, G., Liesa, M., Sahin, E., Ying, H., Bause, A., Li, Y., Stommel, J.M., Dell'antonio, G.*, et al.* (2011). Pancreatic cancers require autophagy for tumor growth. Genes Dev *25*, 717-729.

You, H., Pellegrini, M., Tsuchihara, K., Yamamoto, K., Hacker, G., Erlacher, M., Villunger, A., and Mak, T.W. (2006). FOXO3a-dependent regulation of Puma in response to cytokine/growth factor withdrawal. J Exp Med *203*, 1657-1663.

Zhan, F., Huang, Y., Colla, S., Stewart, J.P., Hanamura, I., Gupta, S., Epstein, J., Yaccoby, S., Sawyer, J., Burington, B.*, et al.* (2006). The molecular classification of multiple myeloma. Blood *108*, 2020-2028.

CHAPTER 4

BIK EXPRESSION IN BREAST CANCER CELLS PROMOTES LIMITED UPREGULATION OF AUTOPHAGY BUT DOES NOT PROMOTE CELL SURVIVAL

4.1 Introduction

Autophagy (self-eating) is a cellular catabolic process that sequesters and recycles intracellular components such as cytoplasmic contents, protein aggregates, and damaged organelles. Hence, it acts as a cytoprotective mechanism under stressful conditions such as starvation, hypoxia, endoplasmic reticulum stress and/or mitochondrial damage (Kaur and Debnath, 2015; Kimmelman, 2011; White et al., 2015). These stressors commonly exist in tumors, and therefore elevated autophagy can promote cancer cell survival by subverting apoptosis (Kaur and Debnath, 2015). Excessive autophagy, however, can lead to Type-II programmed cell death (PCD-II) also referred to as autophagic cell death (Kaur and Debnath, 2015; Kimmelman, 2011; Marino et al., 2014). Therefore, a fine regulation of this process is critical in cancer cells to tip the balance towards survival.

4.1.1 Overview of the autophagic pathway

Autophagy is initiated by the formation of double membrane-bound vacuoles known as autophagosomes to enclose cellular cargo destined for degradation. Autophagosomes subsequently fuse with lysosomes to create autolysosomes where the cargo degradation takes place by lysosomal hydrolases (Das et al., 2012; Dikic and Elazar, 2018; Kaur and Debnath, 2015). The molecular machinery involved in this process and the sequence of events is briefly discussed here (Figure 4.1 A). Autophagosomes are formed through a 3-step process called initiation, nucleation, and expansion. At the initiation step, a kinase complex consisting of ULK1/ULK2 kinases, autophagy related 13 (ATG-13), FIP200 and ATG101 (hereafter referred to as the ULK1 complex) assembles at the phagophore assembly site (PAS) (Kaur and Debnath, 2015; Mizushima et al.,

2011). Membranes required for this process are most commonly derived from the endoplasmic reticulum (*ER*) but other membranous organelles such as the Golgi apparatus, plasma membrane, recycling endosomes as well as the *ER*-Mito contact sites can donate membranes depending on the nature of the stress and selected cargo (Axe et al., 2008; Hamasaki et al., 2013; Kaur and Debnath, 2015; Ravikumar et al., 2010). The ULK1 complex then facilitates the nucleation step by phosphorylating Beclin1 on Ser14 (Figure 4.1 A) (Russell et al., 2013), which forms a crucial component of a second kinase complex made up of phosphoinositide 3-kinase (PI3K) VPS34, VPS15 and co-activator ATG14L (hereafter referred to as the VPS34 complex) (Figure 4.1 A) (Mizushima et al., 2011). Once activated, this complex converts phosphatidylinositol 4,5-bisphosphate (PIP2) to phosphatidylinositol 3,4,5-triphosphate (PIP3), which serves as a membrane-bound localized signal that facilitates the assembly of protein scaffolds for membrane expansion (Dikic and Elazar, 2018; Funderburk et al., 2010). Subsequent expansion proceeds by the action of two ubiquitin-like conjugation systems with the end goal of lipidating microtubule-associated protein 1A/1B-light chain 3 (LC3 I) (Figure 4.1 B). This process is crucial for phagophore expansion, autophagosome sealing as well as later recognition of the autophagy receptors (Dikic and Elazar, 2018; Kaur and Debnath, 2015). The first conjugation system produces a dimeric ATG-5~ATG-12-ATG16L (~denotes conjugation whereas – denotes noncovalent complex formation) complex with E3-like activity critical for LC3 I lipidation in the second conjugation system (Mizushima et al., 2011). This complex is formed by a two-step process (Figure 4.1 B). First, ATG-5 and ATG-12 are conjugated by the action of E1- and E2-like enzymes ATG-7 and ATG-10 respectively, followed by ATG-5~ATG12 forming a complex with ATG-16L (Kaur and Debnath, 2015). The second conjugation system produces lipidated LC3 I required for the phagophore

expansion and sealing process. It involves proteolytic processing of ATG8/LC3 by ATG-4, leading to the formation of LC3 I (Figure 4.1 B) (Mizushima et al., 2011). Subsequently, E1- and E2-like enzymes ATG-7 and ATG-3 along with the ATG-5~ATG12-ATG16L complex, which possesses E3-like activity to carry out conjugation of phosphatidylethanolamine (PE) with LC3 I generating LC3 II (Figure 4.1 B) (also called LC3~PE) (Dikic and Elazar, 2018; Kaur and Debnath, 2015). Thus, ATG-5 in association with ATG-12 and ATG-16L plays a crucial role throughout the phagophore expansion process. Following the expansion and sealing, autophagosomes undergo maturation wherein ATGs, and PIP3 are gradually removed by ATG-4A and MMTRs, which act as a protease and a phosphatase respectively (Dikic and Elazar, 2018). Mature autophagosomes fuse with lysosomes through SNAREs such as SYN17, SNAP29, and SYN6, forming autolysosomes where the cargo degradation occurs (Dikic and Elazar, 2018; Itakura et al., 2012). Building blocks such as amino acids generated from this process are released in the cytosol for recycling. Thus, autophagy supplies nutrients during starvation.

4.1.2 Autophagy in tumor suppression and promotion

Autophagy was initially thought to be a tumor-suppressing mechanism. This was due to the observation that monoallelic loss of the gene coding for Beclin1 was found in more than 40% cases of human prostate, breast and ovarian cancers (Aita et al., 1999; Liang et al., 1999). Furthermore, Beclin1 heterozygous mice are predisposed to develop lung and liver cancers as well as lymphomas (Qu et al., 2003; Yue et al., 2003). However, in the genetically engineered mouse model of hereditary breast cancer, Beclin1 allelic deletion actually reduces tumorigenesis, which is opposite to what would be expected if Beclin1 was a tumor suppressor. As well, mutations of

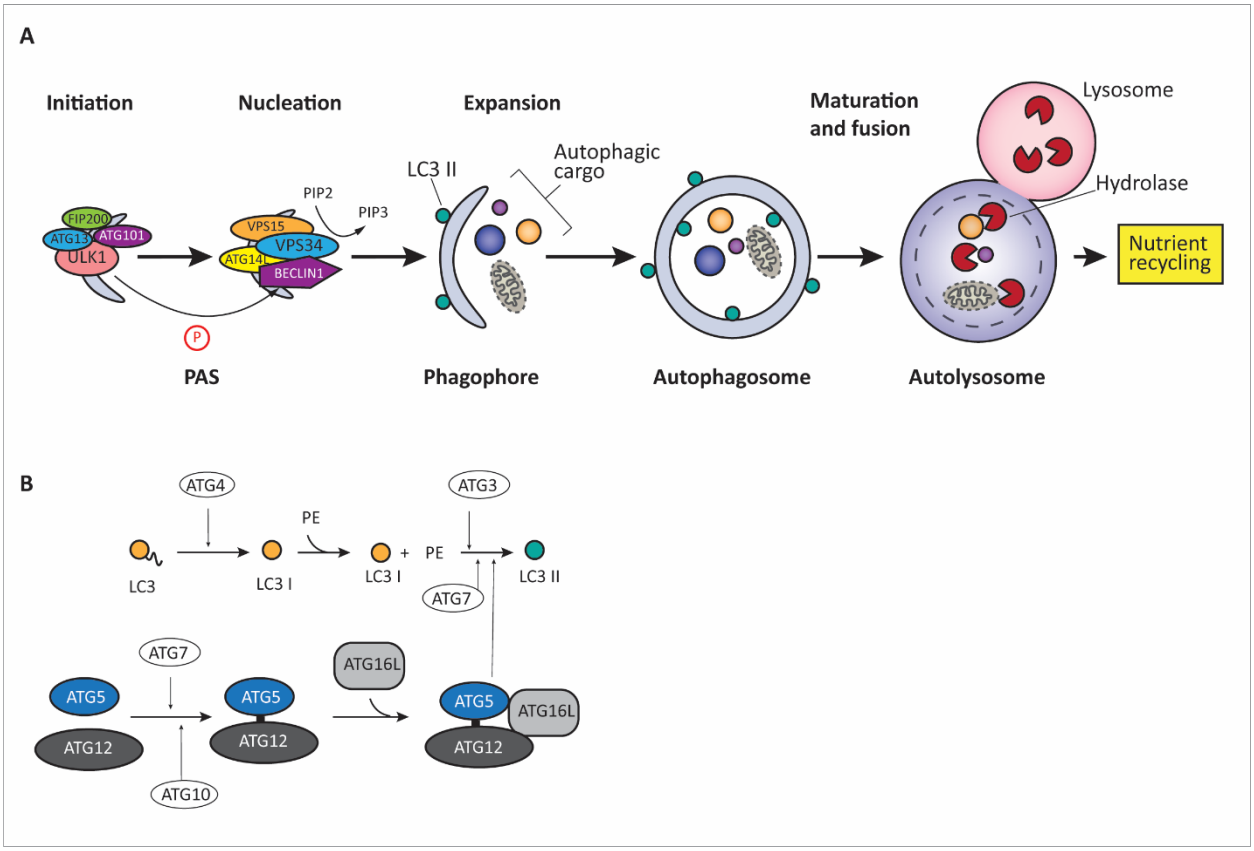

Figure 4.1 Sequence of events in the autophagic pathway. A. Cartoon depicting the generation of PAS, cargo enclosure and fusion of the autophagosomes with lysosomes where aggregated proteins and damaged organelles are degraded by lysosomal hydrolases and recycled. **B.** The depiction of the two ubiquitin-like conjugation systems with the end goal of converting LC3 I to LC3 II.

other essential autophagy genes are also not frequently found in human cancers, suggesting that autophagy may not have a tumor-suppressing role (Lawrence et al., 2014; Vogelstein et al., 2013; White, 2015). Additionally, Takamura et al. demonstrated that liver-specific or mosaic deletions of essential autophagy genes *Atg5* and *Atg7* only produced benign liver tumors (Takamura et al., 2011) that did not progress to frank cancers, suggesting that autophagy deficiency could initiate tumor formation but is not sufficient to drive oncogenic progression. Thus, altogether, the evidence supporting tumor-suppressing role of autophagy is limited.

On the contrary, autophagy as a tumor-promoting pathway has been well established due to its intricate involvement in cell survival. Crucially, mice deficient in *Atg3*, *Atg5*, *Atg7*, *Atg12,* and *Atg16* do not survive past 1 day after birth (Komatsu et al., 2005; Yoshii et al., 2017). As well, adult mice with conditional *Atg7* deletion, when subjected to fasting, do not survive beyond 24 hrs, which suggests a crucial role autophagy plays to promote survival (Karsli-Uzunbas et al., 2014). In the context of cancer, the role of *Atg5* and *Atg7* is well studied in the mutant Ras-driven lung and pancreatic cancer models (White, 2015). *Atg5* or *Atg7* deficiency in these tumors increased cell death and reduced tumor burden, suggesting autophagy was promoting tumor cell survival (Guo et al., 2013; Rao et al., 2014). Furthermore, in rapidly growing tumors, regions of hypoxia or nutrient starvation exist where autophagic stimulation promotes cell survival (Degenhardt et al., 2006). Autophagy has also been demonstrated to promote therapeutic resistance. For instance, treatment of mouse lymphoma tumors with alkylating agents induced autophagy and its inhibition with lysosomal acidification inhibitor chloroquine (CQ) or siRNA silencing of autophagic machinery led to extensive cell killing (Amaravadi et al., 2007). The clinical application of this

approach is being tested in many clinical trials using a CQ derivative called hydroxychloroquine (HCQ) to inhibit autophagy in combination with chemotherapeutic agents (Kimmelman, 2011). These findings underscore a tumor-promoting role of autophagy and its essential components such as ATG-5 by facilitating cell survival.

4.1.3 Regulation of autophagy by the BCL-2 family proteins

Autophagy is regulated by the BCL-2 family of proteins at the phagophore initiation step. Anti-apoptotic BCL-2 members inhibit autophagic initiation whereas BH3-only pro-apoptotic proteins in most cases stimulate it. Anti-apoptotic members such as BCL-2, BCL-XL, and MCL-1 directly interact with Beclin1, which is a BH3-only protein and a co-activator critical for the activity of PI3 kinase VPS34 (Figure 4.2 A) (Marino et al., 2014). This interaction abrogates VPS34 complex formation preventing the conversion of PIP2 to PIP3 required for phagophore expansion (Marino et al., 2014; Mizushima et al., 2011). Interestingly, BH3-only proteins such as BAD, BID, BIK, PUMA, NOXA and NIX as well as BH3 mimetics can break the interaction between anti-apoptotic BCL-2 members and Beclin-1, allowing the activation of the VPS34 complex (Marino et al., 2014). Thus, protein-protein interactions between pro- and anti-apoptotic proteins regulate autophagic induction in addition to regulating apoptosis.

4.1.4 BIK induces autophagy in the presence or absence of BCL-2

The mechanism whereby BH3-only protein BIK stimulates autophagy has been studied both in the presence or absence of BCL-2 and therefore is more complex than a simple BCL-2 sequestration model (Chang et al., 2010; Chen et al., 2014; Rashmi et al., 2008) (Figure 4.2 B). As previously mentioned, autophagy has both cytoprotective and cytodestructive roles depending on

the context. The first hint of BIK's involvement in autophagy came from the studies of Naumann et al. (Naumann et al., 2003) and Oppermann et al. (Oppermann et al., 2005) with the observation of a non-apoptotic mode of cell death upon BIK expression. These authors using human glioma or melanoma cell lines, demonstrated that ectopic BIK expression induced a type of cell death that did not show classical features of apoptosis such as cytochrome *c* release or caspase activation, and was not blocked by selective caspase inhibitors. This, raised the possibility of autophagic cell death upon BIK expression. Subsequently, Rashmi et al. (Rashmi et al., 2008) investigated BIK induced cell death through an autophagic pathway in the presence or absence of BCL-2. These authors found that ectopic BIK expression in *Bcl-2* $^{+/+}$ and *Bcl-2*$^{-/-}$ mouse embryonic fibroblasts (MEFs) resulted in the classical morphological signs of autophagic activation including cytosolic vacuoles and punctate distribution of autophagic marker GFP-LC3 in the *Bcl-2*$^{-/-}$ MEFs along with reduced cell viability (Figure 4.2 B) (Rashmi et al., 2008). Autophagic cell death in the absence of BCL-2 was further confirmed by improved cell survival upon treatment with autophagic inhibitors 3-Methyladenine (3-MA) and wortmannin (Rashmi et al., 2008). Conversely, treatment with z-VAD-fmk, which is a pan-caspase inhibitor however reduced cell viability indicating a protective role of caspases in autophagic cell death. Thus, this study demonstrated that BIK promoted autophagic cell death in *Bcl-2* $^{-/-}$ cells and caspases somehow inhibited this process.

The second pathway of BIK induced autophagy has been described in cells expressing endoplasmic reticulum-targeted BCL-2 referred to as BCL-2b5 (Chang et al., 2010). BCL-2 interacts with Beclin1, which prevents Beclin1 association in the VPS34 complex with a resulting block in the phagophore formation (Marino et al., 2014). Chang et al. explored the BIK: BCL-2

connection in the context of autophagy (Figure 4.2 B) (Chang et al., 2010). These authors identified a BCL-2 interacting partner nutrient-deprivation autophagy factor-1 (NAF1) that was required for BCL-2 suppression of Beclin1 mediated autophagy (Chang et al., 2010). In lung cancer and melanoma cell lines, BIK was able to displace NAF1 from BCL-2 although the mechanism was not through direct competition, as BIK and NAF-1 bound to different domains on BCL-2. BIK overexpression in this system induced autophagic induction, which was enhanced by NAF-1 silencing. This suggested that in BCL-2 competent cells, BIK stimulated phagophore assembly by dissociating NAF-1 from BCL-2, presumably allowing Beclin1 to activate VPS34 complex. Collectively, these studies demonstrated that BIK could induce autophagy and affect cellular health *in vitro* (Figure 4.2 B). However, the effect of BIK stimulated autophagy on *in vivo* cell survival was not known.

BIK is induced in response to tumor-associated stress stimuli such as hypoxia (Koong et al., 2000), genotoxic insults (Mathai et al., 2005) and growth factor withdrawal (Hur et al., 2004). These stressors also induce autophagy (Eliopoulos et al., 2016; Fang et al., 2015; Lum et al., 2005), which promotes cell survival in glioblastoma (Hu et al., 2012) and breast cancer models (Kimmelman, 2011). These observations implied that BIK upregulation induced autophagy may have a cytoprotective role in cancer. Interestingly, by performing gene expression analysis of *BIK* and *ATG5* in relation to breast cancer patient survival outcomes, I had found that *BIK: ATG-5*-high patients had poorer recurrence-free survival outcomes compared to the only *BIK*-high subset (Pandya et al., 2016). Given that ATG-5 is a critical component required for the phagophore expansion process as well as its established role in cell survival, its association with *BIK* provided

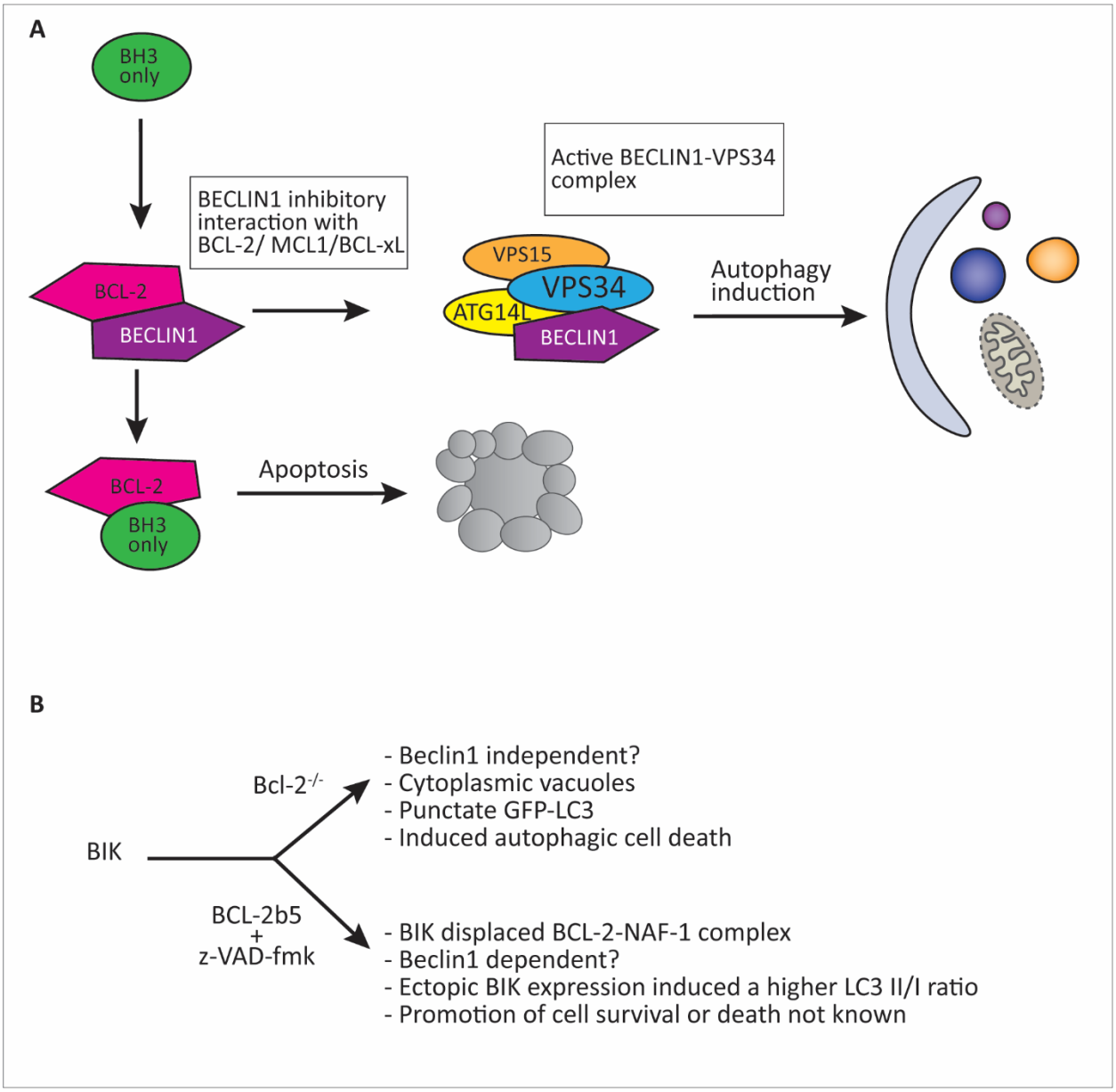

Figure 4.2 Regulation of autophagy by BCL-2 family proteins. A. Anti-apoptotic BCL-2 family proteins sequester Beclin1, which is a co-activator of the VPS34 kinase, preventing initiation of autophagy. BH3-only proteins can relieve this block by competing with anti-apoptotic BCL-2 members for binding. Depending on the intensity of the stress signal, this may induce autophagy or apoptosis. **B.** BIK induced autophagy occurs in the presence or absence of BCL-2 suggesting Beclin1-independent or Beclin1-dependent pathways.

the rationale to investigate BIK stimulated autophagy and tumor cell survival in a breast cancer model. I hypothesized that transient or stable expression of BIK in breast cancer cells may stimulate autophagy leading to improved breast cancer cell survival and may explain a cell-autonomous mechanism whereby *BIK: ATG5* high breast cancer patients show poor survival outcomes.

4.2 Results

In order to determine whether BIK induces autophagy in breast cancer cells, I transiently transfected the breast carcinoma MCF-7 cell line with an expression plasmid encoding human BIK (Figure 4.3 A). Autophagy in cells exists in a basal state and is stimulated by nutrient depletion. Basal autophagy removes misfolded proteins and damaged organelles ensuring optimum cell fitness, whereas autophagic stimulation due to starvation provides essential metabolites such amino and fatty acids as well as glucose to support cell survival (Kaur and Debnath, 2015). To investigate these two states of autophagy, MCF-7 cells transiently expressing BIK were incubated in nutrient-rich or -depleted media called Earl's balanced salt solution (EBSS) in the presence or absence of Bafilomycin A1 (Baf A1). EBSS is a balanced salt solution containing glucose with a physiological pH but lacking in amino acids and serum. It is used to mimic amino acid and growth factor starvation-induced autophagy (Klionsky et al., 2016). Baf A1, a proton pump inhibitor, prevents autolysosomal degradation by blocking the lysosomal acidification required for the activity of acid hydrolases and is used in this assay to account for accelerated cargo degradation. I assessed autophagic flux by measuring the ratio of LC3 II to LC3 I by western blot analysis (Figure 4.3 A). Upon autophagic induction, LC3 I undergoes a conjugation reaction with

phosphatidylethanolamine (PE) producing LC3 II, which is detected as a faster running product on a western blot (Kaur and Debnath, 2015; Klionsky et al., 2016). LC3 II eventually undergoes degradation along with the autophagic cargo. Therefore, a high LC3 II/ I ratio is an indication of increased autophagic flux. Blocked autolysosomal degradation by Baf A1 promotes LC3 II accumulation. Therefore, further elevation in the LC3 II/I ratio with Baf A1 treatment suggests a truly accelerated autophagy. Interestingly, I found that transient BIK expressing cells had a higher LC3 II/I ratio under nutrient-rich conditions compared to mock transfected control, suggesting an increase in the basal autophagic flux (Figure 4.3 B). Furthermore, Baf A1 treatment enhanced this ratio, indicating that BIK stimulated basal autophagy. Conversely, EBSS starvation reduced LC3 II/ I ratio in BIK expressing cells, which may indicate increased lysosomal degradation of LC3 II due to increased autophagy. To test this, I measured autophagic flux in the presence Baf A1, which revealed no additional increase in LC3 II accumulation compared to mock transfected control, suggesting that BIK does not augment starvation-induced autophagy (Figure 4.3 B). These differences were however not statistically significant. Altogether these results indicated that transient BIK expression induces a non-statistically significant basal autophagy but does not affect nutrient-starved autophagic flux.

Cationic lipids such as Lipofectamine 2000 used for transient transfections have been found to induce autophagy and may compound the interpretation of the results (Man et al., 2010). Furthermore, transient transfection can lead to aggregation of the expressed proteins. Therefore, some reports suggest limiting their use in autophagic assays (Mizushima et al., 2010). Hence, I decided to generate stable BIK expressing MCF-7 and MDA-MB-231 cell lines to interrogate BIK

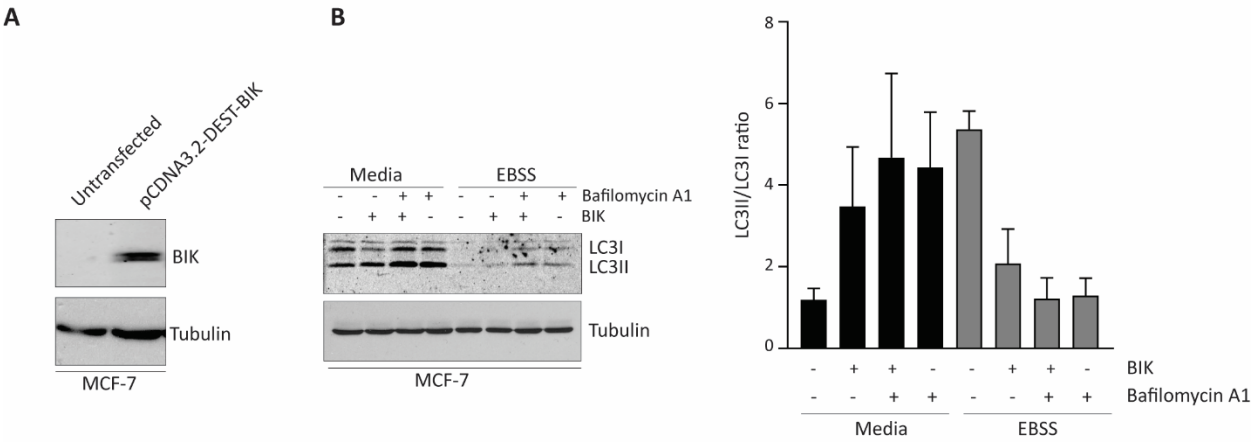

Figure 4.3 Transient BIK expression in breast cancer cells and effect on EBSS stimulated autophagy. A. Western blot analysis of transient BIK expression in MCF-7 cells. **B.** Left: Representative western blot depicting the analysis of basal or EBSS stimulated autophagic flux in response to transient BIK expression. 2.5 x 10^5 MCF-7 cells were mock or pCDNA3.2-DEST-BIK transfected for 24 h followed by a 4 h incubation in regular growth medium or EBSS with or without the proton pump inhibitor Bafilomycin A1 (200 nM). Cell lysates were prepared, and western blotting was performed with the indicated antibodies. Right: Ratio of LC3 II to LC3 I was determined by densitometric analysis of scanned blots using the ImageJ program. Bar graphs depict mean ± SEM calculated from 3 independent experiments. One-way ANOVA was performed to find significance among groups and was found to be non-significant (p= 0.063).

mediated autophagy (Figure 4.4 A). I re-asked the question whether stable BIK expression enhanced basal or nutrient starvation-induced autophagy in this new experimental system. BIK or vector expressing MCF-7 cells were either incubated in nutrient-rich growth medium or challenged with EBSS in the presence or absence of Baf A1. Autophagic flux was measured by taking LC3 II to LC3 I ratio using western blot analysis (Figure 4.4 B). BIK expressing MCF-7 cells had slightly elevated LC3 II production under nutrient-rich conditions. However, Baf A1 treatment failed to augment it further, suggesting BIK did not promote basal autophagy. Upon EBSS starvation, however, BIK expressing cells showed an increase in LC3 II, which was modestly enhanced by Baf A1 treatment implying that BIK may stimulate starvation-induced autophagy in MCF-7 cells (Figure 4.4 B). In BIK expressing MDA-MB-231 cell lines, I found a slight increase in LC3 II levels under nutrient-rich conditions, which was not augmented by Baf A1 treatment indicating that BIK did not induce basal autophagy in these cells. Under EBSS mediated nutrient depletion, both BIK expressing clones showed elevated LC3 II levels however, when I tested this upregulation with Baf A1 treatment, one clone (B33) showed a higher LC3 II levels and the other clone (B28) showed lower LC3 II levels compared to the vector control, suggesting that BIK augmented EBSS mediated autophagy although a clonal variation was observed (Figure 4.4 B). In conclusion, in stable BIK expressing MCF-7 and MDA-MB-231 cell lines, BIK expression modestly increased starvation-induced autophagy, but basal autophagic flux remained unaffected.

Next, I decided to investigate autophagy in the presence of a different autophagic stimulus rapamycin, which inhibits upstream regulator mammalian target of rapamycin complex 1 (mTORC1) (Ballou and Lin, 2008). mTORC1 inhibition de-represses the assembly of ULK1 kinase

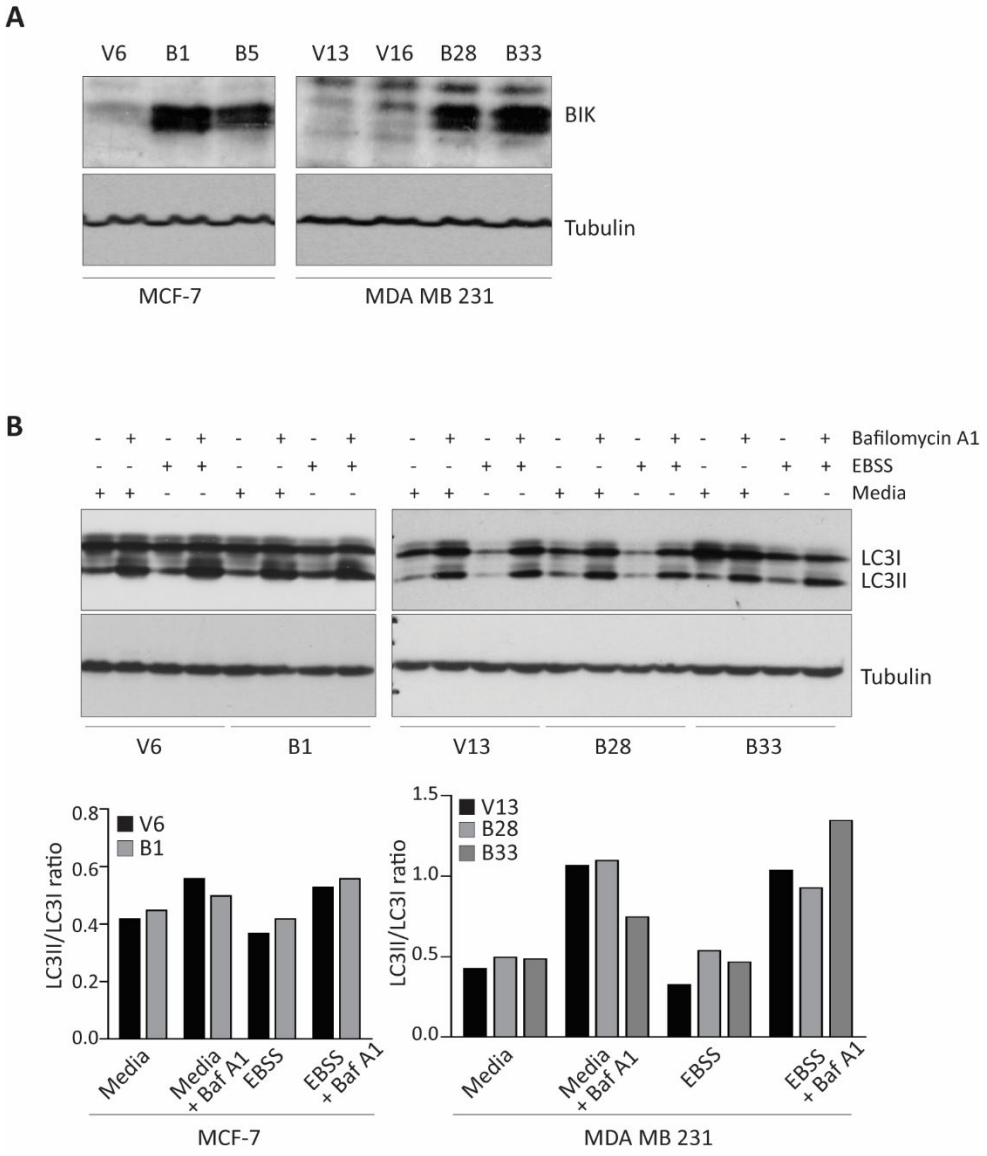

Figure 4.4 Stable BIK expression in breast cancer cell lines and effect on EBSS stimulated autophagy. A. Western blot analysis depicting stable vector or BIK expressing MCF-7 or MDA MB 231 cell lines. Note that since V13 clone of MDA MB 231 cell line showed the lowest endogenous BIK expression, it was used for further experiments. **B.** Top: Western blots depicting the analysis of basal or EBSS stimulated autophagic flux in the presence of stable BIK expression. 2.5 x 10^5 Vector or BIK expressing MCF-7 or MDA MB 231 cells were incubated in regular growth medium or EBSS for 4 h with or without proton pump inhibitor Bafilomycin A1 (200 nM). Cell lysates were prepared, and western blotting was performed with the indicated antibodies. Bottom: Ratio of LC3 II to LC3 I was determined by densitometric analysis of scanned blots using the ImageJ program.

complex and stimulates phagophore formation (Ballou and Lin, 2008). Stable BIK or vector expressing MCF-7 or MDA-MB-231 cells were treated with rapamycin with or without Baf A1 treatments to evaluate BIK augmentation of rapamycin-induced autophagy (Figure 4.5). Autophagic flux was measured by LC3 II to LC3 I ratio calculation (Figure 4.5 A). In the MCF-7 group, BIK expressing clone B5 displayed increased LC3 II formation in both basal and rapamycin stimulated conditions, indicating that BIK promoted autophagic induction in the presence or absence of mTORC1 inhibition. This was confirmed by further accumulation of LC3 II upon Baf A1 block of autolysosomal degradation, suggesting BIK enhanced basal and rapamycin stimulated autophagy in clone B5. In the other BIK expressing clone B1 however, LC3 II levels remained unchanged under basal conditions as well as following Baf A1 inhibition, suggesting an inhibitory role of BIK in basal autophagy. Furthermore, upon rapamycin stimulation, clone B1 did not show a change in the autophagic flux, whereas with Baf A1 treatment, the autophagic flux reduced as indicated by reduced LC3 II levels compared to the vector control (Figure 4.5 A). In conclusion, the two BIK expressing MCF-7 clones showed opposite results, confounding the interpretation of results.

I also evaluated autophagic flux in BIK expressing MDA-MB-231 cell lines upon rapamycin treatment. BIK expressing clone B28 showed increased LC3 II levels compared to vector control under basal conditions, but Baf A1 block did not confirm true autophagic stimulation, suggesting a lack of BIK effect on basal autophagy. Augmentation of rapamycin-induced autophagy was also not observed in this BIK expressing clone (Figure 4.5 B). Furthermore, a second BIK expressing clone B33 showed reduced LC3 II levels under basal and rapamycin-induced conditions with or without

Baf A1 block, suggesting an inhibitory role of BIK on basal and rapamycin-induced autophagy (Figure 4.5 B). Collectively this data showed that one of the MCF-7 stable BIK expressing cell lines displayed increased basal and rapamycin stimulated autophagic flux. MDA-MB-231 cell lines stably expressing BIK however, did not show any kind of autophagic induction. Altogether these results suggested a very limited autophagic stimulation by BIK.

Finally, in order to determine the role of BIK induced autophagy in breast cancer cell survival under basal and nutrient-starved conditions, I challenged vector or BIK expressing stable MCF-7 or MDA-MB- 231 cells in EBSS starvation medium and measured cell growth by MTT assay (Figure 4.6). BIK expressing MCF-7 cell lines did not show enhanced growth in nutrient-replete or deficient conditions suggesting that BIK-induced autophagy did not affect steady-state maintenance of cellular fitness nor did it promote cell survival upon nutrient stress in MCF-7 cells. Furthermore, BIK expressing MDA-MB-231 cells, had a lower cell survival in nutrient-rich conditions whereas their survival was unchanged upon nutrient starvation. This suggested a growth inhibitory role of BIK under nutrient availability. Thus, altogether this data showed that BIK might only marginally affect autophagy and confer no survival advantage in the basal or nutrient starved states.

Overall, the results suggested that BIK did not induce autophagy in general. While these data are preliminary examinations of *in vitro* conditions, they did not reveal robust autophagic signaling in response to BIK. Thus the BIK association with poor patient outcome may be driven by non-autophagic mechanisms.

4.3 Discussion

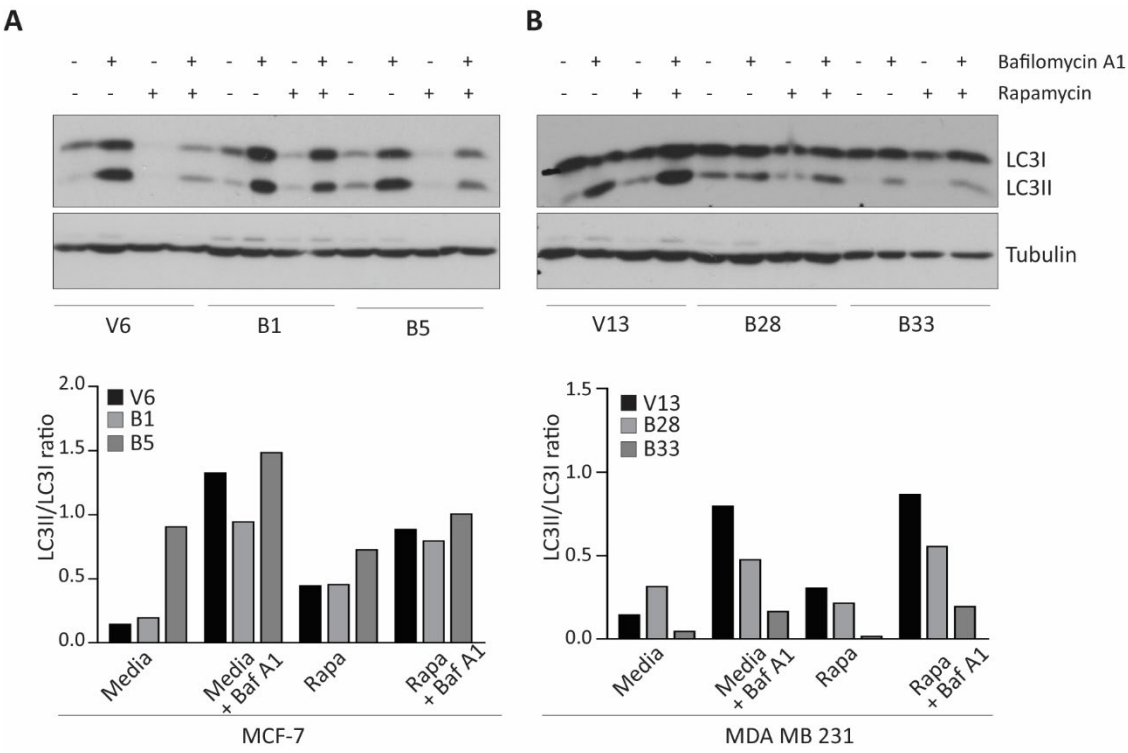

Figure 4.5 Rapamycin stimulated autophagy in BIK expressing cell lines. A. Top: Western blots depicting the analysis of basal or rapamycin stimulated autophagic flux in the presence of stable BIK expression. 2.5 x 10^5 vector or BIK expressing MCF-7 or MDA MB 231 cells were treated with vehicle or 0.5 µM Rapamycin for 12 h with or without proton pump inhibitor Bafilomycin A1 (200 nM) during the last 4 h of treatments. Cell lysates were prepared, and western blotting was performed with the indicated antibodies. Bottom: Ratio of LC3 II to LC3 I was determined by densitometric analysis of scanned blots using the ImageJ program.

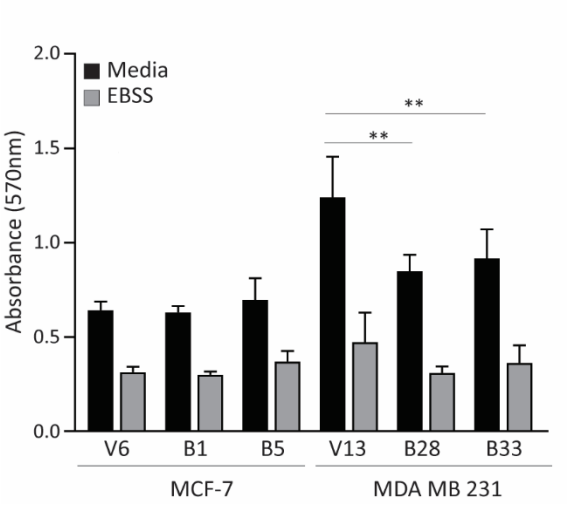

Figure 4.6 BIK expression does not improve cell survival. Vector or BIK expressing MCF-7 or MDA MB 231 cells were incubated in EBSS or growth media for 4 h followed by replacement of EBSS with growth media. 48 h later MTT assay was performed. Bar graphs depict the mean ± SEM of 3 independent experiments. One-way ANOVA was performed followed Sidak's post-hoc test to determine significance among groups. (** $p<0.01$).

I investigated BIK's involvement in promoting breast cancer cell survival by the autophagic pathway. The premise for this investigation was the observation that the combined signature of *BIK* and *ATG-5* mRNA levels correlated with poor patient prognosis. Previous studies reported that exogenous BIK expression might promote autophagy in certain settings (Chang et al., 2010; Rashmi et al., 2008). Some of these studies however overexpressed BIK (Chang et al., 2010; Rashmi et al., 2008), used hBIK in mouse cells (Rashmi et al., 2008) or selectively activated autophagy by using caspase inhibitors (Chang et al., 2010). Also, investigation of autophagy concerning BIK is confounded by the fact that BIK is not induced in response to nutrient starvation (Chang et al., 2010) or *ER* stress (Mathai et al., 2005) where a rescue mechanism such as autophagy plays a crucial role. Therefore, it is important to study BIK's role in a setting where it is physiologically induced. Additionally, observations including our data show that BIK overexpression reduces cellular health (Naumann et al., 2003; Rashmi et al., 2008). Thus BIK may not directly promote cell survival and cause cancer aggression, warranting exploration of alternative mechanisms of tumor promotion.

Our observation in patient tumors that BIK-high patients do poorly raises two important questions. Firstly, how is BIK upregulation achieved in tumors? Moreover, secondly, how does upregulated BIK affect tumor biology to promote cancer aggression? In this regard, an investigation into therapy-induced BIK expression and exploration of non-canonical functions such as recently discovered failed apoptosis may uncover a link between BIK upregulation and poor patient outcomes.

References

Aita, V.M., Liang, X.H., Murty, V.V., Pincus, D.L., Yu, W., Cayanis, E., Kalachikov, S., Gilliam, T.C., and Levine, B. (1999). Cloning and genomic organization of beclin 1, a candidate tumor suppressor gene on chromosome 17q21. Genomics *59*, 59-65.

Amaravadi, R.K., Yu, D., Lum, J.J., Bui, T., Christophorou, M.A., Evan, G.I., Thomas-Tikhonenko, A., and Thompson, C.B. (2007). Autophagy inhibition enhances therapy-induced apoptosis in a Myc-induced model of lymphoma. The Journal of clinical investigation *117*, 326-336.

Axe, E.L., Walker, S.A., Manifava, M., Chandra, P., Roderick, H.L., Habermann, A., Griffiths, G., and Ktistakis, N.T. (2008). Autophagosome formation from membrane compartments enriched in phosphatidylinositol 3-phosphate and dynamically connected to the endoplasmic reticulum. The Journal of cell biology *182*, 685-701.

Ballou, L.M., and Lin, R.Z. (2008). Rapamycin and mTOR kinase inhibitors. Journal of Chemical Biology *1*, 27-36.

Chang, N.C., Nguyen, M., Germain, M., and Shore, G.C. (2010). Antagonism of Beclin 1-dependent autophagy by BCL-2 at the endoplasmic reticulum requires NAF-1. The EMBO Journal *29*, 606-618.

Chen, S., Zhou, L., Zhang, Y., Leng, Y., Pei, X.Y., Lin, H., Jones, R., Orlowski, R.Z., Dai, Y., and Grant, S. (2014). Targeting SQSTM1/p62 induces cargo loading failure and converts autophagy to apoptosis via NBK/Bik. Mol Cell Biol *34*, 3435-3449.

Das, G., Shravage, B.V., and Baehrecke, E.H. (2012). Regulation and function of autophagy during cell survival and cell death. Cold Spring Harbor perspectives in biology *4*.

Degenhardt, K., Mathew, R., Beaudoin, B., Bray, K., Anderson, D., Chen, G., Mukherjee, C., Shi, Y., Gelinas, C., Fan, Y.*, et al.* (2006). Autophagy promotes tumor cell survival and restricts necrosis, inflammation, and tumorigenesis. Cancer cell *10*, 51-64.

Dikic, I., and Elazar, Z. (2018). Mechanism and medical implications of mammalian autophagy. Nature Reviews Molecular Cell Biology *19*, 349-364.

Eliopoulos, A.G., Havaki, S., and Gorgoulis, V.G. (2016). DNA Damage Response and Autophagy: A Meaningful Partnership. Frontiers in Genetics *7*.

Fang, Y., Tan, J., and Zhang, Q. (2015). Signaling pathways and mechanisms of hypoxia-induced autophagy in the animal cells. Cell biology international *39*, 891-898.

Funderburk, S.F., Wang, Q.J., and Yue, Z. (2010). The Beclin 1-VPS34 complex--at the crossroads of autophagy and beyond. Trends in cell biology *20*, 355-362.

Guo, J.Y., Karsli-Uzunbas, G., Mathew, R., Aisner, S.C., Kamphorst, J.J., Strohecker, A.M., Chen, G., Price, S., Lu, W., Teng, X.*, et al.* (2013). Autophagy suppresses progression of K-ras-induced lung tumors to oncocytomas and maintains lipid homeostasis. Genes & development *27*, 1447-1461.

Hamasaki, M., Furuta, N., Matsuda, A., Nezu, A., Yamamoto, A., Fujita, N., Oomori, H., Noda, T., Haraguchi, T., Hiraoka, Y.*, et al.* (2013). Autophagosomes form at ER-mitochondria contact sites. Nature *495*, 389-393.

Hu, Y.L., DeLay, M., Jahangiri, A., Molinaro, A.M., Rose, S.D., Carbonell, W.S., and Aghi, M.K. (2012). Hypoxia-induced autophagy promotes tumor cell survival and adaptation to antiangiogenic treatment in glioblastoma. Cancer Res *72*, 1773-1783.

Hur, J., Chesnes, J., Coser, K.R., Lee, R.S., Geck, P., Isselbacher, K.J., and Shioda, T. (2004). The Bik BH3-only protein is induced in estrogen-starved and antiestrogen-exposed breast cancer cells and provokes apoptosis. Proceedings of the National Academy of Sciences of the United States of America *101*, 2351-2356.

Itakura, E., Kishi-Itakura, C., and Mizushima, N. (2012). The hairpin-type tail-anchored SNARE syntaxin 17 targets to autophagosomes for fusion with endosomes/lysosomes. Cell *151*, 1256-1269.

Karsli-Uzunbas, G., Guo, J.Y., Price, S., Teng, X., Laddha, S.V., Khor, S., Kalaany, N.Y., Jacks, T., Chan, C.S., Rabinowitz, J.D.*, et al.* (2014). Autophagy is required for glucose homeostasis and lung tumor maintenance. Cancer Discov *4*, 914-927.

Kaur, J., and Debnath, J. (2015). Autophagy at the crossroads of catabolism and anabolism. Nature reviews Molecular cell biology *16*, 461-472.

Kimmelman, A.C. (2011). The dynamic nature of autophagy in cancer. Genes & development *25*, 1999-2010.

Klionsky, D.J., Abdelmohsen, K., Abe, A., Abedin, M.J., Abeliovich, H., Acevedo Arozena, A., Adachi, H., Adams, C.M., Adams, P.D., Adeli, K.*, et al.* (2016). Guidelines for the use and interpretation of assays for monitoring autophagy (3rd edition). Autophagy *12*, 1-222.

Komatsu, M., Waguri, S., Ueno, T., Iwata, J., Murata, S., Tanida, I., Ezaki, J., Mizushima, N., Ohsumi, Y., Uchiyama, Y.*, et al.* (2005). Impairment of starvation-induced and constitutive autophagy in Atg7-deficient mice. The Journal of cell biology *169*, 425-434.

Koong, A.C., Denko, N.C., Hudson, K.M., Schindler, C., Swiersz, L., Koch, C., Evans, S., Ibrahim, H., Le, Q.T., Terris, D.J.*, et al.* (2000). Candidate genes for the hypoxic tumor phenotype. Cancer Res *60*, 883-887.

Lawrence, M.S., Stojanov, P., Mermel, C.H., Robinson, J.T., Garraway, L.A., Golub, T.R., Meyerson, M., Gabriel, S.B., Lander, E.S., and Getz, G. (2014). Discovery and saturation analysis of cancer genes across 21 tumour types. Nature *505*, 495-501.

Liang, X.H., Jackson, S., Seaman, M., Brown, K., Kempkes, B., Hibshoosh, H., and Levine, B. (1999). Induction of autophagy and inhibition of tumorigenesis by beclin 1. Nature *402*, 672-676.

Lum, J.J., Bauer, D.E., Kong, M., Harris, M.H., Li, C., Lindsten, T., and Thompson, C.B. (2005). Growth factor regulation of autophagy and cell survival in the absence of apoptosis. Cell *120*, 237-248.

Man, N., Chen, Y., Zheng, F., Zhou, W., and Wen, L.P. (2010). Induction of genuine autophagy by cationic lipids in mammalian cells. Autophagy *6*, 449-454.

Marino, G., Niso-Santano, M., Baehrecke, E.H., and Kroemer, G. (2014). Self-consumption: the interplay of autophagy and apoptosis. Nature reviews Molecular cell biology *15*, 81-94.

Mathai, J.P., Germain, M., and Shore, G.C. (2005). BH3-only BIK regulates BAX,BAK-dependent release of Ca2+ from endoplasmic reticulum stores and mitochondrial apoptosis during stress-induced cell death. The Journal of biological chemistry *280*, 23829-23836.

Mizushima, N., Yoshimori, T., and Levine, B. (2010). Methods in mammalian autophagy research. Cell *140*, 313-326.

Mizushima, N., Yoshimori, T., and Ohsumi, Y. (2011). The role of Atg proteins in autophagosome formation. Annu Rev Cell Dev Biol *27*, 107-132.

Naumann, U., Schmidt, F., Wick, W., Frank, B., Weit, S., Gillissen, B., Daniel, P., and Weller, M. (2003). Adenoviral natural born killer gene therapy for malignant glioma. Hum Gene Ther *14*, 1235-1246.

Oppermann, M., Geilen, C.C., Fecker, L.F., Gillissen, B., Daniel, P.T., and Eberle, J. (2005). Caspase-independent induction of apoptosis in human melanoma cells by the proapoptotic Bcl-2-related protein Nbk / Bik. Oncogene *24*, 7369.

Pandya, V., Glubrecht, D., Vos, L., Hanson, J., Damaraju, S., Mackey, J., Hugh, J., and Goping, I.S. (2016). The pro-apoptotic paradox: the BH3-only protein Bcl-2 interacting killer (Bik) is prognostic for unfavorable outcomes in breast cancer. Oncotarget *7*, 33272-33285.

Qu, X., Yu, J., Bhagat, G., Furuya, N., Hibshoosh, H., Troxel, A., Rosen, J., Eskelinen, E.L., Mizushima, N., Ohsumi, Y.*, et al.* (2003). Promotion of tumorigenesis by heterozygous disruption of the beclin 1 autophagy gene. The Journal of clinical investigation *112*, 1809-1820.

Rao, S., Tortola, L., Perlot, T., Wirnsberger, G., Novatchkova, M., Nitsch, R., Sykacek, P., Frank, L., Schramek, D., Komnenovic, V.*, et al.* (2014). A dual role for autophagy in a murine model of lung cancer. Nat Commun *5*, 3056.

Rashmi, R., Pillai, S.G., Vijayalingam, S., Ryerse, J., and Chinnadurai, G. (2008). BH3-only protein BIK induces caspase-independent cell death with autophagic features in Bcl-2 null cells. Oncogene *27*, 1366-1375.

Ravikumar, B., Moreau, K., Jahreiss, L., Puri, C., and Rubinsztein, D.C. (2010). Plasma membrane contributes to the formation of pre-autophagosomal structures. Nature cell biology *12*, 747-757.

Russell, R.C., Tian, Y., Yuan, H., Park, H.W., Chang, Y.-Y., Kim, J., Kim, H., Neufeld, T.P., Dillin, A., and Guan, K.-L. (2013). ULK1 induces autophagy by phosphorylating Beclin-1 and activating VPS34 lipid kinase. Nature cell biology *15*, 741.

Takamura, A., Komatsu, M., Hara, T., Sakamoto, A., Kishi, C., Waguri, S., Eishi, Y., Hino, O., Tanaka, K., and Mizushima, N. (2011). Autophagy-deficient mice develop multiple liver tumors. Genes & development *25*, 795-800.

Vogelstein, B., Papadopoulos, N., Velculescu, V.E., Zhou, S., Diaz, L.A., Jr., and Kinzler, K.W. (2013). Cancer genome landscapes. Science (New York, NY) *339*, 1546-1558.

White, E. (2015). The role for autophagy in cancer. The Journal of clinical investigation *125*, 42-46.

White, E., Mehnert, J.M., and Chan, C.S. (2015). Autophagy, Metabolism, and Cancer. Clinical cancer research : an official journal of the American Association for Cancer Research *21*, 5037-5046.

Yoshii, S.R., Kuma, A., and Mizushima, N. (2017). Transgenic rescue of Atg5-null mice from neonatal lethality with neuron-specific expression of ATG5: Systemic analysis of adult Atg5-deficient mice. Autophagy *13*, 763-764.

Yue, Z., Jin, S., Yang, C., Levine, A.J., and Heintz, N. (2003). Beclin 1, an autophagy gene essential for early embryonic development, is a haploinsufficient tumor suppressor. Proceedings of the National Academy of Sciences of the United States of America *100*, 15077-15082.

CHAPTER 5

BIK-HIGH ER-POSITIVE PATIENTS HAVE WORSE PROGNOSIS POTENTIALLY THROUGH BIK MEDIATED FAILED APOPTOSIS

A modified version of chapter 5 of this thesis is in preparation for publication as Pandya V, Githaka JM, Kirschenman R, Patel N, Veldhoen R, Damaraju S, Mackey J and Goping IS (2018). BIK is a prognostic maker for ER-positive breast cancer and induces sublethal apoptosis to promote cancer aggression (Manuscript in preparation).

5.1 Introduction

Breast cancer is divided into 3 broad subgroups that dictate the course of treatment. Broadly, these are defined as estrogen receptor (ER)/progesterone receptor (PR) positive, HER2 positive and triple negative subtypes. Of these, the ER/PR positive subtype (called ER-positive from here on) has the best outcomes but is associated with substantial morbidity and mortality because it accounts for 70% of all breast cancer cases (Turner et al., 2017). ER-positive breast cancers depend on estrogen and ER signaling to facilitate growth and are treated with endocrine therapies that suppress estrogen effects. The disease-free survival statistics for primary ER-positive breast cancer is greater than 90% after the first diagnosis demonstrating relatively effective first-line therapy (Sopik et al., 2017; Yu et al., 2012). Disease-free survival for locoregional recurrence, however, is reduced to 70% (Aebi et al., 2014), reflecting key gaps in our understanding of treatment resistance.

Apoptosis is a cell death program with tumor-suppressor activities. Inhibition of apoptosis causes cancer, and this was first identified in B-cell lymphomas driven by the anti-apoptotic protein BCL-2 (Erikson et al., 1983; McDonnell et al., 1989). Biological insights into this protein family led to the development of BH3 mimetics that inhibit BCL-2 anti-apoptotic activities, to initiate the cascade of mitochondrial outer membrane permeabilization, caspase activation and cell death (Billard, 2013; Delbridge and Strasser, 2015). In 2016, ABT-199/Venetoclax, attained breakthrough drug designation from the FDA for the treatment of leukemia (Roberts et al., 2016) and is in clinical testing for multiple other cancers (Billard, 2013; Opydo-Chanek et al., 2017). Hence apoptosis is primarily considered a tumor suppressive process and is a target facilitating

tumor cell death and cancer control. Paradoxically, high BCL-2 protein levels are prognostic for favorable outcomes in breast cancer (Berardo et al., 1998; Neri et al., 2006; Pandya et al., 2016; Vargas-Roig et al., 2008). This suggests that attenuating apoptosis limits cancer progression. In line with this, recent studies have shown that low levels of apoptosis are instead oncogenic (Ichim et al., 2015; Ichim and Tait, 2016; Liu et al., 2015). Cultured cells that were exposed to sublethal doses of radiation, chemotherapeutic drugs or the BH3 mimetic ABT-737 became transformed and/or developed more aggressive tumor characteristics (Ichim et al., 2015; Liu et al., 2015; Miles and Hawkins, 2017). Mechanistically, this "failed apoptosis" stimulated apoptotic DNases such as caspase activated DNAse (CAD) and EndoG that induced double-strand breaks (DSBs) in the nuclear DNA leading to genomic instability, oncogenesis, cancer aggression and/or therapeutic resistance (Cartwright et al., 2017; Ichim et al., 2015; Ichim and Tait, 2016; Larsen and Sorensen, 2017; Liu et al., 2015; Miles and Hawkins, 2017). Thus, incompletely executed apoptosis has tumor-promoting consequences in experimental model systems, although the pertinence of this to clinical disease is not yet clear.

BIK is a pro-apoptotic BH3-only member of the BCL-2 family. Our study of 2 independent breast cancer patient cohorts (n=327) showed that BIK is prognostic for relapse and decreased overall survival (Pandya et al., 2016). This negative association suggests that BIK induces failed apoptosis within the context of clinical disease. Typically, the steady-state expression of BIK is modest and is regulated at the transcriptional level in response to various stressors (Bodet et al., 2010; Chinnadurai et al., 2008; Hur et al., 2006; Real et al., 2006; Ritchie et al., 2009; Spender et al., 2009). Importantly, BIK expression is induced upon estrogen starvation or in response to anti-

estrogen treatment of ER-positive cells (Coser et al., 2009; Fu et al., 2007; Hur et al., 2006; Hur et al., 2004; Viedma-Rodriguez et al., 2013; Viedma-Rodriguez et al., 2015; Zhou et al., 2011) indicating that BIK may be specifically relevant to ER-positive breast cancer. Here we show that BIK elevation in endocrine treated ER-positive breast cancer patients is associated with 8.4-fold increased recurrence and mortality but has no prognostic value for ER-negative patients that were treated with other modalities. BIK did not trigger cell death and instead facilitated DNA damage and the evolution of aggressive cancer cells. Thus BIK-induced failed apoptosis in response to endocrine therapy may provide a molecular explanation for recurrence of ER-positive breast cancer.

5.2 Results

5.2.1 *BIK* transcript levels differentially predict prognosis of ER-positive and ER-negative breast cancer patients

To validate the dependence of BIK expression on estrogen, I treated the ER-positive cell line MCF-7 with tamoxifen and active metabolite 4-hydroxytamoxifen (4-HT) and confirmed that BIK was induced in response to endocrine therapy (Figure 5.1 A). I next analyzed the association of *BIK* transcript levels with survival outcomes of ER-positive vs. ER-negative patients. A cut-point (≤1.72) for *BIK* gene expression values was previously determined (Pandya et al., 2016) using ROC curve analysis that dichotomized the patients into *BIK*-high (19%) and *BIK*-low (81%) groups. Next, I plotted 5 -years disease-free and overall survival outcomes of ER-positive and ER-negative patients (Dataset-1, total n=175) with respect to *BIK* gene expression levels (Figure 5.1 B and C). Interestingly, high *BIK* transcript levels showed an association trend with poor disease-free survivals of ER-positive patients, that was not statistically significant (p=0.15, log-rank test,

HR=1.58) (Figure 5.1 B). Intriguingly, in this cohort, high *BIK* transcript levels significantly predicted worse disease-free survival outcomes of ER-negative patients. Analysis of the overall survivals, on the other hand, revealed contrasting results. High *BIK* transcript levels were significantly associated with the 2.42-fold increased rate of cancer associated deaths (p=0.03, log-rank test) in the ER-positive group, whereas for the ER-negative group there was no significant difference between the survival curves nor a trend indicating *BIK* association (Figure 5.1 C). Thus, *BIK* transcript levels predicted poor disease-free outcomes of ER-negative patients yet poor overall survival of ER-positive patients. These confounding results within the same cohort suggest that *BIK* mRNA levels are not correlated with function.

5.2.2 Analysis of BIK protein levels is the most suited approach to study its association with prognosis of ER-positive patients

The steady-state level of BIK protein is regulated by multiple transcriptional and post-translational mechanisms, so it is likely that *BIK* mRNA does not directly predict BIK protein levels. This may explain in part the confounding results of *BIK* mRNA association with outcomes in the ER-positive and –negative subgroups. In order to understand whether *BIK* mRNA and protein levels correlate in breast cancer tumors, I compared these parameters in breast cancer samples. Since we had already collected BIK protein levels from the tissue microarray of Dataset-2 (n=152) (Pandya et al., 2016), I queried whether gene expression data had been collected from this cohort. mRNA information had been collected from 13 of these patients for which we had matching BIK protein level information. In order to decipher a relationship between *BIK* transcript and protein levels in these tumors, I first plotted a scatter diagram of the continuous score values

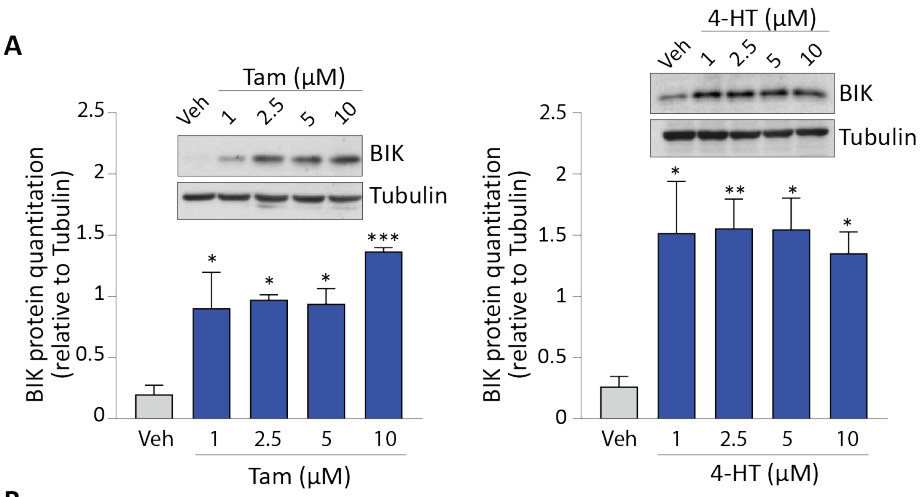
A
Tam (μM)
Veh
1
2.5
5
10
BIK
Tubulin
BIK protein quantitation (relative to Tubulin)
Tam (μM)
4-HT (μM)

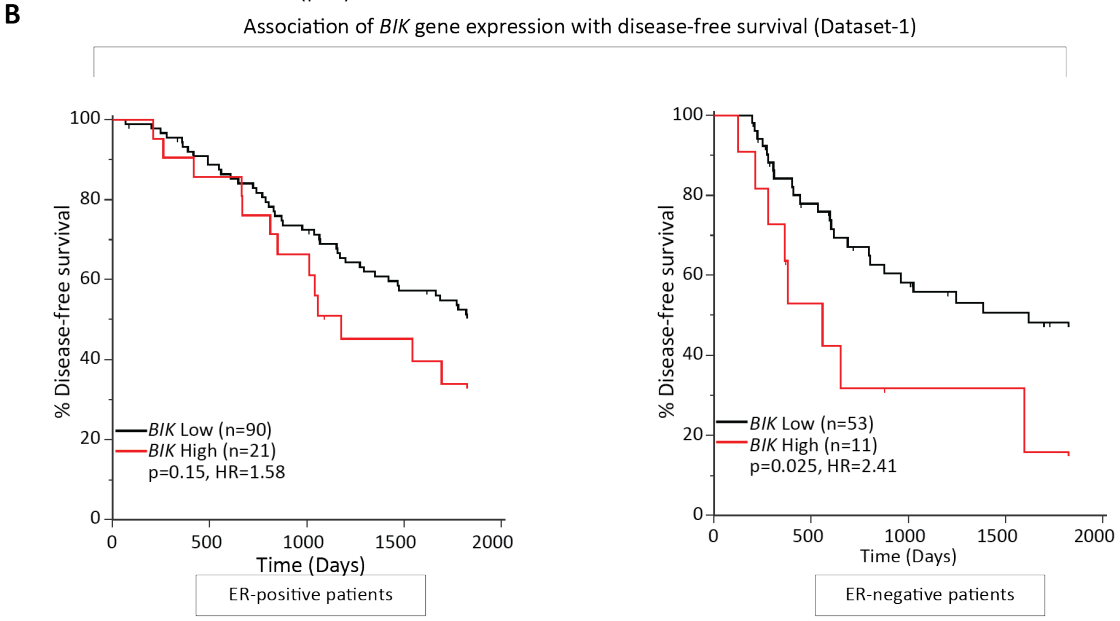
B
Association of BIK gene expression with disease-free survival (Dataset-1)
% Disease-free survival
Time (Days)
BIK Low (n=90)
BIK High (n=21)
p=0.15, HR=1.58
ER-positive patients
BIK Low (n=53)
BIK High (n=11)
p=0.025, HR=2.41
ER-negative patients

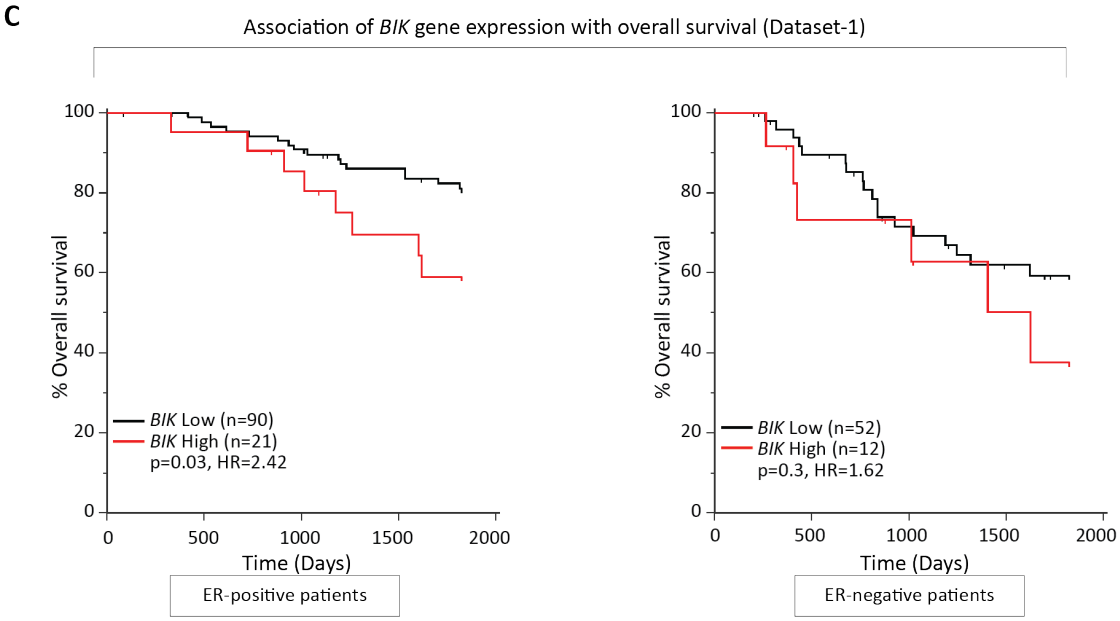
C
Association of BIK gene expression with overall survival (Dataset-1)
% Overall survival
Time (Days)
BIK Low (n=90)
BIK High (n=21)
p=0.03, HR=2.42
ER-positive patients
BIK Low (n=52)
BIK High (n=12)
p=0.3, HR=1.62
ER-negative patients

Figure 5.1 BIK induction in response to anti-estrogen treatment and prediction of survival outcomes in the ER-positive and ER-negative breast cancer. A. Western blots and their quantitation showing BIK upregulation with Tamoxifen (left) and 4-HT treatments (right) of MCF-7 cells for 72 hrs. Error bars indicate SEM of 3 independent experiments. Significance between untreated and treated was determined by One-way ANOVA followed by Dunnet's multiple comparisions test. (* $p<0.05$, * $p<0.01$). **B and C.** Kaplan-Meier survival curves depicting 5 years disease-free or overall survival outcomes of patients stratified in ER-positive anti-estrogen treated vs. ER-negative groups, and their survival outcomes were calculated based on *BIK* mRNA levels in tumor cores. The HR value of greater than 1.0 estimates the predicted risk of poor prognosis. p value was calculated using log-rank analysis.

of *BIK* mRNA and protein levels followed by correlation analysis (Figure 5.2 A). Intriguingly, I found no correlation between mRNA and protein values (Pearson's correlation coeff. r=0.14, p=0.65). Furthermore, using categorical values (BIK-low=0, BIK-high=1) calculated using ROC curve analysis, I performed Chi-squared analysis and Fisher's exact test (used when the sample size is low) to further investigate the relationship between *BIK* gene and protein expression levels (Figure 5.2 B). The null hypothesis that both tests assume prevailed and showed no significant association between *BIK* transcript and protein levels (p=0.44, Chi-squared; p=0.56, Fisher's exact test). Thus, these findings indicated that *BIK* gene and protein levels in breast cancer tumors are not correlated. Importantly, this analysis suggested that analysis of BIK protein and not mRNA levels in ER-positive and –negative patients in relation to the clinical outcome would more accurately identify possible functional roles of BIK in tumors.

In order to identify whether *BIK* transcript or protein levels were the best predictors of survival outcomes, I tested how *BIK* transcript and protein levels predicted survival outcomes in the 13 overlapping patients (Figure 5.2 C). I found that neither the *BIK* gene nor protein levels were associated with patient outcomes (p=0.19 and 0.62 respectively, log-rank test). However, when the BIK association was measured only in the ER-positive patients, a striking trend emerged (Figure 5.2 D). While *BIK* gene expression showed no association with patient outcomes (p=0.50, log-rank test), BIK protein levels were significantly associated with higher recurrence rates in ER-positive patients (p=0.049, log-rank test). In conclusion, since the *BIK* gene and protein expression do not correlate well, estimation of BIK proteins levels is the best method to predict patient survival outcomes. Importantly, assessment of the protein levels would be a true measure

A

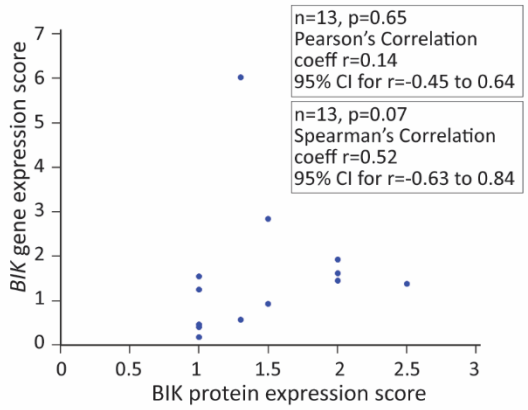

B

Chi-squared analysis and Fisher's exact test

BIK protein expression score	*BIK* gene expression score 0	1	
0	6	1	7(53.8%)
1	4	2	6(46.2%)
	10	3	13
	76.90%	23.10%	

Chi-squared (χ^2)=0.61
DF=1
p=0.44
Contingency coefficient=0.21

Fisher's exact test
p=0.56

C

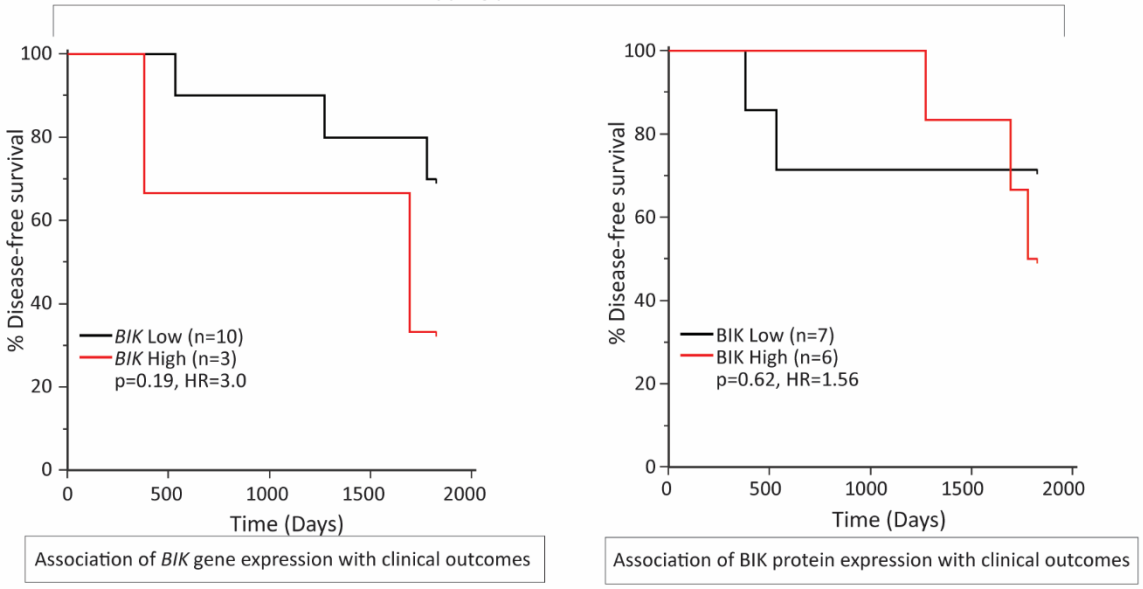

D

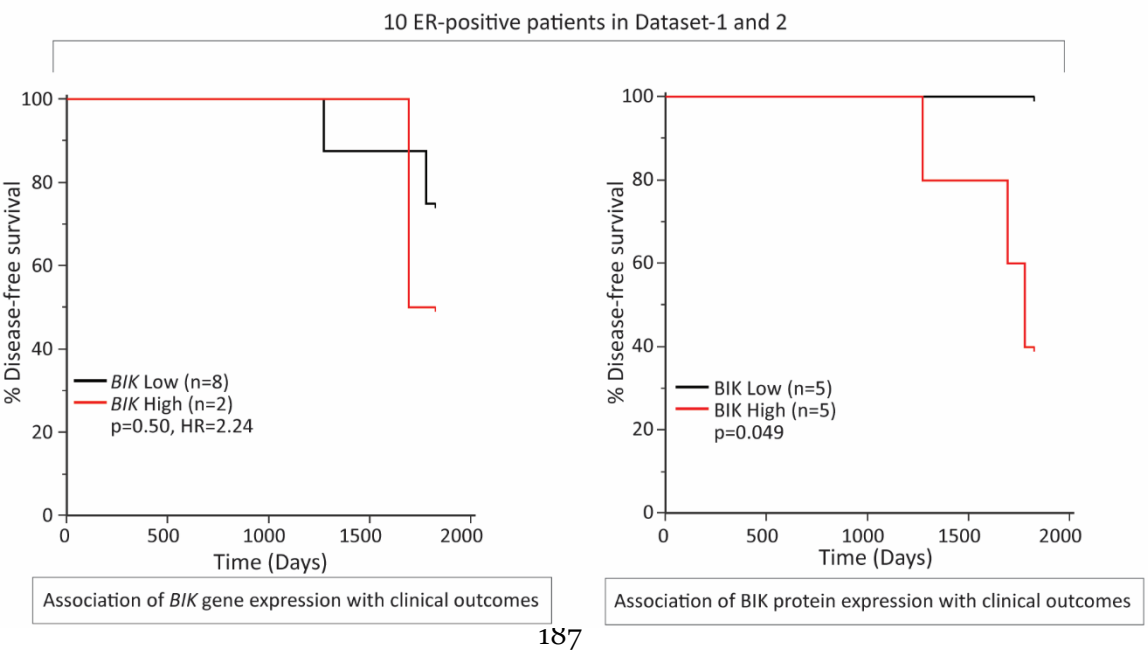

Figure 5.2 *BIK* gene and protein expression correlation in breast cancer and their survival association. A. Scatter diagram depicting the correlation between *BIK* gene and protein expression levels in breast cancer patients (n=13). Pearson's and Spearman's correlation coefficients were calculated with p values. **B.** Top: Contingency table depicting agreement between *BIK* mRNA and proteins levels as categorical variables where 0 indicates BIK-low, and 1 indicates BIK-high. Bottom: Results obtained from Chi-squared and Fisher's exact test analysis. **C.** Kaplan-Meier survival curves depicting 5 years disease-free survival outcomes of 13 overlapping patients stratified in ER-positive vs. ER-negative groups, and their survival outcomes were calculated based on *BIK* mRNA (Left) or protein (Right) levels in tumor cores. **D.** Kaplan-Meier survival curves depicting 5 years disease-free survival outcomes of 10 ER-positive patients present in Dataset-1 and -2 stratified in ER-positive vs. ER-negative groups, and their survival outcomes were calculated based on *BIK* mRNA (Left) or protein (Right) levels in tumor cores. The HR value of greater than 1.0 estimates the predicted risk of poor prognosis. p value was calculated using log-rank analysis.

of the biologically available amounts of protein which may give an insight into the biology of the tumors.

5.2.3 BIK is a prognostic marker for recurrence of ER-positive breast cancer

Given that BIK protein is a more logical marker for functional outcomes analysis and given that BIK protein levels are upregulated in ER-positive breast cancer cells upon treatment with anti-estrogens such as tamoxifen and fulvestrant, I decided to analyze associations of BIK protein levels with outcomes stratified to ER-positive and -negative breast cancers. I analyzed whether BIK protein levels predicted relapse in ER-positive breast cancer patients differently than in ER-negative patients using Dataset-2 (n=152) (Figure 5.3). Using a cut-point determined previously by ROC analysis (Pandya et al., 2016), patient tumors were dichotomized into 2 groups of which 35% were BIK-high, and 65% were BIK-low. Interestingly, within the ER-positive subtype (n=116), BIK-high patients were 8.4 times more likely to relapse (p=0.001, log-rank test) and were 8.1 times more likely to die from the disease (p=0.025, log-rank test), relative to BIK-low patients (Figure 5.3 A and B). Strikingly, 99% of patients with low levels of BIK (n=75) were alive after 5 years, indicating that BIK upregulation had a pro-tumorigenic role in the ER-positive group. On the other hand, BIK had no prognostic value for ER-negative patients (p=0.73, log-rank test). Thus, BIK levels predicted recurrence and mortality specifically in the ER-positive breast cancer, suggesting that BIK contributes to endocrine therapy resistance.

5.2.4 BIK triggers failed apoptosis

I next explored whether BIK is a cause or consequence of tumor relapse. While apoptotic cell death cannot explain aggressive disease, recent cell-based models identified that apoptosis is

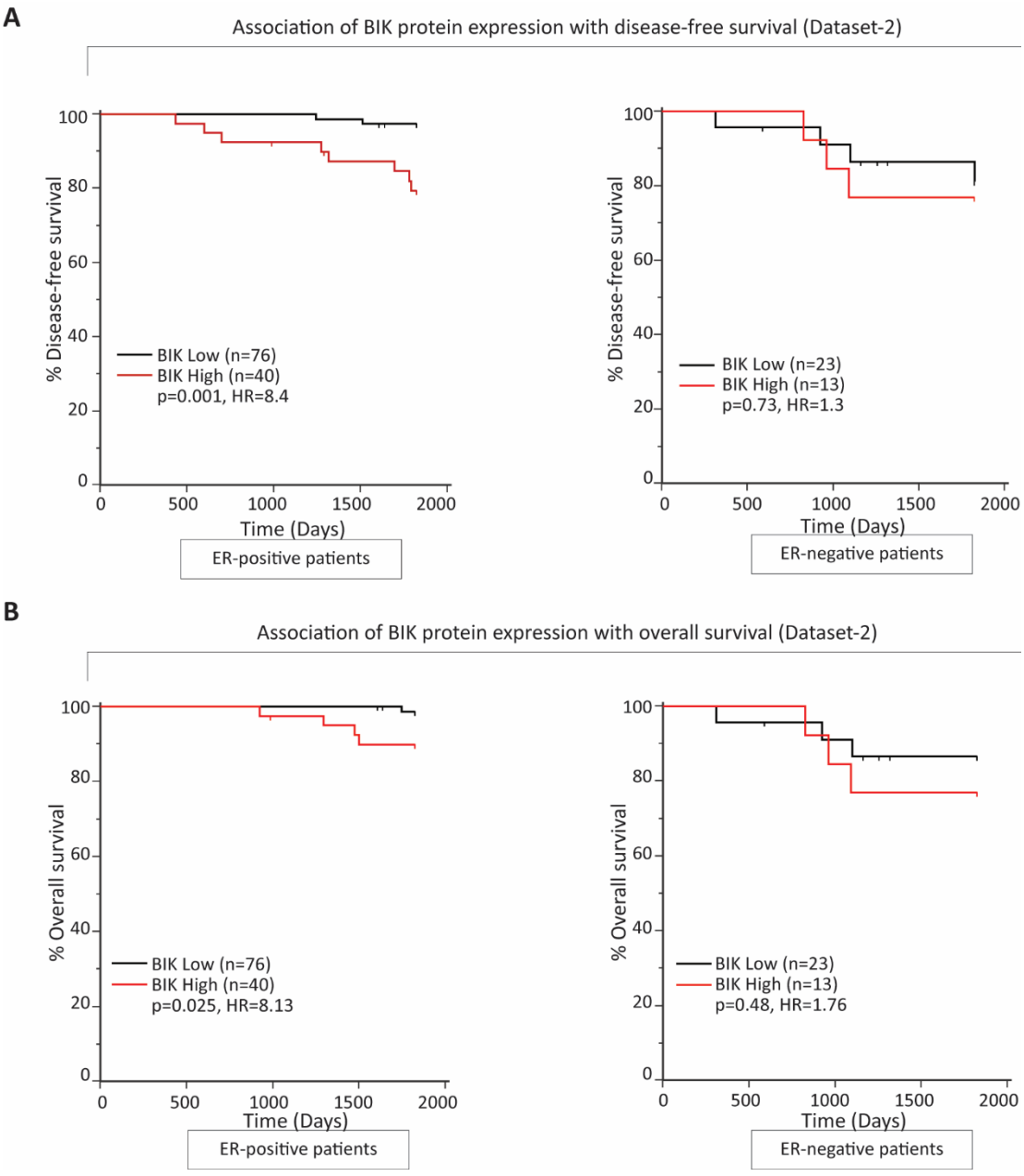

Figure 5.3 BIK protein levels predict poor survival outcomes of ER-positive breast cancer patients. A and B. Kaplan-Meier survival curves depicting 5 years disease-free or overall survival outcomes of patients stratified in ER-positive anti-estrogen treated vs ER-negative groups, and their survival outcomes were calculated based on BIK protein levels in tumor cores. The HR value of greater than 1.0 estimates the predicted risk of poor prognosis. p value was calculated using log-rank analysis.

oncogenic when it is not fully executed (Ichim et al., 2015; Ichim and Tait, 2016; Liu et al., 2015; Miles and Hawkins, 2017). The central theme of these studies was that low-level apoptosis produced DNA damage that led to carcinogenesis and/or increased chemical-induced skin cancers (Ichim et al., 2015; Liu et al., 2015; Miles and Hawkins, 2017). If BIK triggered a similar program, this could provide a molecular link between BIK tumor levels and patient relapse. I, therefore, tested if BIK induced failed apoptosis in a breast cancer model. The ER-positive MCF-7 cell line is a well-studied model for clinical resistance to endocrine therapy (Bacci et al., 2016; Coser et al., 2009; Guest et al., 2016; Martin et al., 2017) and is dependent on BIK-induced apoptosis for sensitivity to anti-estrogen treatment (Fu et al., 2007; Hur et al., 2004). To isolate BIK-dependent effects from anti-estrogen pathways, I generated MCF-7 and MDA-MB-231 cell lines where BIK expression was induced by doxycycline (Dox) (Figure 5.4 A and B). BIK protein levels were titratable in response to increasing doses of Dox and reached maximal amounts at ~75 ng/ml Dox. Immunofluorescence microscopy showed that BIK was expressed in almost all cells (Figures 5.4 A and B bottom panels) and was localized to intracellular reticular structures as expected for an endoplasmic reticulum-localized protein (Mander's coefficient= 0.86) (Figures 5.4 C). The majority of BIK-expressing cells were viable with less than 10% showing apoptotic morphology at the highest Dox concentrations (Figure 5.4 D). To assess long-term survival of BIK-expressing cells, I performed colony formation assays. BIK-expressing cells produced similar numbers of colonies as vector control cells with less than 25% reduction in colony numbers at the highest Dox concentration (Figure 5.5). Colony morphology differed, however, with BIK expression decreasing colony area >2-fold ($p<0.01$, Sidak's post-hoc test) and colony density 1.6-fold ($p<0.001$, Sidak's

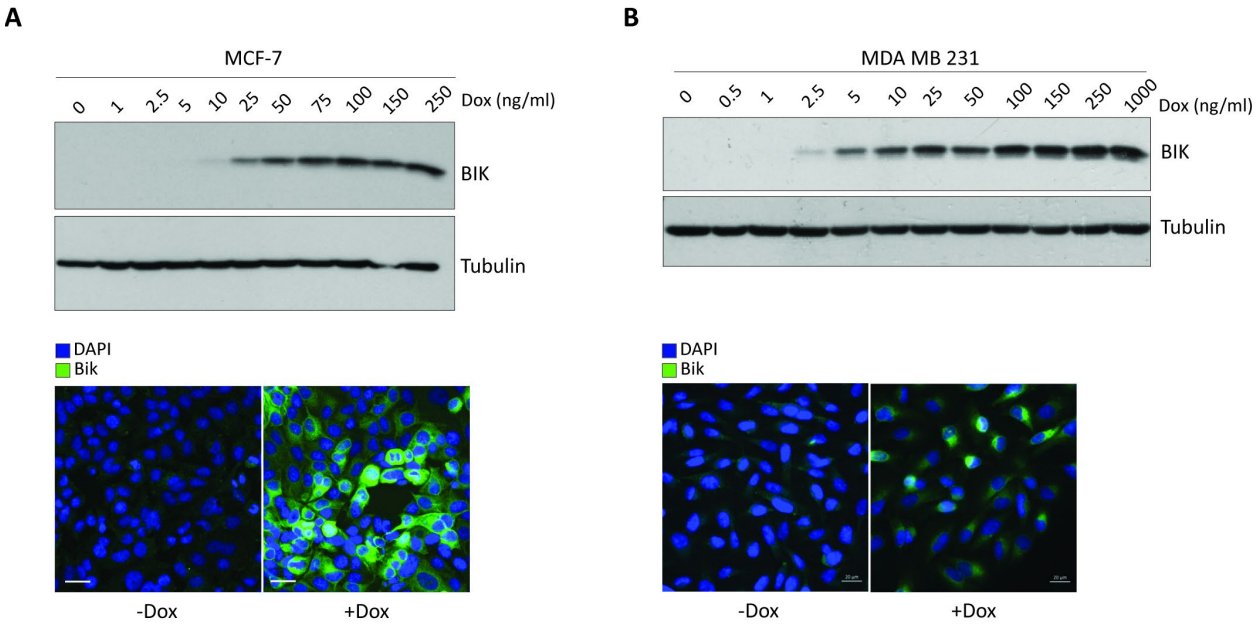
A
MCF-7
0 1 2.5 5 10 25 50 75 100 150 250 Dox (ng/ml)
BIK
Tubulin
DAPI
Bik
-Dox
+Dox
B
MDA MB 231
0 0.5 1 2.5 5 10 25 50 100 150 250 1000 Dox (ng/ml)
BIK
Tubulin
DAPI
Bik
-Dox
+Dox

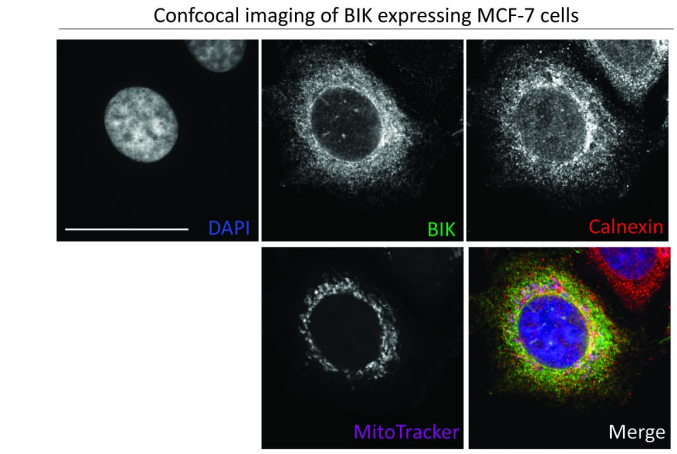
C
Confcocal imaging of BIK expressing MCF-7 cells
DAPI
BIK
Calnexin
MitoTracker
Merge

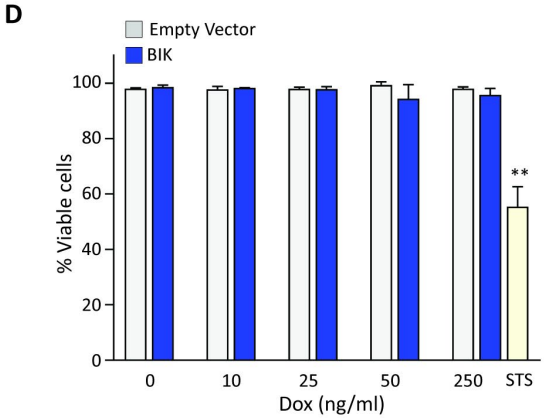
D
Empty Vector
BIK
% Viable cells
100
80
60
40
20
0
**
0
10
25
50
250
STS
Dox (ng/ml)

Figure 5.4 Dox-inducible BIK expression in MCF-7 and MDA MB 231 cells lines and calculation of cell viability. A. Top: Western blot analysis of BIK expression in MCF-7 Tet-On cells using the indicated amounts of Dox. Note the Dox-dose dependent increase in BIK protein levels. Bottom: Immunofluorescence analysis of MCF-7 Tet-On cells in the presence or absence of 250ng/ml of Dox for 24hrs and stained with anti-BIK antibody. Images were acquired using a spinning disk-confocal microscope at 20X magnification. Scale bar 50µM. Note that >95% of the Dox-induced cells are positive for BIK immunostaining. *Contributed by John Maringa Githaka* **B.** Western blot analysis of BIK expression in MDA MB 231 Tet-On cells using the indicated amounts of Dox. Note the Dox-dose dependent increase in BIK protein levels. Bottom: Immunofluorescence analysis of MDA MB 231 Tet-On cells in the presence or absence of 250ng/ml of Dox for 24hrs and stained with anti-Bik antibody. Images were captured using AxioObserver.Z1 inverted florescence microscope at 40X magnification. Scale bar 20 µM. Note that >95% of the Dox-induced cells are positive for BIK immunostaining. **C.** Immunofluorescence analysis of cells expressing BIK to determine its subcellular localization. MCF-7 Tet-On BIK cells stimulated with 250ng/ml of Dox for 24hrs were incubated in the MitoTracker-red, followed by 4%PFA fixation and immunostaining with anti-BIK and -calnexin antibodies. Nuclei were stained using DAPI. Images were acquired using a spinning-disk confocal microscope using a 100X oil immersion objective. Note the reticular staining of BIK and a high degree of correlation with endoplasmic reticulum marker calnexin (Mander's coefficient=0.86). *Contributed by John Maringa Githaka* **D.** Quantitation of viable cells based on the nuclear morphology of anti-γH2AX immunofluorescence analysis. Cells with punctate or no γH2AX staining were considered viable whereas cells with diffuse γH2AX staining were considered apoptotic. At least 200 cells from each treatment were counted. Error bars show SD from 3 independent experiments. (** $p<0.01$, *** $p<0.001$).

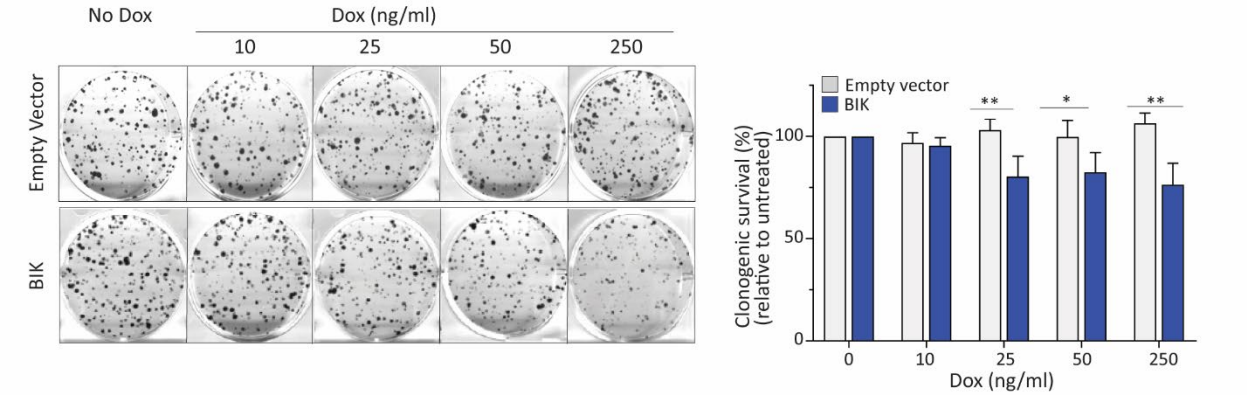

Figure 5.5 Clonogenic survival of BIK expressing cells. Left: Representative images of clonogenic survival assay performed for Empty vector or BIK expressing MCF-7 cells at the indicated Dox stimulation. Right: Bar graph depicting % clonogenic survival relative to untreated cells. Error bars show SD of three independent experiments. One-way ANOVA was performed to determine significance among groups followed by Sidak's post-hoc test. (* $p < 0.05$, ** $p < 0.01$)

post-hoc test) highest Dox concentration (Figure 5.6 A and B). Thus, BIK altered growth characteristics but weakly induced cell death.

Despite this lack of cell death, BIK did initiate apoptotic signaling. MCF-7 cells are null for the caspase-3 gene and respond to apoptotic stimuli through cleavage and activation of caspase-7 (Liang et al., 2001; Orth and Dixit, 1997; Rehm et al., 2003; Yang et al., 2012). BIK expression induced cleavage of caspase-7 that was blocked by the caspase inhibitor z-VAD-fmk (Figure 5.7 A). Additionally, apoptosis is characterized by DNA fragmentation and BIK-expressing cells accumulated DNA double-strand breaks as demonstrated by γH2AX positivity (Figure 5.7 B). The BH3-domain of pro-apoptotic proteins bind to anti-apoptotic BCL-2 proteins to stimulate mitochondrial outer membrane permeabilization (Chinnadurai et al., 2008; Taylor et al., 2008) and BIK-induced γH2AX production was dependent on the BH3 domain (Figure 5.7 C). γH2AX levels were diminished with caspase inhibition (Figure 5.7 A), suggesting that caspase activated DNase (CAD) was the effector molecule producing DNA damage. To confirm this, I depleted cells of CAD and saw a reduction in BIK-induced γH2AX levels (Figure 5.7 D). Thus, BIK initiated the canonical apoptotic pathway consisting of caspase and CAD activation leading to DNA damage, without full execution of cell death.

To identify the block in cell death, I assessed intracellular γH2AX localization (Figure 5.7 E). Typically, in apoptotic cells, γH2AX accumulates at DNA double-strand breaks with diffuse nuclear staining indicative of wide-spread genomic fragmentation (Solier and Pommier, 2014). With BIK expression, <5% of the cells showed apoptotic, diffuse γH2AX nuclear staining (Figure 5.7 E). Instead, γH2AX localization in the majority of BIK expressing cells (22.7%) was to discrete puncta with 3 or more foci per nuclei representing low-level DNA damage. To confirm that the

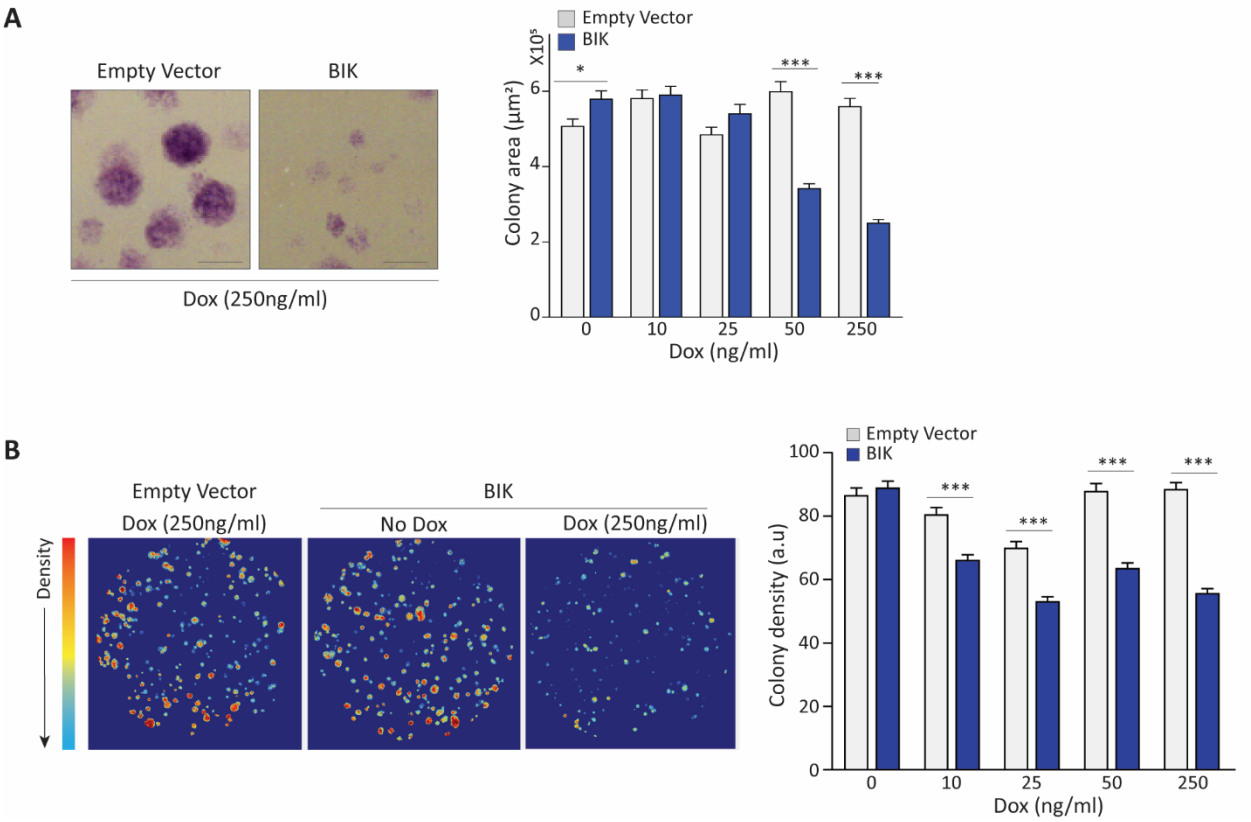

Figure 5.6 Analysis of colony morphology of BIK expressing cells. A. Left: Representative images of colonies formed by MCF-7 Empty Vector or BIK expressing cells at 250ng/ml Dox stimulation. Note the reduction in colony size of cells expressing BIK. Scale bar 1mm. Right: Colony area was calculated for at least 350 colonies from each group from a representative experiment. Error bars show SEM. One-way ANOVA was performed to determine significance among groups followed by Sidak's post-hoc test. (* $p< 0.05$, *** $p< 0.001$). *Contributed by John Maringa Githaka* **B.** Left: Representative images depicting cellular density of Empty Vector or BIK expressing colonies. Red area indicates high density whereas blue areas indicate low density. At least 350 colonies were analysed from a representative experiment and measurements were taken. *Contributed by John Maringa Githaka* Right: Bar graph depicting quantitation of colony density. Note the reduction in the area of the colonies formed by BIK expressing cells. Error bars show SEM. One-way ANOVA was performed to determine significance among groups followed by Sidak's post-hoc test. (*** $p< 0.001$).

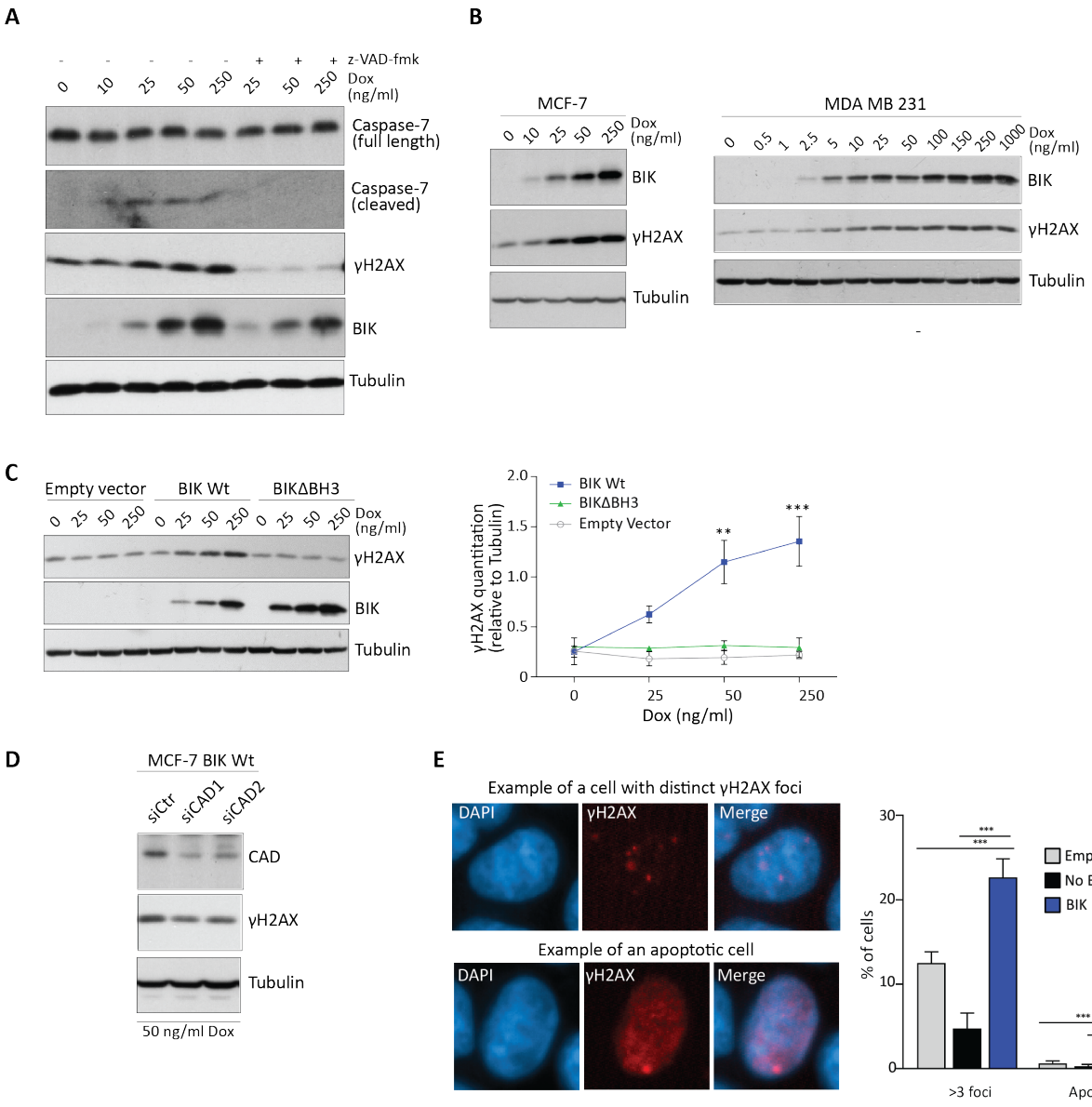
A
z-VAD-fmk
Dox (ng/ml)
Caspase-7 (full length)
Caspase-7 (cleaved)
γH2AX
BIK
Tubulin
B
MCF-7
MDA MB 231
Dox (ng/ml)
BIK
γH2AX
Tubulin
C
Empty vector
BIK Wt
BIKΔBH3
Dox (ng/ml)
γH2AX
BIK
Tubulin
BIK Wt
BIKΔBH3
Empty Vector
γH2AX quantitation (relative to Tubulin)
Dox (ng/ml)
D
MCF-7 BIK Wt
siCtr
siCAD1
siCAD2
CAD
γH2AX
Tubulin
50 ng/ml Dox
E
Example of a cell with distinct γH2AX foci
DAPI
γH2AX
Merge
Example of an apoptotic cell
% of cells
Empty vector
No BIK
BIK
>3 foci
Apoptotic

Figure 5.7 BIK mediated genomic damage requires BH3 domain and is dependent on CAD activity. A. Western blot analysis of MCF-7 Tet-On cells stimulated with Dox dependent BIK expression at the indicated concentrations in the presence or absence of z-VAD-fmk (10μM) for 24hrs. Note caspase-7 activation and γH2AX formation in response to Bik expression and its disappearance upon caspase inhibition. **B.** Western blots depicting increase in γH2AX levels in response to BIK elevation in MCF-7 (Left) or MDA-MB-231 (right) cell lines. **C.** Left: Western blot analysis of MCF-7 Tet-On cells expressing either Empty vector, Wt BIK or BikΔBH3 at the indicated Dox-stimulation for 24hrs. Note the reduction in γH2AX phosphorylation in the absence of BH3 domain of BIK. Densitometric quantitation of western blots was performed using ImageJ. Error bars show SD from three independent experiments. One-way ANOVA was performed to determine significance among groups followed by Tukey's multiple comparisons test. (** $p< 0.01$, *** $p< 0.001$). **D.** Western blot depicting knock-down of CAD using two different siRNAs in the presence of 50 ng/ml Dox stimulation of MCF-7 Tet-On BIK cells. Note the reduction in γH2AX intensity with reduction in CAD levels. **E.** Left: Representative images of γH2AX immunofluorescence analysis depicting cells with punctate γH2AX staining (top panel) representing distinct DSBs or diffuse γH2AX staining (bottom panel) representing apoptotic cells. Right: At least 200 cells from 6 different frames were used for analysis. One-way ANOVA was performed followed by Sidak's multiple comparison's test. (*** $p<0.001$)

DNA damage was in the form of double-strand breaks; I performed comet assays to quantitate DNA double-strand breaks at the single cell level (Figure 5.8). In BIK-expressing cells, 18% of the nuclear DNA contained double-strand breaks versus 5% in vector cells (p=0.007, Student's t-test). Together these data demonstrated that BIK produced DNA double-strand breaks via caspase and CAD nuclease activity. Thus, BIK induced the apoptotic pathway, but despite the accumulation of significant DNA damage, BIK-expressing cells survived and proliferated.

5.2.5 Anti-ER treatment induces DNA damage that is dependent on BIK

Clinical endocrine therapy induces DNA damage (Schiewer and Knudsen, 2016) although the mechanisms are incompletely understood (Carthew et al., 1995; Liu et al., 2003; Wozniak et al., 2007). In certain contexts, the causes of DNA damage are elevated ROS or increased replication stress in the face of insufficient DNA damage repair (DDR) capacity (Kryston et al., 2011; Mehta and Haber, 2014; Woodbine et al., 2011). I first tested whether BIK-induced DNA damage was dependent on ROS. BIK expression did not increase levels of ROS as quantified with the fluorescent ROS indicator CellRox green (Figure 5.9 A). Further BIK-induced γH2AX levels were unaffected by treatment with the ROS scavenger NAC (Figure 5.9 B). This confirmed that CAD and not ROS was the major effector of BIK-induced DNA damage. Next, I examined whether DNA-damage induced upon anti-estrogen treatment was dependent on BIK. I first optimized BIK silencing using two siRNAs and confirmed that γH2AX produced due to BIK expression was lost upon BIK silencing (Figure 5.9 C). Subsequently, I performed the silencing of Tamoxifen or 4-HT induced BIK and looked at modulation in γH2AX levels. Indeed, Tamoxifen and 4-HT treatment of MCF-7 cells induced γH2AX positivity that was lost with BIK knock-down (Figure 5.9 D). These

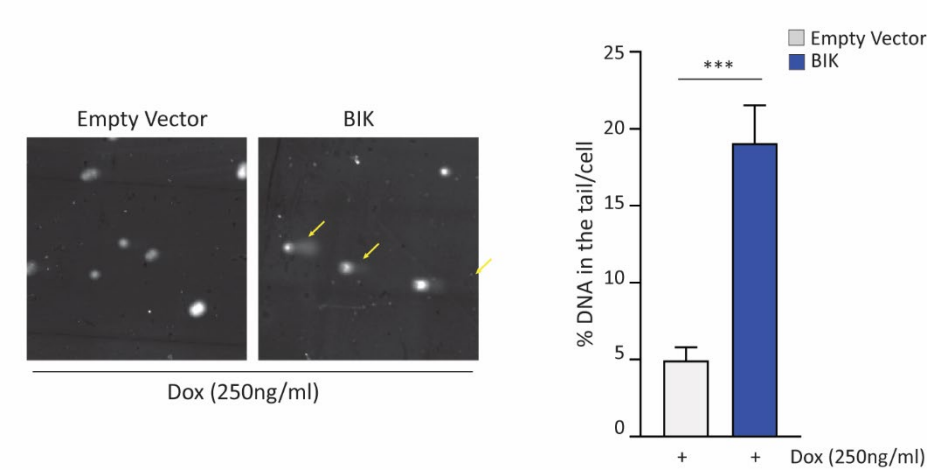

Figure 5.8 Alkaline comet assay demonstrating BIK-induced double-strand breaks. Left: Representative images of comets formed by Empty Vector or BIK expressing MCF-7 cells at the indicated Dox-stimulation. Note the comet tail formation (yellow arrows) with BIK expressing cells. Right: % DNA in the comet tail/cell was quantitated using CaspLab comet analysis program. At least 50 nuclei were analyzed for each group. Error bars show SD of three independent experiments. Student's t-test was performed to determine the significance between the two groups. (*** $p < 0.001$).

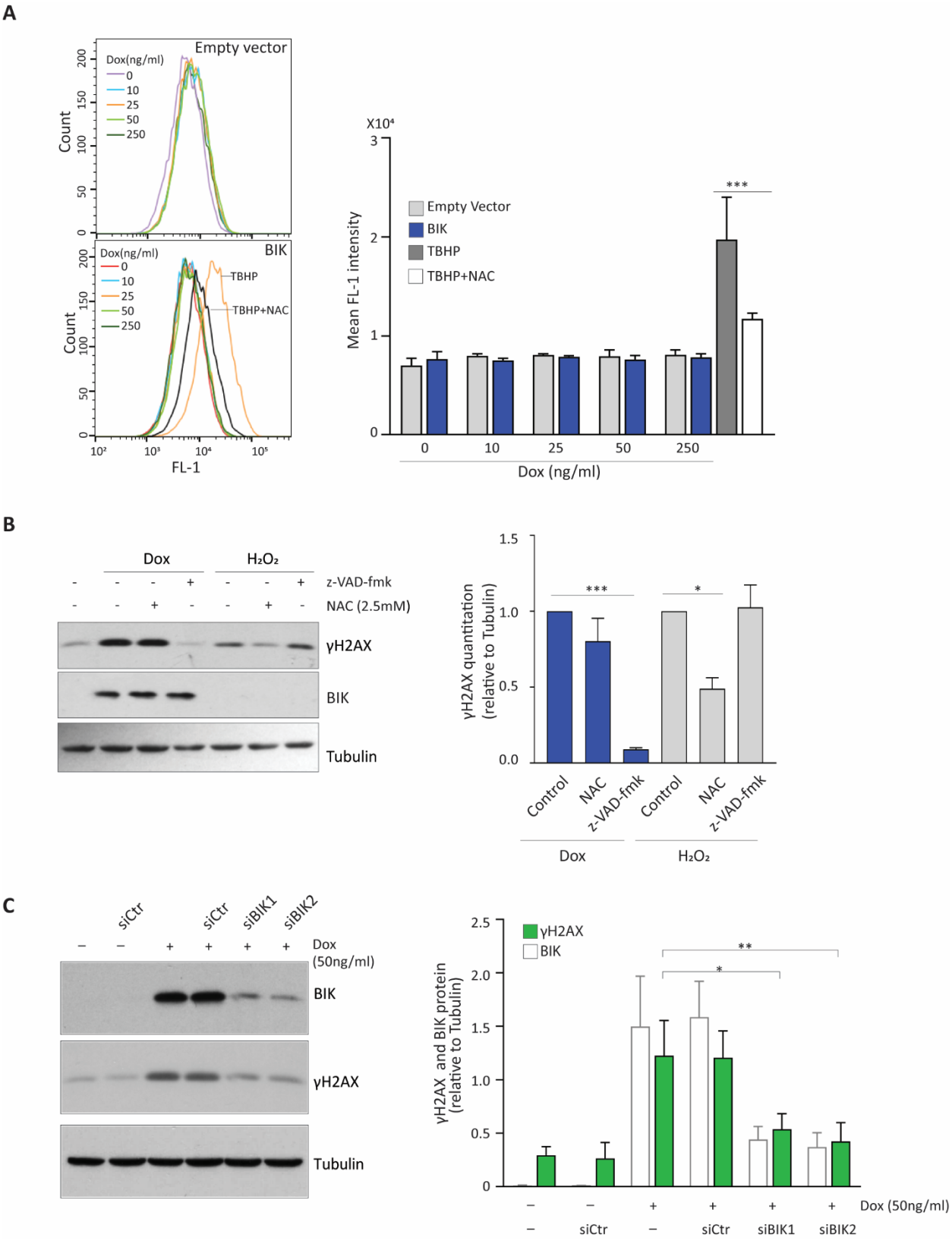
A
Empty vector
Dox(ng/ml)
0
10
25
50
250
Count
BIK
TBHP
TBHP+NAC
FL-1
X10⁴
Mean FL-1 intensity
Empty Vector
BIK
TBHP
TBHP+NAC
***
Dox (ng/ml)
B
Dox
H₂O₂
z-VAD-fmk
NAC (2.5mM)
γH2AX
BIK
Tubulin
γH2AX quantitation (relative to Tubulin)
***
*
Control
NAC
z-VAD-fmk
C
siCtr
siBIK1
siBIK2
Dox (50ng/ml)
γH2AX and BIK protein (relative to Tubulin)
**
*
siCtr
siBIK1
siBIK2

D

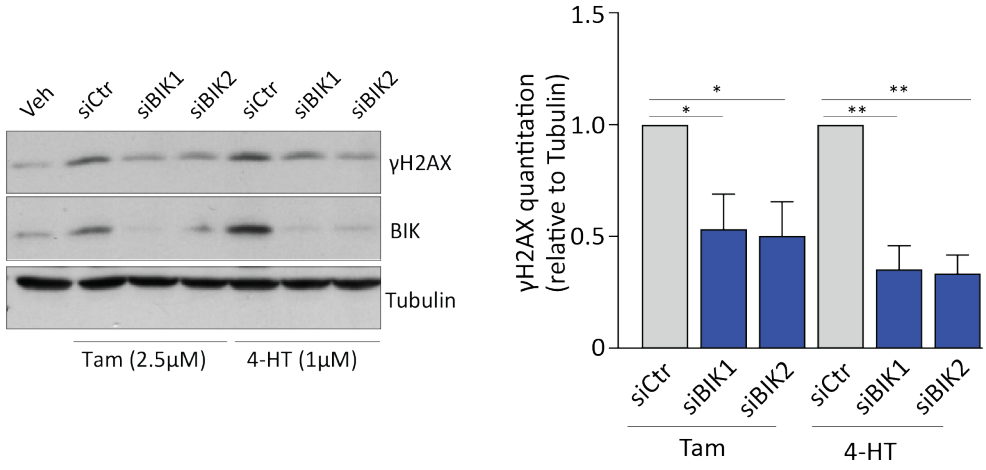

Figure 5.9 Anti-ER treatment induces DNA damage that is dependent on BIK. A. Left: Flow cytometry profiles of ROS measurements by CellRox green reagent for Empty Vector or BIK expressing cells at the indicated Dox-stimulation. Note the overlapping profiles of unstimulated and Dox-stimulated cells. Right: Bar graph depicting mean Fl-1 intensities indicating ROS levels obtained from the flow-cytometric analysis. 50μM TBHP was used as a positive control and 2.5mM NAC as a ROS scavenger. Error bars represent SD from three different experiments. One-way ANOVA was used to determine significance among groups followed by Sidak's post-hoc test. (*** $p < 0.001$). **B.** Left: Western blot depicting BIK mediated γH2AX formation dependent on caspases but not through ROS. Note the loss of γH2AX signal in the presence of pan-caspase inhibitor z-VAD-fmk vs. no change in the presence of ROS scavenger NAC. Right: Densitometric quantitation of western blots from three independent experiments. Error bars show SEM. One-way ANOVA was performed to determine significance among groups followed by Dunnett's post-hoc test. (* $p < 0.05$, *** $p < 0.001$). **C.** Left: Western blot showing siRNA mediated knock down of BIK expression reduces γH2AX formation. MCF-7 Tet-On cells pre-transfected with either scrambled or two BIK specific siRNAs and 24hrs later stimulated with 50ng/ml Dox. Right: Bar graph depicting the densitometric quantitation of BIK and γH2AX levels. Error bars represent the SD of three independent experiments. One-way ANOVA was performed to determine significance among groups followed by Dunnett's multiple comparisons test. (* $p < 0.05$, ** $p<0.01$). **D.** Left: Western blot depicting the formation of γH2AX upon endocrine treatment dependent on BIK upregulation. MCF-7 cells were simultaneously treated with the indicated anti-estrogens and transfected with two different anti-BIK siRNAs for 48 hrs. 20μg of cell lysates were western blotted and probed with the indicated antibodies. Bottom: Densitometric quantitation of western blots from three independent experiments was performed using ImageJ. Error bars represent SEM. One-way ANOVA was performed to determine significance among groups followed by Sidak's multiple comparisons test. (* $p < 0.05$, ** $p<0.01$).

results indicate that endocrine therapy of MCF-7 cells induces DNA damage through a BIK—caspase—CAD axis.

5.2.6 BIK induces an aggressive cell phenotype

Failed apoptosis induces genomic instability and cellular transformation (Ichim and Tait, 2016). In order to determine whether BIK-mediated DNA damage altered cellular characteristics, I expressed BIK continuously for 10 passages, removed Dox and maintained cells in the absence of Dox/BIK. (Figure 5.10 A). BIK protein and DNA damage persisted for the duration of Dox treatment (Figure 5.10 B). I refer to the progeny of these long-term Dox-treated cells with the annotation "LTC" and Dox-concentration during treatment. As an example, BIK-LTC-250 signifies that BIK expression was induced by long-term culture in 250ng/mL Dox. I first tested whether these cells survived 10 passages with high levels of BIK due to compensatory elevation of anti-apoptotic proteins (Figure 5.10 C). BCL-2, BCL-XL or MCL-1 protein levels were not elevated. Furthermore, resistance to BIK mediated apoptosis in an *in vitro* endocrine resistance model was described to occur by GRP78 upregulation that blocked BIK pro-apoptotic activity (Fu et al., 2007; Zhou et al., 2011). Hence, I also probed to test this possibility but did not find a GRP78 upregulation in BIK-LTC-250 cell line (Figure 5.10 C). Anti-apoptotic gene expression and *BIK* gene expression also did not correlate in patient breast tumors (Pandya et al., 2016), indicating that the LTC derived cell lines modeled clinical disease. I next assayed whether long-term BIK expression induced aggressive growth characteristics. I first conducted colony formation assays. The BIK-LTC-250 cells showed significant 1.6-fold ($p<0.001$, Sidak's post-hoc test) increased colony numbers compared to EV-LTC-250 cell line indicating an increased ability to survive and proliferate from isolated single cells (Figure 5.10 D).

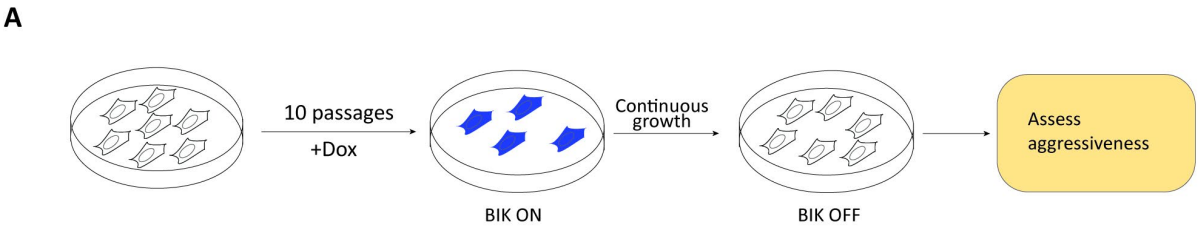
A
10 passages
+Dox
BIK ON
Continuous growth
BIK OFF
Assess aggressiveness

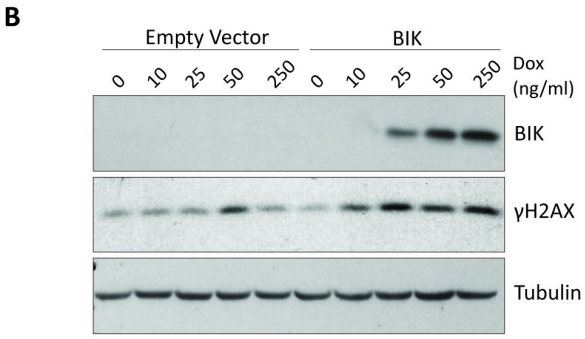
B
Empty Vector
BIK
0 10 25 50 250 0 10 25 50 250
Dox (ng/ml)
BIK
γH2AX
Tubulin

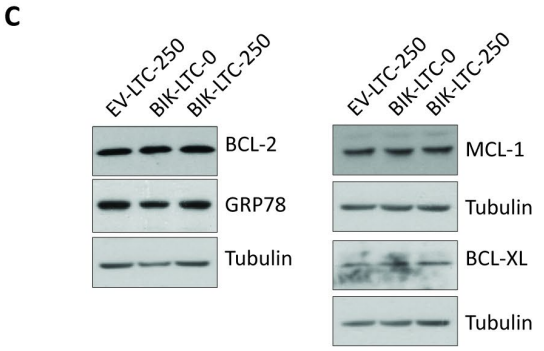
C
EV-LTC-250
BIK-LTC-0
BIK-LTC-250
BCL-2
GRP78
Tubulin
MCL-1
Tubulin
BCL-XL
Tubulin

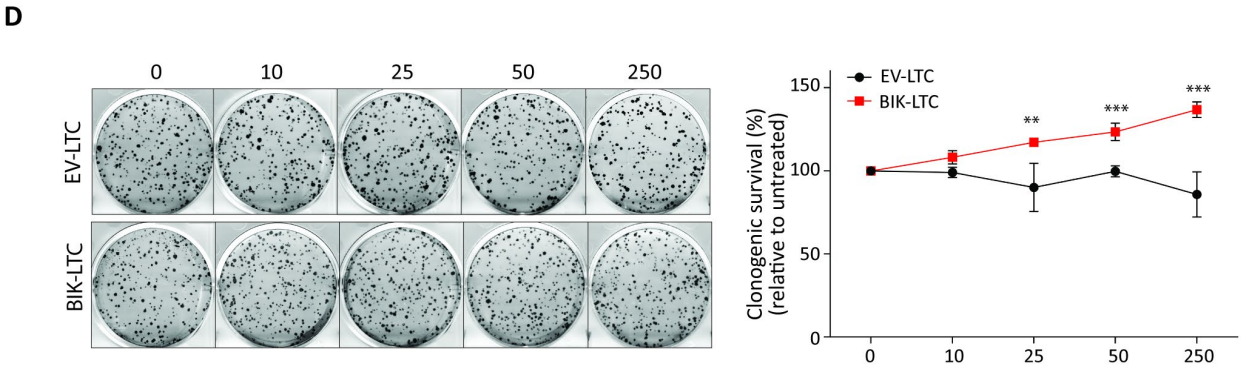
D
0 10 25 50 250
EV-LTC
BIK-LTC
EV-LTC
BIK-LTC
Clonogenic survival (%) (relative to untreated)
150
100
50
0
**
***
***
0 10 25 50 250

Figure 5.10 Long-term BIK expression leads to an elevation in clonogenic survival. A. Experimental scheme depicting generation of 'LTC' cells. **B.** Top: Western blot analysis performed for 'LTC' cells after 10 passages showing the persistence of BIK expression and DNA damage. **C.** Western blot analysis of cell lysates prepared from EV-LTC-250, BIK-LTC-0 and BIK-LTC-250 cell lines to test anti-apoptotic proteins upregulation during long-term culture. Blots were probed with antibodies against BCL-2, BCL-XL, MCL-1 and GRP-78. Tubulin was used as a loading control for individual blots **D.** Left: Representative images from colony formation assay performed for 'LTC' cells. Right: Line graph depicting quantitation of clonogenic potential of BIK-LTC line relative to control. Note the gradual increase in clonogenic potential in BIK-LTC cells. Error bars represent the SD of three independent experiments. One-way ANOVA was performed to determine significance among groups followed by Sidak's post-hoc test. (** $p < 0.01$, *** $p < 0.001$).

Subsequently, to assess growth in a xenograft tumor model, cells were injected into the mammary fat pad of BALB/c nude mice, and tumor volume was monitored for seven weeks. BIK-LTC-250-derived tumors generated significantly larger tumors than EV-LTC-250-derived tumors ($p=0.003$, linear regression analysis) (Figure 5.11 A and B). BIK-LTC-0 cells that had not been treated with Dox generated tumors of similar volume to BIK-LTC-250. Thus, BIK increased colony formation ability and had a moderate stimulatory effect on tumor growth.

I next performed *in vitro* assays of cancer aggressiveness. Anchorage-independent growth and elevated stem-like properties are associated with therapeutic resistance in breast and colon cancer models (Dubrovska et al., 2012; Morata-Tarifa et al., 2017). Adherent cells need attachment to survive, loss of which induces apoptosis. The ability of the cells to grow without attachment is a measure of transformation. This can be tested by the culture of cells in soft agar containing nutrient medium (Borowicz et al., 2014; Horibata et al., 2015). Therefore, I cultured the LTC lines for 7 weeks in soft agar and observed that BIK-LTC-50 and BIK-LTC-250 cells formed ~4 times more anchorage-independent colonies compared to EV-LTC-50 and EV-LTC-250 cells respectively ($p<0.001$, Sidak's post-hoc test) (Figure 5.12 A), confirming the acquisition of anchorage-independent growth potential.

Next, we interrogated if BIK-LTC-250 cells had acquired stem-like properties by mammosphere formation assay (Figure 5.12 B and C). Cancer stem cells are tumor maintaining cells (Beck and Blanpain, 2013). They undergo asymmetric cell division to generate one stem cell and the other progenitor cell that undergoes multiple divisions to populate the tumor (Beck and Blanpain, 2013). Thus, although CSCs rarely divide, they determine the repopulation potential of the tumors. CSC enrichment is associated with therapeutic resistance and disease relapse because

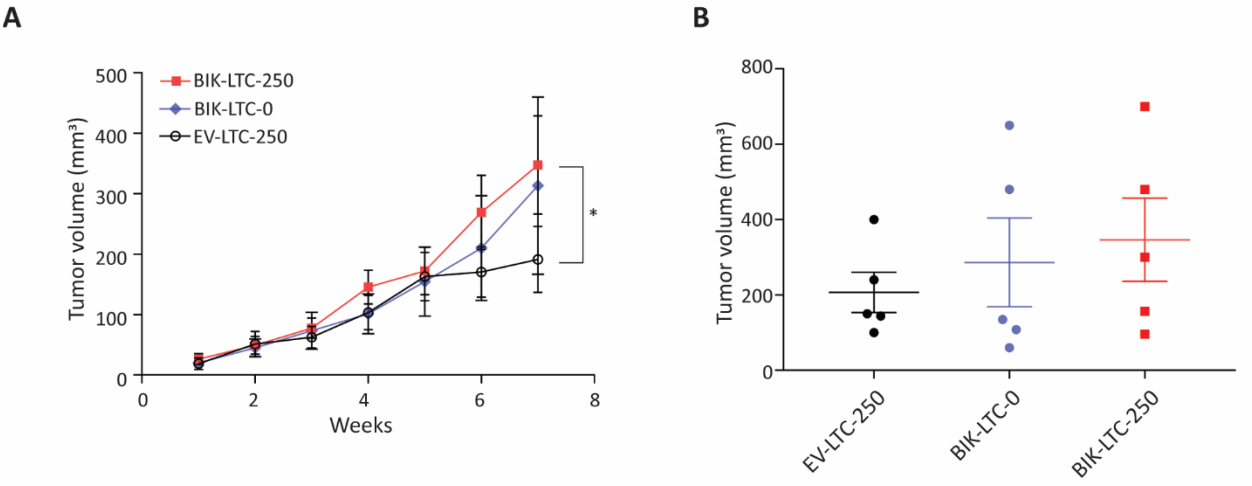

Figure 5.11 Long-term BIK expression leads to a moderate increase in tumor growth rate. A. 5 million EV-LTC-250, BIK-LTC-0 or BIK-LTC-250 cells were orthotopically injected in mouse mammary glands and tumor volume over 7 weeks was measured (n=5 for each group). Linear regression analysis was performed to determine significance in tumor growth rate. *Contributed by Raven Kirschenman* **B.** Plot depicting post-harvest tumor volumes of EV-LTC-250, BIK-LTC-0, and BIK-LTC-250 cell lines (n=5 for each group). One-way ANOVA was performed and no significant difference in endpoint tumor volumes was observed. *Contributed by Namrata Patel*

they rarely divide, hence making cell-division dependent chemotherapies ineffective (Chang, 2016). Mammosphere-forming assays that involve cell culture in low-attachment conditions in the absence of serum assess stem-like properties of cells (Vieira et al., 2014; Zhang et al., 2017). The mammosphere formation efficiency (MFE) of BIK-LTC-250 cells was 1.7-times higher than BIK-LTC-0 or EV-LTC-250 cells ($p<0.001$, Tukey's post-hoc test) (Figure 5.12 B) indicating that BIK-treatment increased the proportion of cancer stem-like cells. Further, I saw a 1.7-fold increase in the mammosphere area of BIK-LTC-250 cells compared to EV-LTC-250 cells ($p<0.001$, Sidak's post-hoc test) (Figure 5.12 C), suggesting an increase in the tumor-initiating potential (Grimshaw et al., 2008). Interestingly, mammospheres formed by BIK-LTC-250 cells were more irregularly-shaped compared to EV-LTC-250 cells as indicated by the isoperimetric quotient which is a measure of circularity (Figure 5.12 C). Departure from spherical morphology is associated with aggressive phenotypes (Liu et al., 2014; Rappa et al., 2008; Wahler et al., 2015; Wang et al., 2014), indicating that BIK-LTC-250 cells had acquired aggressive characteristics. Taken together, these data indicate that BIK expression induces cellular changes that increase colony-formation ability, anchorage-independent growth, and proportion of cancer stem-like cells. These changes persist after down-regulation of BIK and are consistent with a model whereby BIK induced-cellular changes are the result of genomic instability and persistence of mutational changes.

5.3 Discussion

I demonstrated that the pro-apoptotic protein BIK was upregulated in ER-positive breast cancer cells upon treatment with anti-estrogens such as tamoxifen and 4-HT. BIK is a robust apoptotic inducer

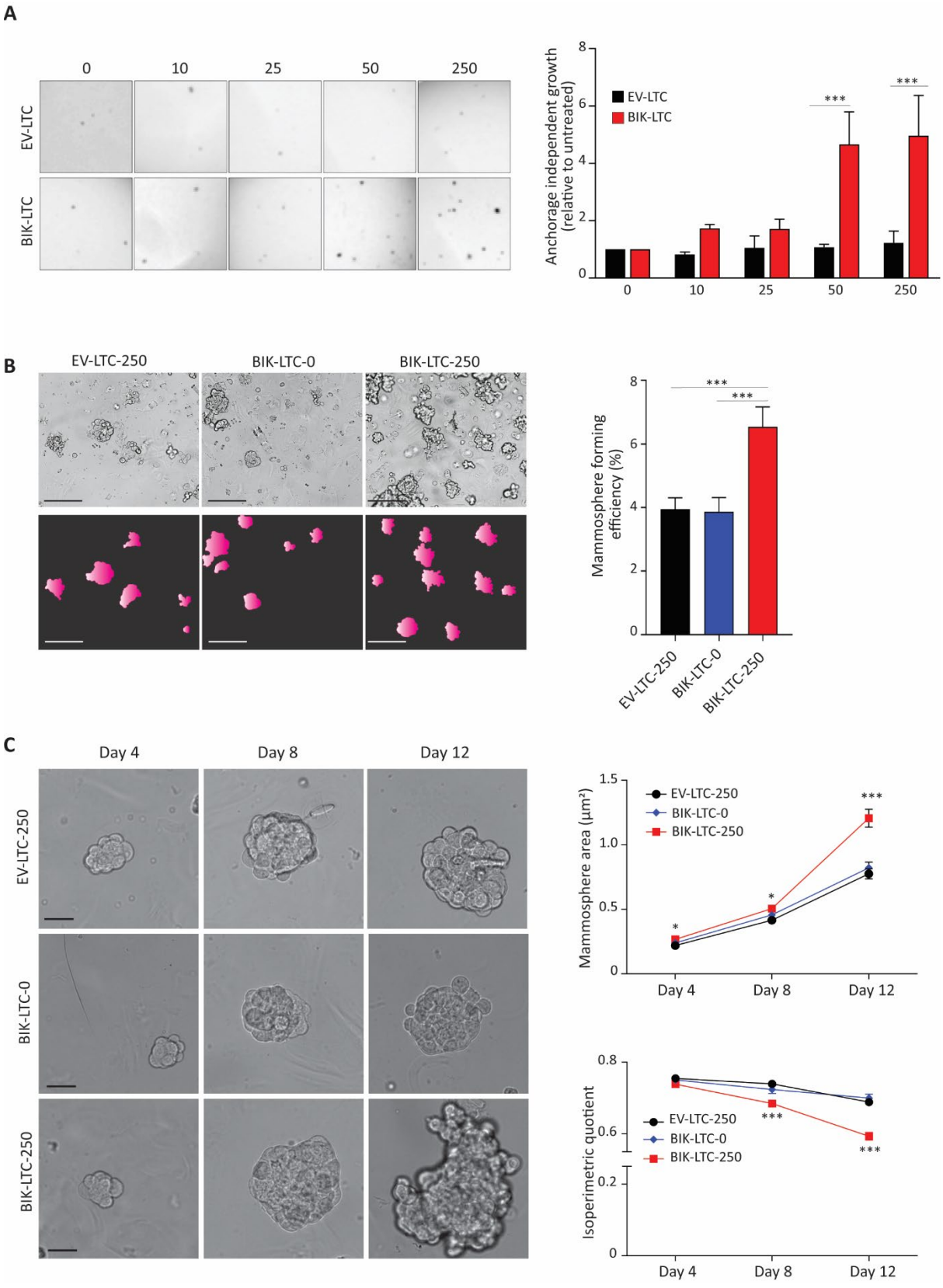
A
0
10
25
50
250
EV-LTC
BIK-LTC
Anchorage independent growth (relative to untreated)
EV-LTC
BIK-LTC
***
***
B
EV-LTC-250
BIK-LTC-0
BIK-LTC-250
Mammosphere forming efficiency (%)
***
***
C
Day 4
Day 8
Day 12
EV-LTC-250
BIK-LTC-0
BIK-LTC-250
Mammosphere area (µm²)
Isoperimetric quotient

Figure 5.12 BIK induces elevated anchorage-independent growth and mammosphere formation. A. Left: Representative images depicting the anchorage-independent growth of LTC cell lines. Right: Quantitation of the number of soft-agar colonies relative to control. Note the drastic increase in soft-agar colony forming potential of BIK-LTC-50 and -250 cell lines. Error bars represent the SD of three independent experiments. One-way ANOVA was performed to ascertain significance among groups followed by Sidak's post-hoc test. (*** $p < 0.001$). **B.** Left: Representative images from mammosphere formation assay performed with EV-LTC-250, BIK-LTC-0, and BIK-LTC-250 cell lines. The top images are original images with necessary brightness/contrast adjustments for clear visual representation. The bottom ones are computer rendered images for better visual presentation. MFE was calculated after 12 days in culture. Scale bar 250µM. Right: Bar graph depicting the quantitation of the mammosphere forming efficiency (MFE) of different LTC cell lines. Note the increase in MFE of BIK-LTC-250 cells. Error bar represent the SD of three independent experiments. One-way ANOVA was performed to ascertain significance among groups followed by Tukey's multiple comparisons test. (*** $p < 0.001$). Contributed by *John Maringa Githaka* **C.** Left: Representative images depicting the size and shapes of mammospheres formed by different LTC cell lines. Note the increase in size and aberration in shape of mammospheres formed by BIK-LTC-250 cell line. Scale bar 50µM. Right top: Plot depicting an increase in mammosphere area over time. Note the sustained increase in mammosphere area of BIK-LTC-250 mammospheres compared to the other two groups. Error bars represent the SEM of three independent experiments. One-way ANOVA was performed to determine significance among groups followed by Dunnett's multiple comparisons test. (* $p < 0.05$, ** $p < 0.01$). Right bottom: Plot depicting the change in circularity over time as a measured by the isoperimetric quotient. Note the significant reduction in mammosphere circularity of BIK-LTC-250 mammospheres compared to the other two groups. Error bars represent the SEM of three independent experiments. One-way ANOVA was performed to determine significance among groups followed by Dunnett's multiple comparisons test. (* $p < 0.05$, ** $p < 0.01$). *Contributed by John Maringa Githaka*

(Bodet et al., 2010; Chinnadurai et al., 2008; Coultas et al., 2004; Germain et al., 2005; Hur et al., 2004; Zhou et al., 2011) and BIK up-regulation is necessary for apoptotic cell death in response to anti-estrogen treatment (Hur et al., 2006; Viedma-Rodriguez et al., 2013; Viedma-Rodriguez et al., 2015). Intriguingly, however, high BIK levels predicted poor disease-free and overall survivals in breast cancer indicative of a tumor-promoting role of BIK. Furthermore, the prognostic value of BIK was specific to ER-positive patients suggesting an interaction of treatment with BIK and poor outcomes. Subsequently I explored the mechanism whereby BIK could contribute to poor patient outcomes. With *in vitro* assays performed on cells expressing titratable amounts of BIK, I demonstrated that although the core apoptotic machinery was activated, overt apoptosis did not occur. Clonogenic survival assays of BIK expressing cells showed that even with continued BIK expression, a large number (~75%) of cells formed colonies. This *in vitro* model suggested that in the face of apoptotic stimuli, some cancer cells can survive and even proliferate.

Apoptotic induction is crucial for the elimination of damaged and potentially neoplastic cells as well as for many anti-cancer therapies to work. Conversely, intriguing correlations between anti-apoptotic upregulation and better patient outcomes have been observed in solid tumors such as breast, colorectal and lung cancers (Berardo et al., 1998; Meterissian et al., 2001; Tomita et al., 2003; Vargas-Roig et al., 2008). Additionally, genetic deletions of pro-apoptotic molecules such BID, PUMA, and caspase-3/7 prevent oncogenesis in some settings (Biswas et al., 2013; Labi et al., 2010; Michalak et al., 2010). Recent studies have demonstrated a process called failed apoptosis, which partly explain these observations. Failed apoptosis is defined as the activation of the apoptotic pathway that does not result in cell death but leads to mutations (Ichim

and Tait, 2016). Weak stimulation of apoptosis using death ligands such as TRAIL and FAS or intrinsic stimuli such as BH3 mimetic and low-dose ionizing radiation (IR) leads to caspase-dependent DNA double strand breaks (DSBs) in the cellular genomes without causing cell death (Ichim et al., 2015; Liu et al., 2015; Lovric and Hawkins, 2010; Miles and Hawkins, 2017). The DNA damage induced by death ligand and BH3 mimetic occurs through CAD whereas low-dose radiation induced DNA damage occurs through a caspase-EndoG axis (Ichim et al., 2015; Liu et al., 2015; Miles and Hawkins, 2017). This DNA damaged has been shown to drive cellular transformation of untransformed cell line such as mouse embryonic fibroblasts (MEFs) and MCF-10A. Furthermore, failed apoptosis has demonstrated tumorigenic effects in mouse xenograft models. For instance, MEFs exposed to BH3 mimetic ABT-737 for long-term gain tumorigenic potential and form subcutaneous tumors in mice while only caspase-3/7 proficient but not deficient MCF-10A cells form subcutaneous tumors when challenged with low-dose IR (Ichim et al., 2015; Liu et al., 2015). Thus, these findings implied that BH3 mimetic treatment or sublethal exposure to ionizing radiation activated the core apoptotic machinery, which led to DNA damage and oncogenesis in cell-based models (Ichim et al., 2015; Liu et al., 2015). Understanding of these observations in the context of therapeutic intervention of cancer patients, their prognosis and the underlying mechanisms were however lacking. Our results provided insight into how endocrine therapy-induced BIK may engage a failed apoptosis in ER-positive cancers, leading to aggressive disease.

I demonstrated that BIK induction does not elevate cellular ROS levels and BIK mediated DNA damage does not occur through ROS but instead though a caspase-CAD axis. Given that BIK

promotes ER Ca^{2+} release (Mathai et al., 2005), this finding was surprising since the mitochondrial overload of Ca^{2+} is known to induce reactive oxygen species (Gorlach et al., 2015; Peng and Jou, 2010). Hence, the lack of ROS production in BIK expressing cells remains unclear. I also showed that tamoxifen or 4-HT treatment of ER-positive breast cancer cells caused BIK dependent DNA damage. These findings provide mechanistic insight into the previous observations that tamoxifen treatment induced double-strand DNA damage in ER-positive cells (Wozniak et al., 2007) and long-term treatment of rats with tamoxifen generated hepatocellular carcinomas (Carthew et al., 1995; Greaves et al., 1993). BIK upregulation in these settings might be partly responsible for genomic instability and mutagenesis. In light of our results with patient tumors, tamoxifen treatment may inflict BIK dependent genomic damage in ER-positive patients leading to mutagenesis, which may provide a means of tumor evolution.

References

Bacci, M., Giannoni, E., Fearns, A., Ribas, R., Gao, Q., Taddei, M.L., Pintus, G., Dowsett, M., Isacke, C.M., Martin, L.A*., et al.* (2016). miR-155 Drives Metabolic Reprogramming of ER+ Breast Cancer Cells Following Long-Term Estrogen Deprivation and Predicts Clinical Response to Aromatase Inhibitors. Cancer Res *76*, 1615-1626.

Beck, B., and Blanpain, C. (2013). Unravelling cancer stem cell potential. Nat Rev Cancer *13*, 727-738.

Berardo, M.D., Elledge, R.M., de Moor, C., Clark, G.M., Osborne, C.K., and Allred, D.C. (1998). bcl-2 and apoptosis in lymph node positive breast carcinoma. Cancer *82*, 1296-1302.

Billard, C. (2013). BH3 mimetics: status of the field and new developments. Mol Cancer Ther *12*, 1691-1700.

Biswas, S., Shi, Q., Wernick, A., Aiello, A., and Zinkel, S.S. (2013). The loss of the BH3-only Bcl-2 family member Bid delays T-cell leukemogenesis in Atm-/- mice. Cell Death Differ *20*, 869-877.

Bodet, L., Menoret, E., Descamps, G., Pellat-Deceunynck, C., Bataille, R., Le Gouill, S., Moreau, P., Amiot, M., and Gomez-Bougie, P. (2010). BH3-only protein Bik is involved in both apoptosis induction and sensitivity to oxidative stress in multiple myeloma. Br J Cancer *103*, 1808-1814.

Borowicz, S., Van Scoyk, M., Avasarala, S., Karuppusamy Rathinam, M.K., Tauler, J., Bikkavilli, R.K., and Winn, R.A. (2014). The soft agar colony formation assay. J Vis Exp, e51998.

Carthew, P., Martin, E.A., White, I.N., De Matteis, F., Edwards, R.E., Dorman, B.M., Heydon, R.T., and Smith, L.L. (1995). Tamoxifen induces short-term cumulative DNA damage and liver tumors in rats: promotion by phenobarbital. Cancer Res *55*, 544-547.

Cartwright, I.M., Liu, X., Zhou, M., Li, F., and Li, C.Y. (2017). Essential roles of Caspase-3 in facilitating Myc-induced genetic instability and carcinogenesis. Elife *6*.

Chang, J.C. (2016). Cancer stem cells: Role in tumor growth, recurrence, metastasis, and treatment resistance. Medicine (Baltimore) *95*, S20-25.

Chinnadurai, G., Vijayalingam, S., and Rashmi, R. (2008). BIK, the founding member of the BH3-only family proteins: mechanisms of cell death and role in cancer and pathogenic processes. Oncogene *27 Suppl 1*, S20-29.

Coser, K.R., Wittner, B.S., Rosenthal, N.F., Collins, S.C., Melas, A., Smith, S.L., Mahoney, C.J., Shioda, K., Isselbacher, K.J., Ramaswamy, S.*, et al.* (2009). Antiestrogen-resistant subclones of MCF-7 human breast cancer cells are derived from a common monoclonal drug-resistant progenitor. Proc Natl Acad Sci U S A *106*, 14536-14541.

Coultas, L., Bouillet, P., Stanley, E.G., Brodnicki, T.C., Adams, J.M., and Strasser, A. (2004). Proapoptotic BH3-only Bcl-2 family member Bik/Blk/Nbk is expressed in hemopoietic and endothelial cells but is redundant for their programmed death. Mol Cell Biol *24*, 1570-1581.

Delbridge, A.R., and Strasser, A. (2015). The BCL-2 protein family, BH3-mimetics and cancer therapy. Cell Death Differ *22*, 1071-1080.

Dubrovska, A., Hartung, A., Bouchez, L.C., Walker, J.R., Reddy, V.A., Cho, C.Y., and Schultz, P.G. (2012). CXCR4 activation maintains a stem cell population in tamoxifen-resistant breast cancer cells through AhR signalling. Br J Cancer *107*, 43-52.

Erikson, J., ar-Rushdi, A., Drwinga, H.L., Nowell, P.C., and Croce, C.M. (1983). Transcriptional activation of the translocated c-myc oncogene in burkitt lymphoma. Proc Natl Acad Sci U S A *80*, 820-824.

Fu, Y., Li, J., and Lee, A.S. (2007). GRP78/BiP inhibits endoplasmic reticulum BIK and protects human breast cancer cells against estrogen starvation-induced apoptosis. Cancer Res *67*, 3734-3740.

Germain, M., Mathai, J.P., McBride, H.M., and Shore, G.C. (2005). Endoplasmic reticulum BIK initiates DRP1-regulated remodelling of mitochondrial cristae during apoptosis. EMBO J *24*, 1546-1556.

Gorlach, A., Bertram, K., Hudecova, S., and Krizanova, O. (2015). Calcium and ROS: A mutual interplay. Redox Biol *6*, 260-271.

Greaves, P., Goonetilleke, R., Nunn, G., Topham, J., and Orton, T. (1993). Two-year carcinogenicity study of tamoxifen in Alderley Park Wistar-derived rats. Cancer Res *53*, 3919-3924.

Grimshaw, M.J., Cooper, L., Papazisis, K., Coleman, J.A., Bohnenkamp, H.R., Chiapero-Stanke, L., Taylor-Papadimitriou, J., and Burchell, J.M. (2008). Mammosphere culture of metastatic breast cancer cells enriches for tumorigenic breast cancer cells. Breast Cancer Res *10*, R52.

Guest, S.K., Ribas, R., Pancholi, S., Nikitorowicz-Buniak, J., Simigdala, N., Dowsett, M., Johnston, S.R., and Martin, L.A. (2016). Src Is a Potential Therapeutic Target in Endocrine-Resistant Breast Cancer Exhibiting Low Estrogen Receptor-Mediated Transactivation. PLoS One *11*, e0157397.

Horibata, S., Vo, T.V., Subramanian, V., Thompson, P.R., and Coonrod, S.A. (2015). Utilization of the Soft Agar Colony Formation Assay to Identify Inhibitors of Tumorigenicity in Breast Cancer Cells. J Vis Exp, e52727.

Hur, J., Bell, D.W., Dean, K.L., Coser, K.R., Hilario, P.C., Okimoto, R.A., Tobey, E.M., Smith, S.L., Isselbacher, K.J., and Shioda, T. (2006). Regulation of expression of BIK proapoptotic protein in human breast cancer cells: p53-dependent induction of BIK mRNA by fulvestrant and proteasomal degradation of BIK protein. Cancer Res *66*, 10153-10161.

Hur, J., Chesnes, J., Coser, K.R., Lee, R.S., Geck, P., Isselbacher, K.J., and Shioda, T. (2004). The Bik BH3-only protein is induced in estrogen-starved and antiestrogen-exposed breast cancer cells and provokes apoptosis. Proc Natl Acad Sci U S A *101*, 2351-2356.

Ichim, G., Lopez, J., Ahmed, S.U., Muthalagu, N., Giampazolias, E., Delgado, M.E., Haller, M., Riley, J.S., Mason, S.M., Athineos, D.*, et al.* (2015). Limited mitochondrial permeabilization causes DNA damage and genomic instability in the absence of cell death. Mol Cell *57*, 860-872.

Ichim, G., and Tait, S.W. (2016). A fate worse than death: apoptosis as an oncogenic process. Nat Rev Cancer *16*, 539-548.

Kryston, T.B., Georgiev, A.B., Pissis, P., and Georgakilas, A.G. (2011). Role of oxidative stress and DNA damage in human carcinogenesis. Mutat Res *711*, 193-201.

Labi, V., Erlacher, M., Krumschnabel, G., Manzl, C., Tzankov, A., Pinon, J., Egle, A., and Villunger, A. (2010). Apoptosis of leukocytes triggered by acute DNA damage promotes lymphoma formation. Genes Dev *24*, 1602-1607.

Larsen, B.D., and Sorensen, C.S. (2017). The caspase-activated DNase: apoptosis and beyond. FEBS J *284*, 1160-1170.

Liang, Y., Yan, C., and Schor, N.F. (2001). Apoptosis in the absence of caspase 3. Oncogene *20*, 6570-6578.

Liu, X., He, Y., Li, F., Huang, Q., Kato, T.A., Hall, R.P., and Li, C.Y. (2015). Caspase-3 promotes genetic instability and carcinogenesis. Mol Cell *58*, 284-296.

Liu, X., Pisha, E., Tonetti, D.A., Yao, D., Li, Y., Yao, J., Burdette, J.E., and Bolton, J.L. (2003). Antiestrogenic and DNA damaging effects induced by tamoxifen and toremifene metabolites. Chem Res Toxicol *16*, 832-837.

Liu, Y., Nenutil, R., Appleyard, M.V., Murray, K., Boylan, M., Thompson, A.M., and Coates, P.J. (2014). Lack of correlation of stem cell markers in breast cancer stem cells. Br J Cancer *110*, 2063-2071.

Lovric, M.M., and Hawkins, C.J. (2010). TRAIL treatment provokes mutations in surviving cells. Oncogene *29*, 5048-5060.

Martin, E.C., Conger, A.K., Yan, T.J., Hoang, V.T., Miller, D.F., Buechlein, A., Rusch, D.B., Nephew, K.P., Collins-Burow, B.M., and Burow, M.E. (2017). MicroRNA-335-5p and -3p synergize to inhibit estrogen receptor alpha expression and promote tamoxifen resistance. FEBS Lett *591*, 382-392.

Mathai, J.P., Germain, M., and Shore, G.C. (2005). BH3-only BIK regulates BAX,BAK-dependent release of Ca2+ from endoplasmic reticulum stores and mitochondrial apoptosis during stress-induced cell death. J Biol Chem *280*, 23829-23836.

McDonnell, T.J., Deane, N., Platt, F.M., Nunez, G., Jaeger, U., McKearn, J.P., and Korsmeyer, S.J. (1989). bcl-2-immunoglobulin transgenic mice demonstrate extended B cell survival and follicular lymphoproliferation. Cell *57*, 79-88.

Mehta, A., and Haber, J.E. (2014). Sources of DNA double-strand breaks and models of recombinational DNA repair. Cold Spring Harb Perspect Biol *6*, a016428.

Meterissian, S.H., Kontogiannea, M., Al-Sowaidi, M., Linjawi, A., Halwani, F., Jamison, B., and Edwardes, M. (2001). Bcl-2 is a useful prognostic marker in Dukes' B colon cancer. Ann Surg Oncol *8*, 533-537.

Michalak, E.M., Vandenberg, C.J., Delbridge, A.R., Wu, L., Scott, C.L., Adams, J.M., and Strasser, A. (2010). Apoptosis-promoted tumorigenesis: gamma-irradiation-induced thymic lymphomagenesis requires Puma-driven leukocyte death. Genes Dev *24*, 1608-1613.

Miles, M.A., and Hawkins, C.J. (2017). Executioner caspases and CAD are essential for mutagenesis induced by TRAIL or vincristine. Cell Death Dis *8*, e3062.

Morata-Tarifa, C., Picon-Ruiz, M., Grinan-Lison, C., Boulaiz, H., Peran, M., Garcia, M.A., and Marchal, J.A. (2017). Validation of suitable normalizers for miR expression patterns analysis covering tumour heterogeneity. Sci Rep *7*, 39782.

Neri, A., Marrelli, D., Roviello, F., DeMarco, G., Mariani, F., DeStefano, A., Megha, T., Caruso, S., Corso, G., Cioppa, T.*, et al.* (2006). Bcl-2 expression correlates with lymphovascular invasion and long-term prognosis in breast cancer. Breast Cancer Res Treat *99*, 77-83.

Opydo-Chanek, M., Gonzalo, O., and Marzo, I. (2017). Multifaceted anticancer activity of BH3 mimetics: Current evidence and future prospects. Biochem Pharmacol *136*, 12-23.

Orth, K., and Dixit, V.M. (1997). Bik and Bak induce apoptosis downstream of CrmA but upstream of inhibitor of apoptosis. J Biol Chem *272*, 8841-8844.

Pandya, V., Glubrecht, D., Vos, L., Hanson, J., Damaraju, S., Mackey, J., Hugh, J., and Goping, I.S. (2016). The pro-apoptotic paradox: the BH3-only protein Bcl-2 interacting killer (Bik) is prognostic for unfavorable outcomes in breast cancer. Oncotarget *7*, 33272-33285.

Peng, T.I., and Jou, M.J. (2010). Oxidative stress caused by mitochondrial calcium overload. Ann N Y Acad Sci *1201*, 183-188.

Rappa, G., Mercapide, J., Anzanello, F., Prasmickaite, L., Xi, Y., Ju, J., Fodstad, O., and Lorico, A. (2008). Growth of cancer cell lines under stem cell-like conditions has the potential to unveil therapeutic targets. Exp Cell Res *314*, 2110-2122.

Real, P.J., Sanz, C., Gutierrez, O., Pipaon, C., Zubiaga, A.M., and Fernandez-Luna, J.L. (2006). Transcriptional activation of the proapoptotic bik gene by E2F proteins in cancer cells. FEBS Lett *580*, 5905-5909.

Rehm, M., Dussmann, H., and Prehn, J.H. (2003). Real-time single cell analysis of Smac/DIABLO release during apoptosis. J Cell Biol *162*, 1031-1043.

Ritchie, A., Gutierrez, O., and Fernandez-Luna, J.L. (2009). PAR bZIP-bik is a novel transcriptional pathway that mediates oxidative stress-induced apoptosis in fibroblasts. Cell Death Differ *16*, 838-846.

Roberts, A.W., Davids, M.S., Pagel, J.M., Kahl, B.S., Puvvada, S.D., Gerecitano, J.F., Kipps, T.J., Anderson, M.A., Brown, J.R., Gressick, L.*, et al.* (2016). Targeting BCL2 with Venetoclax in Relapsed Chronic Lymphocytic Leukemia. N Engl J Med *374*, 311-322.

Schiewer, M.J., and Knudsen, K.E. (2016). Linking DNA Damage and Hormone Signaling Pathways in Cancer. Trends Endocrinol Metab *27*, 216-225.

Solier, S., and Pommier, Y. (2014). The nuclear gamma-H2AX apoptotic ring: implications for cancers and autoimmune diseases. Cell Mol Life Sci *71*, 2289-2297.

Sopik, V., Sun, P., and Narod, S.A. (2017). The prognostic effect of estrogen receptor status differs for younger versus older breast cancer patients. Breast Cancer Res Treat *165*, 391-402.

Spender, L.C., O'Brien, D.I., Simpson, D., Dutt, D., Gregory, C.D., Allday, M.J., Clark, L.J., and Inman, G.J. (2009). TGF-beta induces apoptosis in human B cells by transcriptional regulation of BIK and BCL-XL. Cell Death Differ *16*, 593-602.

Taylor, R.C., Cullen, S.P., and Martin, S.J. (2008). Apoptosis: controlled demolition at the cellular level. Nat Rev Mol Cell Biol *9*, 231-241.

Tomita, M., Matsuzaki, Y., Edagawa, M., Shimizu, T., Hara, M., and Onitsuka, T. (2003). Prognostic significance of bcl-2 expression in resected pN2 non-small cell lung cancer. Eur J Surg Oncol *29*, 654-657.

Turner, N.C., Neven, P., Loibl, S., and Andre, F. (2017). Advances in the treatment of advanced oestrogen-receptor-positive breast cancer. Lancet *389*, 2403-2414.

Vargas-Roig, L.M., Cuello-Carrion, F.D., Fernandez-Escobar, N., Daguerre, P., Leuzzi, M., Ibarra, J., Gago, F.E., Nadin, S.B., and Ciocca, D.R. (2008). Prognostic value of Bcl-2 in breast cancer patients treated with neoadjuvant anthracycline based chemotherapy. Mol Oncol *2*, 102-111.

Viedma-Rodriguez, R., Baiza-Gutman, L.A., Garcia-Carranca, A., Moreno-Fierros, L., Salamanca-Gomez, F., and Arenas-Aranda, D. (2013). Suppression of the death gene BIK is a critical factor for resistance to tamoxifen in MCF-7 breast cancer cells. Int J Oncol *43*, 1777-1786.

Viedma-Rodriguez, R., Ruiz Esparza-Garrido, R., Baiza-Gutman, L.A., Velazquez-Flores, M.A., Garcia-Carranca, A., Salamanca-Gomez, F., and Arenas-Aranda, D. (2015). Involvement of multiple cellular pathways in regulating resistance to tamoxifen in BIK-suppressed MCF-7 cells. Tumour Biol *36*, 6991-7005.

Vieira, A.F., Ribeiro, A.S., Dionisio, M.R., Sousa, B., Nobre, A.R., Albergaria, A., Santiago-Gomez, A., Mendes, N., Gerhard, R., Schmitt, F.*, et al.* (2014). P-cadherin signals through the laminin receptor alpha6beta4 integrin to induce stem cell and invasive properties in basal-like breast cancer cells. Oncotarget *5*, 679-692.

Wahler, J., So, J.Y., Cheng, L.C., Maehr, H., Uskokovic, M., and Suh, N. (2015). Vitamin D compounds reduce mammosphere formation and decrease expression of putative stem cell markers in breast cancer. J Steroid Biochem Mol Biol *148*, 148-155.

Wang, R., Lv, Q., Meng, W., Tan, Q., Zhang, S., Mo, X., and Yang, X. (2014). Comparison of mammosphere formation from breast cancer cell lines and primary breast tumors. J Thorac Dis *6*, 829-837.

Woodbine, L., Brunton, H., Goodarzi, A.A., Shibata, A., and Jeggo, P.A. (2011). Endogenously induced DNA double strand breaks arise in heterochromatic DNA regions and require ataxia telangiectasia mutated and Artemis for their repair. Nucleic Acids Res *39*, 6986-6997.

Wozniak, K., Kolacinska, A., Blasinska-Morawiec, M., Morawiec-Bajda, A., Morawiec, Z., Zadrozny, M., and Blasiak, J. (2007). The DNA-damaging potential of tamoxifen in breast cancer and normal cells. Arch Toxicol *81*, 519-527.

Yang, P.M., Tseng, H.H., Peng, C.W., Chen, W.S., and Chiu, S.J. (2012). Dietary flavonoid fisetin targets caspase-3-deficient human breast cancer MCF-7 cells by induction of caspase-7-associated apoptosis and inhibition of autophagy. Int J Oncol *40*, 469-478.

Yu, K.D., Wu, J., Shen, Z.Z., and Shao, Z.M. (2012). Hazard of breast cancer-specific mortality among women with estrogen receptor-positive breast cancer after five years from diagnosis: implication for extended endocrine therapy. J Clin Endocrinol Metab *97*, E2201-2209.

Zhang, L., Xu, L., Zhang, F., and Vlashi, E. (2017). Doxycycline inhibits the cancer stem cell phenotype and epithelial-to-mesenchymal transition in breast cancer. Cell Cycle *16*, 737-745.

Zhou, H., Zhang, Y., Fu, Y., Chan, L., and Lee, A.S. (2011). Novel mechanism of anti-apoptotic function of 78-kDa glucose-regulated protein (GRP78): endocrine resistance factor in breast cancer, through release of B-cell lymphoma 2 (BCL-2) from BCL-2-interacting killer (BIK). J Biol Chem *286*, 25687-25696.

CHAPTER 6

PERSPECTIVES

6.1 Utility of BIK as a diagnostic tool for ER-positive breast cancer

We identified BIK as a prognostic marker for ER-positive patients and demonstrated that high levels of BIK are associated with worse patient outcomes. This suggests that BIK-high patients may be resistant to endocrine therapy. Chemotherapy of these patients in addition to the standard anti-estrogen treatment may provide therapeutic benefit. Thus, assessment of BIK protein levels can serve as a predictive biomarker for endocrine therapy that can be developed into a diagnostic test for making treatment decisions. Currently, qRT-PCR based tests such as Oncotype Dx have been introduced into clinical practice to better estimate the prognostic outcomes of ER-positive, HER2-negative, node-negative subgroup of breast cancer patients who make up a small portion of the total ER-positive cancers (Xin et al., 2017). On the other hand, prognostic determination using BIK would encompass all ER-positive cancers irrespective of their HER2 and node metastasis status. Oncotype Dx employs a multigene expression signature that includes 16 known genes encoding proteins associated with proliferation (e.g. Ki67, cyclin B1 and survivin), estrogen signaling (e.g. ER, PR, BCL2, SCUBE2) invasion (e.g. stromelysin 3 and cathepsin l2) as well as 5 reference genes (e.g. β-Actin, GAPDH, RPLPO, GUS, TFRC) (Paik, 2007; Xin et al., 2017). Hence, it is a complex assay that requires RNA isolation and the calculation of recurrence score from raw gene expression data. Also, it is run in a single center at the cost of $4500 per test (Breastcancer.org, 2018). In comparison, our study identified a single marker from the BH3-only proteins to predict ER-positive breast cancer prognosis that may well lend itself to the development of a simple, less expensive test. Validation of these results would be necessary with independent cohorts of ER-positive

breast cancer patients before it can be considered/developed as a clinical decision-making tool. Nevertheless, a test of this kind would fit more easily into the current pipeline of ER/PR/HER2 testing that is routinely performed by IHC at local laboratories for under $100 per test. Hence, this kind of assay would be more amenable to less developed nations where it can provide a cost-effective healthcare solution.

6.2 Potential mechanisms determining BIK upregulation in tumors

Steady-state levels of BIK in normal tissues are known to be reasonably low. For instance, Maxfield et al. demonstrated that *BIK* mRNA expression in normal pancreas, lung, colon and breast tissues was lower compared to the corresponding tumor tissues (Maxfield et al., 2015). These low levels in normal tissues are attributed to the conditional expression of *BIK* in response to death stimuli such as low estrogen levels, cytokine stimulation and genotoxic stress (Chinnadurai et al., 2008; Hur et al., 2004; Mathai et al., 2002; Mebratu et al., 2008). These stressors commonly exist in tumors, which may stimulate *BIK* expression through particular transcription factors. As examples, in post-menopausal women circulating levels of estrogen are reduced. Hence, ER-positive breast cancers in such patients encounter estrogen deprivation, which may cause a p53 mediated *BIK* upregulation. As well, some tumors encounter inflammatory responses mediated through pro-inflammatory cytokines such as INF-γ (Zaidi and Merlino, 2011). This cytokine also stimulates *BIK* expression via signal transducer and activator of transcription 1 (STAT1) (Mebratu et al., 2008). Lastly, cancer cells face replicative stress, which leads to genomic damage. Interestingly, *BIK* expression is also stimulated by genotoxic insults through p53

and E2F transcription factors (Mathai et al., 2002; Subramanian et al., 2007). Furthermore, some of the transcription factors (e.g., E2F, STAT1, TEF) that regulate *BIK* expression have also been shown to overexpress in cancer, which in turn, cause *BIK* overexpression in those tumors (Bodet et al., 2010; Mebratu et al., 2008; Reimer et al., 2006; Subramanian et al., 2007). Thus, *BIK* mRNA levels may increase in certain tumors due to existing stressors that are otherwise absent in normal tissues or cultured cells.

Aberrations in the BIK protein turnover could be another likely mechanism determining BIK upregulation in tumors. BIK undergoes constant turn-over through proteasomal and autophagic pathways (Chen et al., 2014; Chinnadurai et al., 2008). This was shown by its stabilization upon treatment with proteasomal (e.g., MG132 and bortezomib) (Hur et al., 2006; Sung et al., 2012; Zhu et al., 2005a; Zhu et al., 2005b) or autophagic (Bafilomycin A1) inhibitors (Chen et al., 2014). Mechanistically, ERK1/2 mediated phosphorylation of BIK promoted its polyubiquitination at Lys 33 (Lopez et al., 2012). As well, BIK ubiquitination was shown to occur through a complex formed by adaptor protein FATE1 and E3 ubiquitin ligase RNF 183, which eventually led to BIK proteasomal degradation (Maxfield et al., 2015). Silencing of either FATE-1 or RNF 183 led to the stabilization of BIK. Importantly, in cancer cells, these regulatory processes are perturbed, which may explain why BIK is detectable in tumors. For instance, autophagy is downregulated in some cancers, and proteasomal machinery might be overwhelmed due to excessive accumulation of misfolded proteins (Marinkovi et al., 2018; Mathew et al., 2007). This may result in elevated levels of proteins, such as BIK, that would otherwise be

degraded. Altogether, this complex level of BIK regulation is encapsulated in the treatment-naive tumors that we analyzed. The tumors that had high levels of BIK, likely had defective BIK-degradation pathways while tumors with low levels of BIK possibly maintained a functional degradation pathway. I propose that once ER-positive breast cancer patients receive anti-estrogen treatment, they would have elevated *BIK* mRNA transcription. Those tumors with high BIK protein prior to treatment would be in a permissive environment (e.g., low FATE1 or RNF 183 levels or mutations preventing their binding to BIK) to further enhance BIK levels given the appropriate stimulation. This proposition is supported by the finding that BIK levels induced by anti-estrogen treatment further increased upon proteasomal inhibition in the ER-positive cancer cells (Hur et al., 2006). Tumors with low BIK prior to treatment, on the other hand, may or may not have the capacity to maintain elevated BIK protein in response to endocrine treatment. Thus, if BIK protein is already high in those tumors that have defects in protein turnover, then the anti-estrogen treatment that induces *BIK* gene transcription would elevate BIK protein levels even further.

6.3 How failed apoptosis may affect patient survival

Apoptosis is generally considered to be a process that once activated culminates in cell death. However, recent research has revealed that apoptotic activation does not always result in cell death. The term “failed apoptosis” was coined by Tait and collogues, which refers to a process wherein cells initiate apoptosis but do not die, and sustain potentially

oncogenic damage such as genomic instability and gene amplification (Ichim and Tait, 2016).

While apoptosis has a tumor-suppressing role, the consequences of failed apoptosis were not well understood. Early clinical observations hinted that apoptosis was linked to aggressive disease and supported the paradigm that it may act as a tumor-promoting mechanism. For instance, contrary to the negative survival association of BCL-2 in lymphomas, high BCL-2 is associated with favorable outcomes in breast (Berardo et al., 1998; Dawson et al., 2010; Neri et al., 2006; Pandya et al., 2016; Vargas-Roig et al., 2008), colorectal (Meterissian et al., 2001; Watson et al., 2005) and non-small cell lung cancers (Anagnostou et al., 2010; Renouf et al., 2009; Tomita et al., 2003). A critical report that analyzed the data from 5 independent studies (total n=11212) involving all types of breast cancer concluded that high BCL-2 levels have a favorable effect on patient prognosis (Dawson et al., 2010). Additionally, high levels of pro-apoptotic BAX are associated with poor prognosis in acute myeloid leukemia (AML) (Kohler et al., 2002), acute lymphocytic leukemia (ALL) (Kaparou et al., 2013; Kohler et al., 2002) and Non-Hodgkin's lymphoma (Bairey et al., 1999). Furthermore, high amounts of activated caspase-3 in breast and, head and neck cancers predicted worse clinical outcomes (Huang et al., 2011). Thus, these studies suggested that enhanced anti-apoptotic signaling was tumor suppressing whereas apoptotic activation was somehow tumor promoting, which stimulated investigations into the pro-tumorigenic role of apoptosis.

In apoptosis, MOMP marks the point of no return, and once caspase activation ensues, various feed-forward mechanisms lead to the full-fledged destruction that ends with cell death (Ichim and Tait, 2016). Despite this prevailing dogma, Albeck et al. published one of the first reports, demonstrating that HeLa cells can survive limited caspase activation achieved through the extrinsic pathway of apoptosis (Albeck et al., 2008). In the normal developmental processes such as macrophage, sperm and stem cell differentiation, as well as in neuronal development and dendritic pruning, caspase activation has been extensively reported (Arama et al., 2003; Julien and Wells, 2017; Kuo et al., 2006; Li et al., 2010; Sordet et al., 2002; Williams et al., 2006). Thus, cell survival with activated caspases routinely occurs although what kind of cell-intrinsic effects it could have in the context of cancer was not clear. Lovric and Hawkins linked caspase activation with genomic mutations (Lovric and Hawkins, 2010). These authors demonstrated that the treatment of human glioblastoma and MEF cells with TRAIL and FAS ligands activated caspase-8 (Lovric and Hawkins, 2010). While this caused some amount of cell death, there was an increase in the mutation frequency of the surviving cells (Lovric and Hawkins, 2010). Crucially, the mutagenesis was dependent on caspase-8, and the caspase-activated DNAse (CAD) as their knockdown reduced the mutation frequency (Lovric and Hawkins, 2010). Thus, cells can not only survive with activated caspases but also accumulate mutations through downstream effectors such as CAD.

Subsequent investigations explored whether the intrinsic apoptotic pathway had any mutagenic effects, which could lead to carcinogenesis. Ichim et al. explored this possibility with a low-dose BH3-mimetic (ABT-737) treatment of cells (Ichim et al., 2015).

This group engaged MOMP in only a few mitochondria, which led to cytochrome *c* release and limited activation of caspases without cell death. Furthermore, activated caspases led to CAD-dependent DSBs and genomic instability defined by gene amplification and chromosomal segregation defects. These results elucidated the mutagenic potential of mitochondrial apoptosis (Ichim et al., 2015). Another study using caspase-3 and -7 deficient^{-} cells reported similar results (Liu et al., 2015). Using sublethal amounts of ionizing radiation, these authors induced caspase-3 activation in non-tumorigenic MCF-10A cells that did not trigger full-fledged apoptosis but inflicted double-strand DNA damage through endonuclease G (EndoG) (Liu et al., 2015). Crucially, shRNA mediated knockdown of EndoG led to a reduction in the radiation-induced transformation frequency of MCF-10A cells, which confirmed that DNA damage was responsible for the cellular transformation. Furthermore, both these reports (Ichim et al., 2015; Liu et al., 2015) provided evidence that caspase-dependent DNA damage conferred tumorigenic potential to MEF or MCF-10A cells, which are otherwise non-tumorigenic. Lastly, caspase-3 and caspase-7 deficient mice when subjected to chemical-induced skin carcinogenesis showed diminished tumor formation, confirming the essential role caspases play in this process (Liu et al., 2015). Thus, these observations linked the intrinsic apoptotic pathway to oncogenesis via genomic damage and provided *in vitro* and *in vivo* evidence that if weakly executed, the intrinsic pathway of apoptosis could inflict genomic damage and facilitate carcinogenesis.

Whether failed apoptosis is induced by anti-cancer treatments in patients and its relevance to disease progression was, however, not known. As well, which BH3-only

sensors can engage failed apoptosis was also unexplored. Using ER-positive breast cancer as a model, I demonstrated that the BH3-only protein BIK was upregulated upon endocrine treatment of ER-positive cancer cells, induced DNA double-strand breaks (DSBs) and predicted poor patient outcomes, signifying the relevance of failed apoptosis in the patient tumor biology. Future studies will likely identify driver mutations resulting from failed apoptosis in tumors upon exposure to stressors such as hypoxia, starvation or chemotherapeutic insults. This will illuminate *de novo* pathways of genomic instability and clonal evolution in cancers.

6.4 BIK-induced DNA damage and its connection to cancer evolution

BIK mediated failed apoptosis generates DNA double-strand breaks (DSBs) that presumably lead to mutations. Cells commonly face four types of DNA damage, which include base modifications, pyrimidine dimers, and single and double strand breaks (DSBs) (Ciccia and Elledge, 2010). Of these, DSBs represent the most lethal type of DNA damage as it threatens the continuity of the blueprint of life. DSBs can arise from endogenous sources such as reactive oxygen species (ROS) and replication-stress or exogenous sources such ionizing radiation in clinical settings, space travel and even through normal decay of uranium in the soil (Mehta and Haber, 2014). Unrepaired DSBs cause broken chromosomes and segregation errors, which can lead to genomic instability and cancer (Gothwal et al., 2016). Therefore, DSB repair pathways have evolved over millions of years to maintain the genomic integrity of cells. Two central repair pathways are called homologous recombination (HR) and non-homologous end joining (NHEJ). NHEJ prevails

during the G1, and early S phases of the cell cycle whereas HR-mediated repair occurs after the DNA is replicated (Branzei and Foiani, 2008; Ceccaldi et al., 2016; Chapman et al., 2012). HR utilizes a healthy sister chromatid as a template during the repair process, which makes it mostly error-free whereas NHEJ mediated repair involves DNA end-ligation making it prone to errors (Ceccaldi et al., 2016; Chapman et al., 2012). To initiate HR, DSBs need to be resected by nucleases and helicases that generate 3′ single-stranded DNA (ssDNA) overhangs onto which the RAD51 recombinase assembles as a nucleoprotein filament (Chapman et al., 2012; Ciccia and Elledge, 2010). This is followed by strand invasion and homologous recombination with the healthy sister chromatid, which is used as a template for repair DNA synthesis (Branzei and Foiani, 2008). HR ends with the action of endonucleases and helicases that resolve correctly repaired DNA molecules (Chapman et al., 2012; Ciccia and Elledge, 2010). On the other hand, during NHEJ, broken ends of the DNA are held in close proximity by the Ku70-Ku80 heterodimeric (Ku) scaffold, which has a propensity to bind at the double-stranded DNA (dsDNA) ends (Chapman et al., 2012; Ciccia and Elledge, 2010). Subsequently, ligase 4 mediates a direct ligation of the DSB ends but in an error-prone manner. This frequently results in small insertions and deletions (indels), or substitutions at the break site. If DSBs from different parts of the chromatin are ligated, it results in translocations leading to genomic instability (Ceccaldi et al., 2016; Chapman et al., 2012; Ciccia and Elledge, 2010). Since, NHEJ occurs during the G1 phase, which occupies >60% of the cell cycle, it dominates the repair process increasing the chances of mutagenesis if the DNA damage is persistent (Chapman et al., 2012). Mutation rates can further increase due to defects in the HR component such as

BRCA1 and BRCA2, which function in the early recruitment of repair proteins or assist RAD51 during the strand invasion step respectively (Prakash et al., 2015; Zámborszky et al., 2016). Considering our results where we see induction of DSBs upon BIK upregulation, if these DSBs are not repaired through HR, it could increase the frequency of mutations such as indels.

Mutational load in breast cancer tumors is relatively well documented. Interestingly, Nik-Zanial et al. sequenced 560 breast tumors and found an average of 664 indels per tumor (Nik-Zainal et al., 2016). Specifically, the ER-positive group had an average of 306 indels with some tumors harboring >5000 of those. Thus, ER-positive tumors harbor the kind of mutations that arise due to error-prone repair. However, how these mutations emerge is not well understood. Investigation of BIK levels in these tumors may provide some answers. I predict that in the ER-positive group, BIK-high tumors may have a higher mutational load than BIK-low tumors. What could this mean in terms of disease outcomes? Interestingly, in the ER-positive cancers, a positive correlation between the mutational load and unfavorable patient prognosis exists (Haricharan et al., 2014). Analysis of the exome sequencing data of 559 ER-positive tumors found a mean somatic mutation load of 62.7 mutations per tumor with a small subset of tumors carrying a significantly higher mutational load (Haricharan et al., 2014). The tumors could be classified into low- and high mutational load (HML) groups wherein HML tumors were associated with poor prognosis compared to the LML group (HR=2.02) (Haricharan et al., 2014). As well, the survival curve of the HML group overlapped with the ER-negative survival curve suggesting an increase in the aggressiveness of the HML tumors

(Haricharan et al., 2014). Considering our results, BIK may contribute to the generation of HML tumors. Both HML and BIK high tumors are associated with poor outcomes, and it would be interesting to determine if the HML tumors in the Haricharan study showed significantly elevated BIK protein. If so, this would suggest that some HML cancers are caused by BIK-mediated failed apoptosis. I also speculate that BIK mediated DNA damage can create mutations in the DNA damage response (DDR) genes, facilitating the generation of a subset of HML tumors found to have defective DNA damage response (Haricharan et al., 2014) and hence, are predisposed to a high level of genomic instability. Thus, BIK mediated failed apoptosis may act as an endogenous mutagenic process in the ER-positive cancers and may partly explain the genesis of HML tumors with poor patient outcomes.

6.5 CAD-induced double-strand DNA breaks and their repair

I demonstrated that BIK expression induces caspase and CAD dependent DSBs. Activated CAD homodimers assemble on dsDNA at the inter-nucleosomal positions and a coordinated nucleophilic attack from both active sites induces a DSB (Larsen and Sorensen, 2017; Widlak et al., 2000). Whether CAD-induced DSBs recruit the canonical DNA repair machinery is not yet clear. Typically, when cells encounter DSBs caused due to ionizing radiation or collapsed replication forks, HR related kinases ataxia telangiectasia mutated (ATM) and ataxia telangiectasia and Rad3 related (ATR) or NHEJ related kinase DNA-dependent protein kinase catalytic subunit (DNA-PKcs) phosphorylate histone 2AX (H2AX) molecules in the vicinity of the DSB on the Ser139 residue (Ceccaldi et al., 2016; Chapman et al., 2012; Ciccia and Elledge, 2010). This phosphorylation is often referred to as γH2AX and marks the site of the damage to facilitate the recruitment of DNA repair factors

(Ceccaldi et al., 2016; Chapman et al., 2012). As well, upon detection of the DNA damage, ATM/ATR–CHK1/CHK2-p53 axis activates a checkpoint that halts cell cycle progression while the repair is in progress (Maréchal and Zou, 2013). If the damage is not resolved, prolonged cell cycle arrest leads to apoptosis. Thus this mechanism safeguards the genomic integrity by prohibiting the transfer of broken or aberrant chromosomes to the daughter cells. Defects in this machinery allow passing of abnormal genetic material to daughter cells, posing a risk of cancer. Interestingly, one study showed that γH2AX phosphorylation of CAD-induced DSBs was not dependent on the ATM/ATR kinases but instead occurred through c-Jun N-terminal kinase (JNK) (Ichim et al., 2015). Interestingly, while JNK mediates γH2AX phosphorylation, it does not have an extensively reported role in the DSB repair. In the Ichim study, whether CAD induced DSBs are actually repaired or not was not addressed (Ichim et al., 2015). However, if there was no repair, cells would die due to extensive DNA damage. On the other hand, in the presence of low-levels of repair, cells may be able to survive although with genomic mutations. A second study interrogated CAD induced DNA damage using a specially engineered expression system wherein CAD activation was achieved without the prior activation of caspases, which allowed the authors to study DNA damaging effects of CAD in isolation (Morgan et al., 2015). Interestingly, isolated CAD activation in the presence of pharmacological inhibitors of ATM and DNA-PKcs led to an increase in the γH2AX intensity. This finding verified that γH2AX phosphorylation of CAD-induced DBSs could occur through other kinases such as JNK. Furthermore, it suggested that CAD-induced DSBs were likely undergoing repair through HR and NHEJ as their inhibition promoted accumulation of further damage marked by

γH2AX. However, a direct assessment of DNA damage such as the one using comet assay was not done, adding some uncertainty with respect to DNA repair. Thus, CAD mediated damage can be repaired in principle, although the individual contributions of HR and NHEJ are not known. One major caveat to these findings that utilized a direct CAD activation is that critical players of DNA damage response pathways including ATM, poly-ADP ribose polymerase (PARP), RAD51 and DNA-PKcs are known substrates of activated caspases (Morgan et al., 2015). Hence, in the context of apoptosis, the repair of CAD-induced DSBs, if it occurs, may be determined by the extent of caspase activation. As well, the caspase substrate specificity may control which repair components are cleaved, thus dictating the choice of the repair pathway. In light of our study, where BIK mediated DNA damage occurs through CAD in the presence of active caspases, it can be theorized that in this scenario the DNA repair remains poor, leading to unstable genomes in the progeny. Our observation that prolonged BIK expression leads to persistent DNA damage and aggressive progeny supports this idea. In the context of breast tumors, recently a large study (n=95561) found that 7% of the unselected patients had mutations in one of the 8 genes involved in HR (*BRCA1*, *BRCA2*, *BARD1*, *CHEK2*, *PALB2*, *PTEN*, *TP53,* and *ATM*) (Kurian et al., 2017). Of all the *BRCA1/2* mutated cases, 10-15% are ER-positive cancers (Lips et al., 2016; Tung et al., 2010). In such tumors, BIK-caspase-CAD mediated damage might lead to severe DNA repair defects leading to the generation of mutations that facilitate tumor evolution. Interestingly, patients with *BRCA2* mutated ER-positive cancers have a worse prognosis than ER-negative cancers (Jonasson et al., 2016). Altogether, BIK mediated DNA

damage coupled with DNA repair deficiency could aggravate mutagenesis and potentially contribute to tumor evolution.

I demonstrated that tamoxifen-mediated BIK upregulation in ER-positive cancer cells leads to DNA damage. Based on this observation, I predict that specific endocrine agents (aromatase inhibitors, tamoxifen or fulvestrant), when used to treat ER-positive tumors, would serve as both BIK inducers and selection agents. Tamoxifen acts by blocking estrogen signaling whereas fulvestrant acts by degrading the estrogen receptor. With such treatments, random mutations generated through the BIK-caspase-CAD axis that confer resistance to endocrine agents may get selected upon therapy. These may include estrogen-independent, constitutively active variants of the estrogen receptor selected by tamoxifen treatment whereas degradation resistant mutants selected by fulvestrant treatment. Tumor cells with such mutations would grow in an estrogen-independent manner and acquire resistance to anti-estrogens. Interestingly, in the primary ER-positive tumors, mutations in the estrogen receptor gene (*ESR1*) are rare (~1% of the tumors) (Fan et al., 2015). However, post-treatment metastatic tumors contain significantly more mutations (11-55%) in the *ESR1* gene (Jeselsohn et al., 2014; Li et al., 2013; Robinson et al., 2013). Additionally, aberrations in other critical regulatory pathways are also implicated in tamoxifen resistance. For instance, amplifications of *ERBB2* (Arpino et al., 2004), *Cyclin D1* (Butt et al., 2005) and *MYC* (Deming et al., 2000) are found in tamoxifen-resistant breast cancer and are associated with poor patient prognosis. These clinical findings support the paradigm that mutagenic pathways such as BIK-caspase-CAD axis activated during the hormonal therapy may partially contribute to these alterations. I anticipate that BIK- high

ER-positive refractory tumors would show enrichment of such mutations that provide growth advantage in response to specific endocrine treatment.

6.6 Harnessing the mutagenic potential of BIK upregulation in immunotherapy

I demonstrated that tamoxifen-induced BIK expression generates DNA double-strand breaks in breast cancer cells. Resulting mutations in the gene coding regions may give rise to abnormal splice variants as well as deleted or truncated forms of proteins. Their proteasomal processing and association with the major histocompatibility complex (MHC-I) would display the neoantigens on the cell surface. Thus, BIK-high endocrine treated patients may likely have tumors that are more immunogenic.

Breast cancer shows an interesting relationship with the immune response. The overall mutational burden in breast cancer has been found to be low compared to sun-exposure associated melanoma (Mar et al., 2013) or smoking-associated lung cancers (Vonderheide et al., 2017). Interestingly, however, nearly 70% of the breast cancers show lymphocytic invasion, which is associated with improved survival outcomes, suggesting a good immune response in the face of developing cancer (Pusztai et al., 2016). This presents an attractive therapeutic opportunity. Advancing breast cancer immunotherapy has been a high priority due to its demonstrated effectiveness in other malignancies such as lung and bladder cancers as well as melanoma (Vonderheide et al., 2017). Efforts to harness this potential for breast cancer immunotherapy mainly utilize three approaches (i) immune checkpoint inhibitors, (ii) adoptive cell transfer and (iii) therapeutic vaccines. The basis of immune checkpoint inhibitor treatment is programmed cell death protein 1 (PD-1) found on the surface of T-cells (Dine et al., 2017). A ligand of PD-1 called PD-L1 is found on

normal and cancer cells. The interaction between PD1-PD-L1 acts as an “off switch” that downregulates T-cell mediated immune response, preventing autoimmunity. Cancer cells exploit this mechanism by expressing PD-L1 on their surface, which prevents their recognition and facilitates immune evasion. Immune checkpoint inhibitors such as anti-PD-1 or anti-PD-L1 antibodies such as pembrolizumab and nivolumab work by preventing recognition of cancer cells as “self”, which reinvigorates the T-cell immune response against neoantigens (Vonderheide et al., 2017). These inhibitors are now FDA approved for use in melanoma, lung and bladder cancers and show excellent prognosis for advanced disease (Vonderheide et al., 2017). Interestingly, in unselected breast cancer cohorts, only 20% of the tumors have >1% cells expressing PD-L1. On the other hand, in non-small cell lung cancers more than 55% of the tumors show >5% cells expressing PD-L1 (Vonderheide et al., 2017; Yu et al., 2016), which might explain the relative ineffectiveness of immune-checkpoint inhibitors in breast cancer. This suggests a need to identify specific subsets of breast tumors that might have high levels of PD-L1 expression accompanied by a high mutational load. Anti-PD-L1 immunotherapy in these patients may suppress recognition of cancer cells as “self” hence promoting tumor regression. Intriguingly, PD-L1 expression is upregulated in response to DSBs and correlates with γH2AX levels in cancer cell lines and primary tumors (Osoegawa et al., 2018; Sato et al., 2017). I demonstrated that tamoxifen mediated BIK upregulation generated double-strand breaks, which may give rise to neoantigens. Thus, BIK high tamoxifen-treated patients are likely to have high PD-L1 expression along with elevated neoantigen presentation, making them an ideal subset for immune checkpoint inhibitor therapy.

Which neoantigens are produced by failed apoptosis is not currently known. However, it is likely that BIK mediated, genomic damage may produce a specific signature of neoantigens. Immuno-profiling of these neoantigens might identify a pattern unique to the tamoxifen-treated BIK-high tumors. These findings may aid in the efforts to develop therapeutic vaccines or adoptive cell transfer therapy (e.g., CAR T-cell therapy) for this subset of breast cancer patients.

6.7 Alternative mechanisms of BIK induced cancer aggression

I demonstrated that continued BIK expression for 10 passages produced aggressive progeny, which could be attributed to DNA damage mediated cancer cell evolution. Other studies that described failed apoptosis also implicated DNA damage as the driver of cellular transformation and carcinogenesis (Ichim et al., 2015; Liu et al., 2015). Apoptosis can cause cell aggression through other routes as well. Recently anastasis was described as a process by which cells that are on the brink of death manage to survive and proliferate (Tang et al., 2012). Interestingly, it was demonstrated that cells transiently exposed to apoptotic stimuli showed typical morphological features of apoptosis but upon recovery in fresh medium, reattached, proliferated and showed an elevated migratory phenotype (Sun et al., 2017). Initial findings suggested that new transcription was required for the apoptosis reversal as actinomycin D mediated blockade of transcription before recovery led to irreversible cell death (Tang et al., 2012). In a subsequent study, using RNAseq analysis performed at different stages of post-treatment recovery, it was discovered that two distinct groups of genes were upregulated (i.e., early vs. late response genes). Transcript and protein levels of some of the early response genes (*EGR1*, *c-FOS*, *SNAIL*, *c-JUN*) were elevated (Sun et al.,

2017). Of these, c-Jun and c-Fos form a heterodimeric activator protein (AP-1) complex that binds to AP-1 specific sites in the genome and upregulates transcription of genes associated with proliferation, survival, hypoxia, and angiogenesis (Mechta-Grigoriou et al., 2001). As well, their role in a variety of cancers has been defined as proto-oncogenic (Piechaczyk and Blanchard, 1994). Thus, c-Jun/Fos upregulation upon recovery from apoptosis suggested that cells were undergoing a survival response. Furthermore, Sun et al. found that activated TGF-β signaling, and Snail induction promoted cell migration, implying an epithelial to mesenchymal transition (EMT) after recovery from apoptosis (Sun et al., 2017). Considering our study, in certain situations, BIK up- and downregulations (e.g., between two doses of anti-estrogens) may lead to a cycle of apoptotic activation followed by recovery, creating an anastasis-like scenario. In that case, activation of survival and migratory genes may confer a survival advantage and the ability to migrate towards nutrient and oxygen-rich sites resulting in increased metastasis.

Another possible mechanism whereby BIK may contribute to cancer relapse is through the enrichment of the cancer stem cell (CSC) pool. This explanation is supported by our observation that long-term expression of BIK leads to an increase in the number of mammospheres. CSCs are tumor maintaining cells (Beck and Blanpain, 2013). They undergo asymmetric cell division to generate a self-renewing stem cell and a progenitor differentiating cell that populates the bulk of the tumor (Beck and Blanpain, 2013). Since CSCs rarely divide, they are resistant to conventional chemotherapies that depend on cell division (Vitale et al., 2017). As well, they have a better ability to repair DNA damage and resist cell death as demonstrated in glioblastoma and lung cancer models (Vitale et al.,

2017). CSCs also avoid cell death by upregulating BCL-2 family proteins (Ito et al., 2004; Vitale et al., 2017). Clinically, CSC enrichment has been associated with therapeutic resistance and refractory disease (Chang, 2016). Conceivably, BIK mediated CSC enrichment might explain the high rate of disease relapse in BIK-high patients. I hypothesize that CSC enrichment upon BIK elevation may occur through three distinct mechanisms. Firstly, CSCs may repair BIK mediated DNA damage promptly and survive better than the progenitors or differentiated cells. This may lead to enhanced survival of CSCs over time and promote their enrichment in the population. Secondly, BIK mediated DNA damage may change the mutational landscape and transcriptome of the differentiated cells such that they revert to CSCs. An example of such a scenario is available. In an injury-induced repopulation model of hair plucking, it was described that extraction of the stem cell-rich hair root stimulates reversion of the surrounding progenitors to stem cells resulting in hair regrowth (Beck and Blanpain, 2013; Ito et al., 2004). Thirdly, BIK mediated DNA damage may stimulate self-renewal of quiescent CSCs leading to an increase in their proportion. Interestingly, tamoxifen pre-treatment of MCF-7 cells or M05 (spontaneously derived ER-positive, tamoxifen sensitive mouse tumor) tumors resulted in increased mammosphere forming potential of the progeny, although a mechanistic explanation for this observation was not proposed (Raffo et al., 2013). Tamoxifen-induced BIK upregulation and enhancement of stem cell pool may provide a possible explanation for this observation. In the context of our study, it is possible that BIK-high tamoxifen treated tumors may have a higher stem cell representation resulting in increased capacity for heterogeneity and development of treatment resistance. Future studies will likely

explore the effects of failed apoptosis on stem-like enrichment in tumors and its consequences.

While so far, I have focused on the cell-autonomous effects of BIK activity in tumor cell evolution, apoptosis can also be tumor promoting in a cell-extrinsic manner. One such mechanism is termed apoptosis-induced proliferation (AiP) where dying cells secret mitogens that stimulate proliferation of the neighboring cells (Soteriou and Fuchs, 2018). AiP is extensively studied in Drosophila where it was demonstrated that in the wing imaginal disk, selective activation of initiator caspases in the presence of executioner caspase inhibitor p35, created an "undead" state of cells. These cells activate JNK in a Dronc (caspase-9 orthologue) dependent manner followed by phosphorylation of transcription factors c-Jun and c-Fos. These transcription factors stimulated the transcription of mitogens such as orthologues of WNT, BMP2 and EGF (Fogarty et al., 2016; Kondo et al., 2006; Soteriou and Fuchs, 2018). These mitogen-activated signaling pathways induced excessive growth of the surrounding tissues possibly by activating the quiescent stem cells in a JNK-dependent manner. Interestingly, DNA damage induced by sublethal doses of the BH3 mimetic ABT-737 also activated JNK (Ichim et al., 2015). In a similar fashion, BIK mediated apoptotic activation may also activate JNK followed by the phosphorylation of c-Jun and c-Fos, leading to the secretion of mitogens that induce proliferation in the surrounding tumor tissue. In support of this, we observed an increase in the number of mammospheres formed by BIK-LTC-250 cells, which indicates an enrichment of stem-like cells in the population. It is possible that secretion of the mitogens that stimulate quiescent stem-cells during long-term BIK expression may have led to this

enrichment. Another possible mode through which this could occur is by a hormone-like lipid compound called prostaglandin E2 (PGE2). It is known to stimulate stem cell proliferation and tissue regeneration (Soteriou and Fuchs, 2018). Interestingly, caspases activated during apoptosis cleave and activate calcium-independent phospholipase A2 (iPLA2), leading to an increased production of arachidonic acid, which is converted to PGE2 via cyclooxygenase 1 (COX1) and COX2. Specifically, in cancer, the effect of PGE2 was shown in a coculture model of lethally irradiated cells mixed with normal cells. Indeed, the presence of dying cells fueled the growth of surrounding cells in culture and in the mouse xenograft models, which was attributed to the caspase-dependent secretion of PGE2 (Huang et al., 2011). The significance of this observation in the context of failed apoptosis lies in the demonstration by Liu et al. where they found that caspase-3 and caspase-7 deficient mice had a reduced potential to develop skin cancers when exposed to known skin-carcinogens (Liu et al., 2015). This finding potentially suggested that diminished PGE2 secretion may have prevented activation of quiescent stem cells and tumor formation. Collectively, these studies highlighted multifaceted ramifications of apoptosis in the context of tumor formation and how BIK might be linked to it.

Our study provided *in vitro* evidence that BIK expression induced failed apoptosis, increased the clonogenic potential of cells, produced more soft-agar colonies and conferred a high mammosphere forming efficiency. High levels of BIK also predicted poor patient outcomes but did not generate larger tumors in mice. It is plausible that in BIK-high breast cancer tumors multiple factors such as genomic instability, elevated survival signaling,

apoptosis induced proliferation and the enrichment of stem cell pool may occur in concert, which may contribute to the overall tumor aggression.

6.8 Concluding remarks

Prior to this thesis, the role of BH3-only proteins in breast cancer pathology was not clear. Since BH3-only proteins induce apoptosis, it was presumed that their high levels in cancer would be associated with good patient prognosis. In chapter 3, we discovered that although BIK is a pro-apoptotic protein, it is associated with worse prognosis of breast cancer patients. This unexpected result indicated that BIK-mediated cell death did not eliminate tumors and instead was associated with disease progression. Whether BIK actively drove this outcome was unknown. To explore this, I investigated whether BIK-mediated autophagy increased cancer cell aggressiveness and while not definitive, results presented in chapter 4 did not strongly support this conclusion. Another critical observation originating from this thesis is that high levels of anti-apoptotic BCL-2, BCL-XL and MCL-1 predict good patient prognosis. While the favorable association of high BCL-2 levels has been previously reported, no molecular explanation was available. Regardless, this observation is contrary to the idea that increased apoptosis would limit disease progression. I directly addressed the question of apoptosis and cancer cell aggressiveness in chapter 5. The results indicated that apoptosis can be tumor promoting and that hence anti-apoptotic signaling might have a favorable impact on patient prognosis.

BIK is induced by endocrine therapy, and therefore I focused on this implication in chapter 5. Strikingly, high-levels of BIK predicted poor prognosis only in the endocrine

treated ER-positive patients but not in the alternatively treated ER-negative group. I showed that BIK upregulation in cells activated caspases, which surprisingly did not result in extensive cell death. Instead, caspase activation promoted DNA double-strand breaks through caspase-activated DNase. Further, continued BIK expression promoted cancer stem cell enrichment along with other aggressive phenotypes. Importantly, BIK induced by tamoxifen treatment also caused DNA damage. I propose that this DNA damage may lead to mutations in genes such as *ESR1*, followed by clonal selection with therapy, which may cause tamoxifen-resistant tumors. Moreover, enrichment of the cancer stem cell pool after the first round of therapy may increase the tumor's potential to recur. This may in part explain the worse prognosis of BIK-high ER-positive patients seen in our patient cohort.

Altogether, in this thesis, I discovered that the pro-apoptotic protein BIK serves as a biomarker of unfavorable outcomes in breast cancer. Further, elevated anti-apoptotic signaling was associated with favorable outcomes, together suggesting that apoptosis may have tumor-promoting effects. Furthermore, with the premise of anti-estrogen mediated upregulation of BIK, we identified that BIK elevation only in the ER-positive tumors predicts a worse prognosis. Subsequent elucidation of a potential tumor-promoting mechanism showed that BIK might promote failed apoptosis upon endocrine therapy, which through DNA damage and cancer-stem-cell enrichment may lead to poor patient outcomes of the BIK-high ER-positive patients.

References

Albeck, J.G., Burke, J.M., Aldridge, B.B., Zhang, M., Lauffenburger, D.A., and Sorger, P.K. (2008). Quantitative analysis of pathways controlling extrinsic apoptosis in single cells. Mol Cell *30*, 11-25.

Anagnostou, V.K., Lowery, F.J., Zolota, V., Tzelepi, V., Gopinath, A., Liceaga, C., Panagopoulos, N., Frangia, K., Tanoue, L., Boffa, D.*, et al.* (2010). High expression of BCL-2 predicts favorable outcome in non-small cell lung cancer patients with non squamous histology. BMC Cancer *10*, 186.

Arama, E., Agapite, J., and Steller, H. (2003). Caspase activity and a specific cytochrome C are required for sperm differentiation in Drosophila. Developmental cell *4*, 687-697.

Arpino, G., Green, S.J., Allred, D.C., Lew, D., Martino, S., Osborne, C.K., and Elledge, R.M. (2004). HER-2 amplification, HER-1 expression, and tamoxifen response in estrogen receptor-positive metastatic breast cancer: a southwest oncology group study. Clin Cancer Res *10*, 5670-5676.

Bairey, O., Zimra, Y., Shaklai, M., Okon, E., and Rabizadeh, E. (1999). Bcl-2, Bcl-X, Bax, and Bak Expression in Short- and Long-Lived Patients with Diffuse Large B-Cell Lymphomas. Clinical Cancer Research *5*, 2860-2866.

Beck, B., and Blanpain, C. (2013). Unravelling cancer stem cell potential. Nat Rev Cancer *13*, 727-738.

Berardo, M.D., Elledge, R.M., de Moor, C., Clark, G.M., Osborne, C.K., and Allred, D.C. (1998). bcl-2 and apoptosis in lymph node positive breast carcinoma. Cancer *82*, 1296-1302.

Bodet, L., Menoret, E., Descamps, G., Pellat-Deceunynck, C., Bataille, R., Le Gouill, S., Moreau, P., Amiot, M., and Gomez-Bougie, P. (2010). BH3-only protein Bik is involved in both apoptosis induction and sensitivity to oxidative stress in multiple myeloma. Br J Cancer *103*, 1808-1814.

Branzei, D., and Foiani, M. (2008). Regulation of DNA repair throughout the cell cycle. Nat Rev Mol Cell Biol *9*, 297-308.

Breastcancer.org (2018). Oncotype DX Test (Breastcancer.org).

Butt, A.J., McNeil, C.M., Musgrove, E.A., and Sutherland, R.L. (2005). Downstream targets of growth factor and oestrogen signalling and endocrine resistance: the potential roles of c-Myc, cyclin D1 and cyclin E. Endocr Relat Cancer *12 Suppl 1*, S47-59.

Ceccaldi, R., Rondinelli, B., and D'Andrea, A.D. (2016). Repair Pathway Choices and Consequences at the Double-Strand Break. Trends Cell Biol *26*, 52-64.

Chang, J.C. (2016). Cancer stem cells: Role in tumor growth, recurrence, metastasis, and treatment resistance. Medicine (Baltimore) *95*, S20-25.

Chapman, J.R., Taylor, M.R., and Boulton, S.J. (2012). Playing the end game: DNA double-strand break repair pathway choice. Mol Cell *47*, 497-510.

Chen, S., Zhou, L., Zhang, Y., Leng, Y., Pei, X.Y., Lin, H., Jones, R., Orlowski, R.Z., Dai, Y., and Grant, S. (2014). Targeting SQSTM1/p62 induces cargo loading failure and converts autophagy to apoptosis via NBK/Bik. Mol Cell Biol *34*, 3435-3449.

Chinnadurai, G., Vijayalingam, S., and Rashmi, R. (2008). BIK, the founding member of the BH3-only family proteins: mechanisms of cell death and role in cancer and pathogenic processes. Oncogene *27 Suppl 1*, S20-29.

Ciccia, A., and Elledge, S.J. (2010). The DNA damage response: making it safe to play with knives. Mol Cell *40*, 179-204.

Dawson, S.J., Makretsov, N., Blows, F.M., Driver, K.E., Provenzano, E., Le Quesne, J., Baglietto, L., Severi, G., Giles, G.G., McLean, C.A.*, et al.* (2010). BCL2 in breast cancer: a favourable prognostic marker across molecular subtypes and independent of adjuvant therapy received. Br J Cancer *103*, 668-675.

Deming, S.L., Nass, S.J., Dickson, R.B., and Trock, B.J. (2000). C-myc amplification in breast cancer: a meta-analysis of its occurrence and prognostic relevance. Br J Cancer *83*, 1688-1695.

Dine, J., Gordon, R., Shames, Y., Kasler, M.K., and Barton-Burke, M. (2017). Immune Checkpoint Inhibitors: An Innovation in Immunotherapy for the Treatment and Management of Patients with Cancer. Asia-Pacific Journal of Oncology Nursing *4*, 127-135.

Fan, W., Chang, J., and Fu, P. (2015). Endocrine therapy resistance in breast cancer: current status, possible mechanisms and overcoming strategies. Future Medicinal Chemistry *7*, 1511-1519.

Fogarty, Caitlin E., Diwanji, N., Lindblad, Jillian L., Tare, M., Amcheslavsky, A., Makhijani, K., Brückner, K., Fan, Y., and Bergmann, A. (2016). Extracellular Reactive Oxygen Species Drive Apoptosis-Induced Proliferation via Drosophila Macrophages. Current Biology *26*, 575-584.

Gothwal, S.K., Patel, N.J., Colletti, M.M., Sasanuma, H., Shinohara, M., Hochwagen, A., and Shinohara, A. (2016). The Double-Strand Break Landscape of Meiotic Chromosomes Is Shaped by the Paf1 Transcription Elongation Complex in Saccharomyces cerevisiae. Genetics *202*, 497-512.

Haricharan, S., Bainbridge, M.N., Scheet, P., and Brown, P.H. (2014). Somatic mutation load of estrogen receptor-positive breast tumors predicts overall survival: an analysis of genome sequence data. Breast Cancer Res Treat *146*, 211-220.

Huang, Q., Li, F., Liu, X., Li, W., Shi, W., Liu, F.F., O'Sullivan, B., He, Z., Peng, Y., Tan, A.C.*, et al.* (2011). Caspase 3-mediated stimulation of tumor cell repopulation during cancer radiotherapy. Nat Med *17*, 860-866.

Hur, J., Bell, D.W., Dean, K.L., Coser, K.R., Hilario, P.C., Okimoto, R.A., Tobey, E.M., Smith, S.L., Isselbacher, K.J., and Shioda, T. (2006). Regulation of expression of BIK proapoptotic protein in human breast cancer cells: p53-dependent induction of BIK mRNA by fulvestrant and proteasomal degradation of BIK protein. Cancer Res *66*, 10153-10161.

Hur, J., Chesnes, J., Coser, K.R., Lee, R.S., Geck, P., Isselbacher, K.J., and Shioda, T. (2004). The Bik BH3-only protein is induced in estrogen-starved and antiestrogen-exposed breast cancer cells and provokes apoptosis. Proc Natl Acad Sci U S A *101*, 2351-2356.

Ichim, G., Lopez, J., Ahmed, S.U., Muthalagu, N., Giampazolias, E., Delgado, M.E., Haller, M., Riley, J.S., Mason, S.M., Athineos, D.*, et al.* (2015). Limited mitochondrial

permeabilization causes DNA damage and genomic instability in the absence of cell death. Mol Cell *57*, 860-872.

Ichim, G., and Tait, S.W. (2016). A fate worse than death: apoptosis as an oncogenic process. Nat Rev Cancer *16*, 539-548.

Ito, M., Kizawa, K., Hamada, K., and Cotsarelis, G. (2004). Hair follicle stem cells in the lower bulge form the secondary germ, a biochemically distinct but functionally equivalent progenitor cell population, at the termination of catagen. Differentiation *72*, 548-557.

Jeselsohn, R., Yelensky, R., Buchwalter, G., Frampton, G., Meric-Bernstam, F., Gonzalez-Angulo, A.M., Ferrer-Lozano, J., Perez-Fidalgo, J.A., Cristofanilli, M., Gomez, H.*, et al.* (2014). Emergence of constitutively active estrogen receptor-alpha mutations in pretreated advanced estrogen receptor-positive breast cancer. Clin Cancer Res *20*, 1757-1767.

Jonasson, J.G., Stefansson, O.A., Johannsson, O.T., Sigurdsson, H., Agnarsson, B.A., Olafsdottir, G.H., Alexiusdottir, K.K., Stefansdottir, H., Munoz Mitev, R., Olafsdottir, K.*, et al.* (2016). Oestrogen receptor status, treatment and breast cancer prognosis in Icelandic BRCA2 mutation carriers. British Journal of Cancer *115*, 776-783.

Julien, O., and Wells, J.A. (2017). Caspases and their substrates. Cell Death And Differentiation *24*, 1380.

Kaparou, M., Choumerianou, D., Perdikogianni, C., Martimianaki, G., Kalmanti, M., and Stiakaki, E. (2013). Enhanced levels of the apoptotic BAX/BCL-2 ratio in children with acute lymphoblastic leukemia and high-risk features. Genet Mol Biol *36*, 7-11.

Kohler, T., Schill, C., Deininger, M.W., Krahl, R., Borchert, S., Hasenclever, D., Leiblein, S., Wagner, O., and Niederwieser, D. (2002). High Bad and Bax mRNA expression correlate with negative outcome in acute myeloid leukemia (AML). Leukemia *16*, 22-29.

Kondo, S., Senoo-Matsuda, N., Hiromi, Y., and Miura, M. (2006). DRONC coordinates cell death and compensatory proliferation. Mol Cell Biol *26*, 7258-7268.

Kuo, C.T., Zhu, S., Younger, S., Jan, L.Y., and Jan, Y.N. (2006). Identification of E2/E3 ubiquitinating enzymes and caspase activity regulating Drosophila sensory neuron dendrite pruning. Neuron *51*, 283-290.

Kurian, A.W., Hughes, E., Handorf, E.A., Gutin, A., Allen, B., Hartman, A.-R., and Hall, M.J. (2017). Breast and Ovarian Cancer Penetrance Estimates Derived From Germline Multiple-Gene Sequencing Results in Women. JCO Precision Oncology, 1-12.

Larsen, B.D., and Sorensen, C.S. (2017). The caspase-activated DNase: apoptosis and beyond. FEBS J *284*, 1160-1170.

Li, F., He, Z., Shen, J., Huang, Q., Li, W., Liu, X., He, Y., Wolf, F., and Li, C.Y. (2010). Apoptotic caspases regulate induction of iPSCs from human fibroblasts. Cell stem cell *7*, 508-520.

Li, S., Shen, D., Shao, J., Crowder, R., Liu, W., Prat, A., He, X., Liu, S., Hoog, J., Lu, C.*, et al.* (2013). Endocrine-therapy-resistant ESR1 variants revealed by genomic characterization of breast-cancer-derived xenografts. Cell Rep *4*, 1116-1130.

Lips, E.H., Debipersad, R., Scheerman, C.E., Mulder, L., Sonke, G.S., van der Kolk, L.E., Wesseling, J., Hogervorst, F.B.L., and Nederlof, P.M. (2016). BRCA1-mutated estrogen receptor positive breast cancer shows BRCAness, suggesting sensitivity to drugs targeting homologous recombination deficiency. Clinical Cancer Research.

Liu, X., He, Y., Li, F., Huang, Q., Kato, T.A., Hall, R.P., and Li, C.Y. (2015). Caspase-3 promotes genetic instability and carcinogenesis. Mol Cell *58*, 284-296.

Lopez, J., Hesling, C., Prudent, J., Popgeorgiev, N., Gadet, R., Mikaelian, I., Rimokh, R., Gillet, G., and Gonzalo, P. (2012). Src tyrosine kinase inhibits apoptosis through the Erk1/2- dependent degradation of the death accelerator Bik. Cell Death Differ *19*, 1459-1469.

Lovric, M.M., and Hawkins, C.J. (2010). TRAIL treatment provokes mutations in surviving cells. Oncogene *29*, 5048-5060.

Mar, V.J., Wong, S.Q., Li, J., Scolyer, R.A., McLean, C., Papenfuss, A.T., Tothill, R.W., Kakavand, H., Mann, G.J., Thompson, J.F.*, et al.* (2013). BRAF/NRAS wild-type melanomas have a high mutation load correlating with histologic and molecular signatures of UV damage. Clin Cancer Res *19*, 4589-4598.

Maréchal, A., and Zou, L. (2013). DNA Damage Sensing by the ATM and ATR Kinases. Cold Spring Harbor Perspectives in Biology *5*, a012716.

Marinkovi, #x, , M., #x, prung, M., Buljuba, #x, #x, , M., and Novak, I. (2018). Autophagy Modulation in Cancer: Current Knowledge on Action and Therapy. Oxidative Medicine and Cellular Longevity *2018*, 18.

Mathai, J.P., Germain, M., Marcellus, R.C., and Shore, G.C. (2002). Induction and endoplasmic reticulum location of BIK/NBK in response to apoptotic signaling by E1A and p53. Oncogene *21*, 2534-2544.

Mathew, R., Karantza-Wadsworth, V., and White, E. (2007). Role of autophagy in cancer. Nat Rev Cancer *7*, 961-967.

Maxfield, K.E., Taus, P.J., Corcoran, K., Wooten, J., Macion, J., Zhou, Y., Borromeo, M., Kollipara, R.K., Yan, J., Xie, Y.*, et al.* (2015). Comprehensive functional characterization of cancer-testis antigens defines obligate participation in multiple hallmarks of cancer. Nat Commun *6*, 8840.

Mebratu, Y.A., Dickey, B.F., Evans, C., and Tesfaigzi, Y. (2008). The BH3-only protein Bik/Blk/Nbk inhibits nuclear translocation of activated ERK1/2 to mediate IFNgamma-induced cell death. J Cell Biol *183*, 429-439.

Mechta-Grigoriou, F., Gerald, D., and Yaniv, M. (2001). The mammalian Jun proteins: redundancy and specificity. Oncogene *20*, 2378.

Mehta, A., and Haber, J.E. (2014). Sources of DNA Double-Strand Breaks and Models of Recombinational DNA Repair. Cold Spring Harbor Perspectives in Biology *6*, a016428.

Meterissian, S.H., Kontogiannea, M., Al-Sowaidi, M., Linjawi, A., Halwani, F., Jamison, B., and Edwardes, M. (2001). Bcl-2 is a useful prognostic marker in Dukes' B colon cancer. Ann Surg Oncol *8*, 533-537.

Morgan, C.W., Diaz, J.E., Zeitlin, S.G., Gray, D.C., and Wells, J.A. (2015). Engineered cellular gene-replacement platform for selective and inducible proteolytic profiling. Proc Natl Acad Sci U S A *112*, 8344-8349.

Neri, A., Marrelli, D., Roviello, F., DeMarco, G., Mariani, F., DeStefano, A., Megha, T., Caruso, S., Corso, G., Cioppa, T.*, et al.* (2006). Bcl-2 expression correlates with lymphovascular invasion and long-term prognosis in breast cancer. Breast Cancer Res Treat *99*, 77-83.

Nik-Zainal, S., Davies, H., Staaf, J., Ramakrishna, M., Glodzik, D., Zou, X., Martincorena, I., Alexandrov, L.B., Martin, S., Wedge, D.C.*, et al.* (2016). Landscape of somatic mutations in 560 breast cancer whole-genome sequences. Nature *534*, 47-54.

Osoegawa, A., Hiraishi, H., Hashimoto, T., Takumi, Y., Abe, M., Takeuchi, H., Miyawaki, M., Okamoto, T., and Sugio, K. (2018). The Positive Relationship Between gammaH2AX and PD-L1 Expression in Lung Squamous Cell Carcinoma. In Vivo *32*, 171-177.

Paik, S. (2007). Development and clinical utility of a 21-gene recurrence score prognostic assay in patients with early breast cancer treated with tamoxifen. Oncologist *12*, 631-635.

Pandya, V., Glubrecht, D., Vos, L., Hanson, J., Damaraju, S., Mackey, J., Hugh, J., and Goping, I.S. (2016). The pro-apoptotic paradox: the BH3-only protein Bcl-2 interacting killer (Bik) is prognostic for unfavorable outcomes in breast cancer. Oncotarget *7*, 33272-33285.

Piechaczyk, M., and Blanchard, J.M. (1994). c-fos proto-oncogene regulation and function. Crit Rev Oncol Hematol *17*, 93-131.

Prakash, R., Zhang, Y., Feng, W., and Jasin, M. (2015). Homologous recombination and human health: the roles of BRCA1, BRCA2 and associated proteins. Cold Spring Harbor perspectives in biology *7*, a016600 016610.011101/cshperspect.a016600.

Pusztai, L., Karn, T., Safonov, A., Abu-Khalaf, M.M., and Bianchini, G. (2016). New Strategies in Breast Cancer: Immunotherapy. Clin Cancer Res *22*, 2105-2110.

Raffo, D., Berardi, D.E., Pontiggia, O., Todaro, L., de Kier Joffe, E.B., and Simian, M. (2013). Tamoxifen selects for breast cancer cells with mammosphere forming capacity and increased growth rate. Breast Cancer Res Treat *142*, 537-548.

Reimer, D., Sadr, S., Wiedemair, A., Goebel, G., Concin, N., Hofstetter, G., Marth, C., and Zeimet, A.G. (2006). Expression of the E2F family of transcription factors and its clinical relevance in ovarian cancer. Ann N Y Acad Sci *1091*, 270-281.

Renouf, D.J., Wood-Baker, R., Ionescu, D.N., Leung, S., Masoudi, H., Gilks, C.B., and Laskin, J. (2009). BCL-2 Expression is Prognostic for Improved Survival in Non-small Cell Lung Cancer. Journal of Thoracic Oncology *4*, 486-491.

Robinson, D.R., Wu, Y.-M., Vats, P., Su, F., Lonigro, R.J., Cao, X., Kalyana-Sundaram, S., Wang, R., Ning, Y., Hodges, L.*, et al.* (2013). Activating ESR1 mutations in hormone-resistant metastatic breast cancer. Nature Genetics *45*, 1446.

Sato, H., Niimi, A., Yasuhara, T., Permata, T.B.M., Hagiwara, Y., Isono, M., Nuryadi, E., Sekine, R., Oike, T., Kakoti, S.*, et al.* (2017). DNA double-strand break repair pathway regulates PD-L1 expression in cancer cells. Nature Communications *8*, 1751.

Sordet, O., Rébé, C., Plenchette, S., Zermati, Y., Hermine, O., Vainchenker, W., Garrido, C., Solary, E., and Dubrez-Daloz, L. (2002). Specific involvement of caspases in the differentiation of monocytes into macrophages. Blood *100*, 4446-4453.

Soteriou, D., and Fuchs, Y. (2018). A matter of life and death: stem cell survival in tissue regeneration and tumour formation. Nat Rev Cancer *18*, 187-201.

Subramanian, T., Vijayalingam, S., Lomonosova, E., Zhao, L.J., and Chinnadurai, G. (2007). Evidence for involvement of BH3-only proapoptotic members in adenovirus-induced apoptosis. J Virol *81*, 10486-10495.

Sun, G., Guzman, E., Balasanyan, V., Conner, C.M., Wong, K., Zhou, H.R., Kosik, K.S., and Montell, D.J. (2017). A molecular signature for anastasis, recovery from the brink of apoptotic cell death. J Cell Biol *216*, 3355-3368.

Sung, E.S., Park, K.J., Choi, H.J., Kim, C.H., and Kim, Y.S. (2012). The proteasome inhibitor MG132 potentiates TRAIL receptor agonist-induced apoptosis by stabilizing tBid and Bik in human head and neck squamous cell carcinoma cells. Exp Cell Res *318*, 1564-1576.

Tang, H.L., Tang, H.M., Mak, K.H., Hu, S., Wang, S.S., Wong, K.M., Wong, C.S., Wu, H.Y., Law, H.T., Liu, K.*, et al.* (2012). Cell survival, DNA damage, and oncogenic transformation after a transient and reversible apoptotic response. Mol Biol Cell *23*, 2240-2252.

Tomita, M., Matsuzaki, Y., Edagawa, M., Shimizu, T., Hara, M., and Onitsuka, T. (2003). Prognostic significance of bcl-2 expression in resected pN2 non-small cell lung cancer. Eur J Surg Oncol *29*, 654-657.

Tung, N., Wang, Y., Collins, L.C., Kaplan, J., Li, H., Gelman, R., Comander, A.H., Gallagher, B., Fetten, K., Krag, K.*, et al.* (2010). Estrogen receptor positive breast cancers in BRCA1 mutation carriers: clinical risk factors and pathologic features. Breast Cancer Research : BCR *12*, R12-R12.

Vargas-Roig, L.M., Cuello-Carrion, F.D., Fernandez-Escobar, N., Daguerre, P., Leuzzi, M., Ibarra, J., Gago, F.E., Nadin, S.B., and Ciocca, D.R. (2008). Prognostic value of Bcl-2 in breast cancer patients treated with neoadjuvant anthracycline based chemotherapy. Mol Oncol *2*, 102-111.

Vitale, I., Manic, G., De Maria, R., Kroemer, G., and Galluzzi, L. (2017). DNA Damage in Stem Cells. Mol Cell *66*, 306-319.

Vonderheide, R.H., Domchek, S.M., and Clark, A.S. (2017). Immunotherapy for Breast Cancer: What Are We Missing? Clinical Cancer Research *23*, 2640-2646.

Watson, N.F., Madjd, Z., Scrimegour, D., Spendlove, I., Ellis, I.O., Scholefield, J.H., and Durrant, L.G. (2005). Evidence that the p53 negative / Bcl-2 positive phenotype is an independent indicator of good prognosis in colorectal cancer: a tissue microarray study of 460 patients. World journal of surgical oncology *3*, 47.

Widlak, P., Li, P., Wang, X., and Garrard, W.T. (2000). Cleavage preferences of the apoptotic endonuclease DFF40 (caspase-activated DNase or nuclease) on naked DNA and chromatin substrates. J Biol Chem *275*, 8226-8232.

Williams, D.W., Kondo, S., Krzyzanowska, A., Hiromi, Y., and Truman, J.W. (2006). Local caspase activity directs engulfment of dendrites during pruning. Nat Neurosci *9*, 1234-1236.

Xin, L., Liu, Y.H., Martin, T.A., and Jiang, W.G. (2017). The Era of Multigene Panels Comes? The Clinical Utility of Oncotype DX and MammaPrint. World J Oncol *8*, 34-40.

Yu, H., Boyle, T.A., Zhou, C., Rimm, D.L., and Hirsch, F.R. (2016). PD-L1 Expression in Lung Cancer. J Thorac Oncol *11*, 964-975.

Zaidi, M.R., and Merlino, G. (2011). The Two Faces of Interferon-γ in cancer. Clinical cancer research : an official journal of the American Association for Cancer Research *17*, 6118-6124.

Zámborszky, J., Szikriszt, B., Gervai, J.Z., Pipek, O., Póti, Á., Krzystanek, M., Ribli, D., Szalai-Gindl, J.M., Csabai, I., Szallasi, Z.*, et al.* (2016). Loss of BRCA1 or BRCA2 markedly increases the rate of base substitution mutagenesis and has distinct effects on genomic deletions. Oncogene *36*, 746.

Zhu, H., Guo, W., Zhang, L., Wu, S., Teraishi, F., Davis, J.J., Dong, F., and Fang, B. (2005a). Proteasome inhibitors-mediated TRAIL resensitization and Bik accumulation. Cancer Biol Ther *4*, 781-786.

Zhu, H., Zhang, L., Dong, F., Guo, W., Wu, S., Teraishi, F., Davis, J.J., Chiao, P.J., and Fang, B. (2005b). Bik/NBK accumulation correlates with apoptosis-induction by bortezomib (PS-341, Velcade) and other proteasome inhibitors. Oncogene *24*, 4993-4999.

BIBLIOGRAPHY

ACS (2016). The Global Burden of Cancer in Women. World Cancer Congress.

Adams, J.M., and Cory, S. (2007a). Bcl-2-regulated apoptosis: mechanism and therapeutic potential. Current opinion in immunology 19, 488-496.

Adams, J.M., and Cory, S. (2007b). The Bcl-2 apoptotic switch in cancer development and therapy. Oncogene 26, 1324-1337.

Ades, F., Tryfonidis, K., and Zardavas, D. (2017). The past and future of breast cancer treatment—from the papyrus to individualised treatment approaches. ecancermedicalscience 11, 746.

Aita, V.M., Liang, X.H., Murty, V.V., Pincus, D.L., Yu, W., Cayanis, E., Kalachikov, S., Gilliam, T.C., and Levine, B. (1999). Cloning and genomic organization of beclin 1, a candidate tumor suppressor gene on chromosome 17q21. Genomics 59, 59-65.

Albeck, J.G., Burke, J.M., Aldridge, B.B., Zhang, M., Lauffenburger, D.A., and Sorger, P.K. (2008). Quantitative analysis of pathways controlling extrinsic apoptosis in single cells. Molecular cell 30, 11-25.

Ali, S., Rasool, M., Chaoudhry, H., P, N.P., Jha, P., Hafiz, A., Mahfooz, M., Abdus Sami, G., Azhar Kamal, M., Bashir, S., et al. (2016). Molecular mechanisms and mode of tamoxifen resistance in breast cancer. Bioinformation 12, 135-139.

Althuis, M.D., Dozier, J.M., Anderson, W.F., Devesa, S.S., and Brinton, L.A. (2005). Global trends in breast cancer incidence and mortality 1973-1997. Int J Epidemiol 34, 405-412.

Altman, D.G. (1991). Practical statistics for medical research (London ;: Chapman and Hall).

Amaravadi, R.K., Yu, D., Lum, J.J., Bui, T., Christophorou, M.A., Evan, G.I., Thomas-Tikhonenko, A., and Thompson, C.B. (2007). Autophagy inhibition enhances therapy-induced apoptosis in a Myc-induced model of lymphoma. The Journal of clinical investigation 117, 326-336.

Amundson, S.A., Myers, T.G., Scudiero, D., Kitada, S., Reed, J.C., and Fornace, A.J., Jr. (2000). An informatics approach identifying markers of chemosensitivity in human cancer cell lines. Cancer Res 60, 6101-6110.

Anagnostou, V.K., Lowery, F.J., Zolota, V., Tzelepi, V., Gopinath, A., Liceaga, C., Panagopoulos, N., Frangia, K., Tanoue, L., Boffa, D., et al. (2010). High expression of BCL-2 predicts favorable outcome in non-small cell lung cancer patients with non squamous histology. BMC Cancer 10, 186.

Anthony J.F. Griffiths, U.o.B.C., Susan R. Wessler, U.o.C.R., Sean B. Carroll, H.H.M.I.U.o.W.-M., and John Doebley, U.o.W.-M. (2015). Introduction to genetic analysis (Eleventh edition. New York, NY : W.H. Freeman & Company, [2015] ©2015).

Arama, E., Agapite, J., and Steller, H. (2003). Caspase activity and a specific cytochrome C are required for sperm differentiation in Drosophila. Developmental cell 4, 687-697.

Armitage, P. (2002). Statistical methods in medical research, G. Berry, and J.N.S. Matthews, eds. (Oxford ;: Blackwell Scientific Publications).

Arpino, G., Green, S.J., Allred, D.C., Lew, D., Martino, S., Osborne, C.K., and Elledge, R.M. (2004). HER-2 amplification, HER-1 expression, and tamoxifen response in estrogen receptor-positive metastatic breast cancer: a southwest oncology group study. Clinical cancer research : an official journal of the American Association for Cancer Research 10, 5670-5676.

Aubrey, B.J., Kelly, G.L., Janic, A., Herold, M.J., and Strasser, A. (2018). How does p53 induce apoptosis and how does this relate to p53-mediated tumour suppression? Cell Death Differ 25, 104-113.

Axe, E.L., Walker, S.A., Manifava, M., Chandra, P., Roderick, H.L., Habermann, A., Griffiths, G., and Ktistakis, N.T. (2008). Autophagosome formation from membrane compartments enriched in phosphatidylinositol 3-phosphate and dynamically connected to the endoplasmic reticulum. The Journal of cell biology 182, 685-701.

Bacci, M., Giannoni, E., Fearns, A., Ribas, R., Gao, Q., Taddei, M.L., Pintus, G., Dowsett, M., Isacke, C.M., Martin, L.A., et al. (2016). miR-155 Drives Metabolic Reprogramming of ER+ Breast Cancer Cells Following Long-Term Estrogen Deprivation and Predicts Clinical Response to Aromatase Inhibitors. Cancer Res 76, 1615-1626.

Bairey, O., Zimra, Y., Shaklai, M., Okon, E., and Rabizadeh, E. (1999). Bcl-2, Bcl-X, Bax, and Bak Expression in Short- and Long-Lived Patients with Diffuse Large B-Cell Lymphomas. Clinical Cancer Research 5, 2860-2866.

Bakhshi, A., Jensen, J.P., Goldman, P., Wright, J.J., McBride, O.W., Epstein, A.L., and Korsmeyer, S.J. (1985). Cloning the chromosomal breakpoint of t(14;18) human lymphomas: clustering around JH on chromosome 14 and near a transcriptional unit on 18. Cell 41, 899-906.

Ballou, L.M., and Lin, R.Z. (2008). Rapamycin and mTOR kinase inhibitors. Journal of Chemical Biology 1, 27-36.

Barres, B.A., and Raff, M.C. (1999). Axonal control of oligodendrocyte development. The Journal of cell biology 147, 1123-1128.

Beck, B., and Blanpain, C. (2013). Unravelling cancer stem cell potential. Nat Rev Cancer 13, 727-738.

Berardo, M.D., Elledge, R.M., de Moor, C., Clark, G.M., Osborne, C.K., and Allred, D.C. (1998). bcl-2 and apoptosis in lymph node positive breast carcinoma. Cancer 82, 1296-1302.

Bergman, L., Beelen, M.L.R., Gallee, M.P.W., Hollema, H., Benraadt, J., and van Leeuwen, F.E. (2000). Risk and prognosis of endometrial cancer after tamoxifen for breast cancer. The Lancet 356, 881-887.

Bertheau, P., Lehmann-Che, J., Varna, M., Dumay, A., Poirot, B., Porcher, R., Turpin, E., Plassa, L.F., de Roquancourt, A., Bourstyn, E., et al. (2013). p53 in breast cancer subtypes and new insights into response to chemotherapy. Breast 22 Suppl 2, S27-29.

Bewick, V., Cheek, L., and Ball, J. (2004). Statistics review 12: survival analysis. Crit Care 8, 389-394.

Bieging, K.T., Mello, S.S., and Attardi, L.D. (2014). Unravelling mechanisms of p53-mediated tumour suppression. Nature Reviews Cancer 14, 359.

Billard, C. (2013). BH3 mimetics: status of the field and new developments. Mol Cancer Ther 12, 1691-1700.

Biswas, S., Shi, Q., Wernick, A., Aiello, A., and Zinkel, S.S. (2013). The loss of the BH3-only Bcl-2 family member Bid delays T-cell leukemogenesis in Atm-/- mice. Cell Death Differ 20, 869-877.

Bodet, L., Menoret, E., Descamps, G., Pellat-Deceunynck, C., Bataille, R., Le Gouill, S., Moreau, P., Amiot, M., and Gomez-Bougie, P. (2010). BH3-only protein Bik is involved in both apoptosis induction and sensitivity to oxidative stress in multiple myeloma. British Journal of Cancer 103, 1808-1814.

Borowicz, S., Van Scoyk, M., Avasarala, S., Karuppusamy Rathinam, M.K., Tauler, J., Bikkavilli, R.K., and Winn, R.A. (2014). The soft agar colony formation assay. J Vis Exp, e51998.

Bouillet, P., Metcalf, D., Huang, D.C., Tarlinton, D.M., Kay, T.W., Kontgen, F., Adams, J.M., and Strasser, A. (1999). Proapoptotic Bcl-2 relative Bim required for certain apoptotic responses, leukocyte homeostasis, and to preclude autoimmunity. Science (New York, NY) 286, 1735-1738.

Bowman, T., Symonds, H., Gu, L., Yin, C., Oren, M., and Van Dyke, T. (1996). Tissue-specific inactivation of p53 tumor suppression in the mouse. Genes & development 10, 826-835.

Boyd, J.M., Gallo, G.J., Elangovan, B., Houghton, A.B., Malstrom, S., Avery, B.J., Ebb, R.G., Subramanian, T., Chittenden, T., Lutz, R.J., et al. (1995). Bik, a novel death-inducing protein shares a distinct sequence motif with Bcl-2 family proteins and interacts with viral and cellular survival-promoting proteins. Oncogene 11, 1921-1928.

Bradbury, A.R., and Olopade, O.I. (2007). Genetic susceptibility to breast cancer. Rev Endocr Metab Disord 8, 255-267.

Branzei, D., and Foiani, M. (2008). Regulation of DNA repair throughout the cell cycle. Nature reviews Molecular cell biology 9, 297-308.

Bravo-Sagua, R., Rodriguez, A.E., Kuzmicic, J., Gutierrez, T., Lopez-Crisosto, C., Quiroga, C., Díaz-Elizondo, J., Chiong, M., Gillette, T.G., Rothermel, B.A., et al. (2013). Cell Death and Survival Through the Endoplasmic Reticulum-Mitochondrial Axis. Current molecular medicine 13, 317-329.

Breastcancer.org (2018). Oncotype DX Test (Breastcancer.org).

Broadinstitute.org (2018). BIK expression in cancer cell lines.

Butt, A.J., McNeil, C.M., Musgrove, E.A., and Sutherland, R.L. (2005). Downstream targets of growth factor and oestrogen signalling and endocrine resistance: the potential roles of c-Myc, cyclin D1 and cyclin E. Endocr Relat Cancer 12 Suppl 1, S47-59.

Capri, S., and Russo, A. (2017). Cost of breast cancer based on real-world data: a cancer registry study in Italy. BMC Health Serv Res 17, 84.

Carter, B.D., Freedman, N.D., and Jacobs, E.J. (2015). Smoking and mortality--beyond established causes. N Engl J Med 372, 2170.

Carthew, P., Martin, E.A., White, I.N., De Matteis, F., Edwards, R.E., Dorman, B.M., Heydon, R.T., and Smith, L.L. (1995). Tamoxifen induces short-term cumulative DNA damage and liver tumors in rats: promotion by phenobarbital. Cancer Res 55, 544-547.

Cartwright, I.M., Liu, X., Zhou, M., Li, F., and Li, C.Y. (2017). Essential roles of Caspase-3 in facilitating Myc-induced genetic instability and carcinogenesis. Elife 6.

Catalanotto, C., Cogoni, C., and Zardo, G. (2016). MicroRNA in Control of Gene Expression: An Overview of Nuclear Functions. Int J Mol Sci 17.

cBioPortal.org (2018). BIK alterations in cancer.

Ceccaldi, R., Rondinelli, B., and D'Andrea, A.D. (2016). Repair Pathway Choices and Consequences at the Double-Strand Break. Trends in cell biology 26, 52-64.

Chang, J.C. (2016). Cancer stem cells: Role in tumor growth, recurrence, metastasis, and treatment resistance. Medicine (Baltimore) 95, S20-25.

Chang, N.C., Nguyen, M., Germain, M., and Shore, G.C. (2010). Antagonism of Beclin 1-dependent autophagy by BCL-2 at the endoplasmic reticulum requires NAF-1. The EMBO Journal 29, 606-618.

Chapman, J.R., Taylor, M.R., and Boulton, S.J. (2012). Playing the end game: DNA double-strand break repair pathway choice. Molecular cell 47, 497-510.

Chen, M., He, H., Zhan, S., Krajewski, S., Reed, J.C., and Gottlieb, R.A. (2001). Bid is cleaved by calpain to an active fragment in vitro and during myocardial ischemia/reperfusion. The Journal of biological chemistry 276, 30724-30728.

Chen, S., Zhou, L., Zhang, Y., Leng, Y., Pei, X.Y., Lin, H., Jones, R., Orlowski, R.Z., Dai, Y., and Grant, S. (2014). Targeting SQSTM1/p62 induces cargo loading failure and converts autophagy to apoptosis via NBK/Bik. Mol Cell Biol 34, 3435-3449.

Chinnadurai, G., Vijayalingam, S., and Rashmi, R. (2008). BIK, the founding member of the BH3-only family proteins: mechanisms of cell death and role in cancer and pathogenic processes. Oncogene 27 Suppl 1, S20-29.

Chipuk, J.E., Moldoveanu, T., Llambi, F., Parsons, M.J., and Green, D.R. (2010). The BCL-2 Family Reunion. Molecular cell 37, 299-310.

Choi, Y.C., Yoon, S., Byun, Y., Lee, G., Kee, H., Jeong, Y., Yoon, J., and Baek, K. (2015). MicroRNA library screening identifies growth-suppressive microRNAs that regulate genes involved in cell cycle progression and apoptosis. Experimental cell research 339, 320-332.

Christensen, E. (1987). Multivariate survival analysis using Cox's regression model. Hepatology (Baltimore, Md) 7, 1346-1358.

Chu, D., Paoletti, C., Gersch, C., VanDenBerg, D.A., Zabransky, D.J., Cochran, R.L., Wong, H.Y., Toro, P.V., Cidado, J., Croessmann, S., et al. (2016). ESR1 Mutations in Circulating Plasma Tumor DNA from Metastatic Breast Cancer Patients. Clinical cancer research : an official journal of the American Association for Cancer Research 22, 993-999.

Ciccia, A., and Elledge, S.J. (2010). The DNA damage response: making it safe to play with knives. Molecular cell 40, 179-204.

Clarke, H.J., Chambers, J.E., Liniker, E., and Marciniak, S.J. (2014). Endoplasmic reticulum stress in malignancy. Cancer cell 25, 563-573.

Colditz, G.A., and Bohlke, K. (2014). Priorities for the primary prevention of breast cancer. CA Cancer J Clin 64, 186-194.

Coleman, M.L., Sahai, E.A., Yeo, M., Bosch, M., Dewar, A., and Olson, M.F. (2001). Membrane blebbing during apoptosis results from caspase-mediated activation of ROCK I. Nature cell biology 3, 339-345.

Coser, K.R., Wittner, B.S., Rosenthal, N.F., Collins, S.C., Melas, A., Smith, S.L., Mahoney, C.J., Shioda, K., Isselbacher, K.J., Ramaswamy, S., et al. (2009). Antiestrogen-resistant subclones of MCF-7 human breast cancer cells are derived from a common monoclonal drug-resistant progenitor. Proceedings of the National Academy of Sciences of the United States of America 106, 14536-14541.

Coultas, L., Bouillet, P., Loveland, K.L., Meachem, S., Perlman, H., Adams, J.M., and Strasser, A. (2005). Concomitant loss of proapoptotic BH3-only Bcl-2 antagonists Bik and Bim arrests spermatogenesis. The EMBO Journal 24, 3963-3973.

Coultas, L., Bouillet, P., Stanley, E.G., Brodnicki, T.C., Adams, J.M., and Strasser, A. (2004). Proapoptotic BH3-only Bcl-2 family member Bik/Blk/Nbk is expressed in hemopoietic and endothelial cells but is redundant for their programmed death. Mol Cell Biol 24, 1570-1581.

Craik, A.C., Veldhoen, R.A., Czernick, M., Buckland, T.W., Kyselytzia, K., Ghosh, S., Lai, R., Damaraju, S., Underhill, D.A., Mackey, J.R., et al. (2010). The BH3-only protein Bad confers breast cancer taxane sensitivity through a nonapoptotic mechanism. Oncogene 29, 5381-5391.

Creighton, C.J. (2012). The molecular profile of luminal B breast cancer. Biologics 6, 289-297.

Curtis, C. (2015). Genomic profiling of breast cancers. Current opinion in obstetrics & gynecology 27, 34-39.

Czabotar, P.E., Lessene, G., Strasser, A., and Adams, J.M. (2014). Control of apoptosis by the BCL-2 protein family: implications for physiology and therapy. Nature reviews Molecular cell biology 15, 49-63.

Daniel, P.T., Pun, K.T., Ritschel, S., Sturm, I., Holler, J., Dorken, B., and Brown, R. (1999). Expression of the death gene Bik/Nbk promotes sensitivity to drug-induced apoptosis in corticosteroid-resistant T-cell lymphoma and prevents tumor growth in severe combined immunodeficient mice. Blood 94, 1100-1107.

Das, G., Shravage, B.V., and Baehrecke, E.H. (2012). Regulation and function of autophagy during cell survival and cell death. Cold Spring Harbor perspectives in biology 4.

Datta, S.R., Dudek, H., Tao, X., Masters, S., Fu, H., Gotoh, Y., and Greenberg, M.E. (1997). Akt phosphorylation of BAD couples survival signals to the cell-intrinsic death machinery. Cell 91, 231-241.

Davies, C., Pan, H., Godwin, J., Gray, R., Arriagada, R., Raina, V., Abraham, M., Alencar, V.H.M., Badran, A., Bonfill, X., et al. (2013). Long-term effects of continuing adjuvant tamoxifen to 10 years versus stopping at 5 years after diagnosis of oestrogen receptor-positive breast cancer: ATLAS, a randomised trial. Lancet (London, England) 381, 805-816.

Dawson, S.J., Makretsov, N., Blows, F.M., Driver, K.E., Provenzano, E., Le Quesne, J., Baglietto, L., Severi, G., Giles, G.G., McLean, C.A., et al. (2010). BCL2 in breast cancer: a favourable prognostic marker across molecular subtypes and independent of adjuvant therapy received. British Journal of Cancer 103, 668-675.

Degenhardt, K., Mathew, R., Beaudoin, B., Bray, K., Anderson, D., Chen, G., Mukherjee, C., Shi, Y., Gelinas, C., Fan, Y., et al. (2006). Autophagy promotes tumor cell survival and restricts necrosis, inflammation, and tumorigenesis. Cancer cell 10, 51-64.

Delbridge, A.R., and Strasser, A. (2015). The BCL-2 protein family, BH3-mimetics and cancer therapy. Cell Death Differ 22, 1071-1080.

DeLong, E.R., DeLong, D.M., and Clarke-Pearson, D.L. (1988). Comparing the areas under two or more correlated receiver operating characteristic curves: a nonparametric approach. Biometrics 44, 837-845.

Deming, S.L., Nass, S.J., Dickson, R.B., and Trock, B.J. (2000). C-myc amplification in breast cancer: a meta-analysis of its occurrence and prognostic relevance. British Journal of Cancer 83, 1688-1695.

Dewson, G., and Kluck, R.M. (2009). Mechanisms by which Bak and Bax permeabilise mitochondria during apoptosis. Journal of Cell Science 122, 2801-2808.

Dijkers, P.F., Medema, R.H., Lammers, J.W., Koenderman, L., and Coffer, P.J. (2000). Expression of the pro-apoptotic Bcl-2 family member Bim is regulated by the forkhead transcription factor FKHR-L1. Current biology : CB 10, 1201-1204.

Dikic, I., and Elazar, Z. (2018). Mechanism and medical implications of mammalian autophagy. Nature Reviews Molecular Cell Biology 19, 349-364.

Dine, J., Gordon, R., Shames, Y., Kasler, M.K., and Barton-Burke, M. (2017). Immune Checkpoint Inhibitors: An Innovation in Immunotherapy for the Treatment and Management of Patients with Cancer. Asia-Pacific Journal of Oncology Nursing 4, 127-135.

Donehower, L.A. (1996). The p53-deficient mouse: a model for basic and applied cancer studies. Semin Cancer Biol 7, 269-278.

Dubrovska, A., Hartung, A., Bouchez, L.C., Walker, J.R., Reddy, V.A., Cho, C.Y., and Schultz, P.G. (2012). CXCR4 activation maintains a stem cell population in tamoxifen-resistant breast cancer cells through AhR signalling. British Journal of Cancer 107, 43-52.

Duroux-Richard, I., Roubert, C., Ammari, M., Presumey, J., Grun, J.R., Haupl, T., Grutzkau, A., Lecellier, C.H., Boitez, V., Codogno, P., et al. (2016). miR-125b controls monocyte adaptation to inflammation through mitochondrial metabolism and dynamics. Blood 128, 3125-3136.

Earnshaw, W.C., Martins, L.M., and Kaufmann, S.H. (1999). Mammalian caspases: structure, activation, substrates, and functions during apoptosis. Annu Rev Biochem 68, 383-424.

Egle, A., Harris, A.W., Bouillet, P., and Cory, S. (2004). Bim is a suppressor of Myc-induced mouse B cell leukemia. Proceedings of the National Academy of Sciences of the United States of America 101, 6164-6169.

Elangovan, B., and Chinnadurai, G. (1997). Functional dissection of the pro-apoptotic protein Bik. Heterodimerization with anti-apoptosis proteins is insufficient for induction of cell death. The Journal of biological chemistry 272, 24494-24498.

Eliopoulos, A.G., Havaki, S., and Gorgoulis, V.G. (2016). DNA Damage Response and Autophagy: A Meaningful Partnership. Frontiers in Genetics 7.

Ellis, H.M., and Horvitz, H.R. (1986). Genetic control of programmed cell death in the nematode C. elegans. Cell 44, 817-829.

Ellis, M.J., and Perou, C.M. (2013). The Genomic Landscape of Breast Cancer as a Therapeutic Roadmap. Cancer discovery 3, 27-34.

Ellis, R.E., Yuan, J.Y., and Horvitz, H.R. (1991). Mechanisms and functions of cell death. Annual review of cell biology 7, 663-698.

Enari, M., Sakahira, H., Yokoyama, H., Okawa, K., Iwamatsu, A., and Nagata, S. (1998). A caspase-activated DNase that degrades DNA during apoptosis, and its inhibitor ICAD. Nature 391, 43-50.

Erikson, J., ar-Rushdi, A., Drwinga, H.L., Nowell, P.C., and Croce, C.M. (1983). Transcriptional activation of the translocated c-myc oncogene in burkitt lymphoma. Proceedings of the National Academy of Sciences of the United States of America 80, 820-824.

Fan, W., Chang, J., and Fu, P. (2015). Endocrine therapy resistance in breast cancer: current status, possible mechanisms and overcoming strategies. Future Medicinal Chemistry 7, 1511-1519.

Fang, Y., Tan, J., and Zhang, Q. (2015). Signaling pathways and mechanisms of hypoxia-induced autophagy in the animal cells. Cell biology international 39, 891-898.

Ferlay, J., Soerjomataram, I., Dikshit, R., Eser, S., Mathers, C., Rebelo, M., Parkin, D.M., Forman, D., and Bray, F. (2015). Cancer incidence and mortality worldwide: sources, methods and major patterns in GLOBOCAN 2012. Int J Cancer 136, E359-386.

Fogarty, Caitlin E., Diwanji, N., Lindblad, Jillian L., Tare, M., Amcheslavsky, A., Makhijani, K., Brückner, K., Fan, Y., and Bergmann, A. (2016). Extracellular Reactive Oxygen Species Drive Apoptosis-Induced Proliferation via Drosophila Macrophages. Current Biology 26, 575-584.

Foulkes, W.D., Smith, I.E., and Reis-Filho, J.S. (2010). Triple-negative breast cancer. N Engl J Med 363, 1938-1948.

Friesen, C., Fulda, S., and Debatin, K.M. (1997). Deficient activation of the CD95 (APO-1/Fas) system in drug-resistant cells. Leukemia 11, 1833.

Fu, Y., Li, J., and Lee, A.S. (2007). GRP78/BiP inhibits endoplasmic reticulum BIK and protects human breast cancer cells against estrogen starvation-induced apoptosis. Cancer Res 67, 3734-3740.

Fuchs, Y., and Steller, H. (2011). Programmed cell death in animal development and disease. Cell 147, 742-758.

Fulda, S. (2009). Tumor resistance to apoptosis. Int J Cancer 124, 511-515.

Fulda, S., Los, M., Friesen, C., and Debatin, K.M. (1998). Chemosensitivity of solid tumor cells in vitro is related to activation of the CD95 system. Int J Cancer 76, 105-114.

Funderburk, S.F., Wang, Q.J., and Yue, Z. (2010). The Beclin 1-VPS34 complex--at the crossroads of autophagy and beyond. Trends in cell biology 20, 355-362.

Garcia, N., Salamanca, F., Astudillo-de la Vega, H., Curiel-Quesada, E., Alvarado, I., Penaloza, R., and Arenas, D. (2005). A molecular analysis by gene expression profiling reveals Bik/NBK overexpression in sporadic breast tumor samples of Mexican females. BMC Cancer 5, 93.

Gaub, M.-P., Bellard, M., Scheuer, I., Chambon, P., and Sassone-Corsi, P. (1990). Activation of the ovalbumin gene by the estrogen receptor involves the Fos-Jun complex. Cell 63, 1267-1276.

Gavathiotis, E., Suzuki, M., Davis, M.L., Pitter, K., Bird, G.H., Katz, S.G., Tu, H.C., Kim, H., Cheng, E.H., Tjandra, N., et al. (2008). BAX activation is initiated at a novel interaction site. Nature 455, 1076-1081.

Germain, D.R., Graham, K., Glubrecht, D.D., Hugh, J.C., Mackey, J.R., and Godbout, R. (2011). DEAD box 1: a novel and independent prognostic marker for early recurrence in breast cancer. Breast cancer research and treatment 127, 53-63.

Germain, M., Mathai, J.P., McBride, H.M., and Shore, G.C. (2005). Endoplasmic reticulum BIK initiates DRP1-regulated remodelling of mitochondrial cristae during apoptosis. The EMBO Journal 24, 1546-1556.

Germain, M., Mathai, J.P., and Shore, G.C. (2002). BH-3-only BIK functions at the endoplasmic reticulum to stimulate cytochrome c release from mitochondria. The Journal of biological chemistry 277, 18053-18060.

Gillissen, B., Essmann, F., Graupner, V., Starck, L., Radetzki, S., Dorken, B., Schulze-Osthoff, K., and Daniel, P.T. (2003). Induction of cell death by the BH3-only Bcl-2 homolog Nbk/Bik is mediated by an entirely Bax-dependent mitochondrial pathway. The EMBO Journal 22, 3580-3590.

Gillissen, B., Essmann, F., Hemmati, P.G., Richter, A., Richter, A., Oztop, I., Chinnadurai, G., Dorken, B., and Daniel, P.T. (2007). Mcl-1 determines the Bax dependency of Nbk/Bik-induced apoptosis. The Journal of cell biology 179, 701-715.

Goping, I.S., Gross, A., Lavoie, J.N., Nguyen, M., Jemmerson, R., Roth, K., Korsmeyer, S.J., and Shore, G.C. (1998). Regulated Targeting of BAX to Mitochondria. The Journal of cell biology 143, 207-215.

Gorlach, A., Bertram, K., Hudecova, S., and Krizanova, O. (2015). Calcium and ROS: A mutual interplay. Redox Biol 6, 260-271.

Gothwal, S.K., Patel, N.J., Colletti, M.M., Sasanuma, H., Shinohara, M., Hochwagen, A., and Shinohara, A. (2016). The Double-Strand Break Landscape of Meiotic Chromosomes Is Shaped by the Paf1 Transcription Elongation Complex in Saccharomyces cerevisiae. Genetics 202, 497-512.

Greaves, P., Goonetilleke, R., Nunn, G., Topham, J., and Orton, T. (1993). Two-year carcinogenicity study of tamoxifen in Alderley Park Wistar-derived rats. Cancer Res 53, 3919-3924.

Green, D.R. (2010). Means to an End: Apoptosis and Other Cell Death Mechanisms (Cold Spring Harbor Laboratory Press).

Grimshaw, M.J., Cooper, L., Papazisis, K., Coleman, J.A., Bohnenkamp, H.R., Chiapero-Stanke, L., Taylor-Papadimitriou, J., and Burchell, J.M. (2008). Mammosphere culture of metastatic breast cancer cells enriches for tumorigenic breast cancer cells. Breast Cancer Res 10, R52.

Guarneri, V., and Conte, P. (2009). Metastatic breast cancer: therapeutic options according to molecular subtypes and prior adjuvant therapy. Oncologist 14, 645-656.

Guest, S.K., Ribas, R., Pancholi, S., Nikitorowicz-Buniak, J., Simigdala, N., Dowsett, M., Johnston, S.R., and Martin, L.A. (2016). Src Is a Potential Therapeutic Target in Endocrine-Resistant Breast Cancer Exhibiting Low Estrogen Receptor-Mediated Transactivation. PloS one 11, e0157397.

Guo, J.Y., Karsli-Uzunbas, G., Mathew, R., Aisner, S.C., Kamphorst, J.J., Strohecker, A.M., Chen, G., Price, S., Lu, W., Teng, X., et al. (2013). Autophagy suppresses progression of K-ras-induced lung tumors to oncocytomas and maintains lipid homeostasis. Genes & development 27, 1447-1461.

Hamasaki, M., Furuta, N., Matsuda, A., Nezu, A., Yamamoto, A., Fujita, N., Oomori, H., Noda, T., Haraguchi, T., Hiraoka, Y., et al. (2013). Autophagosomes form at ER-mitochondria contact sites. Nature 495, 389-393.

Hanahan, D., and Weinberg, R.A. (2011). Hallmarks of cancer: the next generation. Cell 144, 646-674.

Haricharan, S., Bainbridge, M.N., Scheet, P., and Brown, P.H. (2014). Somatic mutation load of estrogen receptor-positive breast tumors predicts overall survival: an analysis of genome sequence data. Breast cancer research and treatment 146, 211-220.

Harris, L.N., Ismaila, N., McShane, L.M., Andre, F., Collyar, D.E., Gonzalez-Angulo, A.M., Hammond, E.H., Kuderer, N.M., Liu, M.C., Mennel, R.G., et al. (2016). Use of Biomarkers to Guide Decisions on Adjuvant Systemic Therapy for Women With Early-Stage Invasive Breast Cancer: American Society of Clinical Oncology Clinical Practice Guideline. J Clin Oncol 34, 1134-1150.

Heath-Engel, H.M., Chang, N.C., and Shore, G.C. (2008). The endoplasmic reticulum in apoptosis and autophagy: role of the BCL-2 protein family. Oncogene 27, 6419.

Hollerer, I., Grund, K., Hentze, M.W., and Kulozik, A.E. (2014). mRNA 3′end processing: A tale of the tail reaches the clinic. EMBO Molecular Medicine 6, 16-26.

Horibata, S., Vo, T.V., Subramanian, V., Thompson, P.R., and Coonrod, S.A. (2015). Utilization of the Soft Agar Colony Formation Assay to Identify Inhibitors of Tumorigenicity in Breast Cancer Cells. J Vis Exp, e52727.

Hu, Y.L., DeLay, M., Jahangiri, A., Molinaro, A.M., Rose, S.D., Carbonell, W.S., and Aghi, M.K. (2012). Hypoxia-induced autophagy promotes tumor cell survival and adaptation to antiangiogenic treatment in glioblastoma. Cancer Res 72, 1773-1783.

Hu, Z., Fan, C., Oh, D.S., Marron, J.S., He, X., Qaqish, B.F., Livasy, C., Carey, L.A., Reynolds, E., Dressler, L., et al. (2006). The molecular portraits of breast tumors are conserved across microarray platforms. BMC genomics 7, 96.

Huang, Q., Li, F., Liu, X., Li, W., Shi, W., Liu, F.F., O'Sullivan, B., He, Z., Peng, Y., Tan, A.C., et al. (2011). Caspase 3-mediated stimulation of tumor cell repopulation during cancer radiotherapy. Nat Med 17, 860-866.

Hur, J., Bell, D.W., Dean, K.L., Coser, K.R., Hilario, P.C., Okimoto, R.A., Tobey, E.M., Smith, S.L., Isselbacher, K.J., and Shioda, T. (2006). Regulation of expression of BIK proapoptotic protein in human breast cancer cells: p53-dependent induction of BIK mRNA by fulvestrant and proteasomal degradation of BIK protein. Cancer Res 66, 10153-10161.

Hur, J., Chesnes, J., Coser, K.R., Lee, R.S., Geck, P., Isselbacher, K.J., and Shioda, T. (2004). The Bik BH3-only protein is induced in estrogen-starved and antiestrogen-exposed breast cancer cells and provokes apoptosis. Proceedings of the National Academy of Sciences of the United States of America 101, 2351-2356.

Ichim, G., Lopez, J., Ahmed, S.U., Muthalagu, N., Giampazolias, E., Delgado, M.E., Haller, M., Riley, J.S., Mason, S.M., Athineos, D., et al. (2015). Limited mitochondrial permeabilization causes DNA damage and genomic instability in the absence of cell death. Molecular cell 57, 860-872.

Ichim, G., and Tait, S.W. (2016). A fate worse than death: apoptosis as an oncogenic process. Nat Rev Cancer 16, 539-548.

Itakura, E., Kishi-Itakura, C., and Mizushima, N. (2012). The hairpin-type tail-anchored SNARE syntaxin 17 targets to autophagosomes for fusion with endosomes/lysosomes. Cell 151, 1256-1269.

Ito, M., Kizawa, K., Hamada, K., and Cotsarelis, G. (2004). Hair follicle stem cells in the lower bulge form the secondary germ, a biochemically distinct but functionally equivalent progenitor cell population, at the termination of catagen. Differentiation 72, 548-557.

Jeffers, J.R., Parganas, E., Lee, Y., Yang, C., Wang, J., Brennan, J., MacLean, K.H., Han, J., Chittenden, T., Ihle, J.N., et al. (2003). Puma is an essential mediator of p53-dependent and -independent apoptotic pathways. Cancer cell 4, 321-328.

Jeselsohn, R., Yelensky, R., Buchwalter, G., Frampton, G., Meric-Bernstam, F., Gonzalez-Angulo, A.M., Ferrer-Lozano, J., Perez-Fidalgo, J.A., Cristofanilli, M., Gomez, H., et al. (2014). Emergence of constitutively active estrogen receptor-alpha mutations in pretreated advanced estrogen receptor-positive breast cancer. Clinical cancer research : an official journal of the American Association for Cancer Research 20, 1757-1767.

Jiang, Q. (2013). Development of new estrogen receptor-targeting therapeutic agents for tamoxifen-resistant breast cancer. 5.

Jiao, S., Wu, M., Ye, F., Tang, H., Xie, X., and Xie, X. (2014). BikDDA, a Mutant of Bik with Longer Half-Life Expression Protein, Can Be a Novel Therapeutic Gene for Triple-Negative Breast Cancer. PloS one 9, e92172.

Jin, Z., McDonald, E.R., 3rd, Dicker, D.T., and El-Deiry, W.S. (2004). Deficient tumor necrosis factor-related apoptosis-inducing ligand (TRAIL) death receptor transport to the cell surface in human colon cancer cells selected for resistance to TRAIL-induced apoptosis. The Journal of biological chemistry 279, 35829-35839.

Jonasson, J.G., Stefansson, O.A., Johannsson, O.T., Sigurdsson, H., Agnarsson, B.A., Olafsdottir, G.H., Alexiusdottir, K.K., Stefansdottir, H., Munoz Mitev, R., Olafsdottir, K., et al. (2016). Oestrogen receptor status, treatment and breast cancer prognosis in Icelandic BRCA2 mutation carriers. British Journal of Cancer 115, 776-783.

Julien, O., and Wells, J.A. (2017). Caspases and their substrates. Cell Death And Differentiation 24, 1380.

Kaparou, M., Choumerianou, D., Perdikogianni, C., Martimianaki, G., Kalmanti, M., and Stiakaki, E. (2013). Enhanced levels of the apoptotic BAX/BCL-2 ratio in children with acute lymphoblastic leukemia and high-risk features. Genet Mol Biol 36, 7-11.

Karsli-Uzunbas, G., Guo, J.Y., Price, S., Teng, X., Laddha, S.V., Khor, S., Kalaany, N.Y., Jacks, T., Chan, C.S., Rabinowitz, J.D., et al. (2014). Autophagy is required for glucose homeostasis and lung tumor maintenance. Cancer Discov 4, 914-927.

Katzenellenbogen, J.A., Mayne, C.G., Katzenellenbogen, B.S., Greene, G.L., and Chandarlapaty, S. (2018). Structural underpinnings of oestrogen receptor mutations in endocrine therapy resistance. Nature Reviews Cancer 18, 377-388.

Kaufmann, T., Tai, L., Ekert, P.G., Huang, D.C., Norris, F., Lindemann, R.K., Johnstone, R.W., Dixit, V.M., and Strasser, A. (2007). The BH3-only protein bid is dispensable for DNA damage- and replicative stress-induced apoptosis or cell-cycle arrest. Cell 129, 423-433.

Kaur, J., and Debnath, J. (2015). Autophagy at the crossroads of catabolism and anabolism. Nature reviews Molecular cell biology 16, 461-472.

Kennecke, H., Yerushalmi, R., Woods, R., Cheang, M.C., Voduc, D., Speers, C.H., Nielsen, T.O., and Gelmon, K. (2010). Metastatic behavior of breast cancer subtypes. J Clin Oncol 28, 3271-3277.

Kerr, J.F.R., Wyllie, A.H., and Currie, A.R. (1972). Apoptosis: A Basic Biological Phenomenon with Wide-ranging Implications in Tissue Kinetics. British Journal of Cancer 26, 239-257.

Kim, H., Rafiuddin-Shah, M., Tu, H.C., Jeffers, J.R., Zambetti, G.P., Hsieh, J.J., and Cheng, E.H. (2006). Hierarchical regulation of mitochondrion-dependent apoptosis by BCL-2 subfamilies. Nature cell biology 8, 1348-1358.

Kimmelman, A.C. (2011). The dynamic nature of autophagy in cancer. Genes & development 25, 1999-2010.

Klionsky, D.J., Abdelmohsen, K., Abe, A., Abedin, M.J., Abeliovich, H., Acevedo Arozena, A., Adachi, H., Adams, C.M., Adams, P.D., Adeli, K., et al. (2016). Guidelines for the use and interpretation of assays for monitoring autophagy (3rd edition). Autophagy 12, 1-222.

Knudson, C.M., Tung, K.S., Tourtellotte, W.G., Brown, G.A., and Korsmeyer, S.J. (1995). Bax-deficient mice with lymphoid hyperplasia and male germ cell death. Science (New York, NY) 270, 96-99.

Kohler, T., Schill, C., Deininger, M.W., Krahl, R., Borchert, S., Hasenclever, D., Leiblein, S., Wagner, O., and Niederwieser, D. (2002). High Bad and Bax mRNA expression correlate with negative outcome in acute myeloid leukemia (AML). Leukemia 16, 22-29.

Komatsu, M., Waguri, S., Ueno, T., Iwata, J., Murata, S., Tanida, I., Ezaki, J., Mizushima, N., Ohsumi, Y., Uchiyama, Y., et al. (2005). Impairment of starvation-induced and constitutive autophagy in Atg7-deficient mice. The Journal of cell biology 169, 425-434.

Konca, K., Lankoff, A., Banasik, A., Lisowska, H., Kuszewski, T., Gozdz, S., Koza, Z., and Wojcik, A. (2003). A cross-platform public domain PC image-analysis program for the comet assay. Mutat Res 534, 15-20.

Kondo, S., Senoo-Matsuda, N., Hiromi, Y., and Miura, M. (2006). DRONC coordinates cell death and compensatory proliferation. Mol Cell Biol 26, 7258-7268.

Konduri, S.D., Medisetty, R., Liu, W., Kaipparettu, B.A., Srivastava, P., Brauch, H., Fritz, P., Swetzig, W.M., Gardner, A.E., Khan, S.A., et al. (2010). Mechanisms of estrogen receptor antagonism toward p53 and its implications in breast cancer therapeutic response and stem cell regulation. Proceedings of the National Academy of Sciences 107, 15081-15086.

Koong, A.C., Denko, N.C., Hudson, K.M., Schindler, C., Swiersz, L., Koch, C., Evans, S., Ibrahim, H., Le, Q.T., Terris, D.J., et al. (2000). Candidate genes for the hypoxic tumor phenotype. Cancer Res 60, 883-887.

Kryston, T.B., Georgiev, A.B., Pissis, P., and Georgakilas, A.G. (2011). Role of oxidative stress and DNA damage in human carcinogenesis. Mutat Res 711, 193-201.

Kuo, C.T., Zhu, S., Younger, S., Jan, L.Y., and Jan, Y.N. (2006). Identification of E2/E3 ubiquitinating enzymes and caspase activity regulating Drosophila sensory neuron dendrite pruning. Neuron 51, 283-290.

Kurian, A.W., Hughes, E., Handorf, E.A., Gutin, A., Allen, B., Hartman, A.-R., and Hall, M.J. (2017). Breast and Ovarian Cancer Penetrance Estimates Derived From Germline Multiple-Gene Sequencing Results in Women. JCO Precision Oncology, 1-12.

Labi, V., Erlacher, M., Krumschnabel, G., Manzl, C., Tzankov, A., Pinon, J., Egle, A., and Villunger, A. (2010). Apoptosis of leukocytes triggered by acute DNA damage promotes lymphoma formation. Genes & development 24, 1602-1607.

Larsen, B.D., and Sorensen, C.S. (2017). The caspase-activated DNase: apoptosis and beyond. FEBS J 284, 1160-1170.

Lauby-Secretan, B., Scoccianti, C., Loomis, D., Benbrahim-Tallaa, L., Bouvard, V., Bianchini, F., Straif, K., and International Agency for Research on Cancer Handbook Working, G. (2015). Breast-cancer screening--viewpoint of the IARC Working Group. N Engl J Med 372, 2353-2358.

Lawrence, M.S., Stojanov, P., Mermel, C.H., Robinson, J.T., Garraway, L.A., Golub, T.R., Meyerson, M., Gabriel, S.B., Lander, E.S., and Getz, G. (2014). Discovery and saturation analysis of cancer genes across 21 tumour types. Nature 505, 495-501.

Lee, S.H., Shin, M.S., Park, W.S., Kim, S.Y., Kim, H.S., Han, J.Y., Park, G.S., Dong, S.M., Pi, J.H., Kim, C.S., et al. (1999). Alterations of Fas (Apo-1/CD95) gene in non-small cell lung cancer. Oncogene 18, 3754-3760.

Levkau, B., Herren, B., Koyama, H., Ross, R., and Raines, E.W. (1998). Caspase-mediated Cleavage of Focal Adhesion Kinase pp125(FAK) and Disassembly of Focal Adhesions in Human Endothelial Cell Apoptosis. The Journal of Experimental Medicine 187, 579-586.

Li, F., He, Z., Shen, J., Huang, Q., Li, W., Liu, X., He, Y., Wolf, F., and Li, C.Y. (2010). Apoptotic caspases regulate induction of iPSCs from human fibroblasts. Cell stem cell 7, 508-520.

Li, H., Zhu, H., Xu, C.J., and Yuan, J. (1998). Cleavage of BID by caspase 8 mediates the mitochondrial damage in the Fas pathway of apoptosis. Cell 94, 491-501.

Li, J., and Yuan, J. (2008). Caspases in apoptosis and beyond. Oncogene 27, 6194.

Li, S., Shen, D., Shao, J., Crowder, R., Liu, W., Prat, A., He, X., Liu, S., Hoog, J., Lu, C., et al. (2013). Endocrine-therapy-resistant ESR1 variants revealed by genomic characterization of breast-cancer-derived xenografts. Cell reports 4, 1116-1130.

Li, W., Laishram, R.S., Ji, Z., Barlow, C.A., Tian, B., and Anderson, R.A. (2012). Star-PAP control of BIK expression and apoptosis is regulated by nuclear PIPKIalpha and PKCdelta signaling. Molecular cell 45, 25-37.

Liang, X.H., Jackson, S., Seaman, M., Brown, K., Kempkes, B., Hibshoosh, H., and Levine, B. (1999). Induction of autophagy and inhibition of tumorigenesis by beclin 1. Nature 402, 672-676.

Liang, Y., Yan, C., and Schor, N.F. (2001). Apoptosis in the absence of caspase 3. Oncogene 20, 6570-6578.

Lindsten, T., Ross, A.J., King, A., Zong, W.X., Rathmell, J.C., Shiels, H.A., Ulrich, E., Waymire, K.G., Mahar, P., Frauwirth, K., et al. (2000). The combined functions of proapoptotic Bcl-2 family members bak and bax are essential for normal development of multiple tissues. Molecular cell 6, 1389-1399.

Lindsten, T., and Thompson, C.B. (2006). Cell death in the absence of Bax and Bak. Cell Death And Differentiation 13, 1272.

Lips, E.H., Debipersad, R., Scheerman, C.E., Mulder, L., Sonke, G.S., van der Kolk, L.E., Wesseling, J., Hogervorst, F.B.L., and Nederlof, P.M. (2016). BRCA1-mutated estrogen receptor positive breast cancer shows BRCAness, suggesting sensitivity to drugs targeting homologous recombination deficiency. Clinical Cancer Research.

Liu, W., Konduri, S.D., Bansal, S., Nayak, B.K., Rajasekaran, S.A., Karuppayil, S.M., Rajasekaran, A.K., and Das, G.M. (2006). Estrogen Receptor-α Binds p53 Tumor Suppressor Protein Directly and Represses Its Function. Journal of Biological Chemistry 281, 9837-9840.

Liu, X., Dai, S., Zhu, Y., Marrack, P., and Kappler, J.W. (2003a). The structure of a Bcl-xL/Bim fragment complex: implications for Bim function. Immunity 19, 341-352.

Liu, X., He, Y., Li, F., Huang, Q., Kato, T.A., Hall, R.P., and Li, C.Y. (2015). Caspase-3 promotes genetic instability and carcinogenesis. Molecular cell 58, 284-296.

Liu, X., Li, P., Widlak, P., Zou, H., Luo, X., Garrard, W.T., and Wang, X. (1998). The 40-kDa subunit of DNA fragmentation factor induces DNA fragmentation and chromatin condensation during apoptosis. Proceedings of the National Academy of Sciences of the United States of America 95, 8461-8466.

Liu, X., Pisha, E., Tonetti, D.A., Yao, D., Li, Y., Yao, J., Burdette, J.E., and Bolton, J.L. (2003b). Antiestrogenic and DNA damaging effects induced by tamoxifen and toremifene metabolites. Chem Res Toxicol 16, 832-837.

Liu, X., Zou, H., Slaughter, C., and Wang, X. (1997). DFF, a heterodimeric protein that functions downstream of caspase-3 to trigger DNA fragmentation during apoptosis. Cell 89, 175-184.

Liu, Y., Nenutil, R., Appleyard, M.V., Murray, K., Boylan, M., Thompson, A.M., and Coates, P.J. (2014). Lack of correlation of stem cell markers in breast cancer stem cells. British Journal of Cancer 110, 2063-2071.

Loibl, S., and Gianni, L. (2017). HER2-positive breast cancer. Lancet (London, England) 389, 2415-2429.

Lomonosova, E., and Chinnadurai, G. (2008). BH3-only proteins in apoptosis and beyond: an overview. Oncogene 27, S2-19.

Lopez-Munoz, E., Hernandez-Zarco, A., Garcia-Hernandez, N., Alvarado-Cabrero, I., Zarco-Espinosa, G., Salamanca-Gomez, F., and Arenas-Aranda, D. (2012). BIK/NBK gene as potential marker of prognostic and therapeutic target in breast cancer patients. Clin Transl Oncol 14, 586-591.

Lopez, J., Hesling, C., Prudent, J., Popgeorgiev, N., Gadet, R., Mikaelian, I., Rimokh, R., Gillet, G., and Gonzalo, P. (2012). Src tyrosine kinase inhibits apoptosis through the Erk1/2- dependent degradation of the death accelerator Bik. Cell Death Differ 19, 1459-1469.

Lovric, M.M., and Hawkins, C.J. (2010). TRAIL treatment provokes mutations in surviving cells. Oncogene 29, 5048-5060.

Lu, Y., Lemon, W., Liu, P.Y., Yi, Y., Morrison, C., Yang, P., Sun, Z., Szoke, J., Gerald, W.L., Watson, M., et al. (2006). A gene expression signature predicts survival of patients with stage I non-small cell lung cancer. PLoS Med 3, e467.

Lum, J.J., Bauer, D.E., Kong, M., Harris, M.H., Li, C., Lindsten, T., and Thompson, C.B. (2005). Growth factor regulation of autophagy and cell survival in the absence of apoptosis. Cell 120, 237-248.

Lynes, E.M., Bui, M., Yap, M.C., Benson, M.D., Schneider, B., Ellgaard, L., Berthiaume, L.G., and Simmen, T. (2012). Palmitoylated TMX and calnexin target to the mitochondria-associated membrane. The EMBO Journal 31, 457-470.

Malhotra, G.K., Zhao, X., Band, H., and Band, V. (2010). Histological, molecular and functional subtypes of breast cancers. Cancer Biol Ther 10, 955-960.

Man, N., Chen, Y., Zheng, F., Zhou, W., and Wen, L.P. (2010). Induction of genuine autophagy by cationic lipids in mammalian cells. Autophagy 6, 449-454.

Mar, V.J., Wong, S.Q., Li, J., Scolyer, R.A., McLean, C., Papenfuss, A.T., Tothill, R.W., Kakavand, H., Mann, G.J., Thompson, J.F., et al. (2013). BRAF/NRAS wild-type melanomas have a high mutation load correlating with histologic and molecular signatures of UV damage. Clinical cancer research : an official journal of the American Association for Cancer Research 19, 4589-4598.

Maréchal, A., and Zou, L. (2013). DNA Damage Sensing by the ATM and ATR Kinases. Cold Spring Harbor perspectives in biology 5, a012716.

Marinkovi, #x, , M., #x, prung, M., Buljuba, #x, #x, , M., and Novak, I. (2018). Autophagy Modulation in Cancer: Current Knowledge on Action and Therapy. Oxidative Medicine and Cellular Longevity 2018, 18.

Marino, G., Niso-Santano, M., Baehrecke, E.H., and Kroemer, G. (2014). Self-consumption: the interplay of autophagy and apoptosis. Nature reviews Molecular cell biology 15, 81-94.

Marino, M., Galluzzo, P., and Ascenzi, P. (2006). Estrogen signaling multiple pathways to impact gene transcription. Curr Genomics 7, 497-508.

Marshansky, V., Wang, X., Bertrand, R., Luo, H., Duguid, W., Chinnadurai, G., Kanaan, N., Vu, M.D., and Wu, J. (2001). Proteasomes Modulate Balance Among Proapoptotic and Antiapoptotic Bcl-2 Family Members and Compromise Functioning of the Electron Transport Chain in Leukemic Cells. The Journal of Immunology 166, 3130-3142.

Martin, E.C., Conger, A.K., Yan, T.J., Hoang, V.T., Miller, D.F., Buechlein, A., Rusch, D.B., Nephew, K.P., Collins-Burow, B.M., and Burow, M.E. (2017). MicroRNA-335-5p and -3p synergize to inhibit estrogen receptor alpha expression and promote tamoxifen resistance. FEBS Lett 591, 382-392.

Masoud, V., and Pagès, G. (2017). Targeted therapies in breast cancer: New challenges to fight against resistance. World Journal of Clinical Oncology 8, 120-134.

Mathai, J.P. (2005). The role of endoplasmic reticulum BIK in p53-mediated apoptosis In Biochemistry (Montreal: McGill University).

Mathai, J.P., Germain, M., Marcellus, R.C., and Shore, G.C. (2002). Induction and endoplasmic reticulum location of BIK/NBK in response to apoptotic signaling by E1A and p53. Oncogene 21, 2534-2544.

Mathai, J.P., Germain, M., and Shore, G.C. (2005). BH3-only BIK regulates BAX,BAK-dependent release of Ca2+ from endoplasmic reticulum stores and mitochondrial apoptosis during stress-induced cell death. The Journal of biological chemistry 280, 23829-23836.

Mathew, R., Karantza-Wadsworth, V., and White, E. (2007). Role of autophagy in cancer. Nat Rev Cancer 7, 961-967.

Maxfield, K.E., Taus, P.J., Corcoran, K., Wooten, J., Macion, J., Zhou, Y., Borromeo, M., Kollipara, R.K., Yan, J., Xie, Y., et al. (2015). Comprehensive functional characterization of cancer-testis antigens defines obligate participation in multiple hallmarks of cancer. Nat Commun 6, 8840.

McDonnell, D.P., and Norris, J.D. (2002). Connections and regulation of the human estrogen receptor. Science (New York, NY) 296, 1642-1644.

McDonnell, J.M., Fushman, D., Milliman, C.L., Korsmeyer, S.J., and Cowburn, D. (1999). Solution Structure of the Proapoptotic Molecule BID: A Structural Basis for Apoptotic Agonists and Antagonists. Cell 96, 625-634.

McDonnell, T.J., Deane, N., Platt, F.M., Nunez, G., Jaeger, U., McKearn, J.P., and Korsmeyer, S.J. (1989). bcl-2-immunoglobulin transgenic mice demonstrate extended B cell survival and follicular lymphoproliferation. Cell 57, 79-88.

McDonnell, T.J., and Korsmeyer, S.J. (1991). Progression from lymphoid hyperplasia to high-grade malignant lymphoma in mice transgenic for the t(14; 18). Nature 349, 254-256.

McIlroy, D., Tanaka, M., Sakahira, H., Fukuyama, H., Suzuki, M., Yamamura, K., Ohsawa, Y., Uchiyama, Y., and Nagata, S. (2000). An auxiliary mode of apoptotic DNA fragmentation provided by phagocytes. Genes & development 14, 549-558.

McIlwain, D.R., Berger, T., and Mak, T.W. (2013). Caspase functions in cell death and disease. Cold Spring Harbor perspectives in biology 5, a008656.

Mebratu, Y.A., Dickey, B.F., Evans, C., and Tesfaigzi, Y. (2008). The BH3-only protein Bik/Blk/Nbk inhibits nuclear translocation of activated ERK1/2 to mediate IFNgamma-induced cell death. The Journal of cell biology 183, 429-439.

Mechta-Grigoriou, F., Gerald, D., and Yaniv, M. (2001). The mammalian Jun proteins: redundancy and specificity. Oncogene 20, 2378.

Mehta, A., and Haber, J.E. (2014). Sources of DNA double-strand breaks and models of recombinational DNA repair. Cold Spring Harbor perspectives in biology 6, a016428.

Ménard, S., Pupa, S.M., Campiglio, M., and Tagliabue, E. (2003). Biologic and therapeutic role of HER2 in cancer. Oncogene 22, 6570.

Meterissian, S.H., Kontogiannea, M., Al-Sowaidi, M., Linjawi, A., Halwani, F., Jamison, B., and Edwardes, M. (2001). Bcl-2 is a useful prognostic marker in Dukes' B colon cancer. Annals of surgical oncology 8, 533-537.

Metz, C.E. (1978). Basic principles of ROC analysis. Seminars in nuclear medicine 8, 283-298.

Michalak, E.M., Vandenberg, C.J., Delbridge, A.R., Wu, L., Scott, C.L., Adams, J.M., and Strasser, A. (2010). Apoptosis-promoted tumorigenesis: gamma-irradiation-induced thymic lymphomagenesis requires Puma-driven leukocyte death. Genes & development 24, 1608-1613.

Miles, M.A., and Hawkins, C.J. (2017). Executioner caspases and CAD are essential for mutagenesis induced by TRAIL or vincristine. Cell Death Dis 8, e3062.

Miquel, C., Borrini, F., Grandjouan, S., Auperin, A., Viguier, J., Velasco, V., Duvillard, P., Praz, F., and Sabourin, J.C. (2005). Role of bax mutations in apoptosis in colorectal cancers with microsatellite instability. American journal of clinical pathology 123, 562-570.

Mizushima, N., Yoshimori, T., and Levine, B. (2010). Methods in mammalian autophagy research. Cell 140, 313-326.

Mizushima, N., Yoshimori, T., and Ohsumi, Y. (2011). The role of Atg proteins in autophagosome formation. Annu Rev Cell Dev Biol 27, 107-132.

Moasser, M.M. (2007). The oncogene HER2: its signaling and transforming functions and its role in human cancer pathogenesis. Oncogene 26, 6469-6487.

Morata-Tarifa, C., Picon-Ruiz, M., Grinan-Lison, C., Boulaiz, H., Peran, M., Garcia, M.A., and Marchal, J.A. (2017). Validation of suitable normalizers for miR expression patterns analysis covering tumour heterogeneity. Sci Rep 7, 39782.

Morgan, C.W., Diaz, J.E., Zeitlin, S.G., Gray, D.C., and Wells, J.A. (2015). Engineered cellular gene-replacement platform for selective and inducible proteolytic profiling. Proceedings of the National Academy of Sciences of the United States of America 112, 8344-8349.

Motoyama, N., Wang, F., Roth, K.A., Sawa, H., Nakayama, K., Nakayama, K., Negishi, I., Senju, S., Zhang, Q., Fujii, S., et al. (1995). Massive cell death of immature hematopoietic cells and neurons in Bcl-x-deficient mice. Science (New York, NY) 267, 1506-1510.

Musgrove, E.A., and Sutherland, R.L. (2009). Biological determinants of endocrine resistance in breast cancer. Nature Reviews Cancer 9, 631.

Nagata, S. (2000). Apoptotic DNA fragmentation. Experimental cell research 256, 12-18.

Nagata, S. (2018). Apoptosis and Clearance of Apoptotic Cells. Annu Rev Immunol 36, 489-517.

Nakano, K., and Vousden, K.H. (2001). PUMA, a novel proapoptotic gene, is induced by p53. Molecular cell 7, 683-694.

Naumann, U., Schmidt, F., Wick, W., Frank, B., Weit, S., Gillissen, B., Daniel, P., and Weller, M. (2003). Adenoviral natural born killer gene therapy for malignant glioma. Hum Gene Ther 14, 1235-1246.

Ndozangue-Touriguine, O., Hamelin, J., and Breard, J. (2008). Cytoskeleton and apoptosis. Biochemical pharmacology 76, 11-18.

Neri, A., Marrelli, D., Roviello, F., DeMarco, G., Mariani, F., DeStefano, A., Megha, T., Caruso, S., Corso, G., Cioppa, T., et al. (2006). Bcl-2 expression correlates with lymphovascular invasion and long-term prognosis in breast cancer. Breast cancer research and treatment 99, 77-83.

Nicholson, R.I., and Johnston, S.R. (2005). Endocrine therapy--current benefits and limitations. Breast cancer research and treatment 93 Suppl 1, S3-10.

Nik-Zainal, S., Davies, H., Staaf, J., Ramakrishna, M., Glodzik, D., Zou, X., Martincorena, I., Alexandrov, L.B., Martin, S., Wedge, D.C., et al. (2016). Landscape of somatic mutations in 560 breast cancer whole-genome sequences. Nature 534, 47-54.

Nikrad, M., Johnson, T., Puthalalath, H., Coultas, L., Adams, J., and Kraft, A.S. (2005). The proteasome inhibitor bortezomib sensitizes cells to killing by death receptor ligand TRAIL via BH3-only proteins Bik and Bim. Mol Cancer Ther 4, 443-449.

Niu, D., Wang, G., and Wang, X. (2015). Up-regulation of cyclin E in breast cancer via estrogen receptor pathway. International Journal of Clinical and Experimental Medicine 8, 910-915.

NobelPrize.org (2018).

O'Lone, R., Frith, M.C., Karlsson, E.K., and Hansen, U. (2004). Genomic targets of nuclear estrogen receptors. Molecular endocrinology (Baltimore, Md) 18, 1859-1875.

Oda, E., Ohki, R., Murasawa, H., Nemoto, J., Shibue, T., Yamashita, T., Tokino, T., Taniguchi, T., and Tanaka, N. (2000). Noxa, a BH3-only member of the Bcl-2 family and candidate mediator of p53-induced apoptosis. Science (New York, NY) 288, 1053-1058.

Okouchi, M., Ekshyyan, O., Maracine, M., and Aw, T.Y. (2007). Neuronal apoptosis in neurodegeneration. Antioxidants & redox signaling 9, 1059-1096.

Opferman, J.T., Iwasaki, H., Ong, C.C., Suh, H., Mizuno, S., Akashi, K., and Korsmeyer, S.J. (2005). Obligate role of anti-apoptotic MCL-1 in the survival of hematopoietic stem cells. Science (New York, NY) 307, 1101-1104.

Opferman, J.T., and Korsmeyer, S.J. (2003). Apoptosis in the development and maintenance of the immune system. Nature immunology 4, 410-415.

Opferman, J.T., Letai, A., Beard, C., Sorcinelli, M.D., Ong, C.C., and Korsmeyer, S.J. (2003). Development and maintenance of B and T lymphocytes requires antiapoptotic MCL-1. Nature 426, 671-676.

Oppermann, M., Geilen, C.C., Fecker, L.F., Gillissen, B., Daniel, P.T., and Eberle, J. (2005). Caspase-independent induction of apoptosis in human melanoma cells by the proapoptotic Bcl-2-related protein Nbk / Bik. Oncogene 24, 7369-7380.

Opydo-Chanek, M., Gonzalo, O., and Marzo, I. (2017). Multifaceted anticancer activity of BH3 mimetics: Current evidence and future prospects. Biochemical pharmacology 136, 12-23.

Ordonez-Mena, J.M., Schottker, B., Mons, U., Jenab, M., Freisling, H., Bueno-de-Mesquita, B., O'Doherty, M.G., Scott, A., Kee, F., Stricker, B.H., et al. (2016). Quantification of the smoking-

associated cancer risk with rate advancement periods: meta-analysis of individual participant data from cohorts of the CHANCES consortium. BMC Med 14, 62.

Orth, K., and Dixit, V.M. (1997). Bik and Bak induce apoptosis downstream of CrmA but upstream of inhibitor of apoptosis. The Journal of biological chemistry 272, 8841-8844.

Osborne, C.K., Wakeling, A., and Nicholson, R.I. (2004). Fulvestrant: an oestrogen receptor antagonist with a novel mechanism of action. British Journal of Cancer 90, S2-6.

Osoegawa, A., Hiraishi, H., Hashimoto, T., Takumi, Y., Abe, M., Takeuchi, H., Miyawaki, M., Okamoto, T., and Sugio, K. (2018). The Positive Relationship Between gammaH2AX and PD-L1 Expression in Lung Squamous Cell Carcinoma. In vivo (Athens, Greece) 32, 171-177.

Paik, S. (2007). Development and clinical utility of a 21-gene recurrence score prognostic assay in patients with early breast cancer treated with tamoxifen. Oncologist 12, 631-635.

Paik, S., Shak, S., Tang, G., Kim, C., Baker, J., Cronin, M., Baehner, F.L., Walker, M.G., Watson, D., Park, T., et al. (2004). A Multigene Assay to Predict Recurrence of Tamoxifen-Treated, Node-Negative Breast Cancer. New England Journal of Medicine 351, 2817-2826.

Pandya, V., Glubrecht, D., Vos, L., Hanson, J., Damaraju, S., Mackey, J., Hugh, J., and Goping, I.S. (2016). The pro-apoptotic paradox: the BH3-only protein Bcl-2 interacting killer (Bik) is prognostic for unfavorable outcomes in breast cancer. Oncotarget 7, 33272-33285.

Paquet, C., Schmitt, E., Beauchemin, M., and Bertrand, R. (2004). Activation of multidomain and BH3-only pro-apoptotic Bcl-2 family members in p53-defective cells. Apoptosis 9, 815-831.

Peng, T.I., and Jou, M.J. (2010). Oxidative stress caused by mitochondrial calcium overload. Ann N Y Acad Sci 1201, 183-188.

Pepper, C., Lin, T.T., Pratt, G., Hewamana, S., Brennan, P., Hiller, L., Hills, R., Ward, R., Starczynski, J., Austen, B., et al. (2008). Mcl-1 expression has in vitro and in vivo significance in chronic lymphocytic leukemia and is associated with other poor prognostic markers. Blood 112, 3807-3817.

Perou, C.M., Sørlie, T., Eisen, M.B., van de Rijn, M., Jeffrey, S.S., Rees, C.A., Pollack, J.R., Ross, D.T., Johnsen, H., Akslen, L.A., et al. (2000). Molecular portraits of human breast tumours. Nature 406, 747.

Piechaczyk, M., and Blanchard, J.M. (1994). c-fos proto-oncogene regulation and function. Critical reviews in oncology/hematology 17, 93-131.

Ponglikitmongkol, M., Green, S., and Chambon, P. (1988). Genomic organization of the human oestrogen receptor gene. The EMBO Journal 7, 3385-3388.

Prakash, R., Zhang, Y., Feng, W., and Jasin, M. (2015). Homologous recombination and human health: the roles of BRCA1, BRCA2 and associated proteins. Cold Spring Harbor perspectives in biology 7, a016600 016610.011101/cshperspect.a016600.

Pusztai, L., Karn, T., Safonov, A., Abu-Khalaf, M.M., and Bianchini, G. (2016). New Strategies in Breast Cancer: Immunotherapy. Clinical cancer research : an official journal of the American Association for Cancer Research 22, 2105-2110.

Qu, X., Yu, J., Bhagat, G., Furuya, N., Hibshoosh, H., Troxel, A., Rosen, J., Eskelinen, E.L., Mizushima, N., Ohsumi, Y., et al. (2003). Promotion of tumorigenesis by heterozygous disruption of the beclin 1 autophagy gene. The Journal of clinical investigation 112, 1809-1820.

Quarrie, L.H., Addey, C.V., and Wilde, C.J. (1996). Programmed cell death during mammary tissue involution induced by weaning, litter removal, and milk stasis. Journal of cellular physiology 168, 559-569.

Raffo, D., Berardi, D.E., Pontiggia, O., Todaro, L., de Kier Joffe, E.B., and Simian, M. (2013). Tamoxifen selects for breast cancer cells with mammosphere forming capacity and increased growth rate. Breast cancer research and treatment 142, 537-548.

Rao, S., Tortola, L., Perlot, T., Wirnsberger, G., Novatchkova, M., Nitsch, R., Sykacek, P., Frank, L., Schramek, D., Komnenovic, V., et al. (2014). A dual role for autophagy in a murine model of lung cancer. Nat Commun 5, 3056.

Rappa, G., Mercapide, J., Anzanello, F., Prasmickaite, L., Xi, Y., Ju, J., Fodstad, O., and Lorico, A. (2008). Growth of cancer cell lines under stem cell-like conditions has the potential to unveil therapeutic targets. Experimental cell research 314, 2110-2122.

Rashmi, R., Pillai, S.G., Vijayalingam, S., Ryerse, J., and Chinnadurai, G. (2008). BH3-only protein BIK induces caspase-independent cell death with autophagic features in Bcl-2 null cells. Oncogene 27, 1366-1375.

Ravikumar, B., Moreau, K., Jahreiss, L., Puri, C., and Rubinsztein, D.C. (2010). Plasma membrane contributes to the formation of pre-autophagosomal structures. Nature cell biology 12, 747-757.

Real, P.J., Sanz, C., Gutierrez, O., Pipaon, C., Zubiaga, A.M., and Fernandez-Luna, J.L. (2006). Transcriptional activation of the proapoptotic bik gene by E2F proteins in cancer cells. FEBS Lett 580, 5905-5909.

Rehm, M., Dussmann, H., and Prehn, J.H. (2003). Real-time single cell analysis of Smac/DIABLO release during apoptosis. The Journal of cell biology 162, 1031-1043.

Reimer, D., Sadr, S., Wiedemair, A., Goebel, G., Concin, N., Hofstetter, G., Marth, C., and Zeimet, A.G. (2006). Expression of the E2F family of transcription factors and its clinical relevance in ovarian cancer. Ann N Y Acad Sci 1091, 270-281.

Renouf, D.J., Wood-Baker, R., Ionescu, D.N., Leung, S., Masoudi, H., Gilks, C.B., and Laskin, J. (2009). BCL-2 Expression is Prognostic for Improved Survival in Non-small Cell Lung Cancer. Journal of Thoracic Oncology 4, 486-491.

Reynaud, K., and Driancourt, M.A. (2000). Oocyte attrition. Molecular and cellular endocrinology 163, 101-108.

Rinkenberger, J.L., Horning, S., Klocke, B., Roth, K., and Korsmeyer, S.J. (2000). Mcl-1 deficiency results in peri-implantation embryonic lethality. Genes & development 14, 23-27.

Ritchie, A., Gutierrez, O., and Fernandez-Luna, J.L. (2009). PAR bZIP-bik is a novel transcriptional pathway that mediates oxidative stress-induced apoptosis in fibroblasts. Cell Death Differ 16, 838-846.

Roberts, A.W., Davids, M.S., Pagel, J.M., Kahl, B.S., Puvvada, S.D., Gerecitano, J.F., Kipps, T.J., Anderson, M.A., Brown, J.R., Gressick, L., et al. (2016). Targeting BCL2 with Venetoclax in Relapsed Chronic Lymphocytic Leukemia. N Engl J Med 374, 311-322.

Robinson, D.R., Wu, Y.-M., Vats, P., Su, F., Lonigro, R.J., Cao, X., Kalyana-Sundaram, S., Wang, R., Ning, Y., Hodges, L., et al. (2013). Activating ESR1 mutations in hormone-resistant metastatic breast cancer. Nature Genetics 45, 1446.

Rowley, J.D. (1982). Identification of the constant chromosome regions involved in human hematologic malignant disease. Science (New York, NY) 216, 749-751.

Russell, R.C., Tian, Y., Yuan, H., Park, H.W., Chang, Y.-Y., Kim, J., Kim, H., Neufeld, T.P., Dillin, A., and Guan, K.-L. (2013). ULK1 induces autophagy by phosphorylating Beclin-1 and activating VPS34 lipid kinase. Nature cell biology 15, 741.

Sabbah, M., Courilleau, D., Mester, J., and Redeuilh, G. (1999). Estrogen induction of the cyclin D1 promoter: Involvement of a cAMP response-like element. Proceedings of the National Academy of Sciences of the United States of America 96, 11217-11222.

Sakahira, H., Iwamatsu, A., and Nagata, S. (2000). Specific Chaperone-like Activity of Inhibitor of Caspase-activated DNase for Caspase-activated DNase. Journal of Biological Chemistry 275, 8091-8096.

Samejima, K., and Earnshaw, W.C. (1998). ICAD/DFF regulator of apoptotic nuclease is nuclear. Experimental cell research 243, 453-459.

Samejima, K., and Earnshaw, W.C. (2005). Trashing the genome: the role of nucleases during apoptosis. Nature reviews Molecular cell biology 6, 677-688.

Sarosiek, K.A., Chi, X., Bachman, J.A., Sims, J.J., Montero, J., Patel, L., Flanagan, A., Andrews, D.W., Sorger, P., and Letai, A. (2013). BID preferentially activates BAK while BIM preferentially activates BAX, affecting chemotherapy response. Molecular cell 51, 751-765.

Sasaki, H., Kotsuji, F., and Tsang, B.K. (2002). Caspase 3-mediated focal adhesion kinase processing in human ovarian cancer cells: possible regulation by X-linked inhibitor of apoptosis protein. Gynecologic oncology 85, 339-350.

Sato, H., Niimi, A., Yasuhara, T., Permata, T.B.M., Hagiwara, Y., Isono, M., Nuryadi, E., Sekine, R., Oike, T., Kakoti, S., et al. (2017). DNA double-strand break repair pathway regulates PD-L1 expression in cancer cells. Nature Communications 8, 1751.

Sattler, M., Liang, H., Nettesheim, D., Meadows, R.P., Harlan, J.E., Eberstadt, M., Yoon, H.S., Shuker, S.B., Chang, B.S., Minn, A.J., et al. (1997). Structure of Bcl-xL-Bak peptide complex: recognition between regulators of apoptosis. Science (New York, NY) 275, 983-986.

Schiewer, M.J., and Knudsen, K.E. (2016). Linking DNA Damage and Hormone Signaling Pathways in Cancer. Trends Endocrinol Metab 27, 216-225.

Sebbagh, M., Renvoize, C., Hamelin, J., Riche, N., Bertoglio, J., and Breard, J. (2001). Caspase-3-mediated cleavage of ROCK I induces MLC phosphorylation and apoptotic membrane blebbing. Nature cell biology 3, 346-352.

Shamas-Din, A., Brahmbhatt, H., Leber, B., and Andrews, D.W. (2011). BH3-only proteins: Orchestrators of apoptosis. Biochim Biophys Acta 1813, 508-520.

Shamas-Din, A., Kale, J., Leber, B., and Andrews, D.W. (2013). Mechanisms of Action of Bcl-2 Family Proteins. Cold Spring Harbor perspectives in biology 5.

Singh, N.P., McCoy, M.T., Tice, R.R., and Schneider, E.L. (1988). A simple technique for quantitation of low levels of DNA damage in individual cells. Experimental cell research 175, 184-191.

Smith, C.L., and O'Malley, B.W. (2004). Coregulator function: a key to understanding tissue specificity of selective receptor modulators. Endocrine reviews 25, 45-71.

Smith, I., Yardley, D., Burris, H., De Boer, R., Amadori, D., McIntyre, K., Ejlertsen, B., Gnant, M., Jonat, W., Pritchard, K.I., et al. (2017). Comparative Efficacy and Safety of Adjuvant Letrozole Versus Anastrozole in Postmenopausal Patients With Hormone Receptor-Positive, Node-Positive Early Breast Cancer: Final Results of the Randomized Phase III Femara Versus Anastrozole Clinical Evaluation (FACE) Trial. J Clin Oncol 35, 1041-1048.

Smith, R.A., Andrews, K., Brooks, D., DeSantis, C.E., Fedewa, S.A., Lortet-Tieulent, J., Manassaram-Baptiste, D., Brawley, O.W., and Wender, R.C. (2016). Cancer screening in the United States, 2016: A review of current American Cancer Society guidelines and current issues in cancer screening. CA Cancer J Clin 66, 96-114.

Solier, S., and Pommier, Y. (2014). The nuclear gamma-H2AX apoptotic ring: implications for cancers and autoimmune diseases. Cell Mol Life Sci 71, 2289-2297.

Sopik, V., Sun, P., and Narod, S.A. (2017). The prognostic effect of estrogen receptor status differs for younger versus older breast cancer patients. Breast cancer research and treatment 165, 391-402.

Sordet, O., Rébé, C., Plenchette, S., Zermati, Y., Hermine, O., Vainchenker, W., Garrido, C., Solary, E., and Dubrez-Daloz, L. (2002). Specific involvement of caspases in the differentiation of monocytes into macrophages. Blood 100, 4446-4453.

Sorlie, T., Perou, C.M., Tibshirani, R., Aas, T., Geisler, S., Johnsen, H., Hastie, T., Eisen, M.B., van de Rijn, M., Jeffrey, S.S., et al. (2001). Gene expression patterns of breast carcinomas distinguish tumor subclasses with clinical implications. Proceedings of the National Academy of Sciences of the United States of America 98, 10869-10874.

Soteriou, D., and Fuchs, Y. (2018). A matter of life and death: stem cell survival in tissue regeneration and tumour formation. Nat Rev Cancer 18, 187-201.

Sotiriou, C., Neo, S.Y., McShane, L.M., Korn, E.L., Long, P.M., Jazaeri, A., Martiat, P., Fox, S.B., Harris, A.L., and Liu, E.T. (2003). Breast cancer classification and prognosis based on gene expression profiles from a population-based study. Proceedings of the National Academy of Sciences of the United States of America 100, 10393-10398.

Sparano, J.A., Gray, R.J., Makower, D.F., Pritchard, K.I., Albain, K.S., Hayes, D.F., Geyer, C.E., Dees, E.C., Goetz, M.P., Olson, J.A., et al. (2018). Adjuvant Chemotherapy Guided by a 21-Gene Expression Assay in Breast Cancer. New England Journal of Medicine 379, 111-121.

Spender, L.C., O'Brien, D.I., Simpson, D., Dutt, D., Gregory, C.D., Allday, M.J., Clark, L.J., and Inman, G.J. (2009). TGF-beta induces apoptosis in human B cells by transcriptional regulation of BIK and BCL-XL. Cell Death Differ 16, 593-602.

Strasser, A., Harris, A.W., Bath, M.L., and Cory, S. (1990). Novel primitive lymphoid tumours induced in transgenic mice by cooperation between myc and bcl-2. Nature 348, 331-333.

Strasser, A., Harris, A.W., and Cory, S. (1993). E mu-bcl-2 transgene facilitates spontaneous transformation of early pre-B and immunoglobulin-secreting cells but not T cells. Oncogene 8, 1-9.

Subramani, R., and Lakshmanaswamy, R. (2017). Pregnancy and Breast Cancer. Prog Mol Biol Transl Sci 151, 81-111.

Subramanian, T., Vijayalingam, S., Lomonosova, E., Zhao, L.J., and Chinnadurai, G. (2007). Evidence for involvement of BH3-only proapoptotic members in adenovirus-induced apoptosis. Journal of virology 81, 10486-10495.

Sulston, J.E., and Horvitz, H.R. (1977). Post-embryonic cell lineages of the nematode, Caenorhabditis elegans. Developmental Biology 56, 110-156.

Sulston, J.E., Schierenberg, E., White, J.G., and Thomson, J.N. (1983). The embryonic cell lineage of the nematode Caenorhabditis elegans. Dev Biol 100, 64-119.

Sun, G., Guzman, E., Balasanyan, V., Conner, C.M., Wong, K., Zhou, H.R., Kosik, K.S., and Montell, D.J. (2017). A molecular signature for anastasis, recovery from the brink of apoptotic cell death. The Journal of cell biology 216, 3355-3368.

Sung, E.S., Park, K.J., Choi, H.J., Kim, C.H., and Kim, Y.S. (2012). The proteasome inhibitor MG132 potentiates TRAIL receptor agonist-induced apoptosis by stabilizing tBid and Bik in human head and neck squamous cell carcinoma cells. Experimental cell research 318, 1564-1576.

Sutton, V.R. (2000). Initiation of Apoptosis by Granzyme B Requires Direct Cleavage of Bid, but Not Direct Granzyme B–Mediated Caspase Activation. 192, 1403-1414.

Takamura, A., Komatsu, M., Hara, T., Sakamoto, A., Kishi, C., Waguri, S., Eishi, Y., Hino, O., Tanaka, K., and Mizushima, N. (2011). Autophagy-deficient mice develop multiple liver tumors. Genes & development 25, 795-800.

Tanenbaum, D.M., Wang, Y., Williams, S.P., and Sigler, P.B. (1998). Crystallographic comparison of the estrogen and progesterone receptor's ligand binding domains. Proceedings of the National Academy of Sciences 95, 5998-6003.

Tang, H.L., Tang, H.M., Mak, K.H., Hu, S., Wang, S.S., Wong, K.M., Wong, C.S., Wu, H.Y., Law, H.T., Liu, K., et al. (2012). Cell survival, DNA damage, and oncogenic transformation after a transient and reversible apoptotic response. Mol Biol Cell 23, 2240-2252.

Taylor, R.C., Cullen, S.P., and Martin, S.J. (2008). Apoptosis: controlled demolition at the cellular level. Nature reviews Molecular cell biology 9, 231-241.

Tomita, M., Matsuzaki, Y., Edagawa, M., Shimizu, T., Hara, M., and Onitsuka, T. (2003). Prognostic significance of bcl-2 expression in resected pN2 non-small cell lung cancer. Eur J Surg Oncol 29, 654-657.

Tong, Y., Yang, Q., Vater, C., Venkatesh, L.K., Custeau, D., Chittenden, T., Chinnadurai, G., and Gourdeau, H. (2001). The Pro-apoptotic Protein, Bik, Exhibits Potent Antitumor Activity That Is Dependent on Its BH3 Domain¹. Molecular Cancer Therapeutics 1, 95-102.

Toss, A., and Cristofanilli, M. (2015). Molecular characterization and targeted therapeutic approaches in breast cancer. Breast Cancer Res 17, 60.

Tremont, A. (2017). Endocrine Therapy for Early Breast Cancer: Updated Review. 17, 405-411.

Tsujimoto, Y., Cossman, J., Jaffe, E., and Croce, C.M. (1985). Involvement of the bcl-2 gene in human follicular lymphoma. Science (New York, NY) 228, 1440-1443.

Tung, N., Wang, Y., Collins, L.C., Kaplan, J., Li, H., Gelman, R., Comander, A.H., Gallagher, B., Fetten, K., Krag, K., et al. (2010). Estrogen receptor positive breast cancers in BRCA1 mutation carriers: clinical risk factors and pathologic features. Breast Cancer Research : BCR 12, R12-R12.

Turner, N.C., Neven, P., Loibl, S., and Andre, F. (2017). Advances in the treatment of advanced oestrogen-receptor-positive breast cancer. Lancet (London, England) 389, 2403-2414.

Vargas-Roig, L.M., Cuello-Carrion, F.D., Fernandez-Escobar, N., Daguerre, P., Leuzzi, M., Ibarra, J., Gago, F.E., Nadin, S.B., and Ciocca, D.R. (2008). Prognostic value of Bcl-2 in breast cancer patients treated with neoadjuvant anthracycline based chemotherapy. Mol Oncol 2, 102-111.

Vaux, D.L., Cory, S., and Adams, J.M. (1988). Bcl-2 gene promotes haemopoietic cell survival and cooperates with c-myc to immortalize pre-B cells. Nature 335, 440-442.

Veis, D.J., Sorenson, C.M., Shutter, J.R., and Korsmeyer, S.J. (1993). Bcl-2-deficient mice demonstrate fulminant lymphoid apoptosis, polycystic kidneys, and hypopigmented hair. Cell 75, 229-240.

Verma, S., Budarf, M.L., Emanuel, B.S., and Chinnadurai, G. (2000). Structural analysis of the human pro-apoptotic gene Bik: chromosomal localization, genomic organization and localization of promoter sequences. Gene 254, 157-162.

Verma, S., Zhao, L.J., and Chinnadurai, G. (2001). Phosphorylation of the pro-apoptotic protein BIK: mapping of phosphorylation sites and effect on apoptosis. The Journal of biological chemistry 276, 4671-4676.

Viedma-Rodriguez, R., Baiza-Gutman, L.A., Garcia-Carranca, A., Moreno-Fierros, L., Salamanca-Gomez, F., and Arenas-Aranda, D. (2013). Suppression of the death gene BIK is a critical factor for resistance to tamoxifen in MCF-7 breast cancer cells. Int J Oncol 43, 1777-1786.

Viedma-Rodriguez, R., Ruiz Esparza-Garrido, R., Baiza-Gutman, L.A., Velazquez-Flores, M.A., Garcia-Carranca, A., Salamanca-Gomez, F., and Arenas-Aranda, D. (2015). Involvement of multiple cellular pathways in regulating resistance to tamoxifen in BIK-suppressed MCF-7 cells. Tumour Biol 36, 6991-7005.

Vieira, A.F., Ribeiro, A.S., Dionisio, M.R., Sousa, B., Nobre, A.R., Albergaria, A., Santiago-Gomez, A., Mendes, N., Gerhard, R., Schmitt, F., et al. (2014). P-cadherin signals through the laminin receptor alpha6beta4 integrin to induce stem cell and invasive properties in basal-like breast cancer cells. Oncotarget 5, 679-692.

Villunger, A., Michalak, E.M., Coultas, L., Mullauer, F., Bock, G., Ausserlechner, M.J., Adams, J.M., and Strasser, A. (2003). p53- and drug-induced apoptotic responses mediated by BH3-only proteins puma and noxa. Science (New York, NY) 302, 1036-1038.

Vitale, I., Manic, G., De Maria, R., Kroemer, G., and Galluzzi, L. (2017). DNA Damage in Stem Cells. Molecular cell 66, 306-319.

Vogelstein, B., Papadopoulos, N., Velculescu, V.E., Zhou, S., Diaz, L.A., Jr., and Kinzler, K.W. (2013). Cancer genome landscapes. Science (New York, NY) 339, 1546-1558.

Vonderheide, R.H., Domchek, S.M., and Clark, A.S. (2017). Immunotherapy for Breast Cancer: What Are We Missing? Clinical Cancer Research 23, 2640-2646.

Wahler, J., So, J.Y., Cheng, L.C., Maehr, H., Uskokovic, M., and Suh, N. (2015). Vitamin D compounds reduce mammosphere formation and decrease expression of putative stem cell markers in breast cancer. J Steroid Biochem Mol Biol 148, 148-155.

Wang, C., Mayer, J.A., Mazumdar, A., Fertuck, K., Kim, H., Brown, M., and Brown, P.H. (2011). Estrogen Induces c-myc Gene Expression via an Upstream Enhancer Activated by the Estrogen Receptor and the AP-1 Transcription Factor. Molecular endocrinology (Baltimore, Md) 25, 1527-1538.

Wang, H.G., Pathan, N., Ethell, I.M., Krajewski, S., Yamaguchi, Y., Shibasaki, F., McKeon, F., Bobo, T., Franke, T.F., and Reed, J.C. (1999). Ca2+-induced apoptosis through calcineurin dephosphorylation of BAD. Science (New York, NY) 284, 339-343.

Wang, R., Lv, Q., Meng, W., Tan, Q., Zhang, S., Mo, X., and Yang, X. (2014). Comparison of mammosphere formation from breast cancer cell lines and primary breast tumors. J Thorac Dis 6, 829-837.

Watson, N.F., Madjd, Z., Scrimegour, D., Spendlove, I., Ellis, I.O., Scholefield, J.H., and Durrant, L.G. (2005). Evidence that the p53 negative / Bcl-2 positive phenotype is an independent indicator of good prognosis in colorectal cancer: a tissue microarray study of 460 patients. World journal of surgical oncology 3, 47.

Weisz, A., and Rosales, R. (1990). Identification of an estrogen response element upstream of the human c-fos gene that binds the estrogen receptor and the AP-1 transcription factor. Nucleic Acids Research 18, 5097-5106.

White, E. (2015). The role for autophagy in cancer. The Journal of clinical investigation 125, 42-46.

White, E., Mehnert, J.M., and Chan, C.S. (2015). Autophagy, Metabolism, and Cancer. Clinical cancer research : an official journal of the American Association for Cancer Research 21, 5037-5046.

Wickerham, D.L., Fisher, B., Wolmark, N., Bryant, J., Costantino, J., Bernstein, L., and Runowicz, C.D. (2002). Association of tamoxifen and uterine sarcoma. J Clin Oncol 20, 2758-2760.

Widlak, P., and Garrard, W.T. (2005). Discovery, regulation, and action of the major apoptotic nucleases DFF40/CAD and endonuclease G. Journal of cellular biochemistry 94, 1078-1087.

Widlak, P., Li, P., Wang, X., and Garrard, W.T. (2000). Cleavage Preferences of the Apoptotic Endonuclease DFF40 (Caspase-activated DNase or Nuclease) on Naked DNA and Chromatin Substrates. Journal of Biological Chemistry 275, 8226-8232.

Williams, D.W., Kondo, S., Krzyzanowska, A., Hiromi, Y., and Truman, J.W. (2006). Local caspase activity directs engulfment of dendrites during pruning. Nature neuroscience 9, 1234-1236.

Willis, S.N., Chen, L., Dewson, G., Wei, A., Naik, E., Fletcher, J.I., Adams, J.M., and Huang, D.C. (2005). Proapoptotic Bak is sequestered by Mcl-1 and Bcl-xL, but not Bcl-2, until displaced by BH3-only proteins. Genes & development 19, 1294-1305.

Woo, E.J., Kim, Y.G., Kim, M.S., Han, W.D., Shin, S., Robinson, H., Park, S.Y., and Oh, B.H. (2004). Structural mechanism for inactivation and activation of CAD/DFF40 in the apoptotic pathway. Molecular cell 14, 531-539.

Woodbine, L., Brunton, H., Goodarzi, A.A., Shibata, A., and Jeggo, P.A. (2011). Endogenously induced DNA double strand breaks arise in heterochromatic DNA regions and require ataxia telangiectasia mutated and Artemis for their repair. Nucleic Acids Research 39, 6986-6997.

Wozniak, K., Kolacinska, A., Blasinska-Morawiec, M., Morawiec-Bajda, A., Morawiec, Z., Zadrozny, M., and Blasiak, J. (2007). The DNA-damaging potential of tamoxifen in breast cancer and normal cells. Arch Toxicol 81, 519-527.

Wu, H., Medeiros, L.J., and Young, K.H. (2018). Apoptosis signaling and BCL-2 pathways provide opportunities for novel targeted therapeutic strategies in hematologic malignances. Blood reviews 32, 8-28.

Wu, Q., Li, J., Zhu, S., Wu, J., Chen, C., Liu, Q., Wei, W., Zhang, Y., and Sun, S. (2017). Breast cancer subtypes predict the preferential site of distant metastases: a SEER based study. Oncotarget 8, 27990-27996.

Xie, X., Xia, W., Li, Z., Kuo, H.P., Liu, Y., Li, Z., Ding, Q., Zhang, S., Spohn, B., Yang, Y., et al. (2007). Targeted expression of BikDD eradicates pancreatic tumors in noninvasive imaging models. Cancer cell 12, 52-65.

Xin, L., Liu, Y.H., Martin, T.A., and Jiang, W.G. (2017). The Era of Multigene Panels Comes? The Clinical Utility of Oncotype DX and MammaPrint. World J Oncol 8, 34-40.

Yang, N., and Goping, I.S. (2013). Apoptosis. Colloquium Series on Building Blocks of the Cell: Cell Structure and Function 1, 1-101.

Yang, P.M., Tseng, H.H., Peng, C.W., Chen, W.S., and Chiu, S.J. (2012). Dietary flavonoid fisetin targets caspase-3-deficient human breast cancer MCF-7 cells by induction of caspase-7-associated apoptosis and inhibition of autophagy. Int J Oncol 40, 469-478.

Ye, D.Z., Jin, S., Zhuo, Y., and Field, J. (2011). p21-Activated kinase 1 (Pak1) phosphorylates BAD directly at serine 111 in vitro and indirectly through Raf-1 at serine 112. PloS one 6, e27637.

Yersal, O., and Barutca, S. (2014). Biological subtypes of breast cancer: Prognostic and therapeutic implications. World J Clin Oncol 5, 412-424.

Yin, X.M., Wang, K., Gross, A., Zhao, Y., Zinkel, S., Klocke, B., Roth, K.A., and Korsmeyer, S.J. (1999). Bid-deficient mice are resistant to Fas-induced hepatocellular apoptosis. Nature 400, 886-891.

Yoshii, S.R., Kuma, A., and Mizushima, N. (2017). Transgenic rescue of Atg5-null mice from neonatal lethality with neuron-specific expression of ATG5: Systemic analysis of adult Atg5-deficient mice. Autophagy 13, 763-764.

Youlden, D.R., Cramb, S.M., Dunn, N.A., Muller, J.M., Pyke, C.M., and Baade, P.D. (2012). The descriptive epidemiology of female breast cancer: an international comparison of screening, incidence, survival and mortality. Cancer Epidemiol 36, 237-248.

Yu, C., Gong, Y., Zhou, H., Wang, M., Kong, L., Liu, J., An, T., Zhu, H., and Li, Y. (2017). Star-PAP, a poly(A) polymerase, functions as a tumor suppressor in an orthotopic human breast cancer model. Cell Death Dis 8, e2582.

Yu, H., Boyle, T.A., Zhou, C., Rimm, D.L., and Hirsch, F.R. (2016). PD-L1 Expression in Lung Cancer. J Thorac Oncol 11, 964-975.

Yu, K.D., Wu, J., Shen, Z.Z., and Shao, Z.M. (2012). Hazard of breast cancer-specific mortality among women with estrogen receptor-positive breast cancer after five years from diagnosis: implication for extended endocrine therapy. J Clin Endocrinol Metab 97, E2201-2209.

Yue, Z., Jin, S., Yang, C., Levine, A.J., and Heintz, N. (2003). Beclin 1, an autophagy gene essential for early embryonic development, is a haploinsufficient tumor suppressor. Proceedings of the National Academy of Sciences of the United States of America 100, 15077-15082.

Yunis, J.J. (1983). The chromosomal basis of human neoplasia. Science (New York, NY) 221, 227-236.

Zaidi, M.R., and Merlino, G. (2011). The Two Faces of Interferon-γ in cancer. Clinical cancer research : an official journal of the American Association for Cancer Research 17, 6118-6124.

Zámborszky, J., Szikriszt, B., Gervai, J.Z., Pipek, O., Póti, Á., Krzystanek, M., Ribli, D., Szalai-Gindl, J.M., Csabai, I., Szallasi, Z., et al. (2016). Loss of BRCA1 or BRCA2 markedly increases the rate of base substitution mutagenesis and has distinct effects on genomic deletions. Oncogene 36, 746.

Zhang, J., Liu, X., Scherer, D.C., van Kaer, L., Wang, X., and Xu, M. (1998). Resistance to DNA fragmentation and chromatin condensation in mice lacking the DNA fragmentation factor 45. Proceedings of the National Academy of Sciences of the United States of America 95, 12480-12485.

Zhang, J.H., and Xu, M. (2000). DNA fragmentation in apoptosis. Cell Research 10, 205.

Zhang, L., Xu, L., Zhang, F., and Vlashi, E. (2017). Doxycycline inhibits the cancer stem cell phenotype and epithelial-to-mesenchymal transition in breast cancer. Cell Cycle 16, 737-745.

Zhou, H., Zhang, Y., Fu, Y., Chan, L., and Lee, A.S. (2011). Novel mechanism of anti-apoptotic function of 78-kDa glucose-regulated protein (GRP78): endocrine resistance factor in breast cancer, through release of B-cell lymphoma 2 (BCL-2) from BCL-2-interacting killer (BIK). The Journal of biological chemistry 286, 25687-25696.

Zhu, H., Guo, W., Zhang, L., Wu, S., Teraishi, F., Davis, J.J., Dong, F., and Fang, B. (2005a). Proteasome inhibitors-mediated TRAIL resensitization and Bik accumulation. Cancer Biol Ther 4, 781-786.

Zhu, H., Zhang, L., Dong, F., Guo, W., Wu, S., Teraishi, F., Davis, J.J., Chiao, P.J., and Fang, B. (2005b). Bik/NBK accumulation correlates with apoptosis-induction by bortezomib (PS-341, Velcade) and other proteasome inhibitors. Oncogene 24, 4993-4999.

Zong, W.X., Lindsten, T., Ross, A.J., MacGregor, G.R., and Thompson, C.B. (2001). BH3-only proteins that bind pro-survival Bcl-2 family members fail to induce apoptosis in the absence of Bax and Bak. Genes & development 15, 1481-1486.

Zou, Y., Peng, H., Zhou, B., Wen, Y., Wang, S.-C., Tsai, E.-M., and Hung, M.-C. (2002). Systemic Tumor Suppression by the Proapoptotic Gene bik. Cancer Research 62, 8-12.

Zweig, M.H., and Campbell, G. (1993). Receiver-operating characteristic (ROC) plots: a fundamental evaluation tool in clinical medicine. Clinical chemistry 39, 561-577.

APPENDIX I

A.1 Overview of the statistical tests used for patient data analysis in the study

A.1.1 Receiver operator curve (ROC) analysis

Gene and protein expression data are usually available in a continuous form. In order to dichotomize it into “low” and “high” groups (also called categorical transformation) with respect to patient survival, ROC analysis is performed with disease recurrence as the classification variable using a statistical program such as MedCalc.

ROC curve analysis allows determination of the diagnostic performance of a test based on the sensitivity and specificity parameters (Metz, 1978; Zweig and Campbell, 1993). In a given n a given population for a specific marker, a clear prediction of recurrence vs. disease-free survival seldom exists due to variations in biology (Figure 1.7). Thus, for every possible cut-off value, four possibilities may exist (i) cases with the disease correctly classified as positive (True positive) (ii) cases with the disease incorrectly classified as negative (False negative) (iii) cases with no disease correctly classified as negative (True negative) and (iv) cases with no disease incorrectly classified positive (False positive). With a ROC curve, the true positive rate (Sensitivity) is plotted on the Y-axis against the false positive rate (100-Specificity) on the X-axis for different cut-off points of a variable (e.g., continuous gene expression values) creating a sensitivity/specificity pair for a particular threshold. The specificity/sensitivity pair that gives the highest area under the curve (AUC), best distinguishes true positives from false positives. A perfect ROC curve passes through the upper left corner (100% sensitivity, 100% specificity) (Figure 1.7). For this study, AUC was determined using the method of DeLong et al. (DeLong et al., 1988).

A.1.2 Chi-squared analysis and Fisher's exact test

These two analyses are employed to interrogate the correlation between two categorical variables. The chi-squared analysis assumes a null hypothesis and employs the following equation to determine the differences between the expected and observed frequencies.

$$\chi^2 = \sum \frac{(f_o - f_e)^2}{f_e}$$

Where f_o is the observed frequency, and f_e is the expected frequency if there is no difference between the variables. The chi-squared analysis gives more accurate results with larger sample sizes. Fisher's exact test produces 2 x 2 frequency tables and employs the following formula, and is usually more suitable for smaller sample sizes.

$$p = \frac{n!(N-n)!R!(N-R)!}{r!(n-r)!(R-r)!(N-n-R+r)!\ N!}$$

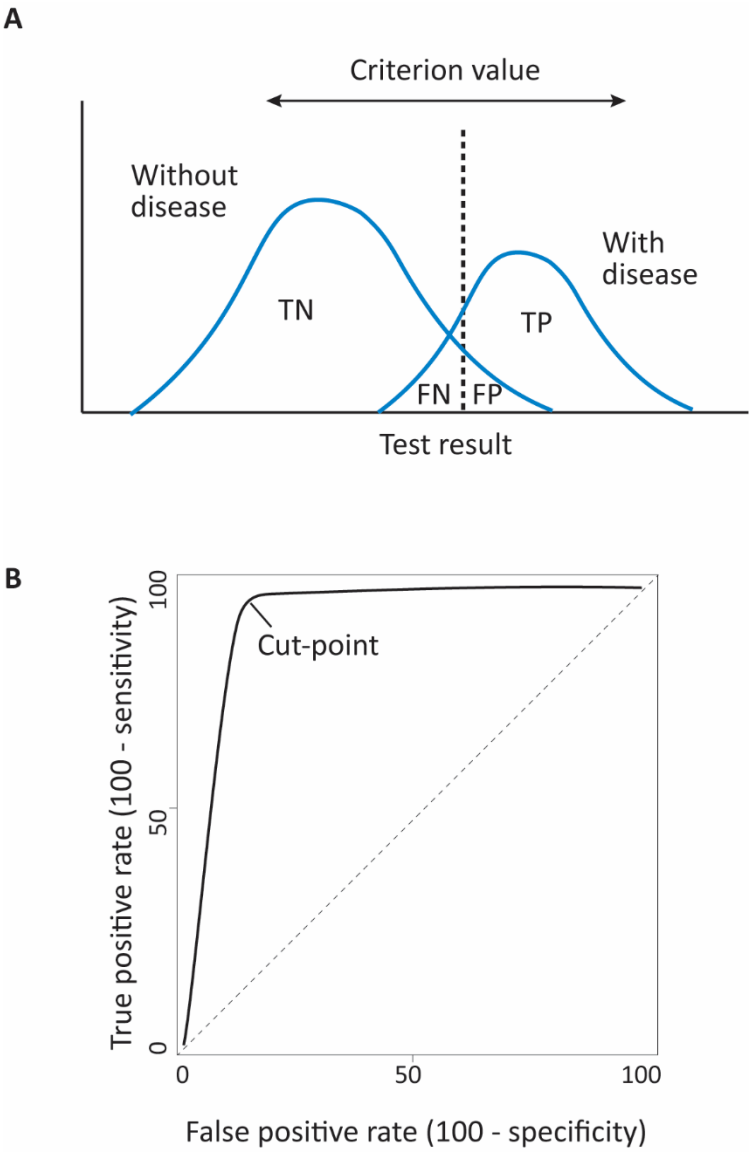

Figure A.1 Distribution of marker expression values for disease-recurrence and utility of ROC analysis A. In the context of disease-recurrence, marker values overlap, giving rise to false positive and false negative results.TN (true negative), FN (false negative), FP (false positive) and TP (true positive) **B.** ROC curve provides a determination of the best cut-point based on the best combination of sensitivity/specificity pair.

Where N is the total sample size, n is the sample size for the first group, r is the number of positive outcomes for the first group and R is the total number of positive outcomes.

A.1.3 Kaplan-Meier survival curves and log-rank test

In order to estimate the individual association of 'high' or 'low' gene/protein expression levels of candidate variables (e.g., *BIK, BCL-2, ATG-5*) with disease recurrence or death, Kaplan-Meier survival curves are plotted, and comparisons between the two survival curves are made using the log-rank test. In this study, Kaplan-Meier survival curves measure the follow-up time from the time of breast cancer diagnosis to the detection of recurrence or death in relation to a specific variable. Variables are dichotomized into a categorical form (0=low, 1=high) using ROC curve analysis as described earlier. The following explanation considers recurrence as an event and describes how the disease-free survival is calculated. The KM survival curve is plotted as cumulative survival S (t) vs. time t (Bewick et al., 2004). S (t) is defined as the observed fraction surviving at least to time t. In order to calculate S (t), the proportions surviving for individual time periods (e.g., p_{t1}, p_{t2}, $p_{t3,}$ etc.), is calculated by the following equation (Bewick et al., 2004):

$$p_t = \frac{r_t - d_t}{r_t}$$

Where p_t is the proportion surviving till time t, r_t is the number alive at the beginning of a specific time period and d_t is the number of recurrences within that time period. Now cumulative proportion surviving S (t) is calculated by the following equation (Bewick et al., 2004):

$$S(t) = p_{t1} \times p_{t2} \times p_{t3} \times \ldots \times p_t$$

Cumulative proportions surviving against the specific survival time is plotted to get a typical stepped survival curve. Statistical significance between the two curves is determined using the log-rank test which assumes a null hypothesis, meaning that there is no significant difference between the two curves. It calculates this by considering the observed number of events compared to the expected number of events using the following equation (Bewick et al., 2004).

$$\chi^2 \ (\log \text{rank}) = \frac{(O_1 - E_1)^2}{E_1} + \frac{(O_2 - E_2)^2}{E_2}$$

Where the O1 and O2 are the total number of observed events in groups 1 and 2, respectively, and E1 and E2 are the total numbers of expected events. E2 (expected number of events for group 2) is calculated by the following equation (Bewick et al., 2004):

$$E_2 = \sum_{i=1}^{t} \frac{d_i}{r_i} \ r_{2i}$$

Where r_{2i} is the number alive from group 2 at the time of event *i, d*i is the number of deaths at specific time t, ri is the total number alive. E1 can be calculated by n – E2 where n is the total number of events. In this study, 5-years disease-free or overall survival of the patients were calculated using the above-described methods using a statistical program called MedCalc Version 17.9.6 (MedCalc Software bvba, Ostend, Belgium; http://www.medcalc.org; 2017). Patients lost to follow-up before 5-years were censored and indicated with a small vertical line on the Kaplan-Meier survival curves.

A.1.4 Cox regression analysis

Cox regression analysis is used to determine associations of the individual as well as multiple variables with patient prognosis. Cox regression measures the instantaneous risk of an event (e.g. death) occurring and assumes that this risk remains proportional in the two groups throughout the time. It utilizes the following equation (Bewick et al., 2004) to compute the hazard:

$$\ln h(t) = \ln h_o(t) + b_1 x_1 + \ldots + b_p x_p$$

Where h(t) is the hazard time t; x_1, $x_2 \ldots x_p$ are the explanatory variables (e.g., mitotic grade, ER status, *BIK,* etc); and $h_o(t)$ is the baseline hazard when all the explanatory variables are zero. The coefficients b_1, $b_2 \ldots b_p$ are calculated from data using a statistical program. For multivariate analyses in this study, a Stepwise model was used which sequentially enters individually significant variables and checks to see and remove the variables that become non-significant after each sequential addition (Christensen, 1987). Using this method, the dependence of variables on each other can be determined. All calculations were done using the MedCalc Version 17.9.6 program (MedCalc Software bvba, Ostend, Belgium; http://www.medcalc.org; 2017).

References

Bewick, V., Cheek, L., and Ball, J. (2004). Statistics review 12: survival analysis. Crit Care *8*, 389-394.

Christensen, E. (1987). Multivariate survival analysis using Cox's regression model. Hepatology *7*, 1346-1358.

DeLong, E.R., DeLong, D.M., and Clarke-Pearson, D.L. (1988). Comparing the areas under two or more correlated receiver operating characteristic curves: a nonparametric approach. Biometrics *44*, 837-845.

Metz, C.E. (1978). Basic principles of ROC analysis. Seminars in nuclear medicine *8*, 283-298.

Zweig, M.H., and Campbell, G. (1993). Receiver-operating characteristic (ROC) plots: a fundamental evaluation tool in clinical medicine. Clinical chemistry *39*, 561-577.